Development and application of LC-MS approaches for studying the plant primary metabolome

Carla Inês Paquim Santos António

A thesis submitted for the degree of Doctor of Philosophy at the University of York

University of York

Department of Chemistry

April 2008

Abstract

Carbohydrates are key compounds in plant metabolism. They are important intermediates of metabolic pathways, such as cell wall formation, glycolysis, the pentose phosphate pathway, and starch and sucrose synthesis in plants. Due to their high polarity, structural variety, and poor UV absorption, carbohydrates are a challenging class of compounds within the plant metabolome to analyse.

While liquid chromatography (LC) coupled to electrospray mass spectrometry (ESI-MS) is an obvious approach, retention of these metabolites on reversed-phase (RP) columns is minimal. Porous graphitic carbon (PGC) and hydrophilic interaction chromatography (HILIC) stationary phases are two alternatives to RP for retention of polar compounds. The suitability of PGC and HILIC was thus investigated for the analysis of polar plant primary metabolites such as carbohydrate-related compounds.

This thesis describes the development and optimisation of robust on-line LC-ESI-MS^n methods using a quadrupole ion trap instrument and MS compatible mobile phases for the simultaneous targeted analysis of a range of primary metabolites, from neutral sugars and sugar phosphates to sugar alcohols, and glycolytic intermediates, using PGC and HILIC stationary phases.

The newly developed LC-MS methods were applied for the analysis of such primary metabolites in extracts of *Arabidopsis thaliana* wild-type Columbia-0 and starchless phosphoglucomutase mutant (*pgm1*) leaf tissues, as well as to extracts of *Lupinus albus* stem tissues that have been subjected to water deficit.

List of contents

Abstract		**ii**
List of contents		**iii**
List of tables		**ix**
List of figures		**x**
List of abbreviations		**xx**
Preface		**xxiv**
Acknowledgements		**xxv**
Author's declaration		**xxvi**
Chapter 1. Introduction		**1**
1.1	Plant carbohydrate metabolism	2
	1.1.1 Monosaccharides	2
	1.1.2 Oligosaccharides and polysaccharides	4
	1.1.3 Hexose phosphate pool	7
	1.1.4 Sucrose synthesis occurs in the cytosol	8
	1.1.5 Starch synthesis occurs in plastids	10
1.2	Plant responses to abiotic stress	12
	1.2.1 Stress involving water deficit	12
	1.2.2 Plant water status	13
	1.2.3 Carbohydrates as compatible solutes in plants under water deficit	14
1.3	*Arabidopsis thaliana*: a model system for plant research	15
1.4	Plant metabolomics	16
1.5	Analytical technologies used in plant metabolomics	19
	1.5.1 Quenching and extraction of plant metabolites	19
	1.5.2 GC-MS	20
	1.5.3 LC-MS	22

1.5.4 CE-MS 24
1.5.5 NMR 24
1.5.6 Direct infusion-MS 25
1.6 Data analysis 26
1.7 High performance liquid chromatography 27
1.7.1 Porous graphitic carbon as a stationary phase in LC 31
1.7.2 Hydrophilic interaction chromatography 32
1.8 Mass spectrometry 34
1.8.1 Ionisation techniques 35
1.8.1.1 Electron ionisation 35
1.8.1.2 Electrospray ionisation 36
1.8.2 Mass analysers 39
1.8.2.1 Quadrupole 40
1.8.2.2 Quadrupole ion trap 44
1.8.2.3 Time-of-flight 48
1.8.2.4 Orthogonal acceleration 51
1.8.3 Detectors 53
1.8.4 Tandem mass spectrometry 53
1.8.4.1 Tandem-in-time 54
1.8.4.2 Tandem-in-space 55
1.8.5 Carbohydrate fragmentation 57
1.9 Aims of this thesis 59

Chapter 2. Experimental methods 61

2.1 Plant material 61
2.1.1 Sowing *Arabidopsis thaliana* on soil 61
2.1.2 Harvesting and storage of *Arabidopsis thaliana* seeds 62
2.1.3 *Arabidopsis thaliana* seed sterilisation 62
2.1.4 *Arabidopsis thaliana* growth-chamber conditions 63
2.1.5 Extraction of metabolites from *Arabidopsis thaliana* tissues 64
2.1.6 *Lupinus albus* growth-chamber conditions 65

2.1.7 Extraction of carbohydrates from *Lupinus albus* tissues 66
2.1.8 Characterisation of soil and *Lupinus albus* water status 66
2.2 Graphitic carbons for solid phase extraction 67
2.3 Mass spectrometric analysis 68
2.3.1 Electrospray quadrupole orthogonal acceleration time-of-flight mass spectrometry (ESI-qoaTOF-MS) 68
2.3.1 Electrospray quadrupole ion trap mass spectrometry (ESI-QIT-MS) 68
2.4 Liquid chromatography-mass spectrometry 69
2.4.1 Porous graphitic carbon liquid chromatography electrospray quadrupole ion trap tandem mass spectrometry for the analysis of *Arabidopsis thaliana* leaf tissues (PGC-LC-ESI-QIT-MS^n) 69
2.4.2 Porous graphitic carbon liquid chromatography electrospray quadrupole ion trap tandem mass spectrometry for the analysis of *Lupinus albus* stem tissues (PGC-LC-ESI-QIT-MS^n) 70
2.4.3 Regeneration of the PGC Hypercarb column (5 µm, 100 mm x 4.6 mm i.d.) 71
2.4.4 Hydrophilic interaction chromatography electrospray quadrupole ion trap tandem mass spectrometry for the analysis of *Arabidopsis thaliana* leaf tissues (HILIC-ESI-QIT-MS^n) 72

Chapter 3. Mass spectrometric studies of sugars, sugar phosphates, and glycolytic intermediates, and evaluation of their retention on carbon-based packing materials 74

3.1 Introduction 74
3.2 Results and discussion 75
3.2.1 Studies of the mass spectrometric behaviour of sugars, sugar phosphates, and glycolytic intermediates 75
3.2.2 Studies of the retention of sugar phosphates and glycolytic intermediate standards on carbon-based sorbents using SPE 88
3.3 Conclusions 94

Chapter 4. Porous graphitic carbon liquid chromatography electrospray ion trap mass spectrometry for the analysis of sugars, sugar phosphates, and glycolytic intermediates from *Arabidopsis thaliana* leaf tissues **95**

4.1 Introduction 95
4.1.1 Aim 98
4.2 Results and discussion 99
4.2.1 PGC-LC-ESI-QIT-MS^n method development 99
4.2.2 Negative ion CID behaviour of standard compounds using PGC-LC-ESI-QIT-MS^n 104
4.2.3 Linearity, limits of detection (LOD), and limits of quantification (LOQ) of the PGC-LC-ESI-QIT-MS method 110
4.2.4 Analytical recoveries of standards added to *A. thaliana* tissue extracts 112
4.2.5 Application of the PGC-LC-ESI-QIT-MS method to the analysis of metabolic intermediates from *A. thaliana* wild-type Col-0 and *pgm1* plants growing in a 16 h light/ 8 h dark photoperiod 113
4.2.6 Application of the PGC-LC-ESI-QIT-MS method to the analysis of metabolite level changes during the diurnal cycle in *A. thaliana* wild-type Col-0 and *pgm1* plants growing in a 12 h light/ 12 h dark regime 116
4.3 Conclusions 118

Chapter 5. Porous graphitic carbon liquid chromatography electrospray ion trap mass spectrometry for the analysis of carbohydrates in *Lupinus albus* stems in response to water deficit **119**

5.1 Introduction 119
5.1.1 Aim 121

5.2 Results and discussion 122
5.2.1 PGC-LC-ESI-QIT-MS^n method development 122
5.2.2 Linearity, limits of detection (LOD), and limits of quantification (LOQ) of the PGC-LC-ESI-QIT-MS method 127
5.2.3 Characterisation of the *L. albus* water status during early/mild/severe water deficit, and recovery conditions 130
5.2.4 PGC-LC-ESI-QIT-MS^n analysis of water soluble carbohydrates from *L. albus* stem extracts 132
5.3 Conclusions 137

Chapter 6. Hydrophilic interaction chromatography electrospray ion trap mass spectrometry for the analysis of carbohydrate-related metabolites from *Arabidopsis thaliana* leaf tissues **138**

6.1 Introduction 138
6.1.1 Aim 140
6.2 Results and discussion 141
6.2.1 HILIC-ESI-QIT-MS^n method development 141
6.2.2 Negative ion CID behaviour of non-reducing RFOs using HILIC-ESI-QIT-MS^n 146
6.2.3 Repeatability, limits of detection (LOD), and limits of quantification (LOQ) of the HILIC-ESI-QIT-MS method 152
6.2.4 Quantification of carbohydrate-related metabolites in *A. thaliana* wild-type Col-0 and *pgm1* leaf extracts using HILIC-ESI-QIT-MS 153
6.3 Conclusions 160

Chapter 7. Concluding remarks and future work **162**

Chapter 8. References **164**

Chapter 9. Outcomes of this PhD **190**

Appendix I

Appendix II

Appendix III

List of tables

Table 3.1 Nominal *m/z* and signal to noise (S/N) values obtained for standard sugars, sugar phosphates, and glycolytic intermediates analysed in positive and negative ion mode ESI-qoaTOF-MS. *nd*, not detected.

Table 3.2 Diagnostic product ions (*m/z*) obtained from $[M-H]^-$ of a range of sugars, sugar phosphates, and glycolytic intermediates using negative ion mode ESI-qoaTOF-MS/MS.

Table 4.1 Nominal *m/z* values, retention times, intra- and inter-day repeatabilities of retention times, LOD, LOQ, and linearity of calibration curves obtained for standard compounds using negative ion PGC-LC-ESI-QIT-MS.

Table 5.1 Nominal *m/z* values, retention times, intra- and inter-day repeatabilities of retention times, LOD, LOQ, and linearity of calibration curves obtained for standard compounds using negative ion PGC-LC-ESI-QIT-MS.

Table 5.2 Soil water content (%), pre-dawn leaf water potential (Ψ_{leafpd}) and leaf, stem stele and stem cortex relative water content (RWC) during the period of water deficit (WD) imposition and rewatering (RW). WW, well watered plants (control).

Table 6.1 Nominal *m/z* values, retention times, intra- and inter-day repeatabilities of retention times, LOD, and LOQ obtained for *myo*-inositol, sugars, sugar alcohols, and sugar phosphate standard compounds using negative ion HILIC-ESI-QIT-MS.

Table 6.2 Linearity of standard curves obtained for Glc, Suc, raffinose, and Glc6P standard compounds using negative ion HILIC-ESI-QIT-MS.

Table 6.3 Metabolite levels (Glc, Suc, raffinose, and Glc6P) determined in *A. thaliana* WT Col-0 and *pgm1* leaf extracts using negative ion mode HILIC-ESI-QIT-MS and PGC-LC-ESI-QIT-MS.

List of figures

Figure 1.1 Reactions in aqueous solution of (a) linear form of D-glucose to yield the anomeric hemiacetals α-D-glucopyranose and β-D-glucopyranose, and (b) linear form of D-fructose to yield the anomeric hemiketals α-D-fructofuranose and β-D-fructofuranose. The cyclic forms are drawn as Haworth projections.

Figure 1.2 Structures and constituent monosaccharides of the (a) non-reducing disaccharide sucrose and (b) reducing disaccharide maltose, drawn as Haworth projections. Shaded areas highlight the anomeric carbons of the molecules.

Figure 1.3 (a) Cellulose, the structural polysaccharide of plant cell walls, is a linear polymer of β(1→4)-linked D-glucose residues. Starch, the food storage polysaccharide of plants, contains (b) α-amylose, a linear polymer of α(1→4)-linked D-glucose residues, and (c) amylopectin, which is branched through α(1→6)-linkages. *n* may be several thousand.

Figure 1.4 Metabolic intermediates of the hexose phosphate pool; they are interconverted by two enzymes: phosphoglucomutase and phosphoglucose isomerase. Hexose phosphates are primary metabolites and key intermediates to many biosynthetic metabolic pathways in plants.

Figure 1.5 Sucrose biosynthetic pathway in cytosol. Carbon assimilated via the Calvin Cycle is partitioned with a fraction exported to the cytosol for sucrose synthesis and glycolysis, and a fraction retained in the chloroplast for starch synthesis. Hexose-P pool, hexose-phosphate pool; Triose-P, triose-phosphates; *TPT*, triose phosphate translocator; Fru1,6BP; fructose-1,6-bisphosphate; Fru6P, fructose-6-phosphate; Glc6P, glucose-6-phosphate; Glc1P, glucose-1-phosphate; UTP, uridine triphosphate; PP_i, pyrophosphate; P_i, inorganic phosphate; UDP, uridine

diphosphate; UDPGlc, uridine diphosphate glucose; Suc6P, sucrose-6-phosphate; *cPGI*, cytosolic phosphoglucose isomerase; *cPGM*, cytosolic phosphoglucomutase; *UGPase*, UDP-glucose pyrophosphorylase; *SPS*, sucrose-phosphate synthase; *SPP*, sucrose-phosphate phosphatase; 1,3BPG; 1,3-bisphosphoglycerate; 3PG, 3-phosphoglycerate; 2PG, 2-phosphoglycerate; PEP, phosphoenolpyruvate; Pyr, pyruvate.

Figure 1.6 Starch biosynthetic pathway in the chloroplast. Carbon assimilated via the Calvin Cycle is partitioned with a fraction retained in the chloroplast for starch synthesis. Hexose-P pool, hexose-phosphate pool; Triose-P, triose-phosphates; *TPT*, triose phosphate translocator; Fru6P, fructose-6-phosphate; Glc6P, glucose-6-phosphate; Glc1P, glucose-1-phosphate; ATP, adenosine triphosphate; PP_i, pyrophosphate; P_i, inorganic phosphate; ADPGlc, adenosine diphosphate glucose; *pPGI*, plastidial phosphoglucose isomerase; *pPGM*, plastidial phosphoglucomutase; *AGPase*, ADP-glucose pyrophosphorylase; *SSs*, starch synthases; *SBEs*, starch-branching enzymes; *PPase*, pyrophosphatase.

Figure 1.7 Diagram showing the connection between the 'omic' technologies. Metabolomics is complementary to transcriptomics and proteomics, but closer to the phenotype. The general flow of information is from genes (genotype) to transcripts to proteins to metabolites (phenotype).

Figure 1.8 Diagram showing the conversion of an aldehyde group into an oxime using methoxylamine. Oximes give two products corresponding to the *E*- and *Z*- isomers, which are resolved by GC-MS.

Figure 1.9 Diagram illustrating the separation in time of different analytes migrating through a column. Each analyte migrates at different rates, each having different partition coefficients (k_D). The analytes elute sequentially from the column and pass through a

detection system. The resulting separation of the analytes generates a chromatogram; the area of each peak is proportional to the concentration of that analyte.

Figure 1.10 Diagram showing (a) the flat surface of PGC and (b) the surface of ODS silica-based materials.

Figure 1.11 Schematic representation of the retention processes on a sulfoalkylbetaine zwitterionic stationary phase. The mechanism of retention is based on the hydrophilic partitioning of the analytes into the water-enriched stationary phase, and weak electrostatic interactions with either the positive or negative charge of the functional group. Adapted from (SeQuant, 2006).

Figure 1.12 Components of a mass spectrometer.

Figure 1.13 Diagram of an electron ionisation source.

Figure 1.14 Diagram of an electrospray source.

Figure 1.15 Charge residue model.

Figure 1.16 Ion evaporation model.

Figure 1.17 Schematic representation of a linear quadrupole mass analyser showing the equations for the potentials applied to the four rods. The green dotted line indicates the general direction of ion movement.

Figure 1.18 Stability diagram in a a_u-q_u space showing the regions of stable ion trajectories in the *x*- and *y*- directions in a quadrupole mass analyser. *u* represents either *x* or *y*.

Figure 1.19 Stability regions for two ions with different *m/z* values (M1 and M2) as a function of *U* and *V* in a quadrupole mass analyser. Scanning along the operating line, maintaining the *U/V* ratio constant, allows ions of different *m/z* values to be transmitted through the quadrupole.

Figure 1.20 Cross-section of a quadrupole ion trap mass analyser showing the radial (r_0) and axial (z_0) directions.

Figure 1.21 Diagram showing the regions of stability along the *r* and *z* axis in the quadrupole ion trap. The common *r* and *z* stability area used in

commercial ion traps is circled in green.

Figure 1.22 Diagram showing simultaneous ion stability in both the *r*- and *z*-directions in the quadrupole ion trap. In the 'mass-selective instability mode', the ion trap operates in rf-only mode along the mass-selective instability line, $a_z=0$. Ion trajectories become unstable when q_z=0.908.

Figure 1.23 Schematic representation of the relative positions of ions with three different *m/z* values along the mass-selective instability line, a_z=0. The effect of ramping the amplitude of the fundamental rf voltage is illustrated from panel a-c; as the fundamental rf voltage increases, the q_z value for each ion also increases. Ions are ejected when q_z=0.908 (red ion, panel c), but the amplitude of the fundamental rf voltage is not ramped high enough to get the higher *m/z* ions (blue and green) out of the trap. These ions are ejected from the trap by applying an additional voltage to the end-cap electrodes at the ions' secular frequencies. The application of a secular frequency creates a 'hole' in the a_z=0 axis, through which the ions can be ejected and detected at q_z values lower than 0.908. This process is called resonance ejection (panel d-f).

Figure 1.24 Schematic principle of a linear time-of-flight mass analyser.

Figure 1.25 Schematic of a TOF mass analyser with an ion reflectron; *KE*, kinetic energy.

Figure 1.26 Schematic of the Applied Biosystems QSTAR Pulsar i quadrupole oaTOF mass spectrometer equipped with an ESI source.

Figure 1.27 Tandem mass spectrometry experiments described using a tandem quadrupole instrument; Q1 and Q2 are quadrupole mass analysers, separated by a collision cell: (a) product ion experiment; (b) precursor ion experiment; (c) neutral loss experiment diagram; (d) selected reaction monitoring experiment.

Figure 1.28 Carbohydrate fragmentation showing nomenclature proposed by Domon and Costello (Domon and Costello, 1988). Superscripts indicate which ring bonds were cleaved to give cross-ring A and X

ions; subscripts indicate which glycosidic bond was broken counting from the non-reducing terminus or from the reducing terminus or aglycone (glycosidic bond linking to the aglycone is numbered zero).

Figure 1.29 Numbering of the C-C bonds used to designate A*i* and X*j* fragments in carbohydrate spectra: (a) 6-membered ring (pyranose) form, and (b) 5-membered ring (furanose) form drawn as Haworth projections.

Figure 1.30 (a) Mechanism of formation of oxonium B*i* ions and Y*j* ions in the positive ion mode; (b) mechanism of formation of B*i* and Y*j* ions in the negative ion mode.

Figure 3.1 (a) Positive ion mode and (b) negative ion mode ESI-qoaTOF-MS analysis of a standard mixture containing: Glc, Suc, Pyr, PEP, Glc1P, Tre6P and Fru1,6BP (each 50 μg/mL).

Figure 3.2 CID MS^2 product ion spectrum of Glc ($[M-H]^-$ at *m/z* 179).

Figure 3.3 CID MS^2 product ion spectrum of Tre ($[M-H]^-$ at *m/z* 341).

Figure 3.4 CID MS^2 product ion spectrum of Suc6P ($[M-H]^-$ at *m/z* 421).

Figure 3.5 CID MS^2 product ion spectrum of Fru1,6BP ($[M-H]^-$ at *m/z* 339).

Figure 3.6 CID MS^2 product ion spectrum of PEP ($[M-H]^-$ at *m/z* 167).

Figure 3.7 CID MS^2 product ion spectrum of Pyr ($[M-H]^-$ at *m/z* 87).

Figure 3.8 Differentiation of the isomeric compounds Glc1P and Glc6P (precursor ion $[M-H]^-$ at *m/z* 259) by ESI-qoaTOF-MS/MS: (a) CID MS^2 product ion spectrum of Glc1P; (b) CID MS^2 product ion spectrum of Glc6P.

Figure 3.9 PGC Hypersep did not retain Glc ($[M-H]^-$ at *m/z* 179; $[M+HCOO]^-$ at *m/z* 225) which was washed through with the water wash.

Figure 3.10 PGC Hypersep elution of Tre ($[M-H]^-$ at *m/z* 341; $[M+HCOO]^-$ at *m/z* 387) with 4:96 (v/v) acetonitrile:water.

Figure 3.11 PGC Hypersep elution of Glc1P ($[M-H]^-$ at *m/z* 259) with 25:75 (v/v) acetonitrile:water + 0.1% FA.

Figure 3.12 PGC Hypersep elution of Tre6P ($[M-H]^-$ at *m/z* 421) with 25:75 (v/v) acetonitrile:water + 0.1% FA.

Figure 3.13 PGC Hypersep elution of PEP ($[M-H]^-$ at *m/z* 167) with 30:70 (v/v) acetonitrile:water + 0.1% FA.

Figure 4.1 Extracted ion chromatograms obtained on PGC-LC-ESI-QIT-MS separation of a 50 µg/mL standard solution of a mixture of intermediary metabolites. HPLC conditions: PGC column (100 mm x 4.6 mm i.d.), 600 µL/min, 20 µL injection, mobile phase composed of (a) acetonitrile and 10% aqueous acetic acid; (b) acetonitrile and 10% aqueous formic acid.

Figure 4.2 Extracted ion chromatograms obtained on PGC-LC-ESI-QIT-MS separation of a 50 µg/mL standard solution of a mixture of intermediary metabolites. HPLC conditions: PGC column (100 mm x 4.6 mm i.d.), 600 µL/min, 20 µL injection, optimised triple stage gradient.

Figure 4.3 Extracted ion chromatogram obtained on PGC-LC-ESI-QIT-MS for a standard solution (10 µM) of disaccharide isomers showing separation of: (1) Tre t_R= 5.96 min, (2) Suc t_R= 7.54 min and (3) Maltose t_R= 8.44 min.

Figure 4.4 (a) Extracted ion chromatograms obtained on PGC-LC-ESI-QIT-MS^n showing the specificity of detection provided by CID MS^n for a standard solution (10 µM) of Suc; (b) CID MS^2 product ion spectrum of Suc (precursor ion $[M+HCOO]^-$ *m/z* 387); (c) CID MS^3 spectrum of Suc (precursor ion *m/z* 341).

Figure 4.5 (a) Extracted ion chromatograms obtained on PGC-LC-ESI-QIT-MS^n showing the specificity of detection provided by CID MS^n for a standard solution (10 µM) of Tre6P; (b) CID MS^2 product ion spectrum of Tre6P (precursor ion $[M-H]^-$ *m/z* 421); (c) CID MS^3 spectrum of Tre6P (precursor ion *m/z* 241).

Figure 4.6 Differentiation of the isomeric compounds Glc1P and Glc6P by ion trap tandem MS: (a) CID MS^2 product ion spectrum of Glc1P *m/z* 259; (b) CID MS^2 product ion spectrum of Glc6P *m/z* 259.

Figure 4.7 Recoveries of different phosphate standards added to accurately weighed *A. thaliana* Col-0 leaf extracts using two extraction

methods: TCA/ether and chloroform/methanol. Values are mean ± SD (n=3 biological replicates, each containing leaves from three rosettes). Each biological replicate is the mean value of n=3-4 independent PGC-LC-ESI-QIT-MS measurements.

Figure 4.8 Metabolite levels (Glc, Suc and Glc6P) determined in *A. thaliana* Col-0 and starchless *pgm1* chloroform/methanol leaf extracts using PGC-LC-ESI-QIT-MS. Plants were grown under a 16 h light/ 8 h dark photoperiod and harvested at developmental stage 6.0. Values are mean ± SD (n=3 biological replicates, each containing leaves from three rosettes). Each biological replicate is the mean value of n=3-4 independent measurements. FW, fresh weight.

Figure 4.9 Metabolite level changes observed over a 12 h light/ 12 h dark cycle in *A. thaliana* wild-type Col-0 (■) and starchless *pgm1* (□) chloroform/methanol leaf extracts using PGC-LC-ESI-MS: (A) Glc, (B) Suc and (C) Glc6P. Rosettes were harvested at the end of the night, 4 h, 8 h, 12 h into the light period, 4 h, 8 h, and again 12 h into the dark period. Values are mean ± SD (n=3 biological replicates, each containing leaves from three rosettes). Each biological replicate is the mean value of n=3-4 independent measurements. FW, fresh weight.

Figure 5.1 Extracted ion chromatograms obtained using mobile phase 1 and negative ion mode PGC-LC-ESI-QIT-MS for the separation of a 50 µg/mL standard mixture of neutral sugars and sugar alcohols. All compounds were detected as formylated molecules $[M+HCOO]^-$.

Figure 5.2 Extracted ion chromatogram obtained on PGC-LC-ESI-QIT-MS for a standard solution (10 µM) of the isomeric compounds: (1) Galactinol t_R= 4.31 min, (2) Suc t_R= 7.12 min and (3) Maltose t_R= 8.34 min, all detected at *m/z* 387 (formylated molecules $[M+HCOO]^-$).

Figure 5.3 (a) Extracted ion chromatograms (mobile phase 1) obtained using negative ion mode PGC-LC-ESI-QIT-MS showing the specificity

of detection provided by CID MS^n for a standard solution (10 μM) of raffinose, detected at *m/z* 549 ($[M+HCOO]^-$); (c) CID MS^3 spectrum of raffinose (precursor ion $[M-H]^-$ at *m/z* 503).

Figure 5.4 Water soluble carbohydrate levels in *Lupinus albus* stems obtained by PGC-LC-ESI-QIT-MS at 4 days after withholding water (DAW; early water stress), 13 DAW (severe water stress), 6 and 26 h after rewatering (RW). (A) Glc, (B) Suc, and (C) raffinose. Data are mean ± SD of n=2-3 biological replicates. Each biological replicate is the mean value of n=2-3 independent PGC-LC-ESI-QIT-MS measurements. DW, dry weight. Control, well watered plants. nd, not detected.

Figure 6.1 Extracted ion chromatograms obtained on negative ion mode HILIC-ESI-QIT-MS separation of a standard solution of neutral sugars (50 μM each) detected as formylated molecules $[M+HCOO]^-$.

Figure 6.2 Extracted ion chromatograms obtained on negative ion mode HILIC-ESI-QIT-MS separation of a standard solution of sugar alcohols and *myo*-inositol (50 μM each) detected as formylated molecules $[M+HCOO]^-$.

Figure 6.3 Extracted ion chromatograms obtained on negative ion mode HILIC-ESI-QIT-MS separation of a standard solution containing neutral sugars (formylated molecules $[M+HCOO]^-$), sugar alcohols (formylated molecules $[M+HCOO]^-$), and sugar phosphates (deprotonated molecules $[M-H]^-$) (50 μM each).

Figure 6.4 Extracted ion chromatograms obtained on HILIC-ESI-QIT-MS separation of different standard solutions containing (a) isomeric disaccharides Suc t_{R1}=9.33 min and Tre t_{R2}= 9.91 min; (b) isomeric monosaccharide phosphates Glc1P t_{R3}=11.04 min and Glc6P t_{R4}= 11.78 min; (c) isomeric disaccharide phosphates Suc6P t_{R5}=11.25 min and Tre6P t_{R6}=11.71 min (50 μM each).

Figure 6.5 Negative ion CID spectra of non-reducing RFOs obtained by HILIC-ESI-QIT-MS^n showing nomenclature of Domon and

Costello (Domon and Costello, 1988; Domon, 2008; personal communication). (a) CID MS^3 spectrum of raffinose (precursor ion $[M-H]^-$ *m/z* 503); (b) CID MS^2 spectrum of stachyose (precursor ion $[M-H]^-$ *m/z* 665); (c) CID MS^2 spectrum of verbascose (precursor ion $[M-H]^-$ *m/z* 827).

Figure 6.6 Typical negative ion base peak chromatogram obtained on separation of an *A. thaliana* Col-0 chloroform/methanol leaf extract (16 h light/8 h dark photoperiod) using (a) HILIC-ESI-QIT-MS and (c) PGC-LC-QIT-MS. The extracted ion chromatograms for Glc ($[M+HCOO]^-$ at *m/z* 225), Suc ($[M+HCOO]^-$ at *m/z* 387), raffinose ($[M+HCOO]^-$ at *m/z* 549), and Glc6P ($[M-H]^-$ at *m/z* 259) obtained using (b) HILIC-ESI-QIT-MS and (d) PGC-LC-ESI-QIT-MS are shown. HPLC conditions: ZIC-HILIC column (150 mm x 2.1 mm i.d.), 0.5 µL injection, flow rate 200 µL/min; Hypercarb PGC column (100 mm x 4.6 mm i.d.), 20 µL injection, flow rate 600 µL/min.

Figure 6.7 Metabolite levels (Glc, Suc, raffinose, and Glc6P) determined in *Arabidopsis thaliana* Col-0 and *pgm1* chloroform/methanol leaf extracts using (A) HILIC-ESI-QIT-MS and (B) PGC-LC-ESI-QIT-MS. Plants were grown under a 16 h light/8 h dark photoperiod and harvested at developmental stage 6.0. Values are mean ± SD (n= 3 biological replicates, each containing leaves from three rosettes). Each biological replicate is the mean value of n=3 independent LC-MS measurements. FW, fresh weight.

Diagram 6.1 Structure of non-reducing RFOs showing carbohydrate fragmentation according to the nomenclature of Domon and Costello (Domon and Costello, 1988; Domon, 2008; personal communication).

Diagram 6.2 Mechanism proposed by the group of Lebrilla (Carroll et al., 1995) for the formation of the cross-ring A-type fragment ions at *m/z* 281 and 221 from the deprotonated anomeric oxygen, after the loss of the fructose moiety by the $[M-H]^-$ ion of the non-reducing

trisaccharide raffinose.

Diagram 6.3 Concerted mechanism proposed by Dallinga and Heerma (Dallinga and Heerma, 1991) for the formation of the cross-ring A-type fragment ions at *m/z* 281 and 221 from the $[M-H]^-$ ion of the non-reducing trisaccharide raffinose.

List of abbreviations

ADP	adenosine diphosphate
ADPGlc	adenosine diphosphate glucose
AGPase	adenosine diphosphate glucose pyrophosphorylase
ATP	adenosine triphosphate
CE	capillary electrophoresis
CID	collision induced dissociation
Col-0	*Arabidopsis thaliana* ecotype Columbia
cPGI	cytosolic phosphoglucose isomerase
cPGM	cytosolic phosphoglucomutase
Da	Dalton
DAW	days after withholding water
dc	direct current
DNA	deoxyribonucleic acid
DW	dry weight
EGTA	ethylene glycol-bis(2-aminoethylether)-*N,N,N',N'*-tetra-acetic acid
EI	electron ionisation
ESI	electrospray ionisation
FA	formic acid
Fru	fructose
Fru1,6BP	fructose-1,6-bisphosphate
Fru6P	fructose-6-phosphate
FTICR	Fourier transform ion cyclotron resonance
FW	fresh weight
FWHM	full-width half maximum
Gal	galactose
GC	gas chromatography
GCB	graphitic carbon black
Glc	glucose

Glc1P	glucose-1-phosphate
Glc6P	glucose-6-phosphate
HILIC	hydrophilic interaction chromatography
HPAEC	high performance anion-exchange liquid chromatography
HPLC	high performance liquid chromatography
i.d.	internal diameter
IRL	internal residue loss
LC	liquid chromatography
LOD	limit of detection
LOQ	limit of quantification
MALDI	matrix assisted laser desorption ionisation
MPa	mega Pascal
MS	mass spectrometry
MS/MS	tandem mass spectrometry
MS^n	multistage tandem mass spectrometry
m/z	mass-to-charge ratio
NMR	nuclear magnetic resonance
NP	normal-phase
oaTOF	orthogonal acceleration time-of-flight
PAD	pulsed amperometric detection
PAR	photosynthetically active radiation
PEP	phospho*enol*pyruvate
2PG	2-phosphoglycerate
3PG	3-phosphoglycerate
PGC	porous graphitic carbon
PGI	phosphoglucose isomerase
pPGI	plastidial phosphoglucose isomerase
PGM	phosphoglucomutase
pgm1	*Arabidopsis thaliana* 'starchless' mutant
pPGM	plastidial phosphoglucomutase
P_i	inorganic phosphate
PP_i	pyrophosphate

PPFD	photosynthetic photon flux density
PREG	polar retention effect on graphite
Pyr	pyruvate
QIT	quadrupole ion trap
QqQ	triple quadrupole
q-TOF	quadrupole time-of-flight
rf	radio frequency
RFOs	raffinose family oligosaccharides
RP	reversed-phase
RSD	relative standard deviation
RW	rewatering
RWC	relative water content
SBE	starch branching enzyme
SD	standard deviation
S/N	signal-to-noise ratio
SPE	solid phase extraction
SPP	sucrose-phosphate phosphatase
SPS	sucrose-phosphate synthase
SS	starch synthase
Suc	sucrose
Suc6P	sucrose-6-phosphate
TCA	trichloroacetic acid
TFA	trifluoroacetic acid
TMS	trimethylsilyl
TOF	time-of-flight
TPT	triose phosphate translocator
t_R	retention time
Tre	trehalose
Tre6P	trehalose-6-phosphate
TW	turgid weight
UDP	uridine diphosphate
UDPGlc	uridine diphosphate glucose

UGPase	uridine diphosphate glucose pyrophosphorylase
UTP	uridine triphosphate
UV	ultra violet
WD	water deficit
WT	wild-type
WW	well watered

Preface

"Passa uma borboleta por diante de mim
E pela primeira vez no Universo eu reparo
Que as borboletas não têm cor nem movimento,
Assim como as flores não têm perfume nem cor.
A cor é que tem cor nas asas da borboleta,
No movimento da borboleta o movimento é que se move,
O perfume é que tem perfume no perfume da flor.
A borboleta é apenas borboleta
E a flor é apenas flor."

Alberto Caeiro *In* O Guardador de Rebanhos (1914)

Com o João descobri a simplicidade do Alberto Caeiro e ao ler este poema quis logo partilhá-lo contigo. Para além desta tese existiu muito mais do que o trabalho científico. Existiu a tua vontade, o teu prazer pela descoberta, o teu rigor na verdade, o teu saber sentir as saudades... o teu gosto por querer acrescentar mais um ponto ao saber do Universo. E se a borboleta é apenas borboleta e a flor é apenas flor, a tua tese é mais do que uma tese.

Muitos Parabéns!

Patrícia António Brilhante

Acknowledgements

First a huge thank you to my supervisor Jane Thomas-Oates not only for letting me pursue a PhD in her group, but also for her continued encouragement, support and advice over the past three years. I would also like to thank Ian Graham's group, in CNAP, for all of their input, support and useful discussions throughout the duration of my PhD.

A huge thanks to all of the members of the JTO group, past and present, who have made it such a great place to work, in particular, Sarah, Emma, João, NJ, Dave, Sally, Barbara, Caroline, Ed, Si, Sally, Kriang, Siân, and Karl. I especially would like to thank Barbara who provided more help and support than she will ever know – 'Obrigada' Ba for being such a nice flat-mate and for your invaluable friendship! I would also like to thank *all* my friends back home (you know who you are!), in particular, the Portuguese 'Yorkies', João and Cristiana, for picking me up at the station three years ago, and for helping me making the first steps in York go so smoothly…

Financial support from the CHEMCELL Marie Curie Early Stage Research Training Fellowship of the European Community's Sixth Framework Programme, and the Treaty of Windsor is gratefully acknowledged. The EU funded project has given me the fantastic opportunity to work in close collaboration with people from all over the world: Argentina, Italy, Poland, and India. I would particularly like to mention my fellows Ines and P. Urban for all their support, and friendship!

Finally, I would like to thank all of my family, above all; Mummy Ana and Papá João for being remarkably good parents, big sister Patrícia, and João "brother-in-law" whose support and encouragement have kept me going through a challenging and sometimes difficult few years – Obrigada! Special 'beijões' go to Robinho, for his friendship, love and support over the last three years, especially the last two months when I was writing this thesis!!! Berlin, here we go!!!

Author's declaration

I hereby declare that the work described in this thesis is my own, except where otherwise acknowledged, and has not been submitted previously for a degree at this or any other university.

Carla Antonio

Chapter 1

Introduction

Chapter 1. Introduction

Plants have a unique metabolism which is due to a range of important features that characterise plant systems. Plants are photosynthetic, being able to utilise energy directly from the sun to convert carbon dioxide and water into carbohydrates and oxygen through a complex series of reactions. These reactions occur in plastids, specialised organelles only found in plants.

Plants are sessile, unable to relocate when faced with diverse environmental and seasonal stimuli, hence must be able to respond rapidly to guarantee survival. Moreover, plants must continuously defend themselves against abiotic stresses, such as extreme temperatures, fluctuations in the availability of light, water, and nutrients (Bray et al., 2000), and biotic stresses, such as herbivory, microbial and pathogen attack (Hammond-Kosak and Jones, 2000). In order to survive, plants have developed versatile multicellular tissues (e.g. roots, tubers, stems, seeds, leaves), which in turn encompass functionally diverse organelles (e.g. nucleus, plastids, vacuoles, mitochondria, etc.) and this inherent flexibility in plant metabolism allows them to adequately react and adapt to such adverse perturbations. Additionally, plants produce several ecologically useful compounds that function in their defense against predators and pathogens.

Plant metabolites can be classified as primary and secondary metabolites. Compounds which participate in ecological interactions between the plant and its environment are traditionally referred to as secondary metabolites. Typical examples of secondary metabolites are terpenoids, alkaloids, and phenolic compounds. Those metabolites involved in metabolic pathways essential for vital functions such as growth and development, are defined as primary metabolites. Typical examples of primary metabolites are carbohydrates, amino acids, organic acids, and fatty-acid derivatives (Croteau et al., 2000).

1.1 Plant carbohydrate metabolism

Carbohydrates are essential compounds found in all plants and are ubiquitous in nature as one of the most abundant class of biomolecules. They play a central role in plant growth and development, and are synthesised and stored in a number of different organelles; sucrose is synthesised in the cytosol whilst starch and its intermediates are synthesised and stored in plastids. Undoubtedly, glucose (monosaccharide), sucrose (disaccharide), cellulose (structural polysaccharide) and starch (storage polysaccharide), are the most widespread carbohydrates throughout the plant kingdom.

1.1.1 Monosaccharides

Monosaccharides are aldehyde or ketone derivatives of polyhydroxy alcohols of chemical formula $(CH_2O)_n$, where n>3, and most naturally occurring monosaccharides have the D-absolute configuration. If the carbonyl group is an aldehyde, the monosaccharide is an aldose (e.g. D-glucose) but if the carbonyl group is a ketone, the monosaccharide is a ketose (e.g. D-fructose).

Monosaccharides have both hydroxyl and aldehyde or ketone functions, and when in solution, they easily react to form reversible intramolecular cyclic hemiacetals or hemiketals, respectively (Figure 1.1). This cyclization reaction causes the former carbonyl carbon to be asymmetric; the resulting pair of diastereomers is known as anomers, and the hemiacetal or hemiketal carbon is referred to as the anomeric carbon. For the D-configuration using Haworth projections, in α anomers the hydroxyl group of the anomeric carbon is drawn pointing down; in β anomers, the hydroxyl group of the anomeric carbon is drawn pointing up. A sugar with a 6-membered ring is known as a pyranose, and a sugar with a 5-membered ring is known as a furanose. The pyranose form of D-glucose is known as D-glucopyranose (Figure 1.1a), and the furanose form of D-fructose is known as D-fructofuranose (Figure 1.1b); D-glucose and D-fructose may each assume

pyranose or furanose forms. In aqueous solution, carbohydrates exist almost exclusively in cyclic forms which are in equilibrium with each other; inter-conversion between α and β anomers and pyranose and furanose forms occurs via the open-chain form which possesses the active aldehyde or ketone.

(a)

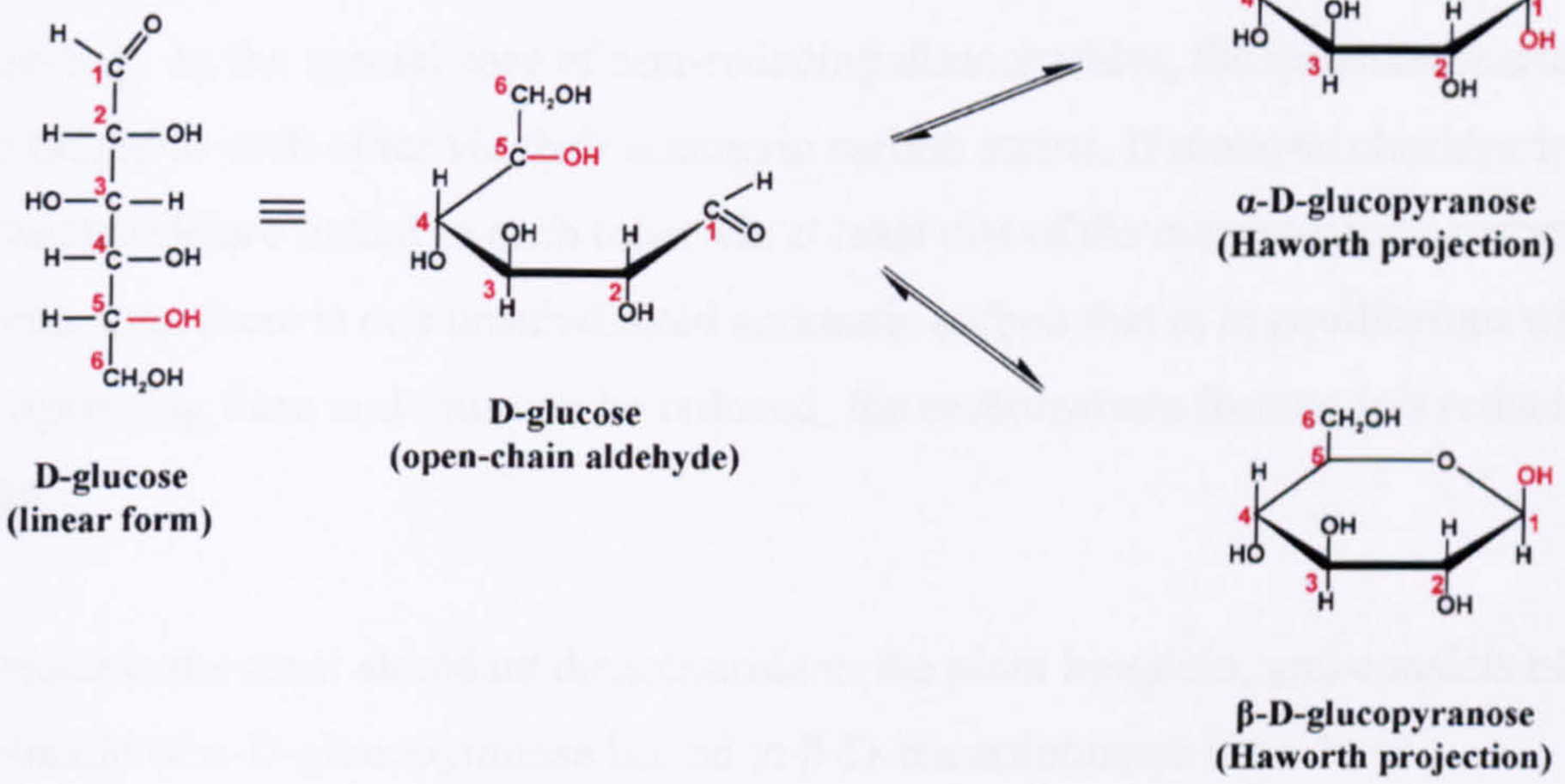

(b)

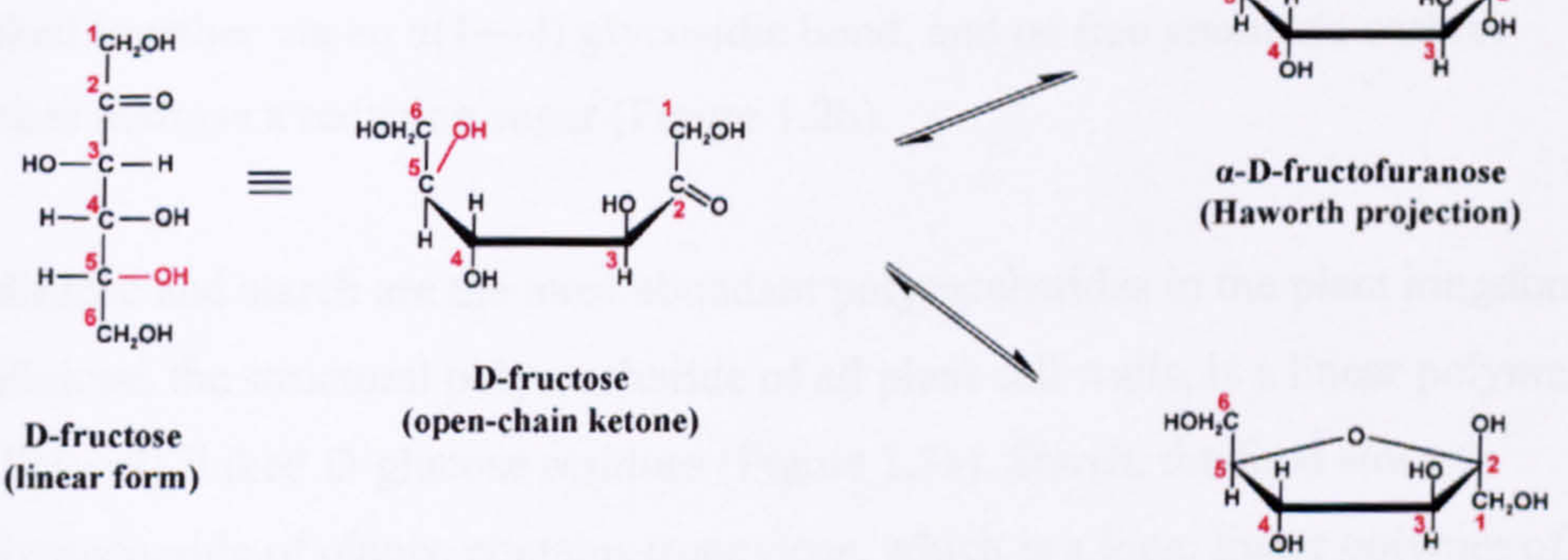

Figure 1.1 Reactions in aqueous solution of (a) linear form of D-glucose to yield the anomeric hemiacetals α-D-glucopyranose and β-D-glucopyranose, and (b) linear form of D-fructose to yield the anomeric hemiketals α-D-fructofuranose and β-D-fructofuranose. The cyclic forms are drawn as Haworth projections.

1.1.2 Oligosaccharides and polysaccharides

Oligosaccharides consist of monosaccharides in their pyranose or furanose forms, linked together by glycosidic bonds to form di-, tri-, tetra-, pentasaccharides, etc.

Carbohydrates can be classified as reducing or non-reducing. If the anomeric oxygen bears a non-hydrogen substituent, which prevents the ring form from being in equilibrium with its open chain form, then it is described as being non-reducing. In the special case of non-reducing disaccharides, the monosaccharides are linked to each other via their anomeric carbon atoms. If monosaccharides in a disaccharide are linked to each other via at least one of the non-anomeric carbon atoms, then there is one unsubstituted anomeric carbon that is in equilibrium with its open ring form and thus can be reduced; the carbohydrate formed is a reducing sugar.

Sucrose is the most abundant disaccharide in the plant kingdom, and consists of a molecule of α-D-glucopyranose linked to β-D-fructofuranose via a 1→2 glycosidic bond; C_1 and C_2 are the anomeric carbon atoms of their respective monosaccharides, thus sucrose is a non-reducing sugar (Figure 1.2a). Conversely, maltose is a disaccharide made up of two α-D-glucopyranose monosaccharides linked together via an α(1→4) glycosidic bond, and its free anomeric carbon makes maltose a reducing sugar (Figure 1.2b).

Cellulose and starch are the most abundant polysaccharides in the plant kingdom. Cellulose, the structural polysaccharide of all plant cell walls, is a linear polymer of β(1→4)-linked D-glucose residues (Figure 1.3a). Starch, the food storage polysaccharide of plants, contains α-amylose, which is a long, linear polymer of α(1→4)-linked D-glucose residues (Figure 1.3b), and amylopectin, which is branched through α(1→6)-linkages (Figure 1.3c). Both cellulose and starch have reducing structures.

(a)

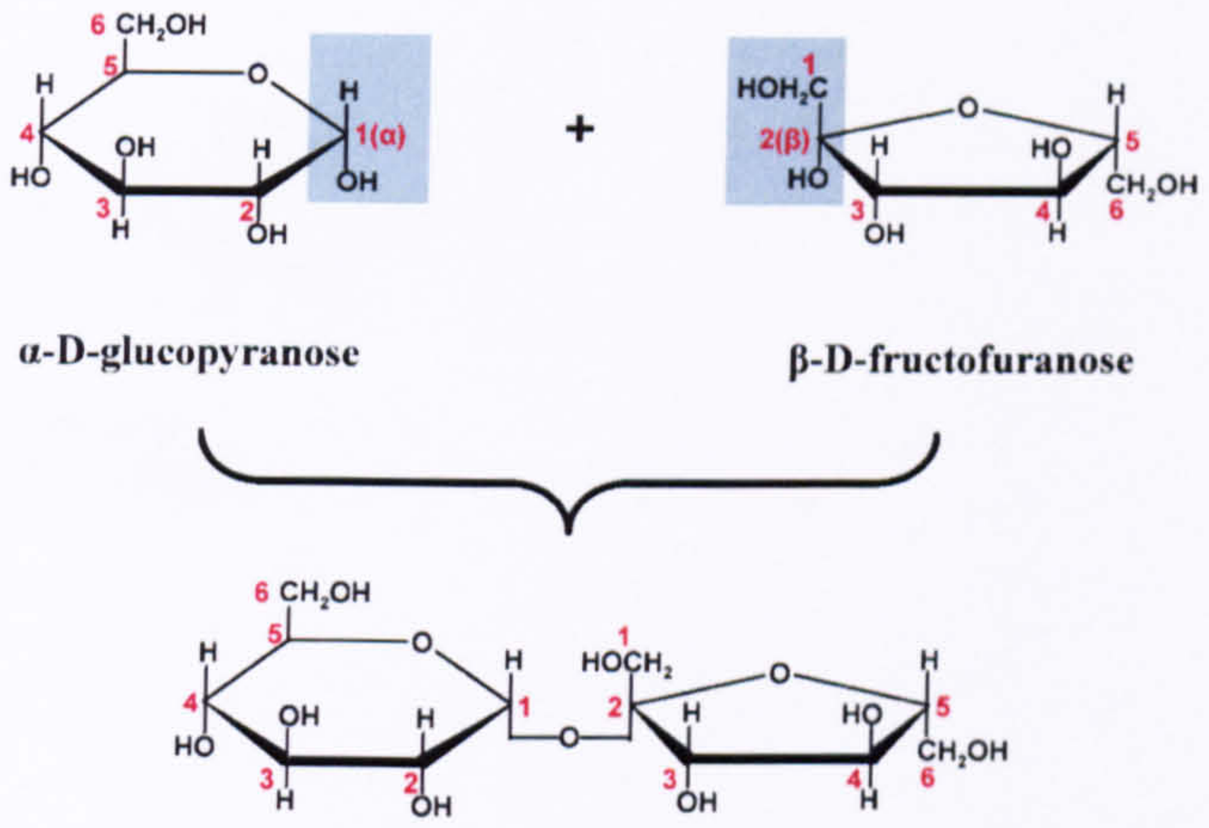

(b)

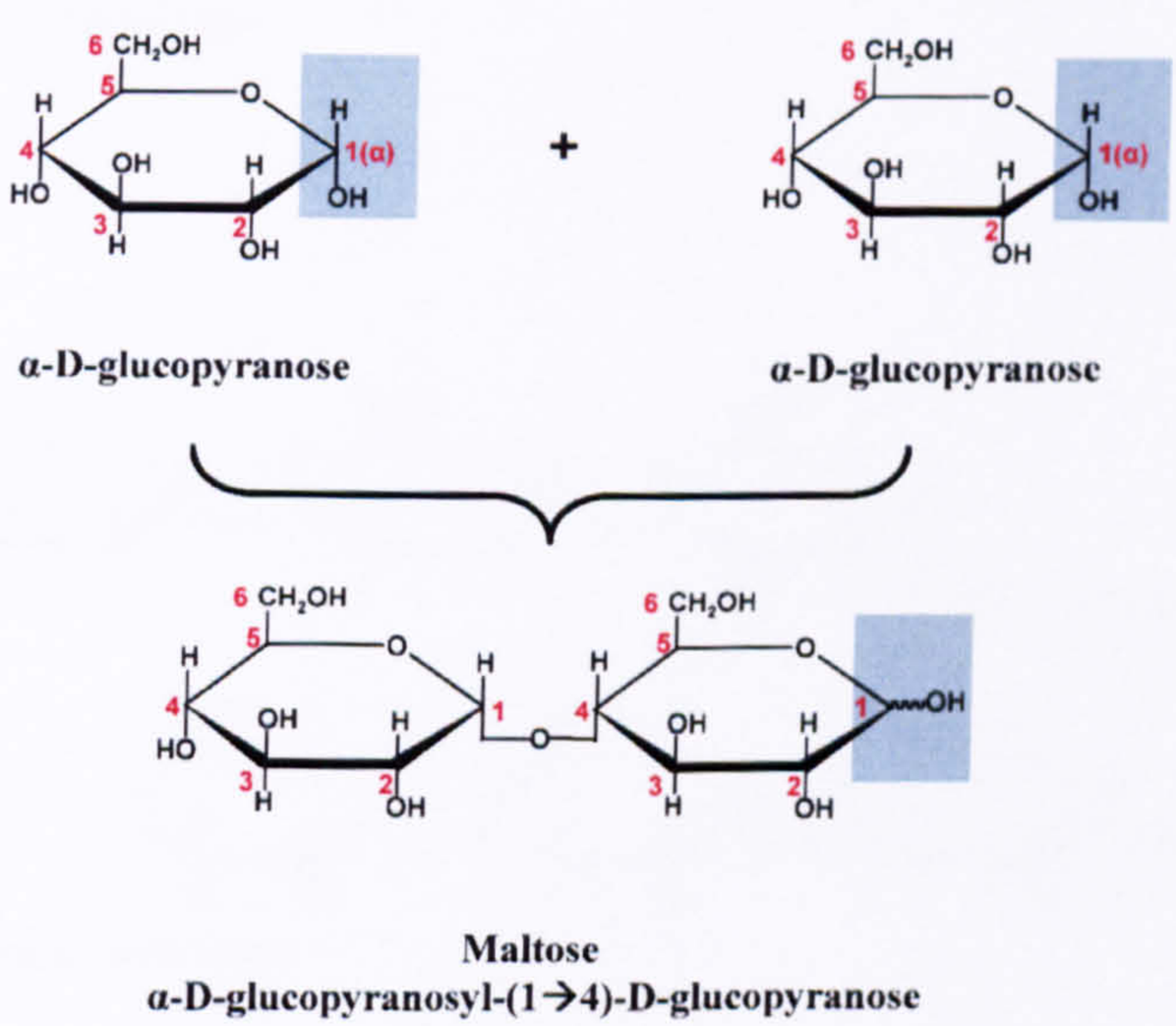

Figure 1.2 Structures and constituent monosaccharides of the (a) non-reducing disaccharide sucrose and (b) reducing disaccharide maltose, drawn as Haworth projections. Shaded areas highlight the anomeric carbons of the molecules.

(a)

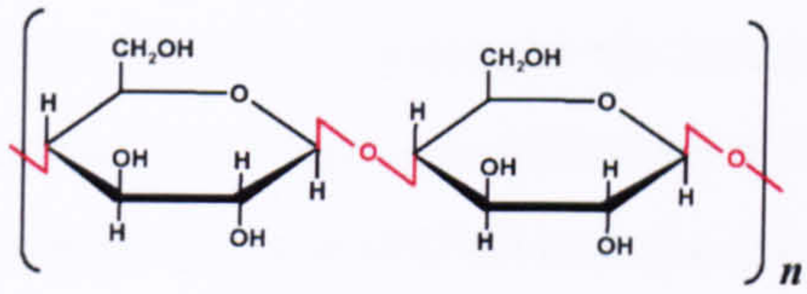

Cellulose
β(1→4)-linkages

(b)

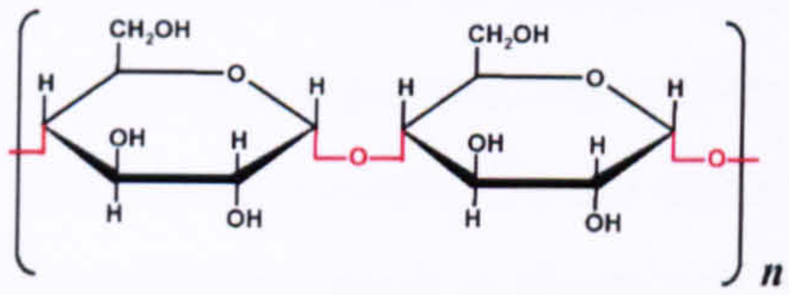

α-Amylose
α(1→4)-linkages

(c)

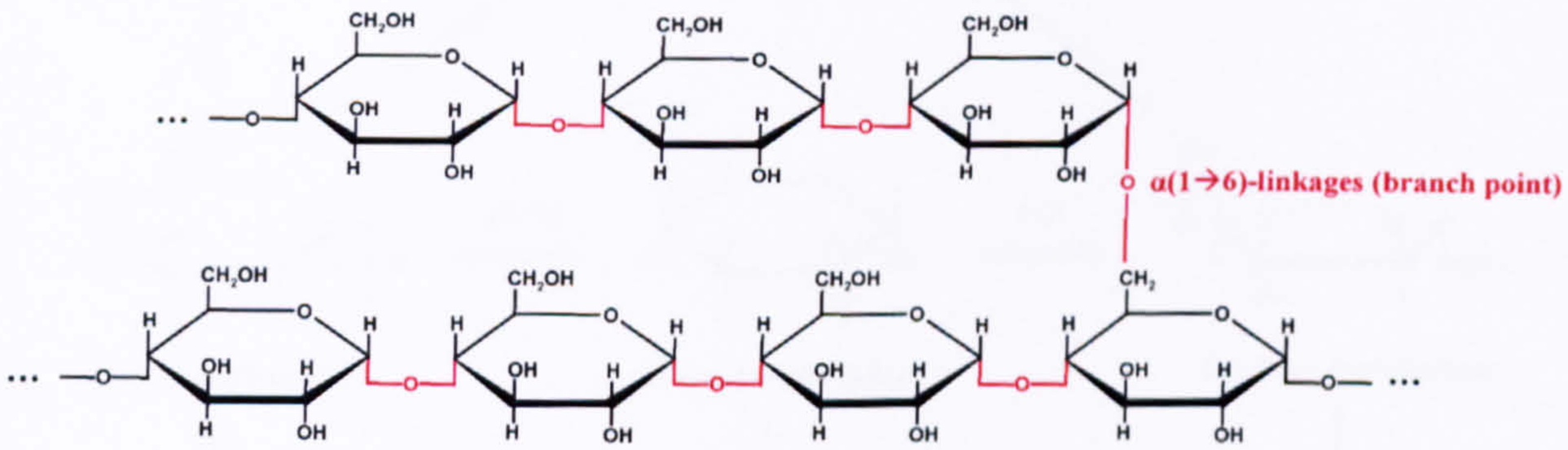

Amylopectin

Figure 1.3 (a) Cellulose, the structural polysaccharide of plant cell walls, is a linear polymer of β(1→4)-linked D-glucose residues. Starch, the food storage polysaccharide of plants, contains (b) α-amylose, a linear polymer of α(1→4)-linked D-glucose residues, and (c) amylopectin, which is branched through α(1→6)-linkages. *n* may be several thousand.

1.1.3 Hexose phosphate pool

Three hexose phosphates, namely glucose-1-phosphate, glucose-6-phosphate, and fructose-6-phosphate comprise the hexose phosphate pool. These three metabolic intermediates are kept in equilibrium by the action of the enzymes phosphoglucomutase (PGM) and phosphoglucose isomerase (PGI). PGM catalyses the interconversion of glucose-1-phosphate and glucose-6-phosphate, and PGI catalyses the interconversion of glucose-6-phosphate and fructose-6-phosphate. In plants, there are two PGM and PGI isoforms, one localised in the cytosol and the other in plastids. The cytosolic (cPGM and cPGI) and plastidial (pPGM and pPGI) isoforms are highly abundant in many plant tissues, including *Arabidopsis thaliana* leaves (Caspar et al., 1985; Periappuram et al., 2000) and *Solanum tuberosum* (potato) tubers (Fernie et al., 2001; Lytovchenko and Fernie, 2003). The hexose phosphate pool contributes intermediates to many biosynthetic metabolic pathways, such as glycolysis, the pentose phosphate pathway, cell wall formation, and starch and sucrose synthesis in plants (Figure 1.4).

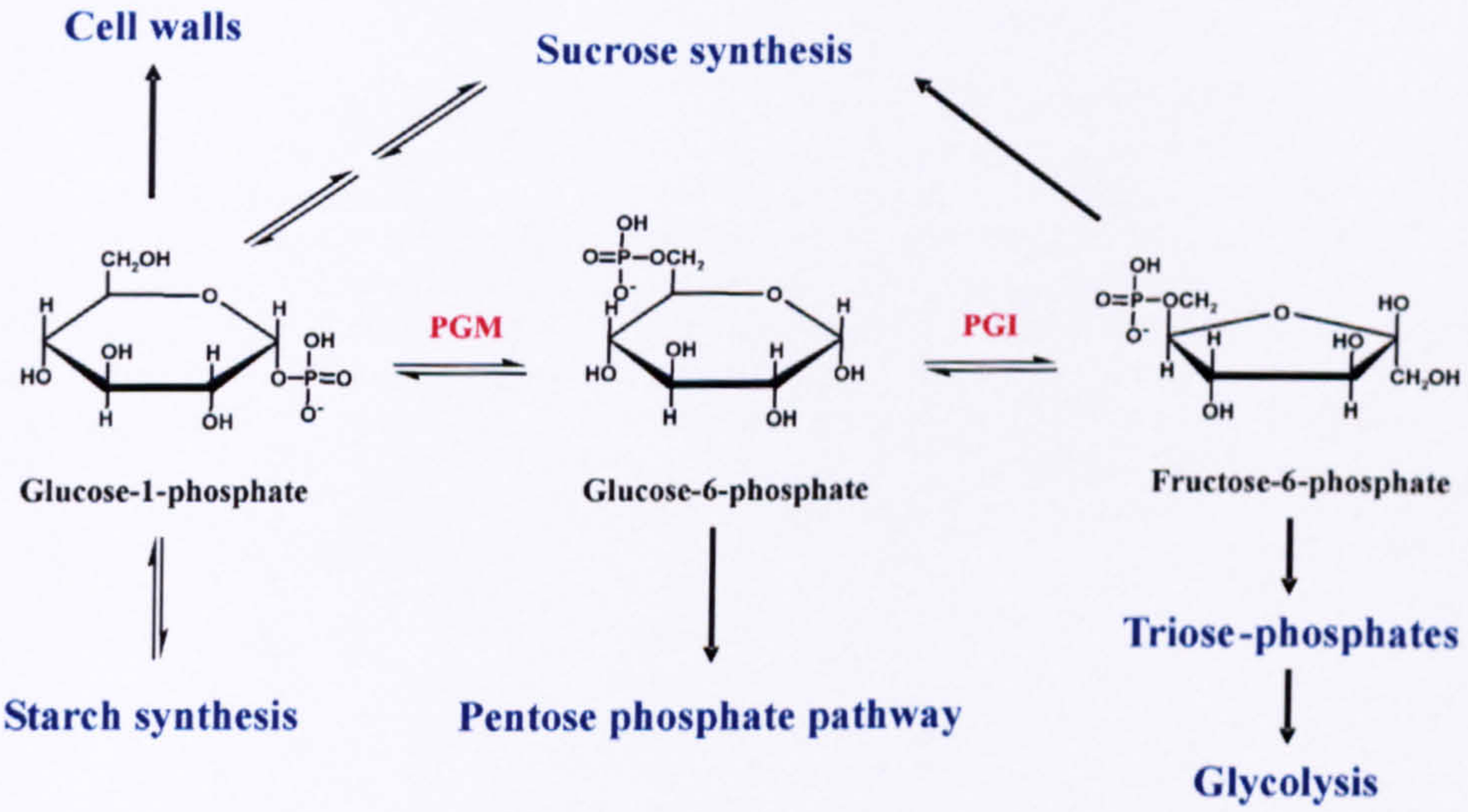

Figure 1.4 Metabolic intermediates of the hexose phosphate pool; they are interconverted by two enzymes: phosphoglucomutase and phosphoglucose isomerase. Hexose phosphates are primary metabolites and key intermediates to many biosynthetic metabolic pathways in plants.

1.1.4 Sucrose synthesis occurs in the cytosol

Sucrose is a major end product of photosynthesis in green leaves during the day. Carbon assimilated into the chloroplast via the Calvin Cycle is partitioned, with a fraction exported to the cytosol for sucrose synthesis and glycolysis, and a fraction retained in the chloroplast for starch synthesis (Figure 1.5). Both the cytosol and chloroplasts contain hexose phosphate pools. The cytosolic hexose phosphate pool is equilibrated by the action of the cytosolic isoforms of cPGI and cPGM. Glucose-1-phosphate (Glc1P) can be reversibly converted to uridine diphosphate glucose (UDPGlc) through the action of UDPGlc pyrophosphorylase (UGPase). The use of fructose-6-phosphate (Fru6P) as substrate results in the synthesis of sucrose-6-phosphate (Suc6P), which is catalysed by sucrose-phosphate synthase (SPS). Sucrose results from dephosphorylation via the action of sucrose-phosphate phosphatase (SPP) (Lunn and MacRae, 2003).

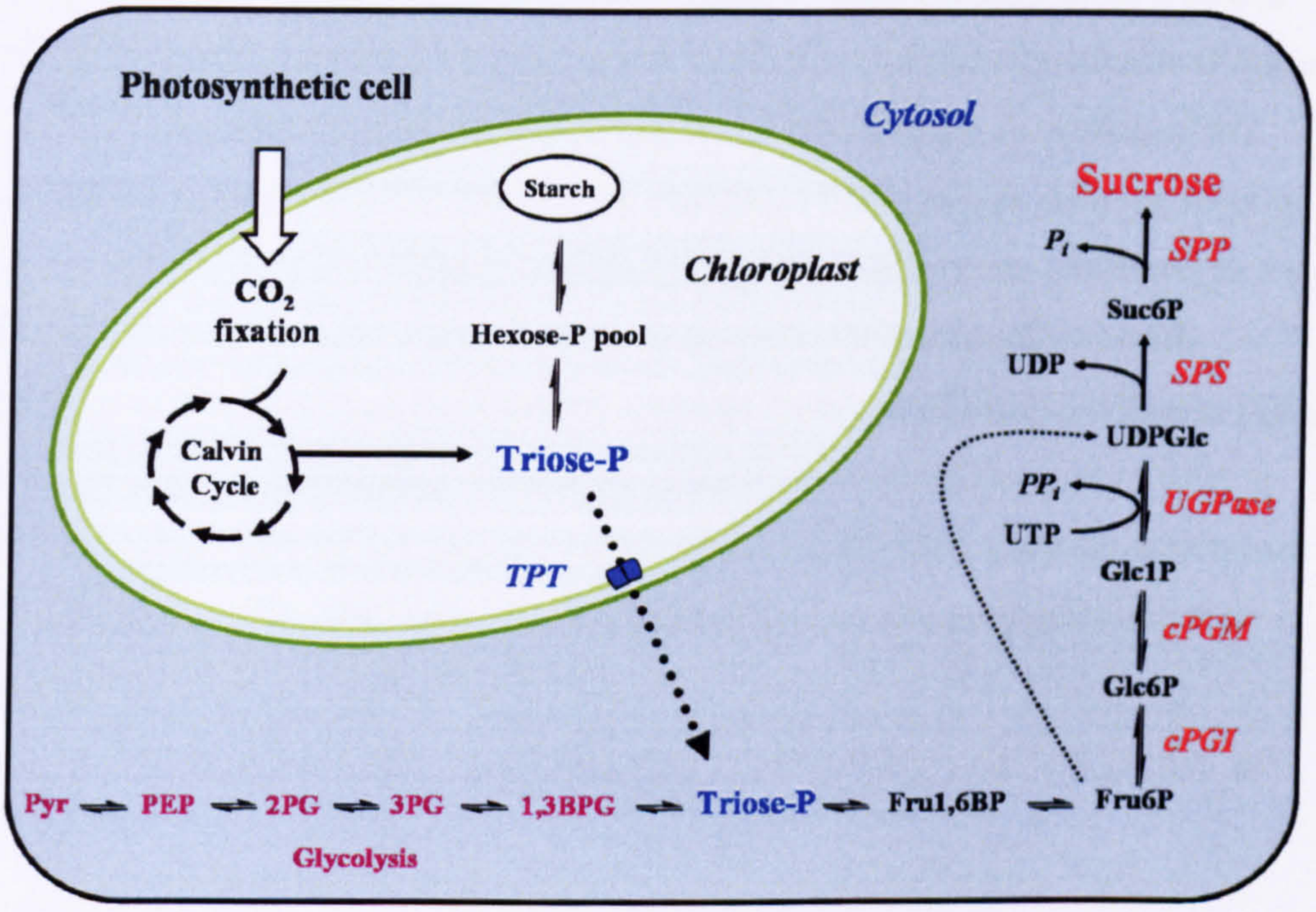

Figure 1.5 Sucrose biosynthetic pathway in cytosol. Carbon assimilated via the Calvin Cycle is partitioned with a fraction exported to the cytosol for sucrose synthesis and glycolysis, and a fraction retained in the chloroplast for starch synthesis. Hexose-P pool, hexose-phosphate pool; Triose-P, triose-phosphates; *TPT*, triose phosphate translocator; Fru1,6BP; fructose-1,6-bisphosphate; Fru6P, fructose-6-phosphate; Glc6P, glucose-6-phosphate; Glc1P, glucose-1-phosphate; UTP, uridine triphosphate; PP_i, pyrophosphate; P_i, inorganic phosphate; UDP, uridine diphosphate; UDPGlc, uridine diphosphate glucose; Suc6P, sucrose-6-phosphate; *cPGI*, cytosolic phosphoglucose isomerase; *cPGM*, cytosolic phosphoglucomutase; *UGPase*, UDP-glucose pyrophosphorylase; *SPS*, sucrose-phosphate synthase; *SPP*, sucrose-phosphate phosphatase; 1,3BPG; 1,3-bisphosphoglycerate; 3PG, 3-phosphoglycerate; 2PG, 2-phosphoglycerate; PEP, phospho*enol*pyruvate; Pyr, pyruvate.

1.1.5 Starch synthesis occurs in plastids

Starch, along with sucrose, is a primary product of photosynthesis in leaves. Starch is synthesised and stored in plastids (chloroplasts), the site of photosynthesis. Carbon assimilated into the chloroplast via the Calvin Cycle is partitioned with a fraction retained in the chloroplast for starch synthesis (Figure 1.6). The plastidial hexose phosphate pool is equilibrated by the action of the plastidial isoforms of pPGI and pPGM. Starch synthesis begins with the reaction catalysed by adenosine diphosphate glucose pyrophosphorylase (AGPase) to form the precursor adenosine diphosphate glucose (ADPGlc), and follows with polymerization reactions catalysed by multiple isoforms of starch synthases (SSs) to form amylose and multiple isoforms of starch-branching enzymes (SBEs) to form amylopectin; the combination of multiple SS and SBE isoforms determines the synthesis of starches with very different structures and properties (Zeeman et al., 2007).

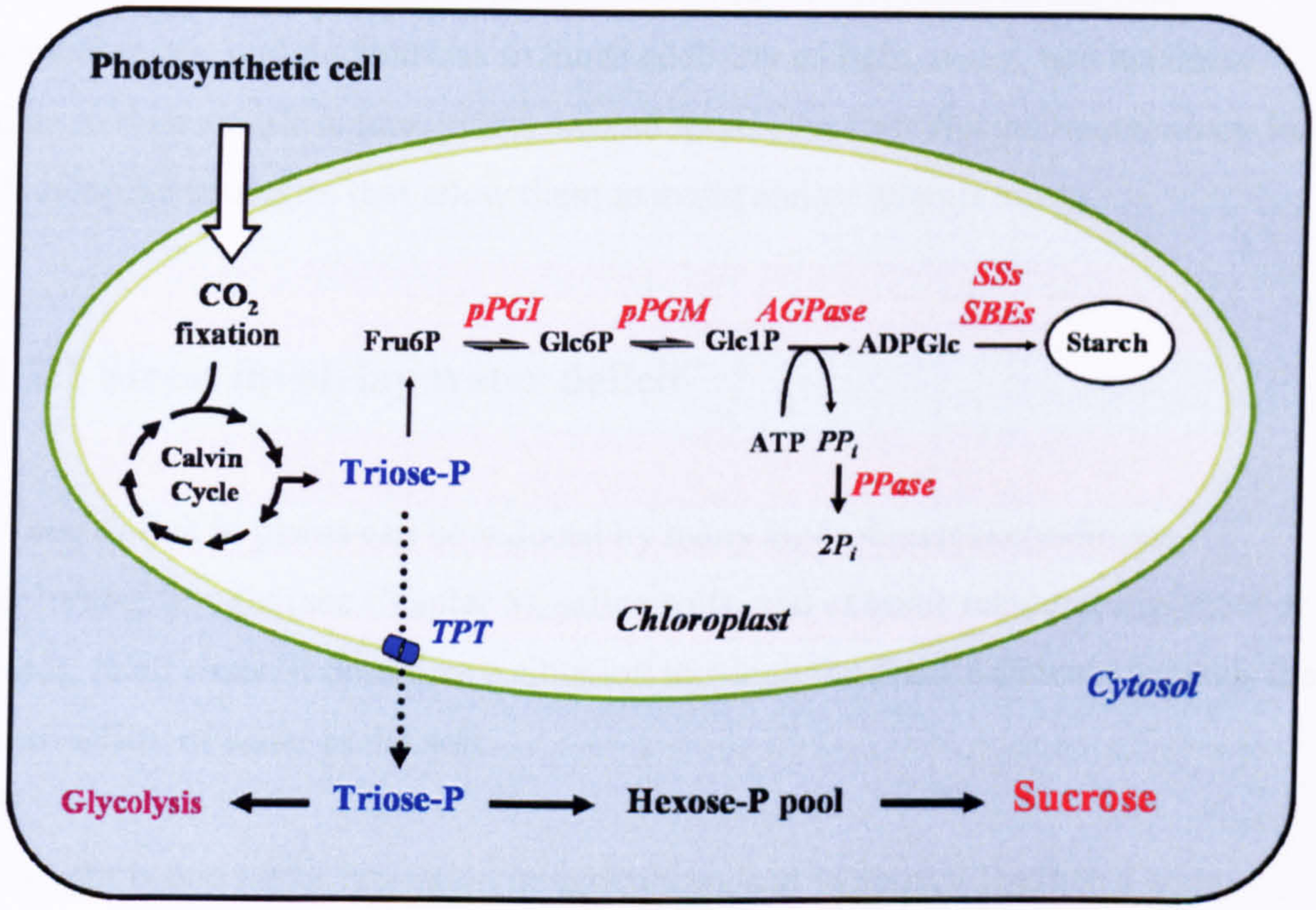

Figure 1.6 Starch biosynthetic pathway in the chloroplast. Carbon assimilated via the Calvin Cycle is partitioned with a fraction retained in the chloroplast for starch synthesis. Hexose-P pool, hexose-phosphate pool; Triose-P, triose-phosphates; *TPT*, triose phosphate translocator; Fru6P, fructose-6-phosphate; Glc6P, glucose-6-phosphate; Glc1P, glucose-1-phosphate; ATP, adenosine triphosphate; PP_i, pyrophosphate; P_i, inorganic phosphate; ADPGlc, adenosine diphosphate glucose; *pPGI*, plastidial phosphoglucose isomerase; *pPGM*, plastidial phosphoglucomutase; *AGPase*, ADP-glucose pyrophosphorylase; *SSs*, starch synthases; *SBEs*, starch-branching enzymes; *PPase*, pyrophosphatase.

1.2 Plant responses to abiotic stresses

Plants are constantly exposed to changing environmental and seasonal conditions that unfavourably affect their growth and development. Consequently, they must continuously defend themselves against abiotic stresses, such as extreme temperatures, and fluctuations in the availability of light, water, and nutrients. Due to their sessile nature, plants depend largely on their flexible metabolism for developing strategies that allow them to avoid and/or tolerate stress.

1.2.1 Stress involving water deficit

Water deficit in plants can be induced by many environmental conditions, including drought (see Chapter 5), saline soils, and extreme temperatures (heat or cold); in all cases, it describes a situation in which the plant's demand exceeds the availability of water in the soil.

Drought is one major limitation in agriculture, and its impact leads to a wide range of plant responses, from changes in gene expression and altered cellular metabolism to huge reductions in crop yield (Chaves and Oliveira, 2004). Thus, understanding the biochemical and physiological mechanisms underlying plant responses to this stress can lead to the development of drought-tolerant crop plants; plants that are able to maintain normal growth and development when the availability of water in the soil is limited. The development of drought-tolerant plants is a major goal of current biotechnological and genetic engineering programmes (Wang et al., 2003; Valliyodan and Nguyen, 2006; Seki et al., 2007), and metabolomics (see Section 1.4), coupled to proteomic and transcriptomic analysis, has recently become one major tool in agriculture for studying plant responses induced by drought (Alvarez et al., 2008; Havlová et al., 2008; Pinheiro et al., 2008).

1.2.2 Plant water status

Two physiological parameters describe the water status of plant cells and tissues: water potential and relative water content. The measurement of the water potential and relative water content is used to evaluate the effect of water deficit on the plant.

Water flows spontaneously down its potential gradient, from regions of higher water potential to regions of lower water potential, a process known as osmosis. Water potential is typically measured as the amount of pressure (mega Pascal units, MPa) needed to stop the movement of water. The plant's water potential (Ψ_w) is given by Equation 1.1:

$$\Psi_w = \Psi_s + \Psi_p \qquad \text{(Equation 1.1)}$$

where Ψ_s is the osmotic potential, determined by the number of solutes dissolved in water, and Ψ_p is the pressure (or turgor) potential, determined by the plant cell water pressure. As solute concentration increases, plant Ψ_w decreases. When water is subjected to negative pressure ($\Psi_p < 0$ MPa), Ψ_w decreases; when water is subjected to positive pressure ($\Psi_p > 0$ MPa), Ψ_w increases.

Plant roots can only extract water from the soil if the water potential in the root is lower than the water potential in the soil. Thus, the plant root must create a water potential gradient so that water flows from the surrounding soil to the root surface; once in the roots, water is transferred to the xylem, the vascular tissue involved in water and mineral transport from the roots to the leaves.

The water potential gradient is triggered by the rate of transpiration inside leaf cells. As water is lost by transpiration from the leaf, the osmotic potential increases (due to a high concentration of solutes, the products of photosynthesis), and leaf water potential is reduced; water available in the soil will flow into the leaf as a result of the developed water potential gradient.

The second physiological parameter used to assess the plant water status is the relative water content (RWC), expressed using Equation 1.2:

$$RWC = [(FW-DW) / (TW-DW)] \times 100 \qquad \text{(Equation 1.2)}$$

where FW is fresh weight, DW is dry weight, and TW is turgid weight. When water uptake by roots matches the water loss by leaves due to transpiration, the RWC typically ranges from 85% to 95%. This is discussed in more detail in Chapter 5.

1.2.3 Carbohydrates as compatible solutes in plants under water deficit

Compatible solutes, also known as compatible osmolytes, are highly soluble plant metabolites that do not inhibit overall cellular metabolism, even at high concentrations. Their accumulation in the plant cell helps to maintain cell volume by decreasing the water potential, which restricts the loss of water to the cell exterior. Hence, they are also referred to as osmoprotectants.

The accumulation of compatible solutes is thought to play an important role in increasing resistance to environmental stresses such as drought (Chaves and Oliveira, 2004; Seki et al., 2007). Common osmolytes include mainly soluble sugars such as glucose, sucrose, trehalose, raffinose family oligosaccharides (RFOs) (e.g. raffinose, stachyose, verbascose), sugar alcohols (e.g. mannitol, sorbitol), and amino acids (e.g. proline).

1.3 *Arabidopsis thaliana*: a model system for plant research

Arabidopsis thaliana (thale cress), a member of the Brassicaceae family, is a dicotyledonous flowering plant that has several advantages that make it an ideal model genetic organism. *A. thaliana* develops, reproduces and responds to stress and disease in a similar way to economically important crop plants; however its relatively small genome size (5 pairs of chromosomes), of around 120 megabases (Mb), makes it an ideal candidate for genomic analysis. For comparison, the genomes of the cereal crops rice*, maize and wheat are 420 Mb, 2500 Mb and 16000 Mb, respectively. Additionally, *A. thaliana*'s small size, short life cycle (about 6 weeks), and exceptional seed production (thousands of seeds per plant), make it an ideal organism for laboratory studies (Meinke et al., 1998).

In 1996, plant scientists established an international collaborative research consortium to sequence the complete genome of *A. thaliana* (The Arabidopsis Genome Initiative). The first results of this multinational effort were published in 1999 with the sequence of the first two chromosomes (Lin et al., 1999; Mayer et al., 1999). One year later, the sequence of the plant's remaining three chromosomes, and a comprehensive overview of the complete genome sequence were reported (Salanoubat et al., 2000; Tabata et al., 2000; The Arabidopsis Genome Initiative, 2000; Theologis et al., 2000).

Coupled with the completion of the genome sequence, many new *A. thaliana* gene knockouts (mutants), deficient in critical enzymes involved in plant metabolic pathways, have been isolated and used to assess gene function through identification and interpretation of the biochemical and phenotypic status during plant growth and development (Thorneycroft et al., 2001). The genetic resources available with the completion of the *A. thaliana* genome sequence, combined with other genetic and biochemical tools have, since then, helped plant researchers to

---

* The genome of the cereal crop rice (*Oryza sativa*) was fully sequenced in 2005 (International Rice Genome Sequencing Project, 2005).

make rapid advances in the understanding of fundamental aspects of plant metabolism (Fernie, 2003). For example, important discoveries in the pathway of leaf starch degradation at night became possible since the completion of the *A. thaliana* genome. *A. thaliana* 'starch excess' mutants, are highly deficient in starch degradation, and characterised by high levels of leaf starch after prolonged periods of darkness (Caspar et al., 1991). These mutants were isolated more than a decade ago; however, the mechanisms regulating leaf starch breakdown have always been difficult to elucidate because multiple isoforms of several different types of enzymes capable of degrading starch are present in the leaves (Smith et al., 2003; Zeeman et al., 2004). With the completion of the *A. thaliana* genome sequence, newly-isolated knockout mutants, deficient in starch degrading enzymes, became rapidly available leading to the discovery of several enzymes involved in leaf starch degradation (Critchley et al., 2001; Yu et al., 2001; Chia et al., 2004; Niittylä et al., 2004). This new evidence produced a radically new picture of the pathway of starch degradation in leaves (Lloyd et al., 2005; Smith et al., 2005; Zeeman et al., 2007).

1.4 Plant metabolomics

Metabolomics has emerged as a functional genomics methodology that together with the well established technologies for high-throughput DNA sequencing (genomics), gene expression profiling (transcriptomics), and protein profiling (proteomics), has the potential to accelerate our understanding of the complex molecular interactions in biological systems (Hall et al., 2002; Bino et al., 2004; Shauer and Fernie, 2006).

The ultimate goal of plant metabolomics is to provide comprehensive, non-biased characterisation of the total complex metabolite pool, 'the metabolome', typical of plant extracts under specific sets of conditions (Fiehn, 2002). The term 'metabolome' was first coined in 1998 by Oliver *et al.* and defined as the quantitative collection of all the low molecular weight compounds present in a

cell or organism in a particular physiological or developmental state (Oliver et al., 1998). Using metabolomics, a better understanding of the correlation between genes (genotype) and the biochemical composition of a plant tissue in response to its environment (phenotype) can be obtained (Figure 1.7), and this information can be further used to assess gene function (genotype); metabolomics is therefore an important tool for functional genomics (Fiehn, 2002; Bino et al., 2004; Shauer and Fernie, 2006). Additionally, and in contrast to transcriptomics and proteomics, metabolomics benefits from the advantage of not being dependent on the availability of organism-specific genome information for useful data analysis (Hall, 2006), and metabolomics-based methods can be applied to other biological systems without the need for re-optimising protocols (Kopka et al., 2004).

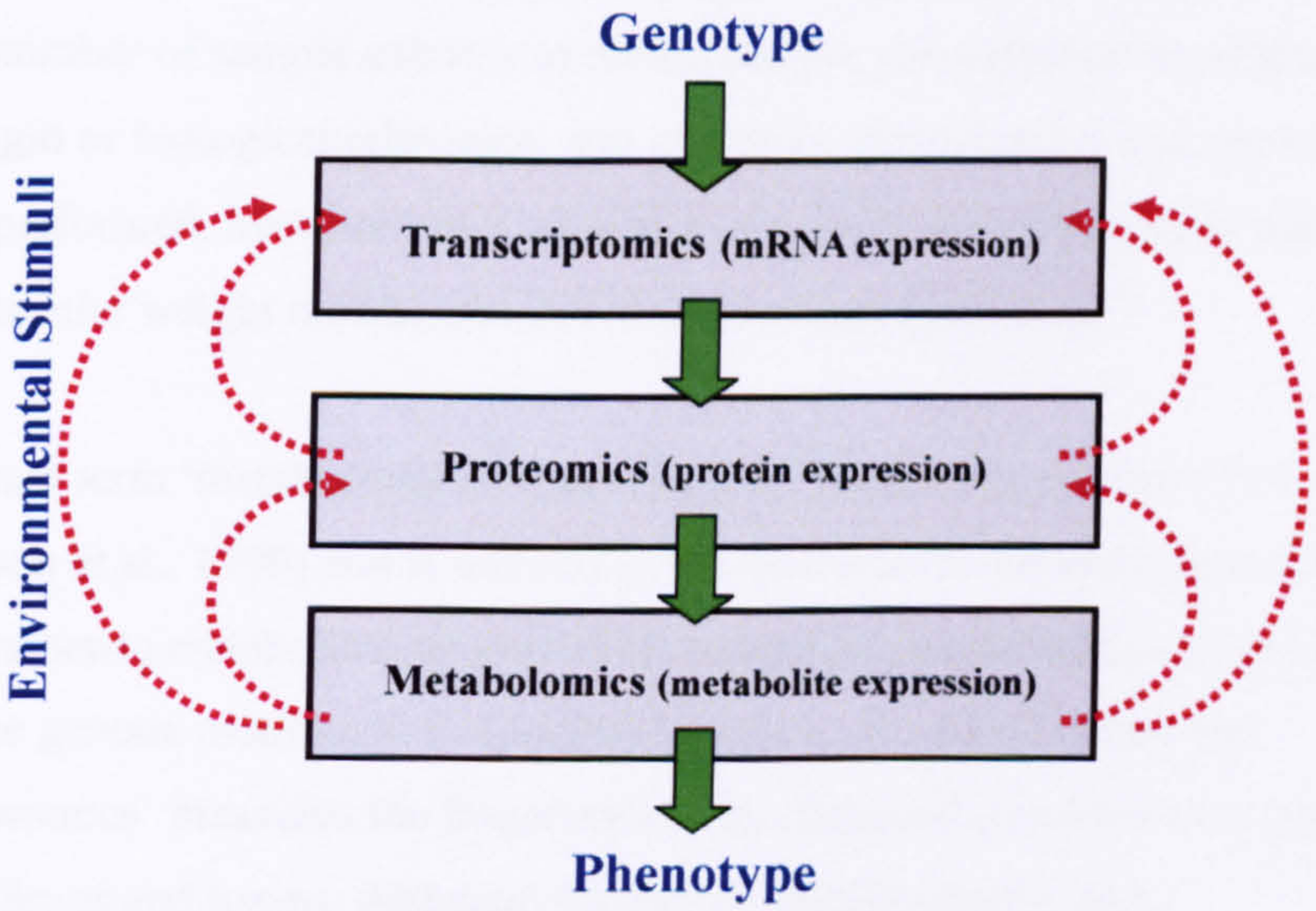

Figure 1.7 Diagram showing the connection between the 'omic' technologies. Metabolomics is *complementary* to transcriptomics and proteomics, but closer to the phenotype. The general flow of information is from genes (genotype) to transcripts to proteins to metabolites (phenotype).

Studies of the plant metabolome include the analysis of a wide range of chemical species, from ionic inorganic compounds to biochemically derived hydrophilic carbohydrates, organic and amino acids, and a range of hydrophobic lipid-related compounds. The plant metabolome also extends over a large dynamic range in

concentrations that can vary from femtomolar to milimolar (Fernie, 2003), and to add to this complexity, more than 200 000 different metabolites are estimated to exist in the plant kingdom (Fiehn, 2001; Fiehn, 2002).

The analysis of the metabolome can be divided into four metabolomics-based approaches: metabolite profiling, metabolite target analyses, metabolite fingerprinting, and metabolomics, as proposed by Fiehn (Fiehn, 2001; Fiehn, 2002). Metabolite profiling aims at identifying and quantitating a selected number of pre-defined metabolites, and often such profiles are focused on a class of compounds such as carbohydrates, lipids, amino acids or those associated with a specific pathway. Metabolite target analysis aims at the qualitative and quantitative analysis of a restricted number of metabolites that participate in a specific pathway. Metabolite fingerprinting aims at global and rapid screening of a large number of sample extracts to obtain sample classification according to their origin or biological relevance, and generally identification and quantification are not performed. Metabolomics aims at a comprehensive analysis in which *all* low molecular weight metabolites are identified and quantified.

The related term 'metabonomics' was coined by Nicholson et al. in 1999 (Nicholson et al., 1999) and is defined as the quantitative measurement of the multiparametric metabolic response of living systems to pathophysiological stimuli or genetic modification; Lindon (Lindon et al., 2003) stated that 'metabonomics' measures the fingerprint of biochemical perturbations caused by disease, drugs and toxins. Although the terms 'metabolomics' and 'metabonomics' are often used interchangeably, the main difference between them is that metabolomics looks at a 'snap-shot' of the metabolome, while metabonomics studies the dynamic changes within a system in response to a stimulus (Ryan and Robards, 2006).

Given these definitions, the work described in this thesis is considered to be a plant 'metabolomics target analysis' study, as it is limited exclusively to the qualitative and quantitative analysis of a restricted number of metabolites (i.e.

carbohydrates and some glycolytic intermediates). As a result, only a very small fraction of the metabolome is the focus of analysis, and signals from all other components are largely ignored, even though the data are recorded and available for further mining at a later date (see Chapter 6).

1.5 Analytical technologies used in plant metabolomics

Currently, there is no single analytical technology that is comprehensive, selective and sensitive enough to give a complete profile of the *total* plant metabolite pool (*true* metabolomics), and a platform of complementary analytical technologies must therefore be employed (Hall et al., 2002; Fernie, 2003; Sumner et al., 2003; Bino et al., 2004; Goodacre et al., 2004; Brown et al., 2005a; Dunn and Ellis, 2005; Hall, 2006).

The analytical technologies most widely used in plant metabolomics are based on hyphenated systems which combine the high sensitivity and specificity provided by mass spectrometry (MS) with robust on-line chromatographic separations, typically gas chromatography (GC) and liquid chromatography (LC). Moreover, the low limits of detection, and the ability to perform tandem MS or multistage MS^n experiments, which provide further structural information, has made MS a popular choice.

1.5.1 Quenching and extraction of plant metabolites

Rapid inactivation of metabolic processes during harvesting of plant material prior to extraction is of utmost importance, especially when measuring intermediary metabolites with high turnover rates (e.g. glycolytic intermediates and sugar phosphates) (de Koning and van Dam, 1992; Stitt and Fernie, 2003; Dunn and Ellis, 2005).

The quenching method most widely used when sampling plant material is by rapidly freezing it at extremely low temperature using liquid nitrogen, and subsequent storage at -80 °C prior to extraction and analysis (Weiner et al., 1987; Jelitto et al., 1992; Fiehn et al., 2000b; Roessner et al., 2000; Fiehn, 2002; Ward et al., 2003; Gullberg et al., 2004; Kopka et al., 2004; Desbrosses et al., 2005). Frozen fresh tissue must then be finely homogenised to allow full extraction of the metabolites. Tissue homogenisation can be performed simply by grinding using a pestle and mortar filled with liquid nitrogen; the most important factor during homogenisation is that the plant material must not thaw (Fiehn, 2002).

No single extraction protocol will cover the complete plant metabolome, and a wide range of extraction protocols can be used. Polar metabolites can be extracted using polar organic solvents such as methanol and methanol-water mixtures which are directly added to fresh frozen tissues at low temperatures. Alternatively, non-polar solvents such as chloroform are used to extract lipophilic metabolites (Fiehn, 2002; Dunn and Ellis, 2005). Combinations of chloroform:methanol:water are also used to separate a methanol:water phase (hydrophilic metabolites) from a chloroform phase (lipophilic metabolites) (Gullberg et al., 2004; Lunn et al., 2006). Most importantly, the three main requirements when performing any extraction protocol are: (i) metabolites are completely extracted (ii) no changes in the metabolites levels occur during extraction, and (iii) metabolites are not destroyed (de Koning and van Dam, 1992).

1.5.2 GC-MS

To date, GC-MS is the most well-established analytical technology used in post-genomic plant metabolomics studies (Fernie, 2003; Fiehn, 2006; Kopka, 2006b). This popularity can be attributed mostly to the pioneering work of Roessner and co-workers at the Max Planck Institute of Plant Molecular Physiology who first approached the use of GC-MS metabolite profiling for the comprehensive, simultaneous quantitative analysis of 150 metabolites, ranging from sugars, to

sugar alcohols, amino acids, and organic acids in potato tuber tissues (*Solanum tuberosum*) (Roessner et al., 2000; Roessner et al., 2001a; Roessner et al., 2001b). Following a similar non-biased approach, Fiehn and co-workers found 326 metabolites in a single *A. thaliana* leaf extract (Fiehn et al., 2000a). Other comprehensive GC-MS methods have been developed and applied to other plant tissues, allowing the identification in a single extract of over 200 metabolites in tomato (*Lycopersicon esculentum*) fruit and leaf tissues (Roessner-Tunali et al., 2003), and the identification of 87 metabolites in several *Lotus japonicus* organs (Desbrosses et al., 2005).

One major limitation of GC-MS is that it can only be used for the analysis of volatile and thermally stable metabolites or metabolites that can be chemically modified to produce volatile derivatives; thus, nonvolatile polar metabolites (mainly primary metabolites such as carbohydrates, amino acids, and organic acids), require derivatisation prior to GC-MS analysis. In addition, GC-MS is not suitable for the analysis of larger oligosaccharides due to their limited volatility, or thermolabile di- and triphosphates (Weckwerth, 2003; Kopka et al., 2004).

Methoxyamination followed by silylation is the standard derivatisation procedure used in routine GC-MS plant metabolomics studies (Fiehn et al., 2000b; Gullberg et al., 2004; Fiehn, 2006; Kopka, 2006b; Kopka, 2006a; Moritz and Johansson, 2008). Essentially, this two-step derivatisation process involves conversion of aldehyde or keto groups into oximes using methoxylamine, followed by conversion of functional groups such as –OH, -COOH, -NH, -SH into trimethylsilyl (TMS) ethers, TMS-esters, TMS-amines or TMS-sulfides, respectively. The methoxyamination step inhibits cyclisation of reducing carbohydrates, and hence, helps to reduce the number of chromatographic peaks due to anomeric α- and β-pyranose and furanose structures (Figure 1.8) (Harvey and Horning, 1973); after silylation, the introduced C=N bond generally forms only *E*- and *Z*-isomers which are chromatographically resolvable by GC-MS (Fiehn et al., 2000b; Kopka, 2006a).

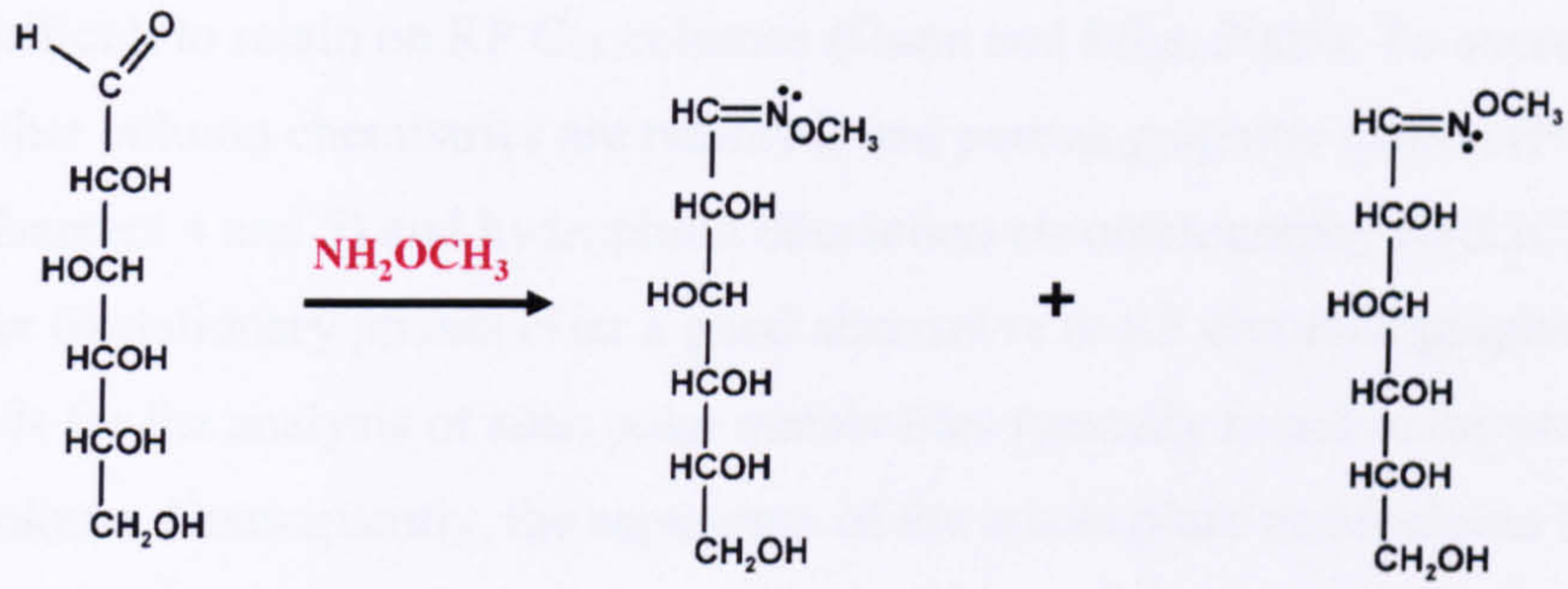

D-glucose **O-methyloximes**

Figure 1.8 Diagram showing the conversion of an aldehyde group into an oxime using methoxylamine. Oximes give two products corresponding to the *E*- and *Z*- isomers, which are resolved by GC-MS.

The main disadvantages of derivatisation protocols derive from the time and sample losses associated with the additional steps in sample handling and the fact that more than one derivatisation product may be formed (Kopka, 2006a).

1.5.3 LC-MS

LC-MS is the most important complementary technology to GC-MS, and methods are becoming very popular in current plant metabolomics studies. They offer the advantage over GC-MS methods of being able to analyse thermolabile, polar metabolites, and high-molecular weight compounds without the need for derivatisation.

The most important factor when developing an LC-MS method is the selection of column chemistry. The majority of LC-MS applications use reversed-phase (RP) C_{18} chromatography. In RP separations, compounds are separated based on their hydrophobicity, with the most hydrophobic compounds eluting last, using a predominantly aqueous based mobile phase. However, it is well known that

highly polar metabolites such as carbohydrates and glycolytic intermediates are very difficult to retain on RP C_{18} columns (Dunn and Ellis, 2005). To overcome this, other column chemistries are required, and porous graphitic carbon (PGC) (see Chapters 4 and 5) and hydrophilic interaction chromatography (HILIC) (see Chapter 6) stationary phases offer a good alternative to RP chromatographic methods for the analysis of such polar metabolites typically found in the plant metabolome. Consequently, the separation of the whole plant metabolome is not achievable using a single chromatographic LC-MS system, and LC-MS-based methods have been mainly used to profile specific compound classes of the plant metabolome, e.g. flavonoids (Sumner et al., 1996) and saponins (Huhman and Sumner, 2002) from leguminous plant extracts, carbohydrates from *Triticum aestivum* stem extracts (Robinson et al., 2007). The coverage of a broader range of the plant metabolome using LC-MS was first approached by Tolstikov and Fiehn who detected a wide range of highly polar metabolites, including raffinose family oligosaccharides (RFOs) and other larger oligosaccharides, amino acids, amino sugars, and sugar nucleotides from *Cucurbita maxima* phloem tissues (Tolstikov and Fiehn, 2002) using a HILIC-type column and electrospray (ESI) MS.

One major problem associated with LC-ESI-MS methods is their susceptibility to ion suppression due to interfering compounds present in the plant matrix (Choi et al., 2001; Matuszewski et al., 2003). The presence of multiple metabolites influences the ionisation and the transfer of analytes from liquid to the gas phase, potentially compromising the accurate quantification of metabolites (Wilson and Brinkman, 2003). A good chromatographic separation prior to ESI-MS is essential to reduce the impact of matrix-induced effects; matrix effects can be tested by performing recovery experiments using plant extracts spiked with authentic standards (Fernie et al., 2004).

1.5.4 CE-MS

Capillary electrophoresis (CE) is an alternative separation technology with potential for metabolome analysis mainly due to its fast analysis and high-efficiency separations, and when combined with MS, it provides the high selectivity and sensitivity required in plant metabolome analysis (Ramautar et al., 2006; Monton and Soga, 2007).

Efforts have been made by Soga and co-workers to demonstrate the power of CE-MS for metabolome analysis using less complex bacterial extracts (Soga et al., 2002), and even leaf extracts of the rice plant *Oryza sativa* (Sato et al., 2004); however, its application to routine plant metabolomics studies is still underused. This is probably related to the fact that the CE-MS interface with electrospray ionisation is more complicated than with LC-MS due to the very low flow of the effluent from the capillary, the need to maintain electrical contact for electrophoretic current, and the need for MS compatible background electrolytes used in the running buffer. All these factors contribute to a poor reproducibility of this analytical technology.

1.5.5 NMR

Nuclear magnetic resonance (NMR) spectroscopy has also been applied to plant metabolomics studies (Ott et al., 2003; Ward et al., 2003; Moing et al., 2004). NMR has several advantages over other analytical platforms currently in use. It does not require prior separation or ionisation of metabolites, is not compound class selective, the signals obtained are highly reproducible, and it is a non-destructive technique, making it easy to combine NMR with other complementary analytical technologies such as GC-MS or LC-MS (Ratcliffe and Shachar-Hill, 2001; Ward and Beale, 2006). However, due to its poor sensitivity and poor dynamic range relative to MS, metabolite profiling of plant samples using NMR can only detect and quantify the most abundant metabolites (Sumner et al., 2003;

Krishnan et al., 2005). In contrast, NMR fingerprinting coupled to multivariate data analysis has become a standard analytical platform in current highthroughput plant metabolomics studies (Krishnan et al., 2005; Ward and Beale, 2006). Its ability to rapidly screen a large number of plant extracts and to discriminate between groups of similar samples has made NMR fingerprinting an appealing analytical technology for defining metabolic phenotypes (e.g. wild-type *versus* knock-out mutant); it is not necessary to assign the NMR signals (Ward et al., 2003; Ratcliffe and Shachar-Hill, 2005). Although less sensitive than MS, NMR constitutes a powerful complementary analytical technology for plant metabolomics studies.

1.5.6 Direct infusion-MS

Fourier transform ion cyclotron resonance-MS (FTICR-MS) is capable of performing accurate mass measurements that allow for empirical formulae determination, and therefore non-isomeric metabolites with the same nominal mass can be identified on the basis of their accurate mass alone (Brown et al., 2005b; Ohta et al., 2007). Direct infusion analyses using FTICR-MS have been adopted for high-throughput metabolome analysis without the prior use of separation. In plant metabolomics studies, the first application of direct infusion FTICR-MS was reported by Aharoni and co-workers for a highthroughput metabolomics study of ripening strawberries and transgenic tobacco flowers (Aharoni et al., 2002). The studies were carried out by comparing the direct infusion FTICR-MS data from strawberry extracts obtained over time during ripening. The data were analysed using multivariate statistical approaches, which highlighted those ions that changed in intensity during ripening. Studies on the *Arabidopsis thaliana* metabolome followed (Hirai et al., 2005; Tohge et al., 2005; Oikawa et al., 2006). These few applications have demonstrated the power of FTICR-MS as a general tool for high-throughput plant metabolomic studies (Hall et al., 2002; Fernie, 2003; Stitt and Fernie, 2003).

1.6 Data analysis

Like proteomics and transcriptomics studies, a typical plant metabolomics experiment generates large multivariate data sets (information) which in turn need to be converted into knowledge (Brown et al., 2005a). Researchers have thus started exploring the use of multivariate statistical methods to get the most out of the information obtained and to aid in the interpretation of the data. These methods can be either unsupervised, where there is no pre-classification of the data, or supervised, where each variable (metabolite) is associated to an already known class (Sumner et al., 2003; Goodacre et al., 2004; Mehrotra and Mendes, 2006; Trygg et al., 2006). The most commonly used unsupervised methods include principal component analysis (PCA) and hierarchical cluster analysis (HCA). PCA is a descriptive technique that gives an overview of all samples and is used to visualize trends and outliers in the data. HCA organises information into a data set forming groups of samples (clusters) for which the degree of association is strong between data in the same cluster and weak between data in different clusters (e.g. wild-type and mutant); it is often applied to the data after transformation with PCA. Supervised methods include partial least squares discriminant analysis (PLS-DA). This is a discriminative method used instead of PCA when additional knowledge about each sample exists.

1.7 High performance liquid chromatography

High performance liquid chromatography (HPLC) is a separation technique by which analytes in a solution are separated in time according to their partitioning behaviour (e.g. hydrophobicity/hydrophilicity) between a stationary phase and a mobile phase. The partitioning principle can be described as an equilibrium (Equation 1.3):

$$A\ (\text{mobile phase}) \rightleftharpoons A\ (\text{stationary phase}) \qquad \text{(Equation 1.3)}$$

with the partition coefficient (k_D) defined as (Equation 1.4):

$$k_D = [A\ (\text{stationary phase})] / [A\ (\text{mobile phase})] \qquad \text{(Equation 1.4)}$$

A solution containing a mixture of compounds to be separated is injected into a flow of liquid (mobile phase) that is pumped through a column containing a solid medium (stationary phase). When the sample contacts with the stationary phase, the analytes are partitioned between the stationary and mobile phases. The analytes with a higher k_D spend longer in the stationary phase than those with a lower k_D; consequently, they take longer to pass through the column. The analytes elute sequentially from the column and pass through a detection system. The result is separation of the analytes and a chromatogram that shows peaks corresponding to the elution of each analyte (Figure 1.9).

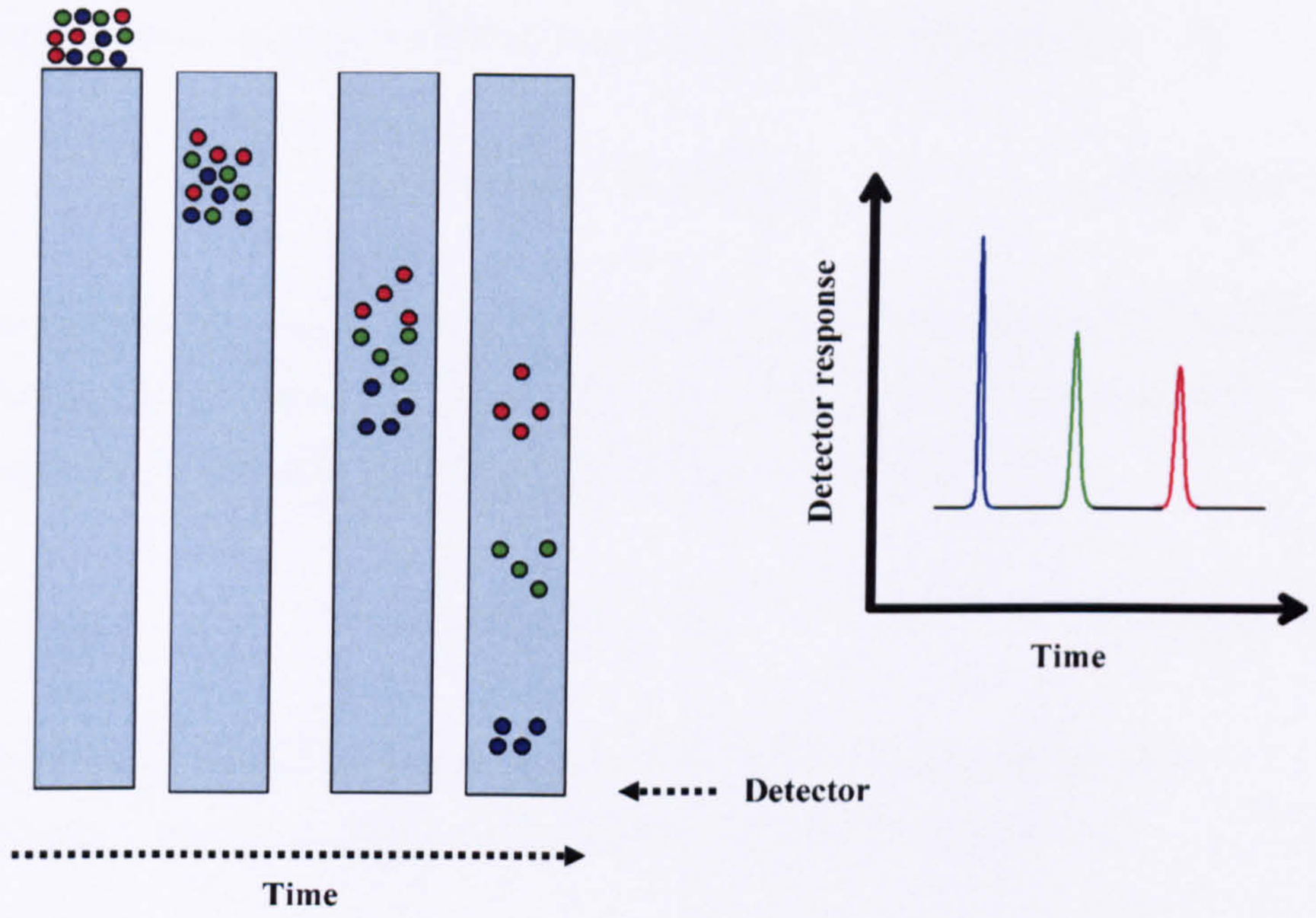

Figure 1.9 Diagram illustrating the separation in time of different analytes migrating through a column. Each analyte migrates at different rates, each having different partition coefficients (k_D). The analytes elute sequentially from the column and pass through a detection system. The resulting separation of the analytes generates a chromatogram.

The capacity factor of a compound (k'_A) can be used to describe the migration rate of a compound on a column (Equation 1.5):

$$k'_A = (t_{RA} - t_M) / t_M \qquad \text{(Equation 1.5)}$$

where (t_{RA}) is the retention time of compound A and (t_M) is the time that the mobile phase takes to pass through the column, often referred to as dead volume (unretained compound).

The capacity factors for two compounds (A and B) can be used to describe the selectivity factor (α), a measure of peak separation (Equation 1.6):

$$\alpha = k'_B / k'_A \qquad \text{(Equation 1.6)}$$

Resolution, R, defines the ability of a column to separate two peaks A and B, with retention times t_{RA}, t_{RB}, and baseline peak widths W_A, W_B (Equation 1.7):

$$R= 2(t_{RB}-t_{RA}) / (W_A + W_B) \qquad \text{(Equation 1.7)}$$

The column efficiency can be calculated using the baseline peak width (W) of the eluting analyte in the resulting chromatogram, and retention time (t_R), and is measured by the number of theoretical plates, N (Equation 1.8):

$$N= 16 (t_R / W)^2 \qquad \text{(Equation 1.8)}$$

Plate height (H) is another term that can be used to measure the column efficiency; the two terms are related by the equation (Equation 1.9):

$$H= L / N \qquad \text{(Equation 1.9)}$$

where L is the length of the column.

Column efficiency can be compromised by band broadening. To better understand the meaning of plate height, the separation of a compound can be described as a series of consecutive, independent equilibration events occurring at adjacent points (or plates) along the column. Each plate is the distance required for an 'equilibration event' to occur; therefore the greater the number of plates, the more efficient the column. Plate height (H) is dependent on the linear flow rate (u, cms^{-1}) of the mobile phase, and can be described using the van Deemter equation (Equation 1.10):

$$H = A + B/u + Cu \qquad \text{(Equation 1.10)}$$

where 'A' describes multiple-path effects (eddy diffusion), 'B' is the longitudinal diffusion and 'C' is the mass transport; these terms can be described in more detail as follows:

(A) Eddy diffusion results from the different paths that molecules of the same analyte can take through a column. Each molecule of a compound may start at the same position, but take paths of different lengths through the column as the mobile phase flows around the particles, causing band broadening. This phenomenon is independent of the velocity of the mobile phase.

(B) Longitudinal diffusion creates band broadening, due to the movement of analyte molecules from areas of high to low concentration. The extent of band broadening depends on the amount of time each compound spends on the column, and so is inversely proportional to the flow rate of the mobile phase.

(C) Mass transport is the major contributor to band broadening, particularly for silica particle-type stationary phases. During separation, analyte molecules are partitioned between the stationary and mobile phase; this process is much faster than the diffusion of a molecule into and out of a silica particle pore, where there is no mobile phase flow. Band broadening occurs due to the difference between partitioning and diffusion. The effects of mass transport are proportional to the velocity of the mobile phase, thus lower mobile phase flow rates lead to better equilibration between partitioning and diffusion and less band broadening.

LC separation efficiencies can be improved by altering several parameters, such as selectivity (e.g. changing mobile phase composition, column packing material), reducing the column internal diameter, and reducing the particle size of the column.

The most commonly used separation mode is RP chromatography, where compounds are separated according to their hydrophobicity with the most hydrophobic compounds eluting last. RP stationary phases are generally made up of silica particles functionalised with hydrophobic alkyl chains, where octadecylsilane (ODS) phases, i.e. phases with a C_{18} functional group covalently bonded to the surface of the silica particle, are the most frequently used in RP-LC. A predominantly aqueous-based mobile phase is used in RP separations.

1.7.1 Porous graphitic carbon as a stationary phase in LC

Porous graphitic carbon (PGC) is stationary phase used in LC. The material was developed by Knox and co-workers (Gilbert et al., 1982; Knox et al., 1986) to provide an alternative to the commonly used silica-based packing materials. The use of silica-based stationary phases commonly restricts the choice of mobile phases to within the pH range of 2-7 due to the limited pH stability of the silica particles. Conversely, PGC stationary phases offer the advantage of stability over the entire pH range of 0-14, allowing separation with strongly acidic (Emery and Lim, 1989; Lim, 1989; Gu and Lim, 1990) and alkaline (Barrett et al., 1998; Buchholz et al., 2001) mobile phases.

The surface of PGC is composed of flat sheets of hexagonally arranged carbon atoms with a satisfied valence (Knox et al., 1986), which is very different from the surface of a typical ODS silica-based material (Figure 1.10). At the edges of the graphite sheets, there are carbon atoms which must have valency-satisfying functional groups attached such as hydrogen, hydroxyl, carbonyl, or carboxylic functions. The flat, layered surface of PGC has been found to be advantageous for the separation of closely related substances (Wan et al., 1995; Reepmeyer et al., 2005; Robinson et al., 2007).

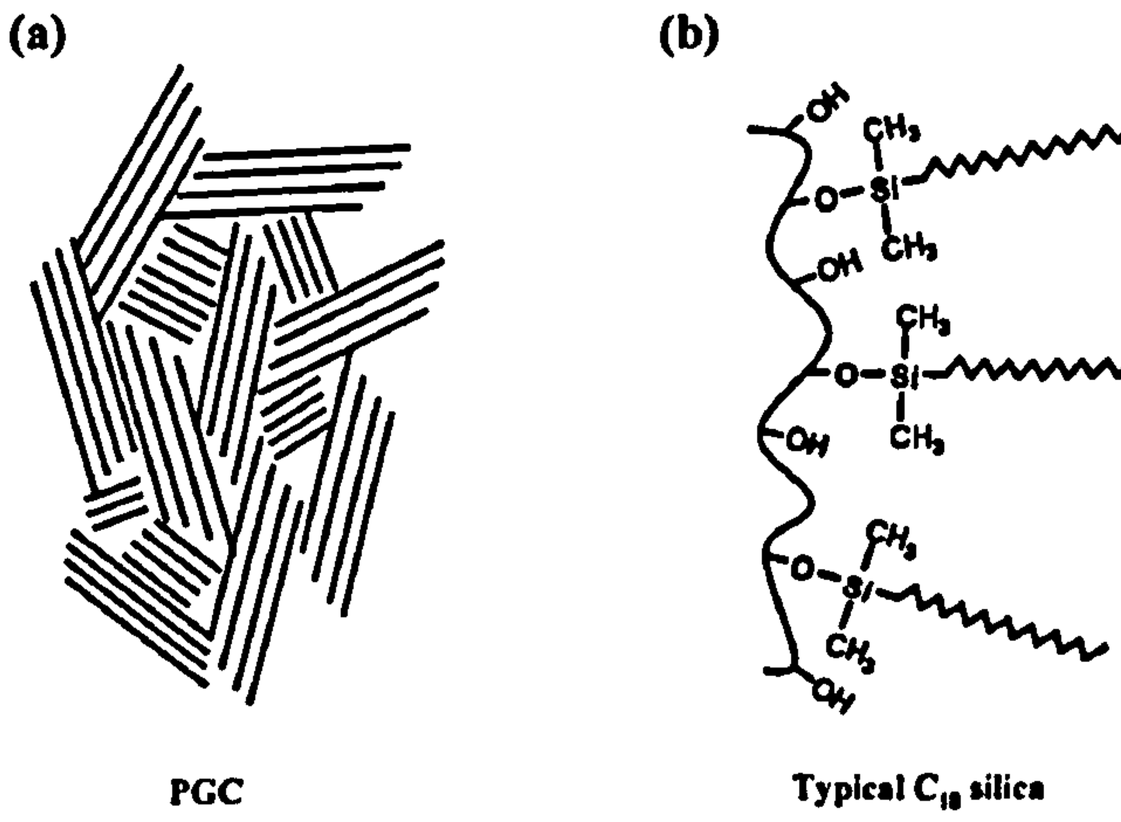

Figure 1.10 Schematic showing (a) the flat surface of PGC and (b) the surface of ODS silica-based materials.

The retention mechanism of PGC has been defined by Knox and Ross as being a balance between two factors: (i) hydrophobic eluent-analyte interactions, and (ii) electronic interactions of polarizable (or polarized) functional groups in the analyte with the delocalized π-electrons of the graphite surface (Knox and Ross, 1997). The second effect is particularly strong when the stereochemistry of the analyte molecules forces the polar group to be close to the graphite surface. They called this retention mechanism the polar retention effect on graphite (PREG), and it appears to be an effect which is additional to the normal hydrophobic and dispersive effects found in conventional RP separations.

The retention of polar compounds on PGC stationary phases has been extensively studied, and PGC-LC-based methods have been reported including for the separation of mono-, di- and oligosaccharides (Koizumi et al., 1991; Davies et al., 1993; Fan et al., 1994; Koizumi, 1996; Barroso et al., 2002; Robinson et al., 2007), some pairs of glycolytic intermediates and sugar phosphates such as 2PG/3PG and Glc6P/Fru6P (Buchholz et al., 2001), nucleosides and their mono-, di- and triphosphates (Xing et al., 2004), phenolic compounds (Hennion et al., 1995; Hanai, 2003).

1.7.2 Hydrophilic interaction chromatography

Another suitable approach for the separation of very polar and hydrophilic compounds is hydrophilic interaction chromatography (HILIC). HILIC performance is orthogonal to RP-LC, and similar to that of normal-phase liquid chromatography (NP-LC), but the non-aqueous mobile phase used in NP-LC is replaced by an eluent containing a high content of water miscible organic solvent (typically acetonitrile in water or volatile buffer) to promote hydrophilic interactions between the analyte and a water-enriched hydrophilic stationary phase.

Silica-based HILIC columns contain a stationary phase that is hydrophilic, e.g. sulfoalkylbetaine zwitterionic functional groups covalently attached to silica particles. Sulfoalkylbetaine zwitterions are known to be potent osmolytes, with a strong ability to bind water, so that water associated with such zwitterions at interfaces exists as bulk liquid water. These water-retaining properties of the zwitterionic stationary phase, combined with a low surface charge that does not promote strong ion exchange interactions, provides a unique environment capable of solvating polar and charged compounds, which enables high performance HILIC separations (Hermström and Irgum, 2006). The separation is known to be achieved by a balance between two factors (i) partitioning of the analytes into this hydrophilic environment, and (ii) weak electrostatic interactions (Figure 1.11) (Alpert, 1990; Alpert et al., 1994).

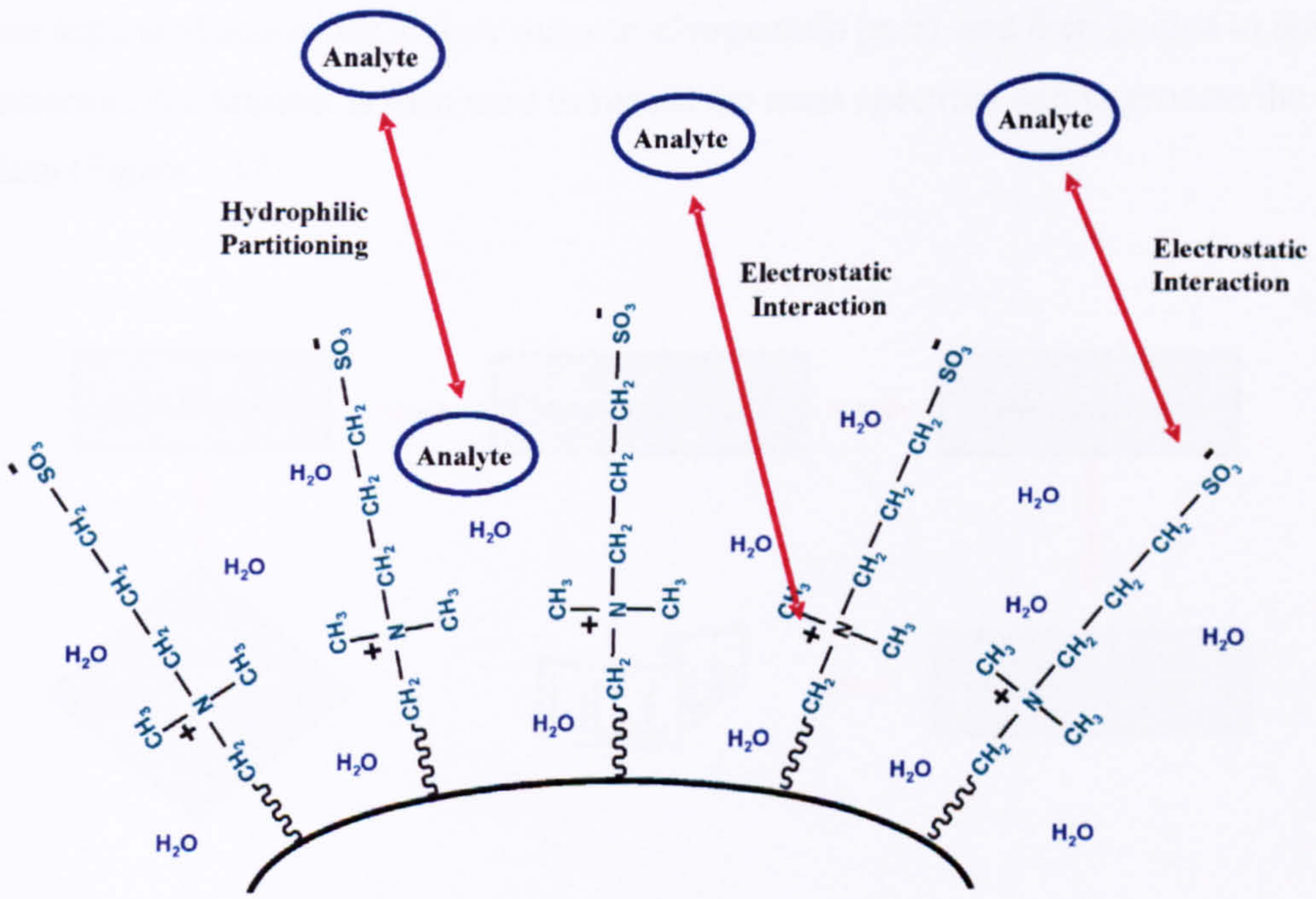

Figure 1.11 Schematic representation of the retention processes on a sulfoalkylbetaine zwitterionic stationary phase. The mechanism of retention is based on the hydrophilic partitioning of the analytes into the water-enriched stationary phase, and weak electrostatic interactions with either the positive or negative charge of the functional group. Adapted from (SeQuant, 2006).

In plant metabolomic studies, the use of HILIC was introduced by Tolstikov and Fiehn (Tolstikov and Fiehn, 2002) who analysed a wide range of polar metabolites from *Cucurbita maxima* phloem tissues; they have demonstrated that HILIC constitutes a complementary separation approach for studying the plant metabolome (see Chapter 6).

1.8 Mass spectrometry

Mass spectrometry (MS) is a powerful analytical tool that can be used to identify both unknown organic and inorganic substances, quantify known compounds, and clarify structures with a high degree of sensitivity and selectivity. The basic principle of mass spectrometers is to convert analyte molecules into gas-phase ions before entering the mass analyser. Within the mass analyser, gas-phase ions are separated according to their mass-to-charge ratio (*m/z*), and then guided to the detector. A computer is then used to record the mass spectrum and to process the data (Figure 1.12).

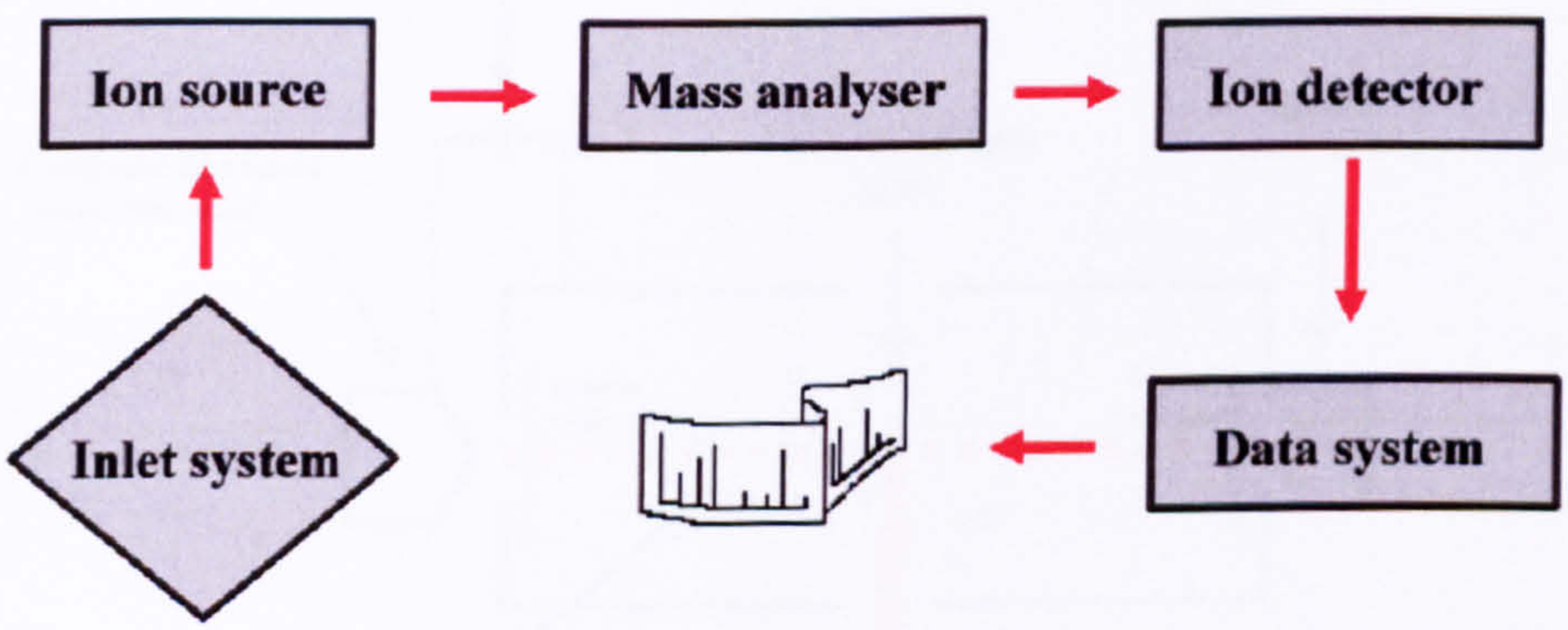

Figure 1.12 Components of a mass spectrometer.

1.8.1 Ionisation techniques

In the ion source, samples are ionised prior to analysis in the mass spectrometer. In plant metabolomics studies, electron ionisation (EI) is the most widely used ionisation technique in GC-MS, and electrospray ionisation (ESI) is the ionisation technique typically used in the analysis of plant extracts by direct infusion, LC-MS, and CE-MS.

1.8.1.1 Electron ionisation

Electron ionisation (EI) was developed by Dempster in 1921 and was one of the first ionisation techniques to be used. An electron ionisation source uses a heated filament to produce electrons of typically of 70 eV energy that are accelerated towards an anode, enabling them to collide with the gaseous analyte molecules injected into the source (Figure 1.13).

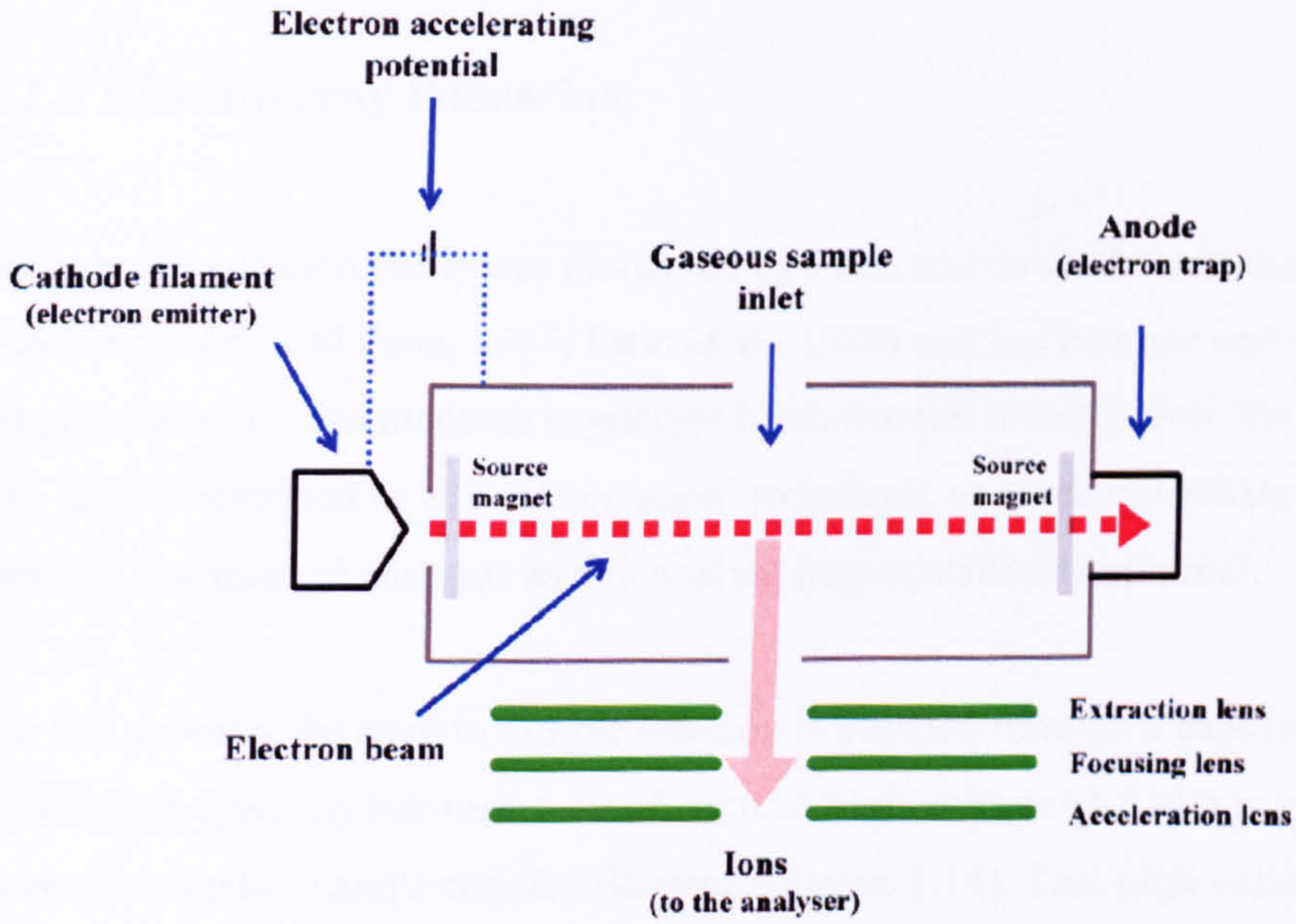

Figure 1.13 Diagram of an electron ionisation source.

The presence of a magnetic field ensures the electrons are focused towards the anode, enhancing their chance of collision with a gaseous analyte molecule. A collision between a gaseous analyte molecule and an electron of 70 eV energy results in the generation of a positive radical molecular ion ($M^{+\bullet}$) (Equation 1.11).

$$M\,(g) + e^- \rightarrow M^{+\bullet}\,(g) + 2\,e^- \qquad \text{(Equation 1.11)}$$

This is a high energy process, as most molecules only require around 10 eV of energy to become ionised, and this excess energy carried by the molecular ion causes it to fragment further in the ion source (Equation 1.12).

$$M^{+\bullet}\,(g) \rightarrow A^+\,(g) + B^\bullet\,(g) \qquad \text{(Equation 1.12)}$$

The fragmentation pattern obtained from the decomposition of the molecular ion produces a highly informative compound-specific mass spectrum, allowing its identification.

1.8.1.2 Electrospray ionisation

Electrospray ionisation (ESI) was pioneered by Fenn and co workers in the late 1980s (Yamashita and Fenn, 1984; Fenn et al., 1989) and has become one of the most popular ionisation methods to analyse biomolecules directly from the liquid phase. ESI is described as a 'soft ionisation' technique, as it generates ions with extremely low internal energies so that analyte fragmentation is minimal.

In the ESI process, the analyte sample solution is pumped through a capillary at a low flow rate, typically between 1-10 μL/min. A high voltage (2-5 kV) is applied between the capillary and a counter electrode (Figure 1.14). This high voltage causes an electric field gradient which induces a charge accumulation on the emerging liquid surface at the capillary tip, producing the 'Taylor cone'. When

the solution that comprises the Taylor cone reaches the Rayleigh limit†, droplets that contain excess charge detach from the Taylor cone giving rise to the emission of a spray of small charged droplets.

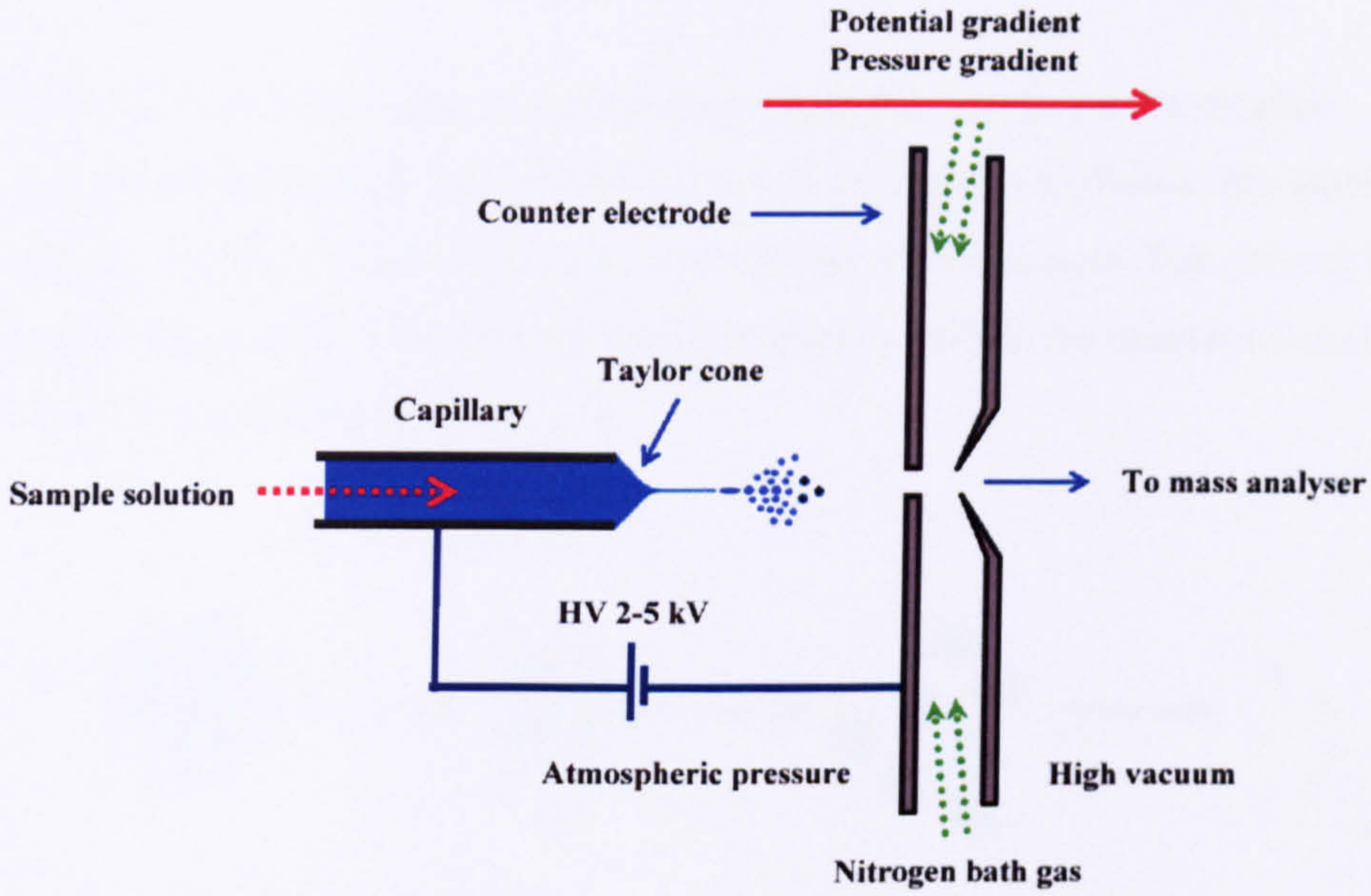

Figure 1.14 Diagram of an electrospray source.

These droplets pass through a pressure and potential gradient towards the mass analyser. Droplets that contain excess positive charge detach from the Taylor cone and move towards the mass analyser. During this transition, the droplets move down a potential and pressure gradient, and reduce in size by evaporation of the solvent or by Coulombic explosion to form fully desolvated ions present in the gas phase. A nitrogen bath gas also aids the evaporation process.

† Rayleigh limit is the point at which Coulombic repulsion of the surface charge is equal to the surface tension of the solution.

Two important mechanisms have been proposed to explain the formation of gas phase ions. The charge residue model (CRM) proposed by Dole and co-workers (Dole et al., 1968) and the ion evaporation model (IEM) proposed by Iribarne and Thomson (Iribarne and Thomson, 1976).

The CRM postulates that at the Rayleigh limit, the charge on the droplet overcomes the surface tension and causes large droplets to divide into smaller and smaller droplets, which eventually consist only of single ions. The driving force for this separation is the increased charge density within the droplet caused by solvent evaporation (Figure 1.15).

Figure 1.15 Charge residue model.

The IEM postulates that the increase in charge density resulting from solvent evaporation causes coulombic repulsion to overcome the liquid's surface tension releasing ions from the droplet's surface (Figure 1.16).

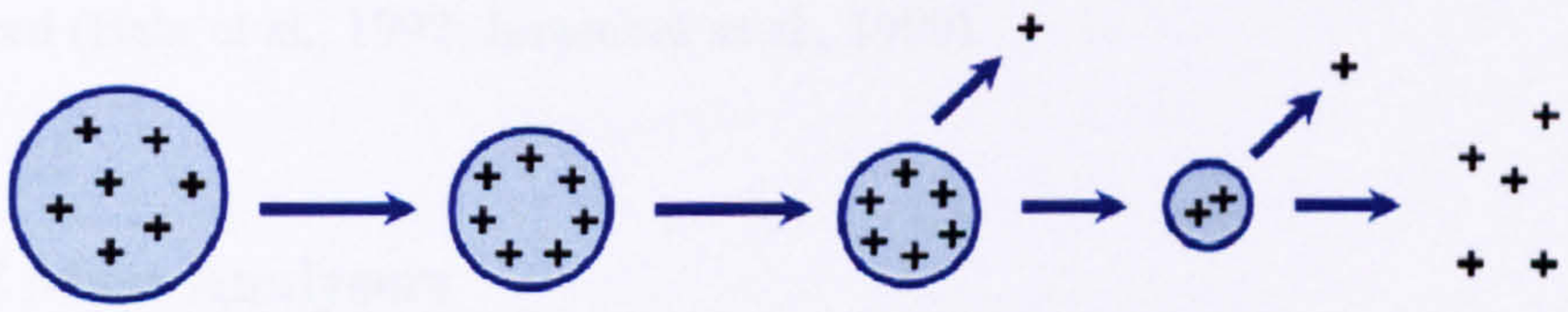

Figure 1.16 Ion evaporation model.

The formation of gas phase ions generates intact protonated $[M+H]^+$ (Equation 1.13) or deprotonated $[M-H]^-$ molecules, that allow the determination of molecular weight. However, ESI may also generate adducts of the analyte with

cations (e.g. Na^+, K^+, NH_4^+) (Equation 1.14) or anions (e.g. CH_3COO^-, Cl^-) (Equation 1.15).

$$M_{(l)} + H^+_{(l)} \rightarrow [M+H]^+_{(g)} \qquad \text{(Equation 1.13)}$$

$$M_{(l)} + Na^+_{(l)} \rightarrow [M+Na]^+_{(g)} \qquad \text{(Equation 1.14)}$$

$$M_{(l)} + CH_3COO^-_{(l)} \rightarrow [M+CH_3COO]^-_{(g)} \qquad \text{(Equation 1.15)}$$

Nanoelectrospray (nanoESI) is a miniaturisation of the traditional electrospray source developed by Wilm and Mann (Wilm and Mann, 1994; Wilm and Mann, 1996). The nanoESI process uses a capillary with an internal diameter of 1-2 μm (20-100 μm for ESI), and has the advantage of operating at much lower flow rates (nL/min), reducing the amount of sample required for a mass spectrometric analysis. Low flow rates produce smaller droplets from the Taylor cone, which may only contain a single ion, and which, due to their small size are more efficiently desolvated, leading to a more efficient sample transfer into the mass spectrometer. In addition, nanospray has also better tolerance towards salt contamination; as droplets are smaller than those formed by ESI, the number of steps required for droplet fission and solvent evaporation events to get down to a single desolvated ion are reduced. Since these steps also serve to concentrate any salt in the droplets, if these steps are reduced then the salt concentration is also reduced (Bahr et al., 1997; Juraschek et al., 1999).

1.8.2 Mass Analysers

Once the ions have been produced, they must be separated according to their mass-to-charge ratios (*m/z*). Mass separation can be achieved using quadrupole-based mass spectrometers, ion-trapping mass spectrometers, and time-of-flight (TOF) mass spectrometers.

The mass spectrometer's resolution and mass accuracy are two analytical attributes important in addressing the issue of the complex plant metabolome (Breitling et al., 2006). Resolution (*R*) is the ability to differentiate between closely related *m/z* values. For a single peak of mass *m*, the resolution is expressed as (Equation 1.16):

$$R = m/\Delta m \qquad \text{(Equation 1.16)}$$

where Δm is the peak width which is commonly defined at half-height (full-width half maximum or FWHM) or 50% of the relative intensity. Mass accuracy is defined as the difference between the measured value and the calculated value (Δm) relative to the calculated value (m) (Balogh, 2004; Breitling et al., 2006). Mass accuracy is usually expressed as a relative error in parts per million (ppm) (Equation 1.17):

$$\text{error (ppm)} = (\Delta m/m) \times 10^6 \qquad \text{(Equation 1.17)}$$

1.8.2.1 Quadrupole

The linear quadrupole mass analyser was first described by Paul and Steinwedel in 1953. It consists of four parallel metal rods positioned along the instrument's *z*-axis that have fixed direct current (dc) and alternating radio frequency (rf) potentials applied to them. Two opposite rods have an applied potential of $+(U- V\cos \omega t)$ and the other two rods have a potential of $-(U- V\cos \omega t)$, where U is a fixed dc voltage and $V\cos\omega t$ is the applied rf voltage of amplitude 'V' and frequency 'ω' (Figure 1.17).

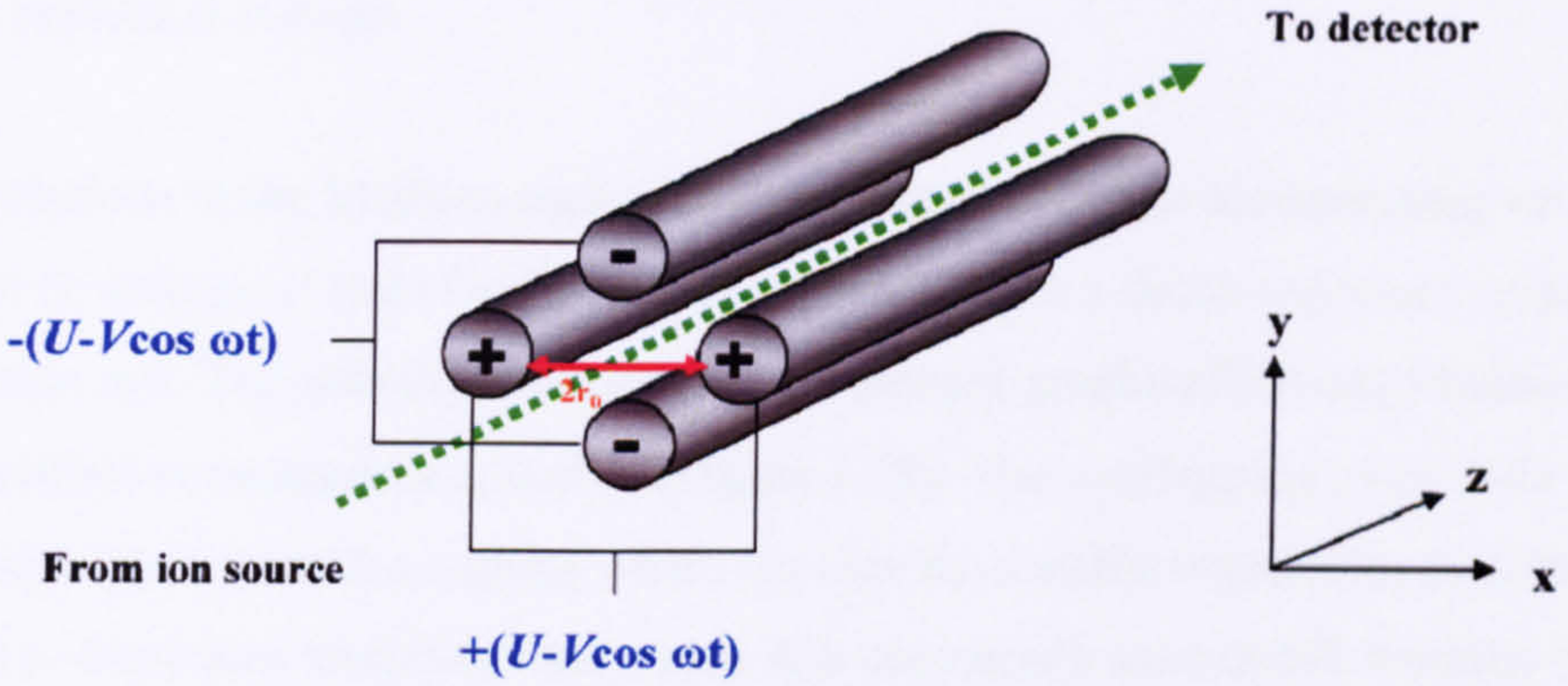

Figure 1.17 Schematic representation of a linear quadrupole mass analyser showing the equations for the potentials applied to the four rods. The green dotted line indicates the general direction of ion movement.

The applied voltages affect the trajectory of ions travelling along the *z*-axis between the four rods. The trajectory of ions depends on the forces induced by the electric fields, so that for given *U* and *V* voltages only ions of a particular *m/z* ratio have stable trajectories along the *x*-*y* directions and are transmitted through the quadrupole mass analyser. All the other ions have unstable trajectories (large amplitudes in the *x*- or *y*- directions), hit the rods and are lost. This mode of operation of linear quadrupoles is called 'mass-selective stability mode'.

The motion of an ion of particular *m/z* value which has a stable trajectory in a quadrupole field and therefore can be transmitted through the quadrupole mass analyser can be described mathematically by the solutions to the second-order linear differential equations described by Mathieu in 1868. This equation is known as the Mathieu equation (Equations 1.18 and 1.19).

$$a_u = 8eU / m\omega^2 r_0^2 \qquad \text{(Equation 1.18)}$$

and

$$q_u = 4eV / m\omega^2 r_0^2 \qquad \text{(Equation 1.19)}$$

where e is the charge on an electron, m is the mass of the ion, ω is the angular frequency, r_0 is the radius of the quadrupole field, U is the fixed dc voltage, and V is the applied rf voltage.

The solutions to the Mathieu equations can be used to define the operating values for the dc voltage U and rf voltage V required to obtain a stable trajectory of ions of certain m/z. The stability areas can be represented graphically using Mathieu's dimensionless parameters a_u and q_u (Figure 1.18). The overlapping areas A-D (circled in green) are the regions where the ions have stable trajectories in both the x- and y- directions simultaneously; area A is commonly used in MS because it involves the application of low potentials.

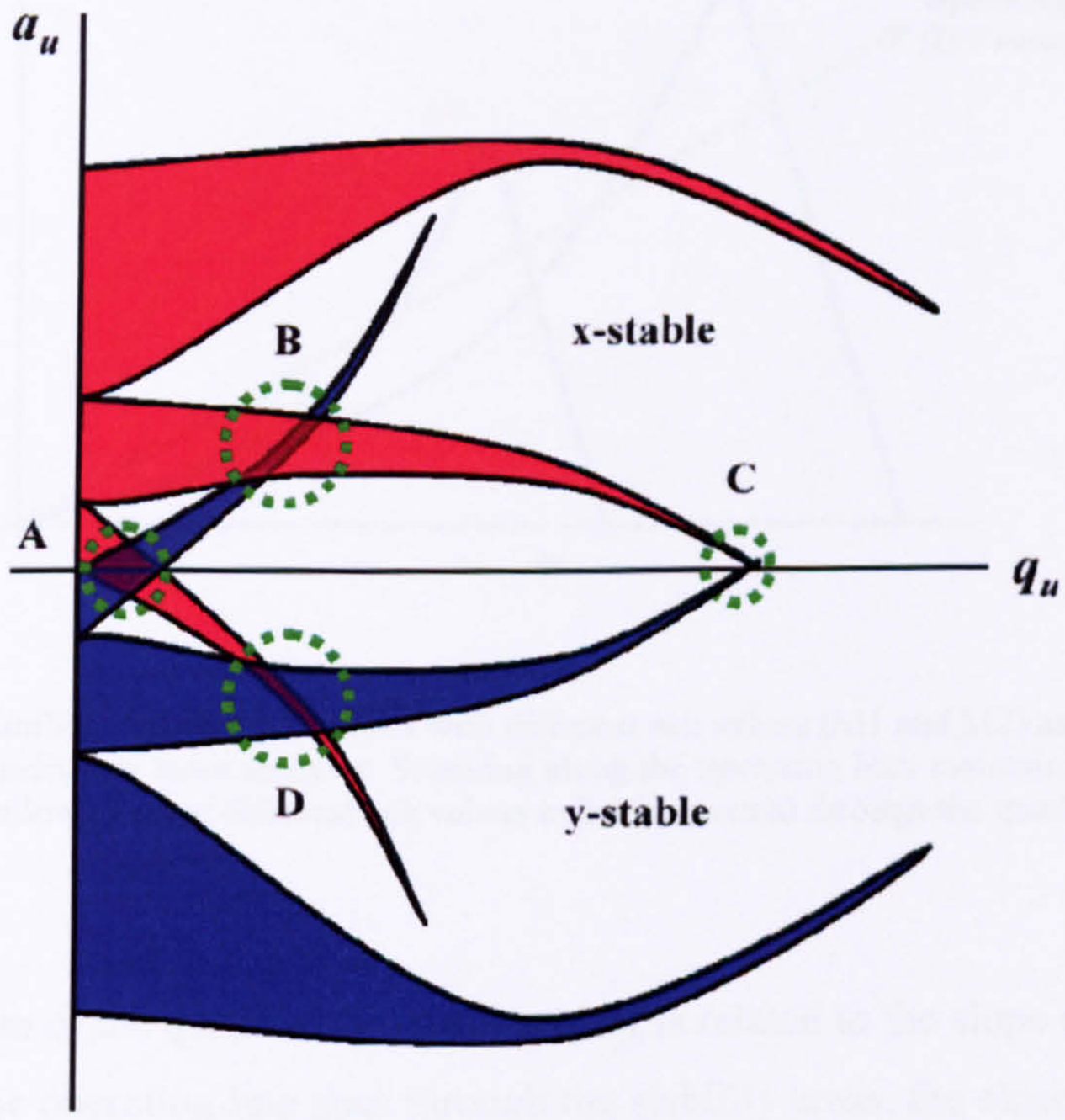

Figure 1.18 Stability diagram in a a_u-q_u space showing the regions of stable ion trajectories in the x- and y- directions in a quadrupole mass analyser. u represents either x or y.

Selective transmission of ions of different *m/z* values can be achieved by changing the values of a_u and q_u, which means changing the applied voltages *U* and *V*. If *U* and *V* are ramped simultaneously whilst maintaining a constant ratio between them, ions of different *m/z* values are sequentially brought within the stability region, and a linear operating line is generated. Scanning along the operating line allows ions of different *m/z* values to be sequentially transmitted through the quadrupole, and a mass spectrum can thus be recorded at the detector (Figure 1.19).

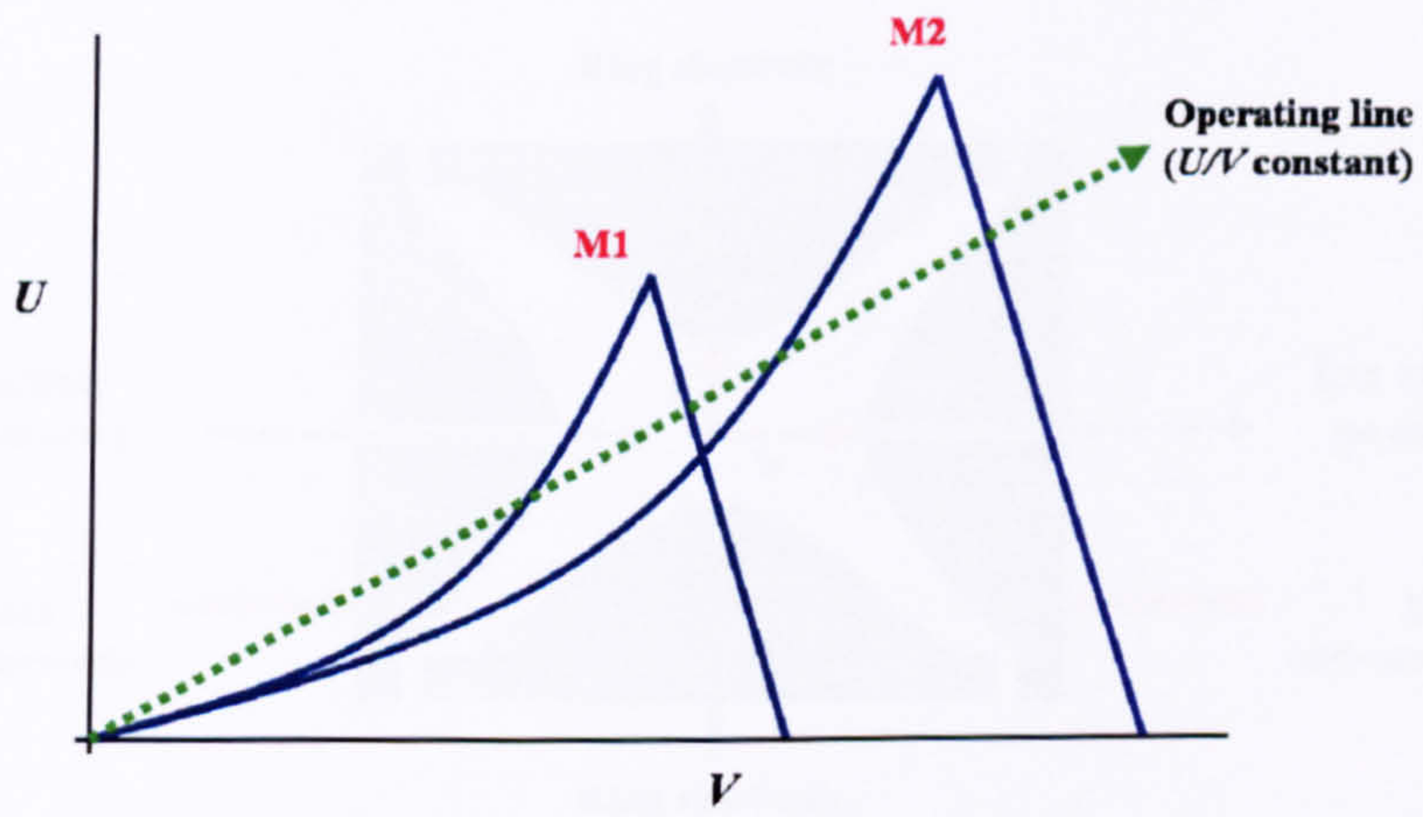

Figure 1.19 Stability regions for two ions with different *m/z* values (M1 and M2) as a function of *U* and *V* in a quadrupole mass analyser. Scanning along the operating line, maintaining the *U/V* ratio constant, allows ions of different *m/z* values to be transmitted through the quadrupole.

The resolution of the quadrupole mass analyser is related to the slope of the line. As long as the operating line goes through the stability areas, the closer the line is to the apex of the stability region, the higher the resolution.

1.8.2.2 Quadrupole ion trap

The quadrupole ion trap (QIT) mass analyser was developed in parallel with the quadrupole in the early 1950s by Paul and Steinwedel (Paul and Steinwedel, 1953). The QIT consists of three electrodes: two identical end-cap electrodes and a ring electrode. They have hyperbolic-shaped inner surfaces and each of the end-cap electrodes contains a small, centrally positioned hole; ions formed in the source are transported into the trap via the entrance end-cap electrode, and ions exit the trap at the other end via the exit end-cap electrode (Figure 1.20).

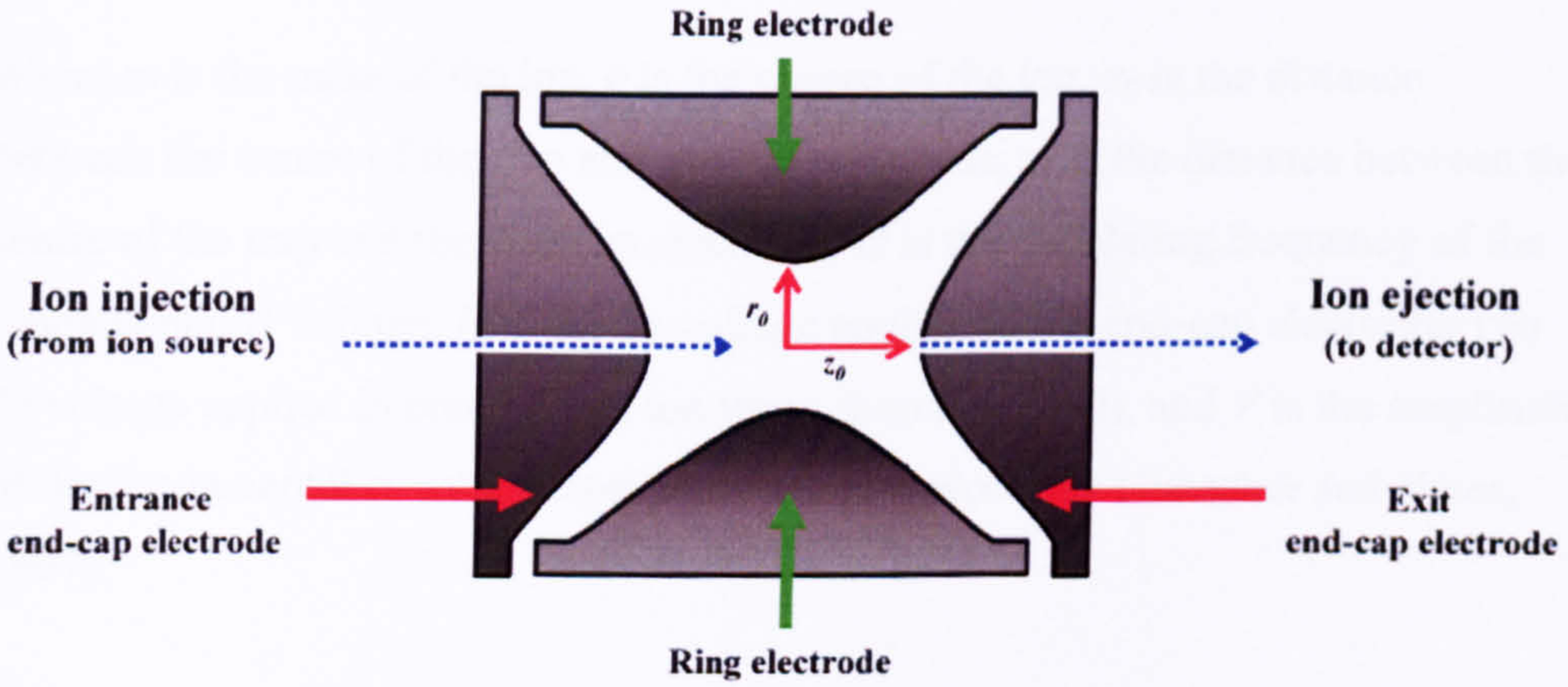

Figure 1.20 Cross-section of a quadrupole ion trap mass analyser showing the radial (r_0) and axial (z_0) directions.

An oscillating rf voltage known as the 'fundamental rf' is applied to the ring electrode to focus ions towards the centre of the trap. A dc voltage may be applied to the end-cap electrodes; however, in modern commercial ion traps the dc voltage is set to zero. The applied rf voltage creates a three-dimensional quadrupolar field in the ion trap, and ions formed in the source can be trapped in stable trajectories for a certain length of time in this region between the three electrodes. Modern ion traps are filled with helium, often called 'damping' or 'buffer' gas to help maintain ions in the trap by damping their kinetic energy (collisional cooling);

collisions between the helium gas and the analyte ions focuses their trajectories towards the centre of the trap (Stafford et al., 1984). For an ion to be stored inside the ion trap, it needs to have a stable trajectory in both the *r*- (radial) and *z*- (axial) directions. The motion of the ions that have a stable trajectory inside the trap can again be described mathematically using the solutions to the Mathieu equation and the stability areas can be represented graphically using Mathieu's dimensionless parameters a_z and q_z (Equations 1.20 and 1.21).

$$a_z = -16eU / m(r_0^2 + 2z_0^2)\Omega^2 \qquad \text{(Equation 1.20)}$$

and

$$q_z = 8eV / m(r_0^2 + 2z_0^2)\Omega^2 \qquad \text{(Equation 1.21)}$$

where m is the mass of the ion, e is the charge of the ion, r_0 is the distance between the centre of the trap and the ring electrode, z_0 is the distance between the centre of the trap and the end-cap electrode, Ω is the oscillating frequency of the fundamental rf voltage, U is the dc voltage applied to the end-cap electrodes (no dc voltage applied in commercial ion traps, therefore U=0), and V is the amplitude of the fundamental rf voltage applied to the ring electrode (Jonscher and Yates, 1997).

The stability diagram in a a_z-q_z space of stable ion trajectories in the *r*- and *z*- directions (blue and red shaded regions, respectively) is represented in Figure 1.21. The overlapping area, circled in green, is the region in the a_z-q_z space where radial and axial stability overlaps, and ions are stable in both directions inside the trap. In contrast to the 'mass-selective stability mode' of operation of linear quadrupoles where ions of a small *m/z* range are stable at a time, commercial ion traps operate in 'mass-selective instability mode' where ions formed in the source are stored in the trap, then sequentially ejected according to their *m/z* value, and reach the detector. In the 'mass-selective instability mode', the ion trap operates in rf-only mode (no dc voltage applied; U=0) along the line a_z=0 (Figure 1.22) (Stafford et al., 1984; Jonscher and Yates, 1997; March, 1997).

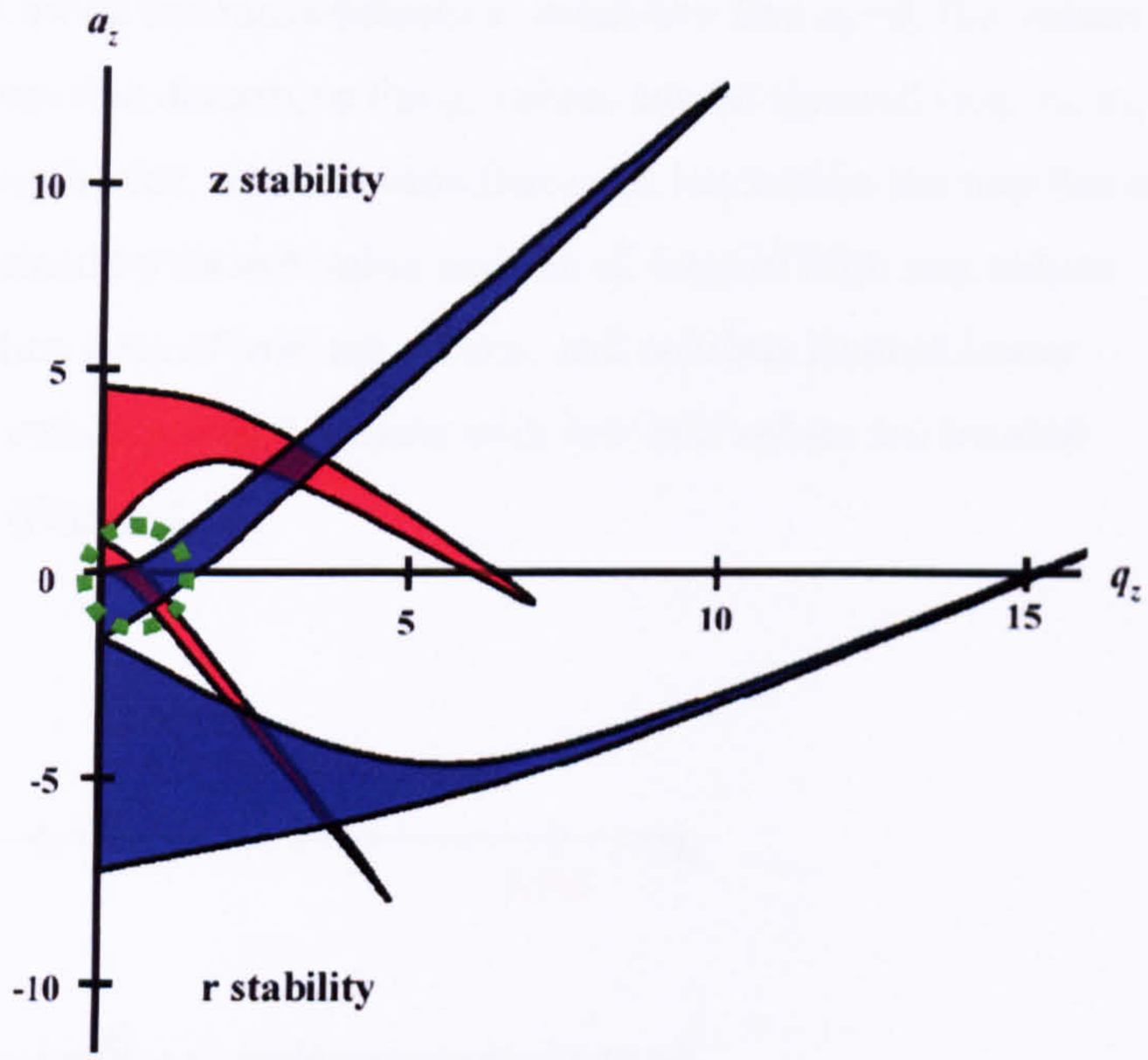

Figure 1.21 Diagram showing the regions of stability along the *r* and *z* axis in the quadrupole ion trap. The common *r* and *z* stability area used in commercial ion traps is circled in green.

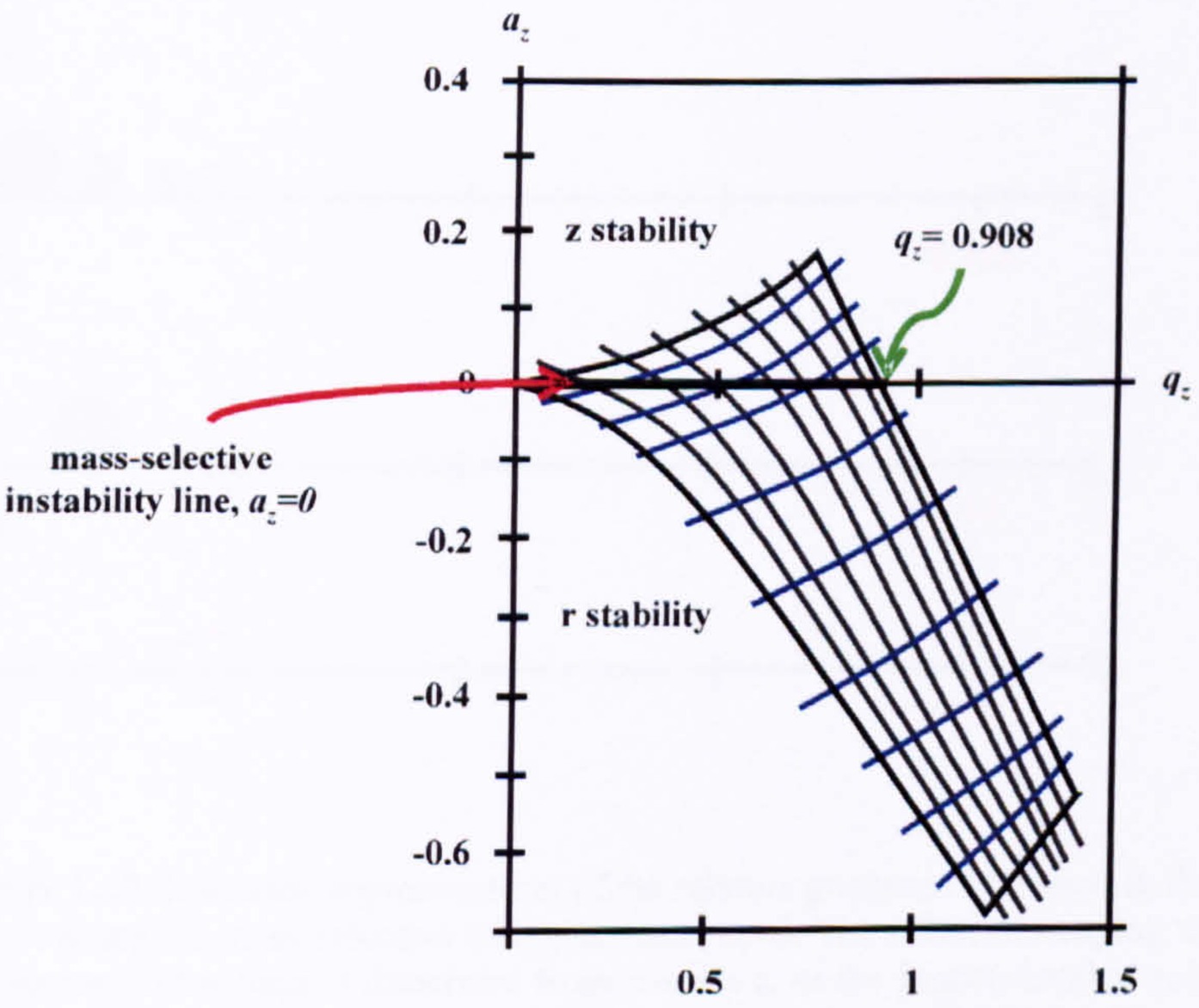

Figure 1.22 Diagram showing simultaneous ion stability in both the *r*- and *z*- directions in the quadrupole ion trap. In the 'mass-selective instability mode', the ion trap operates in rf-only mode along the mass-selective instability line, $a_z=0$. Ion trajectories become unstable when q_z=0.908.

As the ion trap operates along the mass-selective instability line $a_z=0$, the values of many of the parameters that determine the q_z values can be ignored (e.g. r_0, z_0, and Ω are the same for each ion), which means that each ion within the trap has a defined q_z value, determined by its *m/z* value and the rf. Ions of high *m/z* values have smaller q_z values than ions of low *m/z* values, and are thus located lower along the q_z axis on the stability diagram; ions with low *m/z* values are located higher along the q_z axis (Figure 1.23).

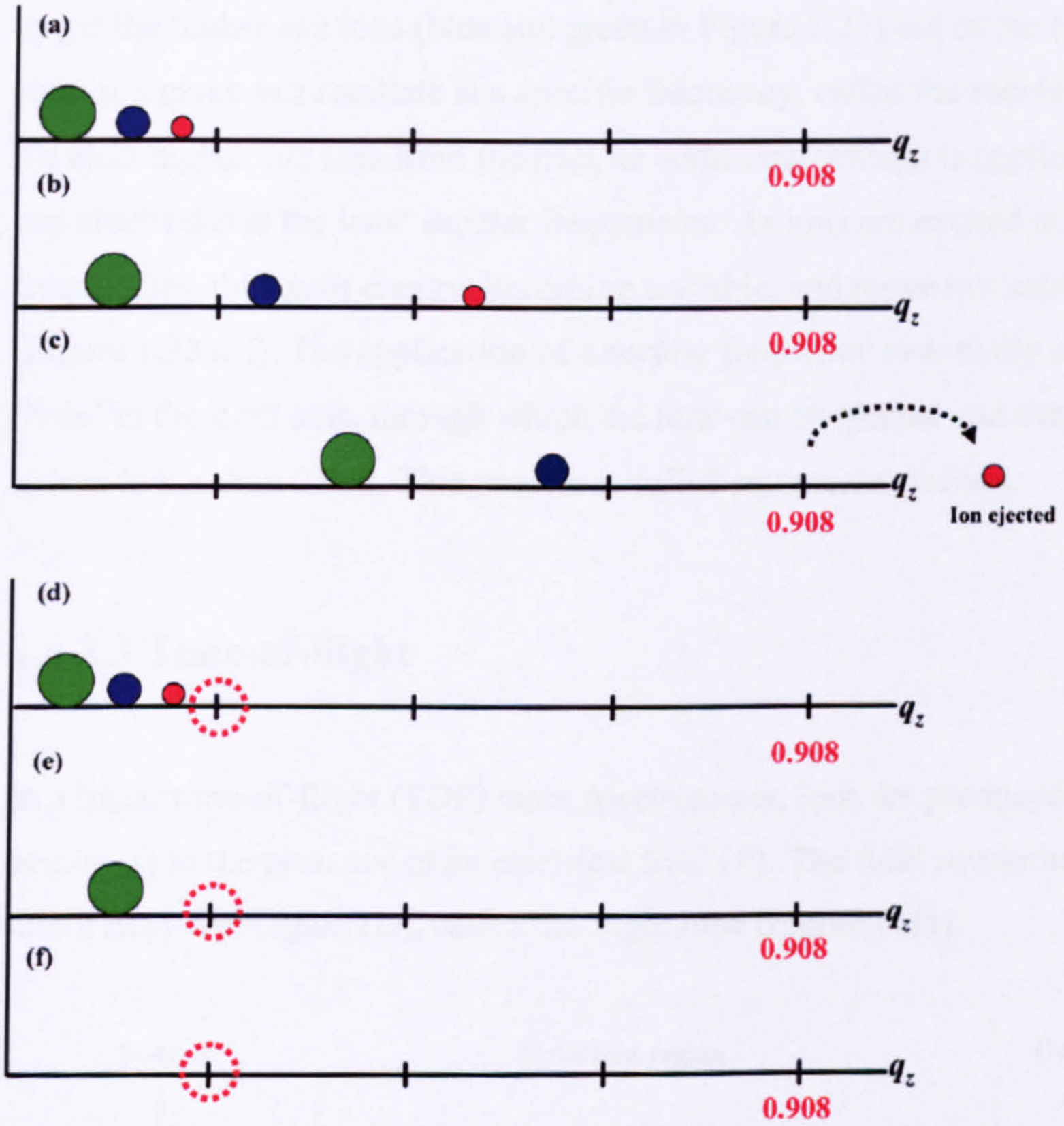

Figure 1.23 Schematic representation of the relative positions of ions with three different *m/z* values along the mass-selective instability line, $a_z=0$. The effect of ramping the amplitude of the fundamental rf voltage is illustrated from panel a-c; as the fundamental rf voltage increases, the q_z value for each ion also increases. Ions are ejected when $q_z=0.908$ (red ion, panel c), but the amplitude of the fundamental rf voltage is not ramped high enough to get the higher *m/z* ions (blue and green) out of the trap. These ions are ejected from the trap by applying an additional voltage to the end-cap electrodes at the ions' secular frequencies. The application of a secular frequency creates a 'hole' in the $a_z=0$ axis, through which the ions can be ejected and detected at q_z values lower than 0.908. This process is called resonance ejection (panel d-f).

As the amplitude of the fundamental rf voltage is ramped from low to high voltage, the q_z value of all the ions increases. When it reaches q_z=0.908 (q_{eject}), the ions are no longer stable and are ejected from the trap via the exit end-cap electrode (red ions, panel c), and detected using an electron multiplier system (Stafford et al., 1984; Jonscher and Yates, 1997; March, 1997). A mass spectrum is generated by sequentially ejecting ions in order of increasing *m/z*.

However, the amplitude of the fundamental rf voltage is not ramped high enough to get the higher *m/z* ions (blue and green in Figure 1.23) out of the trap. Trapped ions of a given *m/z* oscillate at a specific frequency, called the secular frequency. To eject higher *m/z* ions from the trap, an additional voltage is applied to the end-cap electrodes at the ions' secular frequencies. As ions are excited at their secular frequencies, they gain energy, becoming unstable, and move towards the end-caps (Figure 1.23 d-f). The application of a secular frequency essentially creates a 'hole' in the a_z=0 axis, through which the ions can be ejected and detected at q_z values lower than 0.908. This process is called resonance ejection.

1.8.2.3 Time-of-flight

In a linear time-of-flight (TOF) mass spectrometer, ions are produced in the source (*s*) in the presence of an electrical field (*V*). The field accelerates the ions into a field-free region (*D*), called the flight tube (Figure 1.24).

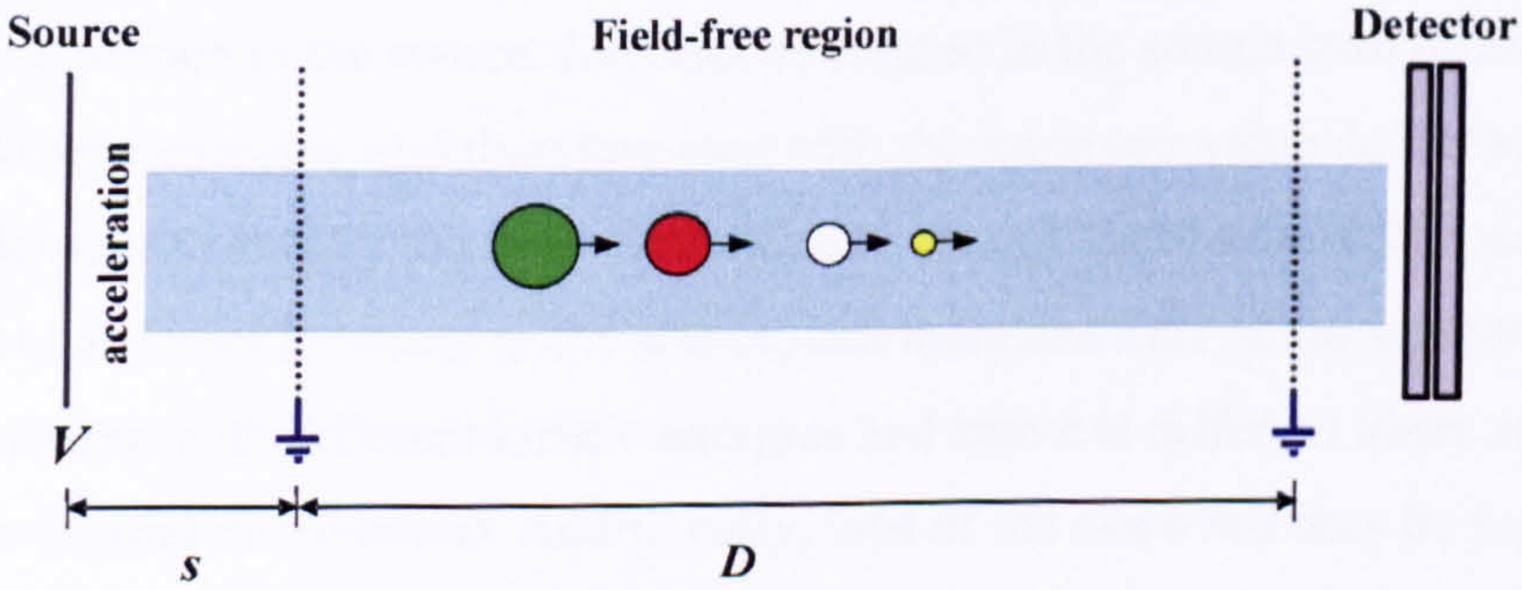

Figure 1.24 Schematic principle of a linear time-of-flight mass analyser.

Ions are separated as a function of their velocities (v), which are dependent on their mass (m) and charge (z); high mass ions take longer to reach the detector than low mass ions. By accelerating an ion with mass (m), and charge (z) through a potential difference (V), the ion acquires kinetic energy (KE) (Equation 1.22):

$$KE = zV = 1/2\ mv^2 \qquad \text{(Equation 1.22)}$$

The time (t) required to travel through the drift region (D) is given by (Equation 1.23):

$$t = D/v \qquad \text{(Equation 1.23)}$$

Rearranging Equation 1.5 and substituting for v (Equation 1.24):

$$KE = zV = mD^2/2t^2 \qquad \text{(Equation 1.24)}$$

Rearranging for t (Equation 1.25):

$$t^2 = m/z\ (D^2/2V) \qquad \text{(Equation 1.25)}$$

If D and V remain constant, then m/z values can be determined by measuring the time that ions take to travel all the way through the field-free region between the source and the detector. However, the resolution obtained using simple linear TOF instruments is poor due to spatial and velocity spreads of ions of the same m/z value formed in the source. Ions can be formed in the source with different initial kinetic energies, and therefore ions with the same m/z value do not arrive at the detector at exactly the same time (kinetic energy distribution). Ions can be formed at different locations in the source, and therefore ions of the same m/z can be accelerated with different kinetic energies and arrive at different times at the detector (spatial distribution). Additionally, ions of the same m/z may be formed in the source at different times, and thus ions of the same m/z do not all arrive at

the detector at the same time due to their different time of formation (temporal distribution) (Cotter, 1992; Chernushevich et al., 2001).

To compensate for some of the variation in kinetic energy distributions between ions, and therefore improve the resolution of TOF instruments, Mamyrin and co-workers (Mamyrin et al., 1973) incorporated a reflectron at the end of the flight tube (Figure 1.25).

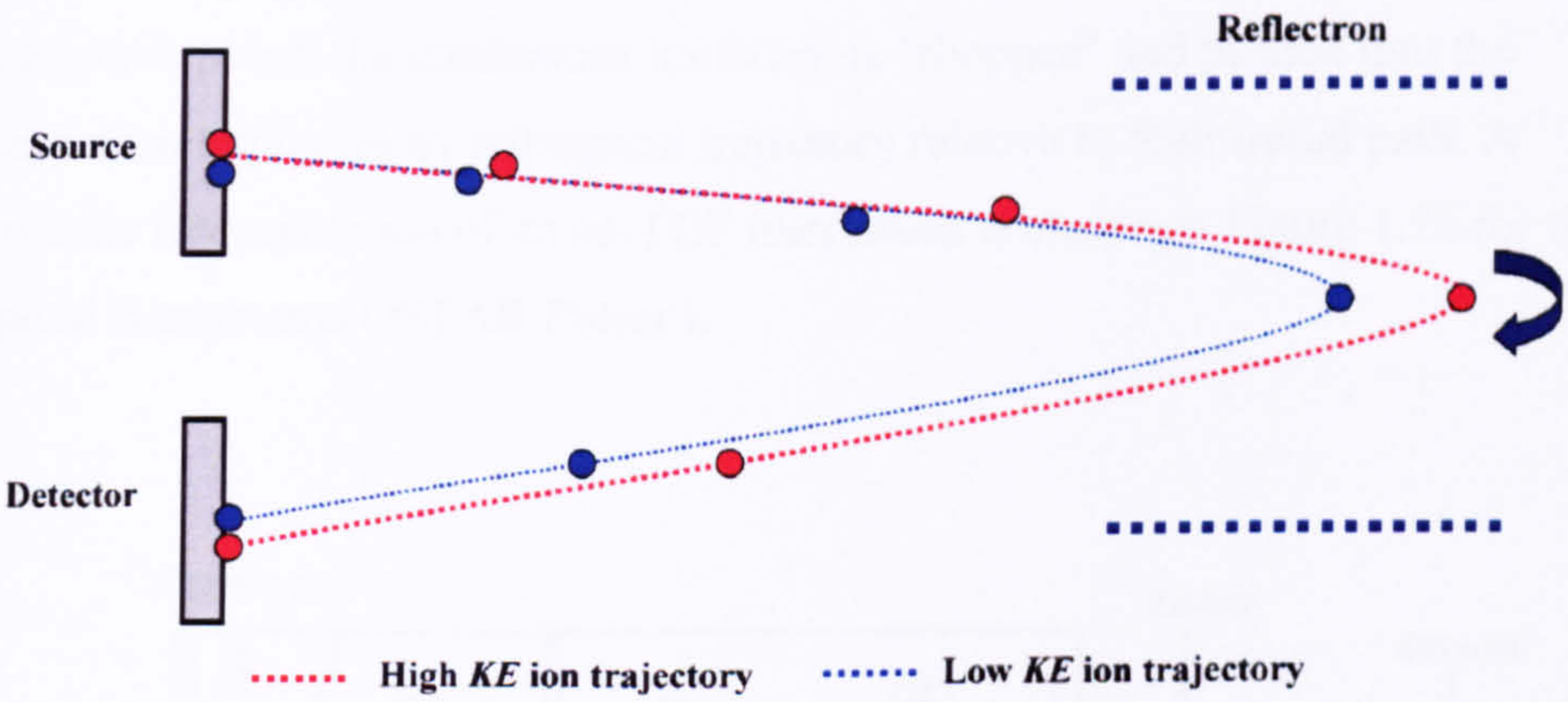

Figure 1.25 Schematic of a TOF mass analyser with an ion reflectron; *KE*, kinetic energy.

In a reflectron, an electric field is applied which reflects ions according to their kinetic energy. Ions of the same *m/z* value but different kinetic energies enter the reflectron, turn around and are reaccelerated back through the reflectron, exiting with energies identical to their incoming energy but with velocities in the opposite direction. The focusing action of a reflectron results from the fact that ions with higher kinetic energies enter the reflectron more deeply, so that these ions spend more time in the reflectron and arrive at the detector at the same time as the slower ions; increased resolution is thus achieved in this manner.

1.8.2.4 Orthogonal acceleration

Orthogonal acceleration into a TOF (oaTOF) was first described at the Bendix Corporation in 1964 and rediscovered in 1989 by Guilhaus and co-workers (Dawson and Guilhaus, 1989; Coles and Guilhaus, 1993; Guilhaus et al., 2000). The use of orthogonal acceleration was developed to couple TOFs with a continuous ion beam sources, such as ESI, by means of accelerating ions through a direction which is perpendicular to the TOF's axis. To move ions into the direction of the TOF, an accelerator voltage ('pusher') is used to create a short electrostatic pulse; the continuous ion beam is 'chopped' and pushed into the acceleration region on an orthogonal trajectory relative to their initial path. A schematic representation of an oa-TOF instrument is shown in Figure 1.26 for the Applied Biosystems QSTAR Pulsar i.

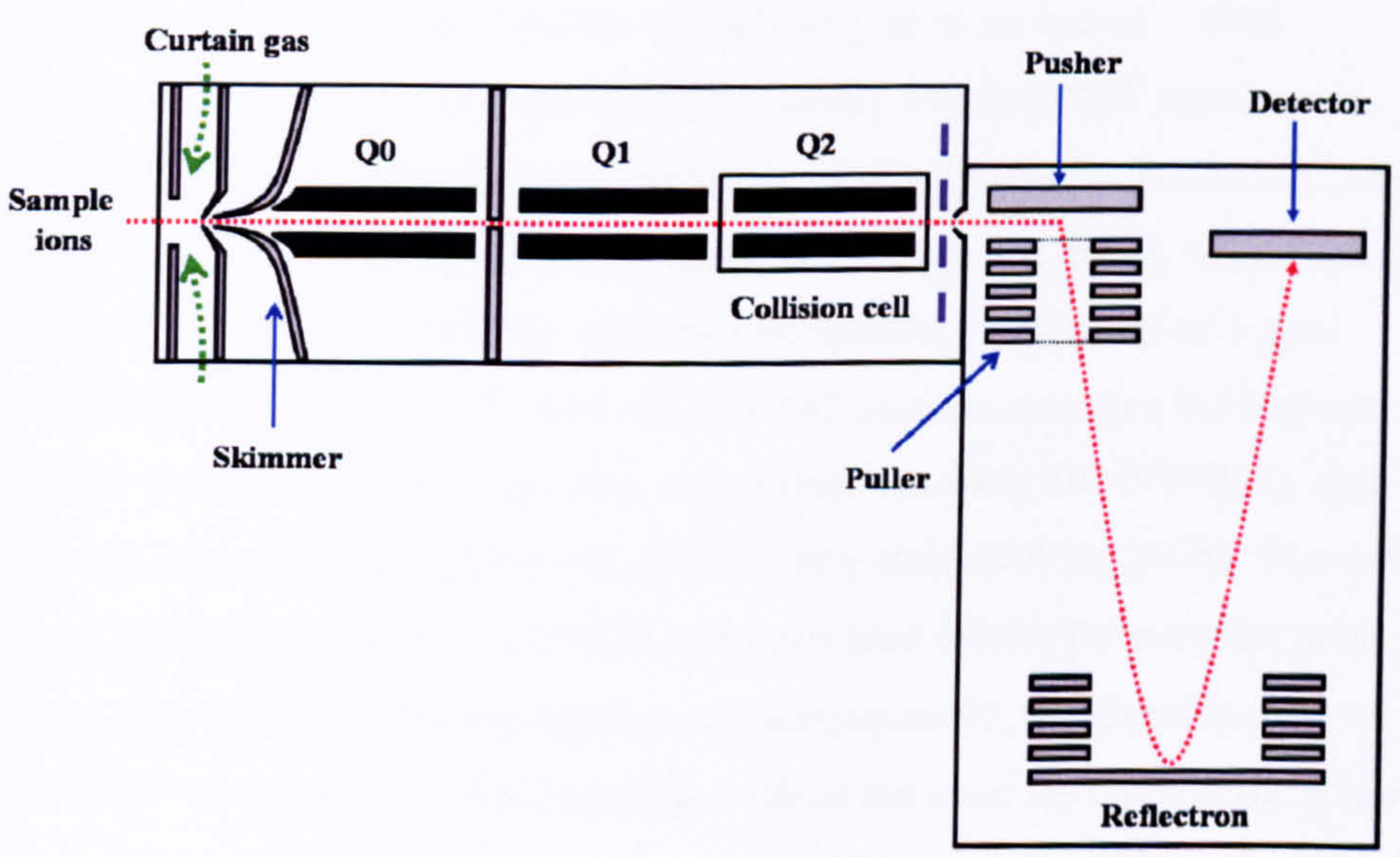

Figure 1.26 Schematic of the Applied Biosystems QSTAR Pulsar i quadrupole oaTOF mass spectrometer equipped with an ESI source.

The Applied Biosystems QSTAR Pulsar i is a hybrid quadrupole oa-TOF instrument that can be equipped with either ESI or MALDI sources; only ESI is used and described in this thesis. The rf-only quadrupole Q_0 focuses and transmits all ions from the ESI source into the quadrupole mass filter Q_1. In MS mode, Q_1 operates in rf-only mode to transmit ions over a wide range of *m/z* values through the collision cell quadrupole (Q_2) into the TOF mass analyser. Ions enter the TOF from the collision cell quadrupole (Q_2) where they are then orthogonally 'pushed', creating a discrete packet of ions; this allows a starting time for the ion's flight to be recorded. Ions enter the field-free region where they are separated according to their *m/z* value before being detected, using a multichannel plate (MCP); ions with greater *m/z* values take longer to travel the flight tube than ions with smaller *m/z* values.

Generally, quadrupole mass analysers are relatively low-cost instruments, and are the most common mass analysers in existence today. These instruments operate at unit mass resolution, and are capable of analysing up to an *m/z* of ~ 4000 (Rodrigues et al., 2008; Wang and Griffiths, 2008). Modern TOF instruments, equipped with reflectrons, offer high resolution and improved mass accuracy over quadrupole-based mass analysers (including quadrupole ion traps), with mass resolving power of 10^4 (FWHM), and mass accuracies in the order of 5 ppm (Wang and Griffiths, 2008). To date, FTICR-MS instruments have the highest resolving power of all mass analysers, with values reaching 10^6 (FWHM), and mass accuracies of < 2 ppm (Balogh, 2004; Wang and Griffiths, 2008). The ultra-high resolution provided by the FTICR mass analyser allows for accurate mass measurements (elemental composition), and subsequently, the identification of metabolites with similar nominal masses, without the need for chromatographic separations prior to mass spectrometric analysis (Brown et al., 2005b; Breitling et al., 2006; Ohta et al., 2007).

1.8.3 Detectors

Once separated according to their *m/z* values, ions must be detected (collected) and their abundances measured. Detectors are generally based on the electron multiplier principle. In an electron multiplier, ions leaving the mass analyser collide with the metal surface of a conversion dynode and create a cascade of electrons. The electrons are passed down a chain of dynodes, creating further cascades of electrons at each surface. Eventually the electrons reach ground potential at the final dynode where they can be measured as a current; the amplification of the initial signal can reach 10^7. There are two classes of detectors: single point ion collectors and multipoint or array collectors. Point ion collectors detect ions sequentially at one point. These detectors are used after mass analysers such as the quadrupole, where each ion of different *m/z* is scanned in, one *m/z* at a time and each *m/z* can then be detected. Multipoint collectors detect all ions simultaneously and when a series of electron multipliers are placed into arrays on a plate, they are known as multichannel plates (MCPs). They are particularly useful with TOF mass analysers as they detect most ions of a single *m/z* at the same time even if they spread spatially over the whole plate.

1.8.4 Tandem mass spectrometry

Soft ionisation techniques, such as ESI, introduce little internal energy and give little information on structure as few fragments are generated. To be able to obtain detailed structural information from such intact species, further fragmentation can be achieved by collision of the analyte ions with inert gas molecules (He, Ar, or N_2) in a process called collision induced dissociation (CID). In this process, part of the ion's kinetic energy is converted into internal energy which causes the ion to dissociate into characteristic fragment ions. CID is generally carried out on a tandem MS instrument, which allows for two or more sequential stages of mass spectrometric analysis.

1.8.4.1 Tandem-in-time

Tandem-in-time instruments are ion-trapping mass spectrometers such as quadrupole ion traps (QIT-MS), which allow for multiple stages of mass spectrometric analysis, which are separated in time. In these instruments, ions from the ion source are allowed into the trap, and specific precursor ions of a given *m/z* value can be isolated in the trap and fragmented to generate structurally diagnostic ions. In modern ion traps, the precursor ion is isolated in the trap by applying to the end-cap electrodes a broadband waveform which has a window corresponding to the secular frequency of the precursor ion; all ions except the selected precursor ion become unstable and are ejected from the trap. Now that the precursor ion has been isolated, an auxiliary rf voltage (known as the 'tickle' voltage) is applied to the end-cap electrodes at the secular frequency of the precursor. This voltage increases the kinetic energy of the precursor ion, which increases the amplitude of the ion's trajectory in the trap, and causes it to move away from the centre of the trap. These excited ions collide with the helium gas molecules, and this causes some of the kinetic energy to be converted into internal energy, inducing fragmentation by CID and generation of product ions (MS^2 analysis). Because these fragment ions do not resonate at the same secular frequency as the precursor ion, they cool back towards the centre of the trap and do not undergo further fragmentation. A fragment ion can then be selected as a precursor ion, be isolated inside the trap, and subjected to CID to generate further structural information (MS^3 analysis). This process can be repeated to 'n' stages of mass spectrometry to generate MS^n data, and the same mass analyser is used to carry out the successive stages of analysis. Ions are scanned out of the trap by means of the mass-instability mode of operation, and detected, to produce a tandem mass spectrum. The ability to perform multiple stages of MS is a unique feature of ion trapping instruments which has exceptional power in structural elucidation.

1.8.4.2 Tandem-in-space

Tandem-in-space instruments have two mass analysers separated by a collision cell and allow for two sequential stages of mass spectrometric analysis (MS/MS); MS/MS is achieved through spatial separation of the precursor and fragment ions. Examples of these instruments include triple quadrupoles (QqQ), and quadrupole time-of-flight instruments (q-TOF). There are four MS/MS experiments that can be performed in current tandem mass spectrometers (Figure 1.27). These are described for a tandem quadrupole instrument where Q1 and Q2 are quadrupole mass analysers separated by a collision cell.

In a product ion experiment a precursor ion is selected by the first mass analyser (Q1), fragmented in the collision cell, and the product ions are analysed in the second mass analyser (Q2) (Figure 1.27a). In a precursor ion experiment, Q2 is set to only allow ions of a specific *m/z* ratio to be transmitted to the detector, while Q1 scans the mass range. A signal is observed only when a precursor ion selected in Q1 fragments in the collision cell to produce the selected product ion with fixed *m/z* value (Figure 1.27b). A neutral loss experiment identifies precursor ions that fragment by loss of a specific neutral. Q1 is scanned while Q2 is scanned at a set mass difference from Q1 corresponding to the neutral molecule, and only precursor ions that result in fragment ions formed by the loss of that specific neutral are transmitted to the detector (Figure 1.27c). Selected reaction monitoring (SRM) involves fixing both mass analysers to a particular *m/z* value. Q1 is set to select a precursor ion while Q2 is set to select a known fragment ion. Q2 detects a signal if the selected precursor ion is present and fragments to produce the known product ion (Figure 1.27d).

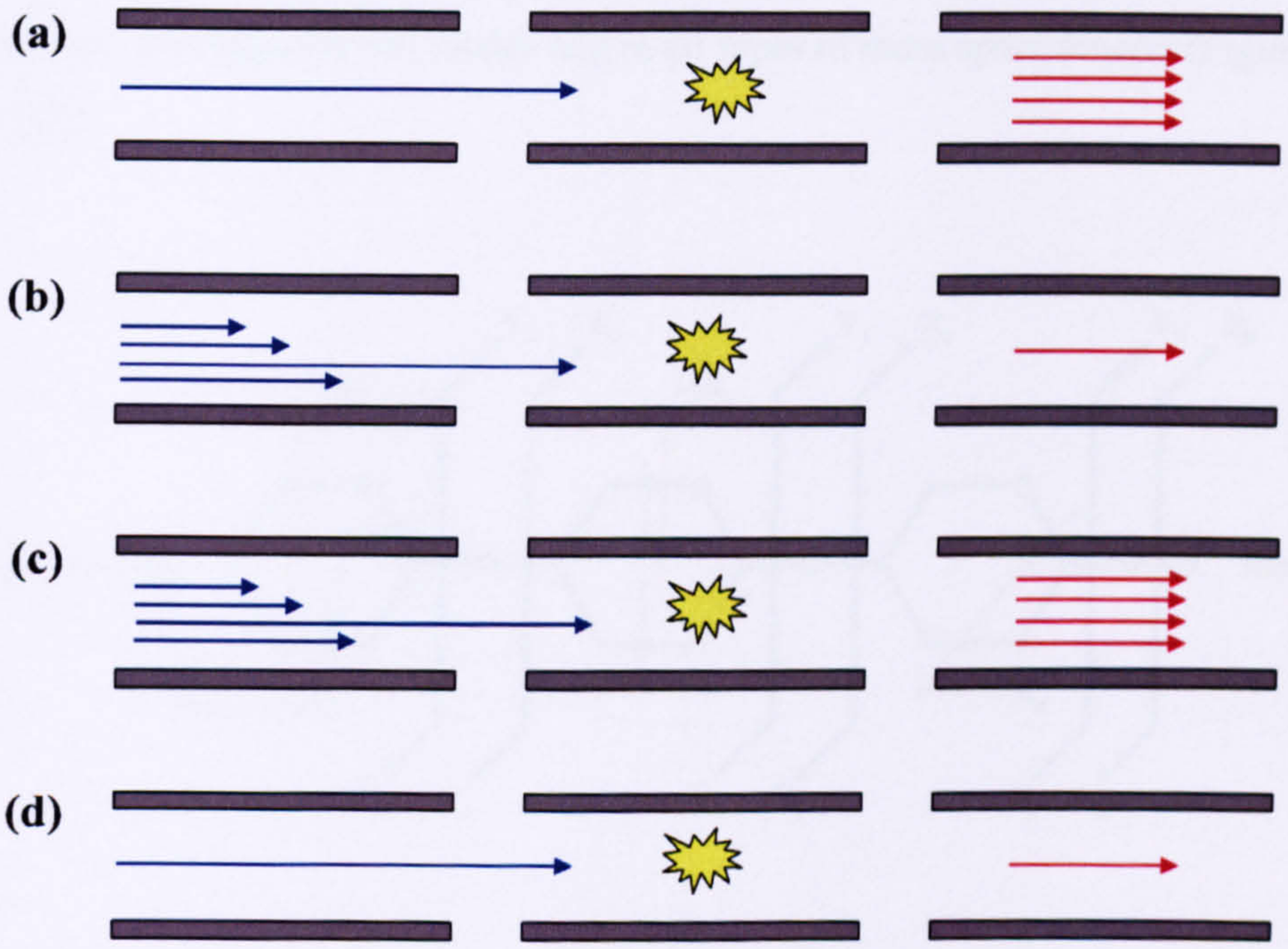

Figure 1.27 Tandem mass spectrometry experiments described using a tandem quadrupole instrument; Q1 and Q2 are quadrupole mass analysers, separated by a collision cell: (a) product ion experiment; (b) precursor ion experiment; (c) neutral loss experiment diagram; (d) selected reaction monitoring experiment.

1.8.5 Carbohydrate fragmentation

Mass spectrometry and tandem mass spectrometry are well-established methods for the analysis of carbohydrates. A systematic nomenclature system for carbohydrate fragmentation has been proposed by Domon and Costello (Domon and Costello, 1988), and the fragmentation is applicable to ions produced in both positive and negative ion modes and in all types of mass spectrometer (Figure 1.28).

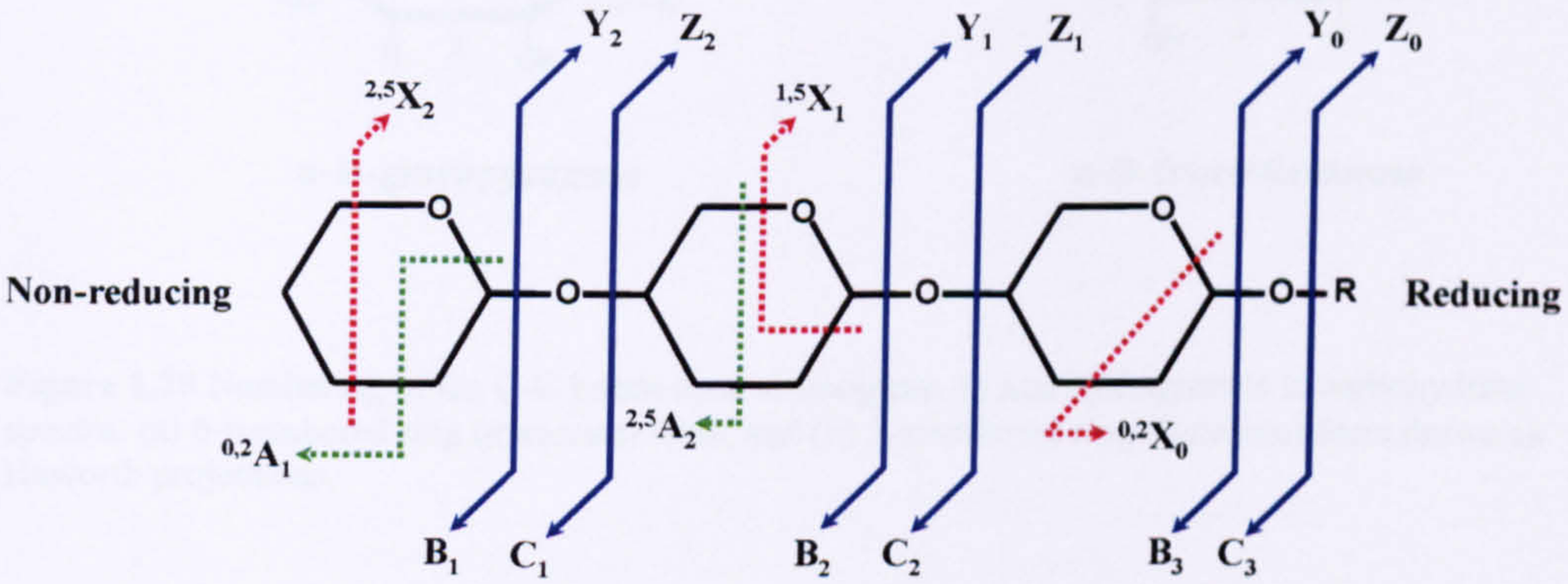

Figure 1.28 Carbohydrate fragmentation showing nomenclature proposed by Domon and Costello (Domon and Costello, 1988). Superscripts indicate which ring bonds were cleaved to give cross-ring A and X ions; subscripts indicate which glycosidic bond was broken counting from the non-reducing terminus or from the reducing terminus or aglycone (glycosidic bond linking to the aglycone is numbered zero).

Fragment ions that result from direct cleavage of the glycosidic bond and that contain a terminal monosaccharide unit (non-reducing terminus) are designated A*i*, B*i* and C*i* ions. The subscripts *i* indicate the number of the glycosidic bond that was cleaved, and this is counted from the non-reducing terminus. Alternatively, fragment ions that contain the aglycone (or the reducing terminus) are designated X*j*, Y*j*, and Z*j* ions. The subscripts *j* indicate the number of the interglycosidic bond that was cleaved, counted from the aglycone (or reducing terminus); the glycosidic bond linking to the aglycone is numbered zero.

In addition, the C-C bonds of the monosaccharide ring can also be cleaved to generate cross-ring fragments. Cross-ring fragments that contain the non-reducing terminus are designated ^{k,l}A*i* ions, and those that contain the aglycone (or reducing terminus) are ^{k,l}X*j* ions. The superscripts *k* and *l* indicate the monosaccharide ring bonds that were cleaved. The numbering of the C-C bonds in a 6-membered ring (pyranose) and 5-membered ring (furanose) forms are represented in Figure 1.29.

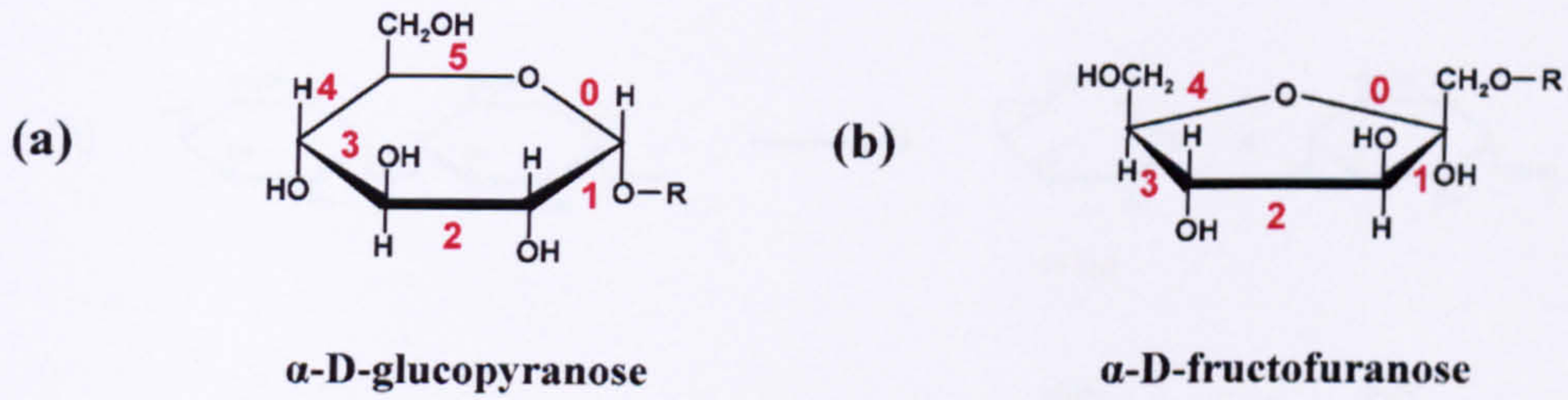

Figure 1.29 Numbering of the C-C bonds used to designate A*i* and X*j* fragments in carbohydrate spectra: (a) 6-membered ring (pyranose) form, and (b) 5-membered ring (furanose) form drawn as Haworth projections.

In the positive ion mode, B*i* ions (oxonium ions) are formed by simple cleavage of the protonated glycosidic bond, and when the cleavage of the glycosidic bond is followed by H-transfer, Y*j* ions are formed (Figure 1.30a). In the negative ion mode, this type of fragmentation follows a more complex pathway. It has been proposed that the deprotonated molecule undergoes epoxide formation accompanied by opening of the ring followed by cleavage of the glycosidic bond to form Y*j* ions; competitive H-transfer may occur to generate B*i* ions (Domon and Costello, 1988) (Figure 1.30b).

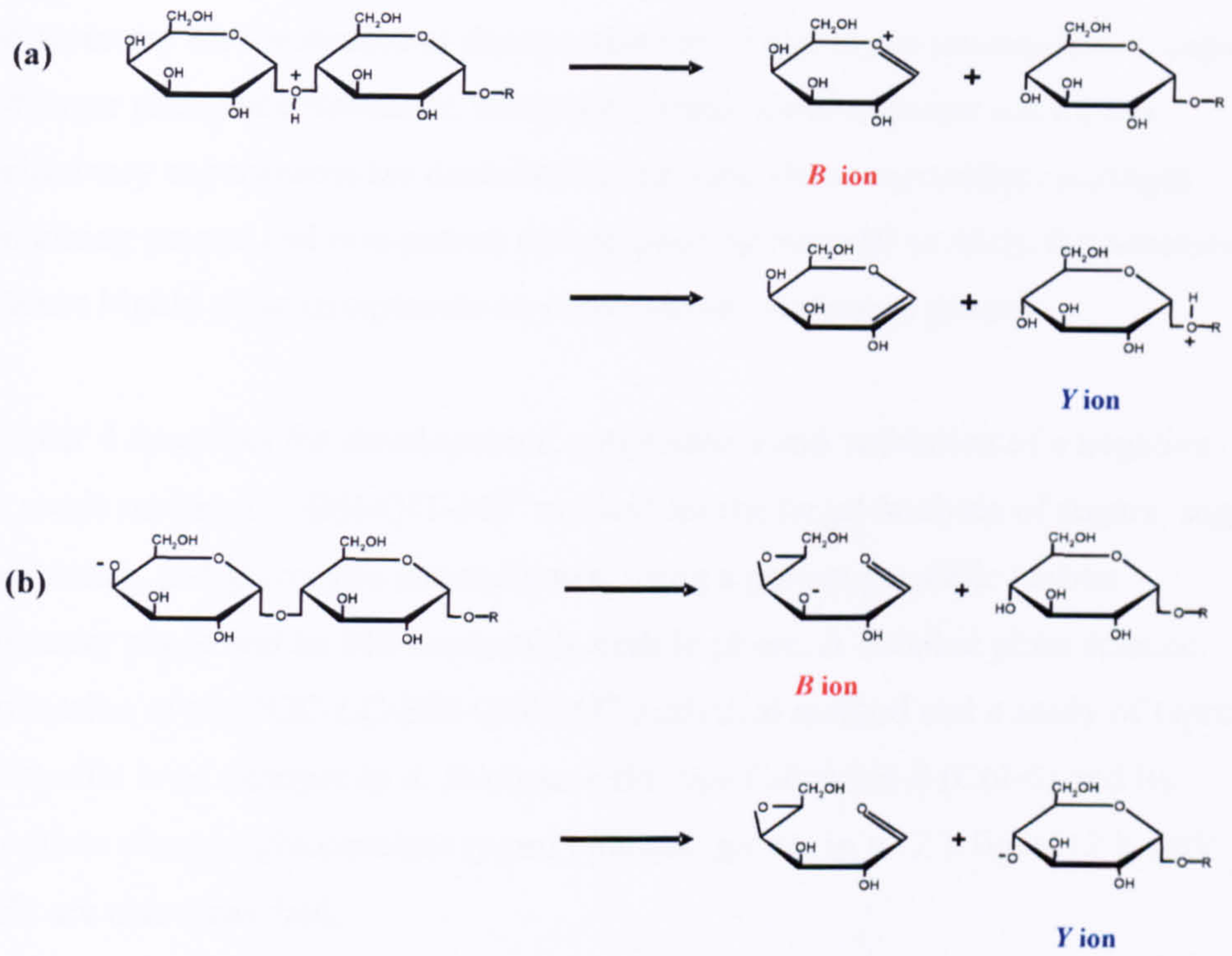

Figure 1.30 (a) Mechanism of formation of oxonium B*i* ions and Y*j* ions in the positive ion mode; (b) mechanism of formation of B*i* and Y*j* ions in the negative ion mode.

1.9 Aims of this thesis

The aim of the work described in this thesis was to develop and implement new LC-MS approaches for studying key plant primary metabolites, using *A. thaliana* as the model system. The methods development aspects described were driven by the need to develop sensitive LC-MS-based methods, able to separate and identify sugars, sugar phosphates, and some glycolytic intermediates, that are predominantly polar compounds. Although *A. thaliana* was used as an ideal model system for establishing and optimising the LC-MS-based separations, the methods developed clearly have applicability for the analysis of these central metabolites in other biological systems.

Chapter 3 describes the use of mass spectrometry and CID tandem mass spectrometry for the structural characterisation of glycolytic intermediates, sugars and sugar phosphate standards, using both positive and negative ion modes. Preliminary experiments are described using solid phase extraction cartridges containing porous and non-porous carbon packing material to study the retention of these highly polar compounds on carbon-based stationary phases.

Chapter 4 describes the development, optimisation and validation of a negative ion mode on-line LC-ESI-QIT-MS^n method for the target analysis of sugars, sugar phosphates, and glycolytic intermediates, using a porous graphitic carbon stationary phase and an MS compatible mobile phase. A detailed plant science application of the PGC-LC-ESI-QIT-MS^n analytical method and a study of typical metabolite level changes in *A. thaliana* wild-type Columbia-0 (Col-0) and its starchless phosphoglucomutase (*pgm1*) mutant, grown in a 12 h light/ 12 h dark cycle are also described.

Chapter 5 describes the development and application of a negative ion mode on-line PGC-ESI-MS^n for studying the changes in carbohydrate levels of *Lupinus albus* stem tissues in response to different water deficit stresses: early stress, severe stress, and rewatering.

Chapter 6 describes the development and use of hydrophilic interaction chromatography for the analysis of carbohydrate-related metabolites from *A. thaliana* wild-type Col-0 and *pgm1* leaf tissues. Data obtained using this method were compared to those obtained using a PGC-LC column, as described in Chapter 4.

Chapter 2

Experimental methods

Chapter 2. Experimental methods

2.1 Plant material

Arabidopsis thaliana ecotype Columbia (Col-0) was used as the wild-type (WT) control throughout the study and *Arabidopsis thaliana* starchless *pgm1* (Caspar et al., 1985) was the mutant line used. Both *A. thaliana* Col-0 and *pgm1* mutant plants were first grown in the greenhouse through a complete life cycle in order to obtain seed stock for further experiments.

Lupinus albus lyophilised plant material (stems) was provided by collaborators at the Plant Sciences Division, Instituto de Tecnologia Química e Biológica (ITQB, Oeiras, Portugal), as part of a major collaborative project entitled 'Screening for stress responsive metabolites'. This project is funded by the British Council under the Treaty of Windsor Anglo-Portuguese Joint Research Programme.

2.1.1 Sowing *Arabidopsis thaliana* on soil

An aliquot (approximately 0.5 mL) of *A. thaliana* seeds was transferred into a 2.0 mL polypropylene microfuge tube containing 0.5-1.0 mL of sterile deionised water. Seeds were cold-treated at 4 °C and imbibed in the dark for four days. Seeds were sown onto F2 compost (Levington Horticulture, Ipswich, UK) in shallow trays consisting of individual 4 x 4 cm pots (P40, Cookson Plantpak, Maldon, UK), with several seeds per pot. A propagator lid was placed on each tray and trays were transferred to a greenhouse set to a long-day photoperiod (16 h light/ 8 h dark, 20-22 °C/17 °C) and photosynthetic photon flux density (PPFD) of 100 μmol m^{-2} s^{-1}. Seedlings were thinned out to one per pot after germination. One week after germination, propagator lids were removed.

2.1.2 Harvesting and storage of *Arabidopsis thaliana* seeds

When siliques began to turn brown, *A. thaliana* plants were prepared for seed harvesting by bagging each plant using waxed bags, one bag per plant. Bags were sealed around the stem with masking tape. When plants had browned completely, the plant stems were cut off at the base, and the bag was sealed completely. Harvesting occurred a week after bagging. Dried plant material was gently hand-pressed from the outside the bag, and the seeds were poured into a fine meshed sieve positioned on a clean piece of paper to remove plant debris. Sieved and cleaned seeds were transferred to labelled polypropylene conical tubes. Tubes containing dried seeds were tightly sealed and stored in the dark at 4 °C.

2.1.3 *Arabidopsis thaliana* seed sterilisation

One klorsept 7 tablet (Jencons Scientific, UK) was dissolved in 14.0 mL of deionised water with 5 µL of Triton X-100 (Sigma, Poole, UK). A solution containing 1.0 mL of the klorsept solution and 9.0 mL of 95% ethanol was prepared and mixed. To each polypropylene microfuge tube (2.0 mL) containing an aliquot of seeds (approximately 0.5 mL), 1.0 mL of the ethanol/klorsept solution was added. The tubes were capped and seeds sterilized for 6 minutes, shaking the tubes every 30 s to1 min. The ethanol/klorsept solution was discarded, leaving the seeds in the polypropylene microfuge tube. Approximately 1.0 mL of 95% ethanol was added to each tube. The tubes were capped, shaken and seeds were allowed to settle. The ethanol was then discarded. The washing step was repeated three times and on the last wash, remaining traces of ethanol were removed using a pipette. Seeds were spread up the sides of the polypropylene microfuge tubes, to aid drying and tubes were left uncapped at the back of the flow hood until dry.

2.1.4 *Arabidopsis thaliana* growth-chamber conditions

A. thaliana WT Col-0 and starchless *pgm1* mutant (Caspar et al., 1985) sterilised seeds were spread over plates containing ½-strength Murashige and Skoog medium (Murashige and Skoog, 1962). Seeds were cold-treated at 4 °C and imbibed in the dark for 4 days. Plates with cold-treated seeds were positioned vertically in a controlled-environment growth chamber set to: long-day photoperiod (16 h light/8 h dark), temperature 22/17 °C, humidity 70/60% (day/night regime), and photosynthetic photon flux density (PPFD) of 150 µmol m^{-2} s^{-1}. Seeds were allowed to germinate into the Murashige and Skoog medium for 9-10 days. Seedlings were then sown onto F2 compost (Levington Horticulture, Ipswich, UK) in shallow trays consisting of individual 4x4 cm pots (P40, Cookson Plantpak, Maldon, UK). A propagator lid was placed on each tray, and trays were transferred to the growth chamber. Rosettes were harvested at developmental growth stage 6.0 (first flower open) (Boyes et al., 2001) and quenched by immediately freezing in the light at the temperature of liquid nitrogen, and stored at -80 °C prior to extraction and analysis.

For the analysis of metabolite changes over the diurnal cycle, *A. thaliana* WT Col-0 and *pgm1* mutant plants were grown in controlled-environment growth chambers set to: photoperiod 12 h light/12 h dark cycle, temperature 22/17 °C, humidity 70/60% (day/night regime), and photosynthetic photon flux density (PPFD) of 150 µmol photons m^{-2} s^{-1}. Five week old rosettes were harvested at the end of the night period, 4 h, 8 h, and 12 h into the light period, and 4 h, and 8 h into the dark period, and again at the end of the night. Plant material was quenched by immediately freezing in liquid nitrogen, and stored at -80 °C prior to extraction and analysis.

2.1.5 Extraction of metabolites from *Arabidopsis thaliana* tissues

Metabolites were extracted from *A. thaliana* plant tissues in trichloroacetic acid (TCA)/ether using a method adapted from Weiner *et al.* (Weiner et al., 1987) and Jelitto *et al.* (Jelitto et al., 1992). Leaf material was ground to a fine powder in liquid nitrogen in a pre-cooled mortar and pestle. Approximately 50 mg frozen plant material was transferred to a polypropylene microfuge tube (2.0 mL) containing 500 µL ice-cold 16% (v/v) TCA in diethylether, vortex-mixed and stored on ice for 30 min. To the tube was added 500 µL 16% (v/v) aqueous TCA containing 5 mM ethylene glycol-bis(2-aminoethylether)-*N,N,N',N'*-tetraacetic acid (EGTA) and the mixture was homogenised and stored on ice for 2 h to achieve complete inactivation of the enzymes and extraction of metabolites. The extract was then centrifuged for 4 min at 17900 *g* at 4 °C and the upper phase discarded. The water phase was washed with 800 µL diethylether saturated with water, centrifuged as above, and the upper phase discarded. The ether washing step was repeated three times. The pH of the extract was then modified with 1 µL 2.5 M KOH aliquots until the pH reached 5-6. The final neutralised extract was then frozen in liquid nitrogen and stored at -80 °C prior to analysis. All plant extracts were centrifuged for 10 min at 17900 *g* at 4 °C and filtered through 0.22 µm Cameo syringe filters (Sigma, Poole, UK) prior to LC-mass spectrometric analysis.

Alternatively, metabolites were extracted from *A. thaliana* plant tissues in chloroform/methanol using a method adapted from Lunn *et al.* (Lunn et al., 2006). Leaf material was ground to a fine powder in liquid nitrogen in a pre-cooled mortar and pestle. Approximately 10 mg frozen plant material was transferred to a polypropylene microfuge tube (2.0 mL) containing 250 µL ice-cold 3:7 (v/v) chloroform/methanol, vortex-mixed, and the frozen mixture was incubated at -20 °C for 2 h to stop metabolism and extract water soluble metabolites, including sugars and sugar phosphates. To the tube was added 200 µL ice-cold water and the tube was warmed to 4 °C with repeated shaking. The extract was then

centrifuged for 10 min at 17900 *g* at 4 °C. The upper aqueous-methanol phase was transferred to a new polypropylene microfuge tube (1.5 mL) and kept at 4 °C. The lower chloroform phase was re-extracted by adding 200 µL ice-cold water, centrifuged as described above and the second aqueous-methanol phase was added to the first. The combined extract was evaporated to dryness using a centrifugal concentrator (Savant SpeedVac system, Thermo Electron Corporation, Runcorn, UK).

Tissue extracts were reconstituted in 100 µL water, centrifuged for 30 min at 6800 *g* at 20 °C, and introduced into sample vials fitted with 100 µL inserts (Thermo Electron Corporation, Runcorn, UK) for porous graphitic carbon (PGC) LC-mass spectrometric analysis.

Tissue extracts were reconstituted in 100 µL 50:50 (v/v) acetonitrile:water, centrifuged for 30 min at 6800 *g* at 20 °C, and filtered through a 0.2 µm PVDF membrane syringe filter (VWR International Ltd, Lutterworth, UK) into sample vials fitted with 100 µL inserts (Thermo Electron Corporation, Runcorn, UK) for hydrophilic interaction chromatography (HILIC) LC-mass spectrometric analysis.

.

2.1.6 *Lupinus albus* growth-chamber conditions

Collaborators at the Plant Sciences Division, Instituto de Tecnologia Química e Biológica (ITQB, Oeiras, Portugal) were responsible for the growth, harvesting, and lyophilisation of *L. albus* plant material prior to extraction and LC-mass spectrometric analysis which was carried out at the University of York (UK). *L. albus* plants (cv. Rio Maior) were cultivated on a sterilised soil, peat, sand mixture (1:1:1, v/v) in controlled-environment growth chambers: photon flux density 290–320 µmol m^{-2} s^{-1} photosynthetically active radiation (PAR), photoperiod (12 h), temperature (19/25 °C, night/day) and relative humidity (65-70%). Twenty-three days after sowing, water deficit (WD) was induced by withholding watering (this caused a natural and slow induction of WD). Plants

were collected 4 and 13 days after withholding water, and 6 and 26 h after rewatering (RW). Control plants were watered throughout the whole period. Sample collection took place 3-5 h after the beginning of the light period. The stem was cut at both extremities (cotyledon level and the shoot/root junction) to separate the vascular (stele) and cortical (cortex) tissues. A small vertical incision produced at the cotyledon extremity allowed the cortex to be peeled off the stele. As the separation occurred at the vascular cambium level, the stele included both the parenchymatous pith tissue and the xylem while the cortex included parenchymatous tissue and the phloem. Stele and cortex tissues were immediately frozen in liquid nitrogen, lyophilised, and stored at -80 °C prior to extraction and LC-mass spectrometric analysis at the University of York (UK).

2.1.7 Extraction of carbohydrates from *Lupinus albus* tissues

Water soluble carbohydrates were extracted from *L. albus* lyophilised stem tissues (cortex and stele) in chloroform/methanol as described in Section 2.1.5. Tissue extracts were reconstituted in 100 µL water, centrifuged for 30 min at 6800 *g* at 20 °C, and introduced into sample vials fitted with 100 µL inserts (Thermo Electron Corporation, Runcorn, UK) for PGC-LC-mass spectrometric analysis.

2.1.8 Characterisation of soil and *Lupinus albus* water status

Collaborators at the Plant Sciences Division, Instituto de Tecnologia Química e Biológica (ITQB, Oeiras, Portugal) characterised the soil and plant water status. The progression of WD was monitored by measuring the soil water content using a ThetaProbe soil moisture sensor (ML2x ThetaProbe coupled with ThetaMeter type HH2 from Delta-T Devices), and the predawn leaf water potential (Ψ_{leafpd}) using a Sholander pressure chamber (PMS instrument Co, Corvallis, Oregon, USA). The effect of WD in leaflets and stems (cortex and stele) was evaluated by

means of relative water content (RWC) according to Rodrigues *et al.* (Rodrigues et al., 1995).

2.2 Graphitic carbons for solid phase extraction

To investigate the retention of sugar phosphates on carbon-based packing materials, Hypersep (Thermo Hypersil-Keystone, Runcorn, UK) solid phase extraction (SPE) columns containing 200 mg of porous graphitic carbon (PGC) and Envicarb (Supelco, Bellefonte, PA, USA) SPE columns containing 250 mg of non-porous graphitic carbon black (GCB) were used for preliminary experiments. Positive pressure from an air line was controlled manually and used to force the liquid over the packing material.

The protocol for elution applied for both porous and non-porous graphitic carbon SPE columns was as follows: (i) the packing material was conditioned with 2.0 mL 80:20 (v/v) acetonitrile:water modified with 0.1% formic acid (FA) followed by 2.0 mL of water; (ii) 1.0 mL of standard solution was applied to each SPE column; (iii) the packing material was washed with 2.0 mL of water; and (iv) compounds were eluted with 2.0 mL of 4:96 (v/v) acetonitrile:water, 10:90 (v/v) acetonitrile:water, 25:75 (v/v) acetonitrile:water, 25:75 (v/v) acetonitrile:water modified with 0.1% FA, and 30:70 (v/v) acetonitrile:water modified with 0.1% FA.

Fractions (1.0 mL) were collected in a polypropylene microfuge tube (1.5 mL), evaporated to dryness using a centrifugal concentrator (Savant SpeedVac, Thermo Electron Corporation, Runcorn, UK), reconstituted in 500 µL 50:50 (v/v) methanol:water and stored at -20 °C prior to ESI-qoaTOF-MS analysis.

2.3 Mass spectrometric analysis

2.3.1 Electrospray quadrupole orthogonal acceleration time-of-flight mass spectrometry (ESI-qoaTOF-MS)

Electrospray quadrupole orthogonal acceleration time-of-flight (ESI-qoaTOF) MS and collision induced dissociation (CID) tandem mass spectrometry (MS/MS) experiments were carried out on an Applied Biosystems API QSTAR Pulsar i mass spectrometer (Foster City, CA, USA). Samples were dissolved in 50:50 (v/v) methanol:water and were continuously infused into the microspray ion source at a flow rate of 0.2 μL/min using the integral syringe driver. The instrument was operated in either positive or negative ion modes over the *m/z* range 50-500. In the positive ion mode, the declustering and focusing potentials were set to 65 and 265 V, respectively, and the capillary voltage to 5800 V. In the negative ion mode, the declustering and focusing potentials were set to -65 and -265 V, respectively, and the capillary voltage set to -3500 V. The collision energy setting for tandem mass spectrometry experiments was varied between 10 and 28 V in positive ion mode and between -8 and -35 V in negative ion mode. Nitrogen was used as the nebulising, curtain and collision gases. Spectra were acquired using the Analyst software, version 1.1 (Applied Biosystems, Foster City, CA, USA).

2.3.2 Electrospray quadrupole ion trap mass spectrometry (ESI-QIT-MS)

Electrospray quadrupole ion trap MS and CID analyses were carried out on an LCQ DECA XP Plus mass spectrometer (Thermo Fisher Scientific, San Jose, CA, USA), equipped with a Thermo Finnigan orthogonal electrospray interface.

Samples were dissolved in 50:50 (v/v) methanol:water and were directly infused into the electrospray ion source using the integrated syringe pump typically set to deliver the solution at a flow rate of 3 μL/min. The negative ion mode was selected for MS and product ion experiments using the following optimised conditions: ion source voltage -3.0 kV, capillary voltage -20 V, tube lens offset -60 V, capillary temperature 250 °C, sheath and auxiliary gases 40 (arbitrary units). Mass spectra were acquired over the scan range *m/z* 50-800. Precursor ions were selected with an isolation width of 2 *m/z* units and activated for 30 ms. CID MS^n experiments used helium as the collision gas and normalized collision energy settings were in the range 20-35%, depending on the compound. Data were processed using Xcalibur 1.3 software (Thermo Finnigan, now Thermo Fisher Scientific, San Jose, CA, USA).

2.4 Liquid chromatography-mass spectrometry

2.4.1 Porous graphitic carbon liquid chromatography electrospray quadrupole ion trap tandem mass spectrometry for the analysis of *Arabidopsis thaliana* leaf tissues (PGC-LC-ESI-QIT-MS^n)

LC-MS analyses were carried out on a Surveyor HPLC coupled to a quadrupole ion trap mass spectrometer (LCQ DECA XP Plus, Thermo Fisher Scientific, San Jose, CA, USA), equipped with a Thermo Finnigan orthogonal electrospray interface. Chromatographic separations were performed on a PGC Hypercarb column (5 μm, 100 mm x 4.6 mm i.d.; Thermo Electron Corporation, Runcorn, UK). The flow rate was 600 μL/min, the sample injection volume was 20 μL and the PGC column was used at ambient temperature (25 °C). The triple stage mobile phase was composed of (A) water, (B) acetonitrile, and (C) 15% aqueous formic acid (FA) (Sigma).

The LC run time was 20 min using the gradient elution profile: 0-5 min, 96% A 4% B to 92% A 8% B; 5-7 min, 92% A 8% B to 75% A 25 % B and maintained for 3 min; 10-20 min, 75% A 25 % B to 25% B 75% C followed by column re-equilibration: 20-22 min, 25% B 75% C to 50% A 50% B and maintained for 5 min; 27-30 min, 50% A 50% B to 96% A 4% B and maintained for 10 min.

The ion trap mass spectrometer was operated in the negative ion mode with the following ionisation conditions: ion source voltage set to -3.0 kV, capillary voltage -20 V, tube lens offset -60 V, capillary temperature 300 °C, sheath gas 40 (arbitrary units) and auxiliary gas 30 (arbitrary units). Mass spectra were acquired over the scan range *m/z* 50-800. Precursor ions were selected with an isolation width of 2 *m/z* units and activated for 30 ms. CID-MS^n experiments used helium as the collision gas and normalized collision energy settings were in the range 20-35%, depending on the compound. Data were processed using Xcalibur 1.3 software (Thermo Finnigan, now Thermo Fisher Scientific, San Jose, CA, USA).

2.4.2 Porous graphitic carbon liquid chromatography electrospray quadrupole ion trap tandem mass spectrometry for the analysis of *Lupinus albus* stem tissues (PGC-LC-ESI-QIT-MS^n)

LC-MS analyses were performed on a Surveyor HPLC system coupled to a quadrupole ion trap mass spectrometer (LCQ DECA XP Plus, Thermo Fisher Scientific, San Jose, CA, USA), equipped with a Thermo Finnigan orthogonal electrospray interface. Chromatographic separations were carried out using a PGC Hypercarb column (5 µm, 100 mm x 4.6 mm i.d.; Thermo Electron Corporation, Runcorn, UK) at a flow rate of 600 µL/min. The sample injection volume was 20 µL and the PGC column was used at ambient temperature (25 °C). Two binary mobile phases were used during method development. Mobile phase 1 was composed of (A) water and (B) acetonitrile. Mobile phase 2 was composed of (A) water containing 0.1% (v/v) FA and (B) acetonitrile containing 0.1% (v/v) FA.

The gradient elution profile was as follows: 0-5 min, 96% A + 4% B to 92% A + 8% B; 5-7 min, 92% A + 8% B to 75% A + 25 % B, and maintained for 3 min, followed by column re-equilibration: 10-12 min, 75% A + 25% B to 50% A + 50% B, and maintained for 4 min; 16-18 min, 50% A + 50% B to 96% A + 4% B and maintained for 10 min. Compounds were detected in the negative ion mode with the ion source voltage set to -3.0 kV, capillary voltage -20 V, tube lens offset -60 V, capillary temperature 300 °C, sheath gas 40 (arbitrary units) and auxiliary gas 30 (arbitrary units). Mass spectra were acquired over the scan range *m/z* 50-1000. Precursor ions were selected with an isolation width of 2 *m/z* units and activated for 30 ms. CID-MS^n experiments used helium as the collision gas and normalized collision energy settings were in the range 20-35%, depending on the compound. Data were processed using Xcalibur 1.3 software (Thermo Finnigan, now Thermo Fisher Scientific, San Jose, CA, USA).

2.4.3 Regeneration of the PGC Hypercarb column (5 µm, 100 mm x 4.6 mm i.d.)

The analytical size PGC Hypercarb column was regenerated using a method described by Thermo (Thermo Electron Corporation, Runcorn, UK). Solvents used for regeneration were HPLC grade and purchased from Fisher (Fisher Scientific, Loughborough, UK). The column was inverted and plumbed into the Surveyor LC system (Thermo Fisher Scientific, San Jose, CA, USA) with the outlet tubing running to waste. 50:50 (v/v) water:tetrahydrofuran (THF) modified with 0.5% trifluoroacetic acid (TFA) (Sigma, Poole, UK) was pumped through the column at a flow rate of 500 µL/min for 30 min. This was followed by 50:50 (v/v) water:THF modified with 0.1 M aqueous NaOH (BDH, Poole, UK) at a flow rate of 500 µL/min for 30 min. 50:50 (v/v) water:THF modified with 0.5% TFA was pumped through the column again at a flow rate of 500 µL/min for 15 min. The column was rinsed with 95:5 (v/v) methanol:water at a flow rate of 900 µL/min for 30 min. The column was re-inverted and plumbed back into the system.

Alternatively, the PGC Hypercarb column was regenerated using a protocol adapted from Reepmeyer and co-workers (Reepmeyer et al., 2005). The column was inverted and plumbed into the Surveyor LC system with the outlet tubing running to waste. The column was back flushed with acetone at a flow rate of 200 µL/min overnight, followed by 95:5 (v/v) methanol:water at a flow rate of 400 µL/min for 60 min. The column was re-inverted and plumbed back into the system.

2.4.4 Hydrophilic interaction chromatography electrospray quadrupole ion trap tandem mass spectrometry for the analysis of *Arabidopsis thaliana* leaf tissues (HILIC-ESI-QIT-MS^n)

HILIC-MS analyses were carried out on a Surveyor HPLC coupled to a quadrupole ion trap mass spectrometer (LCQ DECA XP Plus, Thermo Fisher Scientific, San Jose, CA, USA), equipped with a Thermo Finnigan orthogonal electrospray interface. Chromatographic separations were performed on a zwitterionic ZIC-HILIC stationary phase (3.5 µm, 150 mm x 2.1 mm i.d., SeQuant, Umeå, Sweden). The flow rate was 200 µL/min, the sample injection volume was 0.5 µL, and the HILIC column was used at ambient temperature (25 °C). The solution used for washing the auto sampler syringe and injection needle was composed of 95:5 (v/v) acetonitrile:water.

Mobile phase A was composed of acetonitrile modified with 0.1% (v/v) FA, and mobile phase B was composed of 5 mM ammonium acetate modified with 0.1% (v/v) FA (pH 4), adapted from Cubbon *et al.* (Cubbon et al., 2007). The gradient elution profile started with a linear increase of 10% B to 90% B in 19 min. The mobile phase was allowed to return to the starting conditions within 1 min, followed by column re-equilibration for 10 min. The ion trap MS was operated in the negative ion mode with the ion source voltage set to -3.0 kV, capillary voltage -20 V, tube lens offset -60 V, capillary temperature 300 °C, sheath gas 40 (arbitrary units) and auxiliary gas 30 (arbitrary units). Mass spectra were acquired

over the scan range *m/z* 50-1000. Precursor ions were selected with an isolation width of 2 *m/z* units and activated for 30 ms. CID-MS^n experiments used helium as the collision gas and normalized collision energy settings were in the range 20-35%, depending on the compound. Data were processed using Xcalibur 1.3 software (Thermo Finnigan, now Thermo Fisher Scientific, San Jose, CA, USA).

Chapter 3

Mass spectrometric studies of sugars, sugar phosphates, and glycolytic intermediates, and evaluation of their retention on carbon-based packing materials

Chapter 3. Mass spectrometric studies of sugars, sugar phosphates, and glycolytic intermediates, and evaluation of their retention on carbon-based packing materials

3.1 Introduction

In this chapter, the mass spectrometric behaviour of authentic standard compounds ranging from neutral sugars, to sugar phosphates, and glycolytic intermediates, is described using electrospray ionisation quadrupole orthogonal time-of-flight mass spectrometry (ESI-qoaTOF-MS) in both positive and negative ion modes. Characteristic structural information for each compound was obtained by performing collision induced dissociation (CID) product ion experiments.

Secondly, the retention of authentic standard neutral sugars, sugar phosphates, and glycolytic intermediates on carbon-based packing materials was investigated using both porous graphitic carbon (PGC) and non-porous graphitic carbon black (GCB) solid phase extraction (SPE) columns. The use of SPE columns was a quick and cheap means of evaluating the retention of these compounds on graphitic carbon-based materials, using small volumes of solvents.

These preliminary studies were central to a major study described in the subsequent chapter, aimed at the development and optimisation of an on-line liquid chromatography-mass spectrometry (LC-MS) method using a PGC analytical column for the analysis of sugars, sugar phosphates, and glycolytic intermediates from plant leaf extracts (see Chapter 4).

3.2 Results and discussion

3.2.1 Studies of the mass spectrometric behaviour of sugars, sugar phosphates, and glycolytic intermediates

Standard solutions of a range of different neutral sugars, sugar phosphates and glycolytic intermediates (each 50 μg/mL) were prepared in 50:50 (v/v) methanol:water and each was continuously infused into the ESI source of a quadrupole orthogonal time-of-flight instrument (ESI-qoaTOF-MS), and analysed in positive and negative ion modes (Table 3.1).

In the positive ion mode, protonated molecules $[M+H]^+$ were observed for only the glycolytic intermediate phospho*enol*pyruvate (PEP), detected at *m/z* 169. However, the MS response of these protonated molecules was very low (Table 3.1). Sodiated molecules $[M+Na]^+$ were observed for only the neutral isomeric monosaccharides glucose (Glc) and fructose (Fru), both detected at *m/z* 203, and the neutral isomeric disaccharides Suc and Tre, both detected at *m/z* 365. No signals were observed in positive ion mode ESI-MS analysis for the remaining species. These observations are in agreement to those obtained by March and Stadey in a previous mass spectrometric study of mono- and disaccharides (including Glc, Fru, and Suc) using ESI-qTOF-MS. In that study, positive ion mass spectra of monosaccharides were also dominated by sodiated molecules (March and Stadey, 2005).

In the negative ion mode, ESI-qoaTOF-MS analysis gave better MS response and intense signals for all compounds, which yielded mainly deprotonated molecules $[M-H]^-$ (Table 3.1). Less intense signals for formylated molecules $[M+HCOO]^-$ were also observed for the neutral mono- (Glc, Fru) and disaccharides (Suc, Tre).

Table 3.1 Nominal *m/z* and signal to noise (S/N) values obtained for standard sugars, sugar phosphates, and glycolytic intermediates analysed in positive and negative ion mode ESI-qoaTOF-MS. *nd*, not detected.

Standard compounds	**$[M+H]^+$ (*m/z*)**	**$[M+Na]^+$ (*m/z*)**	**$[M-H]^-$ (*m/z*)**	**$[M+HCOO]^-$ (*m/z*)**
Glucose (Glc)	*nd*	203 (59)	179 (59)	225 (35)
Fructose (Fru)	*nd*	203 (27)	179 (59)	225 (30)
Sucrose (Suc)	*nd*	365 (33)	341 (59)	387 (42)
Trehalose (Tre)	*nd*	365 (27)	341 (59)	387 (40)
Trehalose-6-phosphate (Tre6P)	*nd*	*nd*	421 (59)	*nd*
Sucrose-6-phosphate (Suc6P)	*nd*	*nd*	421 (59)	*nd*
Glucose-1-phosphate (Glc1P)	*nd*	*nd*	259 (59)	*nd*
Glucose-6-phosphate (Glc6P)	*nd*	*nd*	259 (59)	*nd*
Fructose-6-phosphate (Fru6P)	*nd*	*nd*	259 (59)	*nd*
Phospho*enol*pyruvate (PEP)	169 (12)	*nd*	339 (59)	*nd*
Fructose-1,6-bisphosphate (Fru1,6BP)	*nd*	*nd*	167 (59)	*nd*
Pyruvate (Pyr)	*nd*	*nd*	87 (59)	*nd*

Following ESI-qoaTOF-MS analyses of each standard compound, a standard mixture was then prepared in 50:50 (v/v) methanol:water containing seven different analytes (each 50 μg/mL): Glc, Suc, Pyr, PEP, glucose-1-phosphate (Glc1P), trehalose-6-phosphate (Tre6P) and fructose-1,6-bisphosphate (Fru1,6BP). This standard mixture was analysed by ESI-qoaTOF-MS using both positive and negative ion modes (Figure 3.1).

In the positive ion mode ESI-qoaTOF-MS analysis of this standard mixture, only two compounds were observed to ionise, both giving sodiated molecules $[M+Na]^+$: the monosaccharide Glc, detected at *m/z* 203, and the disaccharide Suc, detected at *m/z* 365 (Figure 3.1a). In contrast, in the negative ion mode ESI-qoaTOF-MS analysis of this same standard mixture, all seven compounds were observed to ionise as deprotonated molecules $[M-H]^-$, and less intense signals for formylated molecules $[M+HCOO]^-$ were also observed for the neutral sugars Glc and Suc (Figure 3.1b).

Because the negative ion mode ESI-qoaTOF-MS analysis of this mixture of seven different compounds gave higher ion intensities than positive ion mode, and yielded deprotonated molecules $[M-H]^-$ for all, the negative ion mode was selected for further mass spectrometric experiments. Characteristic structural information for each compound listed in Table 3.2 was obtained by performing CID product ion experiments. Deprotonated molecules $[M-H]^-$ were selected as precursor ions for CID product ion experiments. The nomenclature for carbohydrate fragmentation proposed by Domon and Costello (Domon and Costello, 1988) was used in assigning the CID MS^2 product ion spectra of the neutral and phosphorylated carbohydrates. Diagnostic product ions for each authentic standard compound have been determined and are listed in Table 3.2.

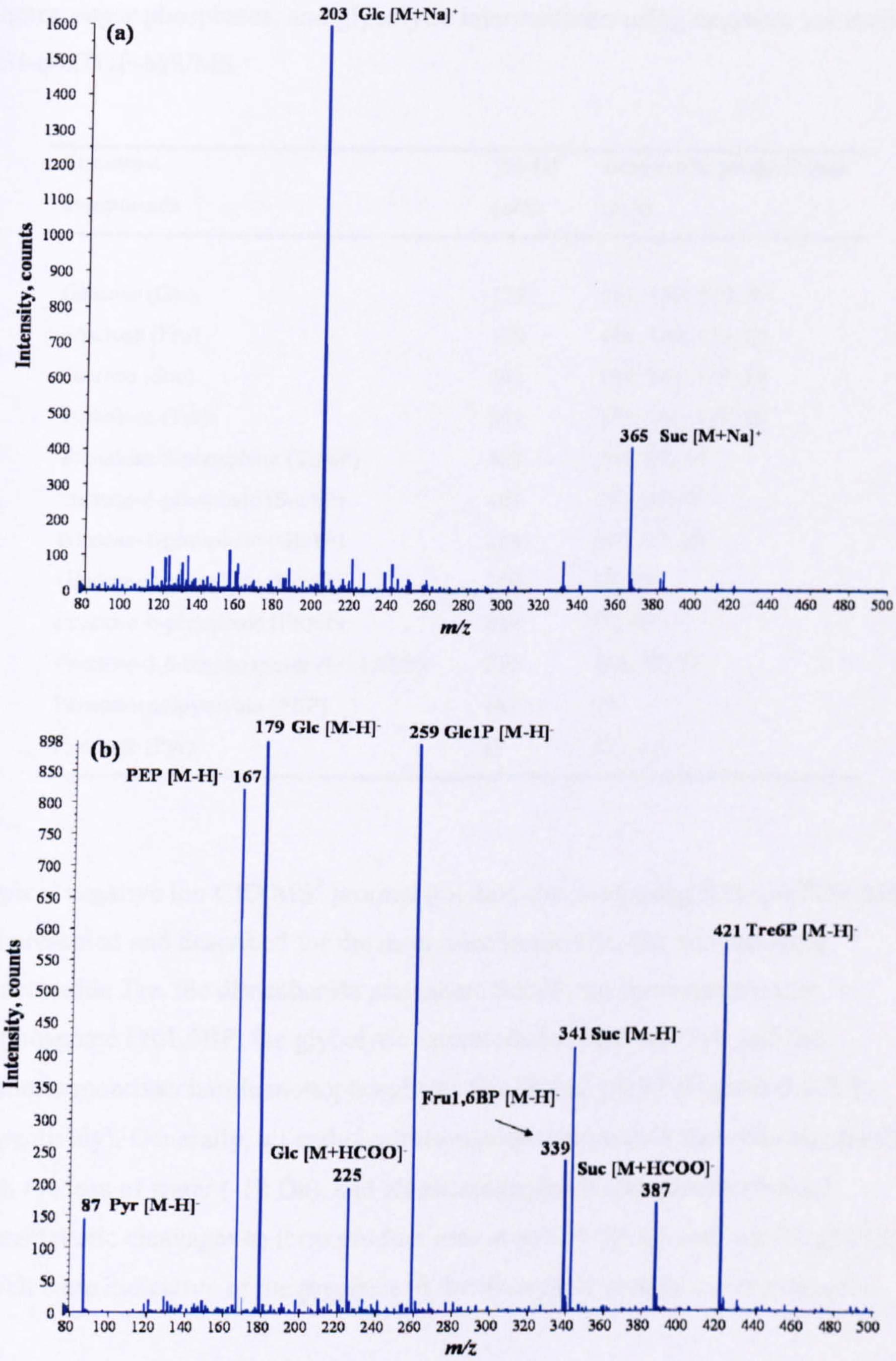

Figure 3.1 (a) Positive ion mode and (b) negative ion mode ESI-qoaTOF-MS analysis of a standard mixture containing: Glc, Suc, Pyr, PEP, Glc1P, Tre6P and Fru1,6BP (each 50 μg/mL).

Table 3.2 Diagnostic product ions (*m/z*) obtained from $[M-H]^-$ of a range of sugars, sugar phosphates, and glycolytic intermediates using negative ion mode ESI-qoaTOF-MS/MS.

Standard compounds	$[M-H]^-$ (*m/z*)	Diagnostic product ions (*m/z*)
Glucose (Glc)	179	161, 149, 119, 89
Fructose (Fru)	179	161, 149, 119, 89
Sucrose (Suc)	341	179, 161, 119, 89
Trehalose (Tre)	341	179, 161, 119, 89
Trehalose-6-phosphate (Tre6P)	421	241, 97, 79
Sucrose-6-phosphate (Suc6P)	421	241, 97, 79
Glucose-1-phosphate (Glc1P)	259	241, 97, 79
Glucose-6-phosphate (Glc6P)	259	97, 79
Fructose-6-phosphate (Fru6P)	259	97, 79
Fructose-1,6-bisphosphate (Fru1,6BP)	339	241, 97, 79
Phosphoenolpyruvate (PEP)	167	79
Pyruvate (Pyr)	87	43

Typical negative ion CID MS^2 product ion data obtained using ESI-qoaTOF-MS are presented and described for the monosaccharide Glc, the non-reducing disaccharide Tre, the disaccharide phosphate Suc6P, the monosaccharide bisphosphate Fru1,6BP, the glycolytic intermediates PEP and Pyr, and the isomeric monosaccharide monophosphates Glc1P and Glc6P (Figures 3.2-3.8, respectively). Generally, all carbohydrate-related compounds showed dehydration with the loss of water (-18 Da), and all phosphorylated compounds showed characteristic cleavages to form product ions at *m/z* 79 $[PO_3]^-$ and *m/z* 97 $[H_2PO_4]^-$ which were indicative of the presence of the phosphate moiety in the molecule.

The CID MS^2 product ion spectrum of Glc ($[M-H]^-$ at *m/z* 179) produced an intense ion at *m/z* 161 which according to the nomenclature for carbohydrate fragmentation proposed by Domon and Costello (Domon and Costello, 1988) corresponds to a B_1 ion formed by the loss of one molecule of water (-18 Da), and multiple cross ring cleavages to form A-type ions at *m/z* 149 ($^{0,1}A_1$), *m/z* 119 ($^{0,2}A_1$), *m/z* 89 ($^{0,3}A_1$), and *m/z* 59 ($^{0,4}A_1$) which are formed by the neutral loss of one, two, three, and four molecules of CH_2O (-30 Da), respectively (March and Stadey, 2005; Taylor et al., 2005). Product ions at *m/z* 131, 101 and 71 correspond to the combined neutral loss of one, two and three molecules of CH_2O (-30 Da), respectively, plus a neutral loss of one molecule of water (-18 Da) as described by March and Stadey in a previous negative ion CID-MS/MS study of monosaccharides using ESI-qTOF-MS (March and Stadey, 2005) (Figure 3.2).

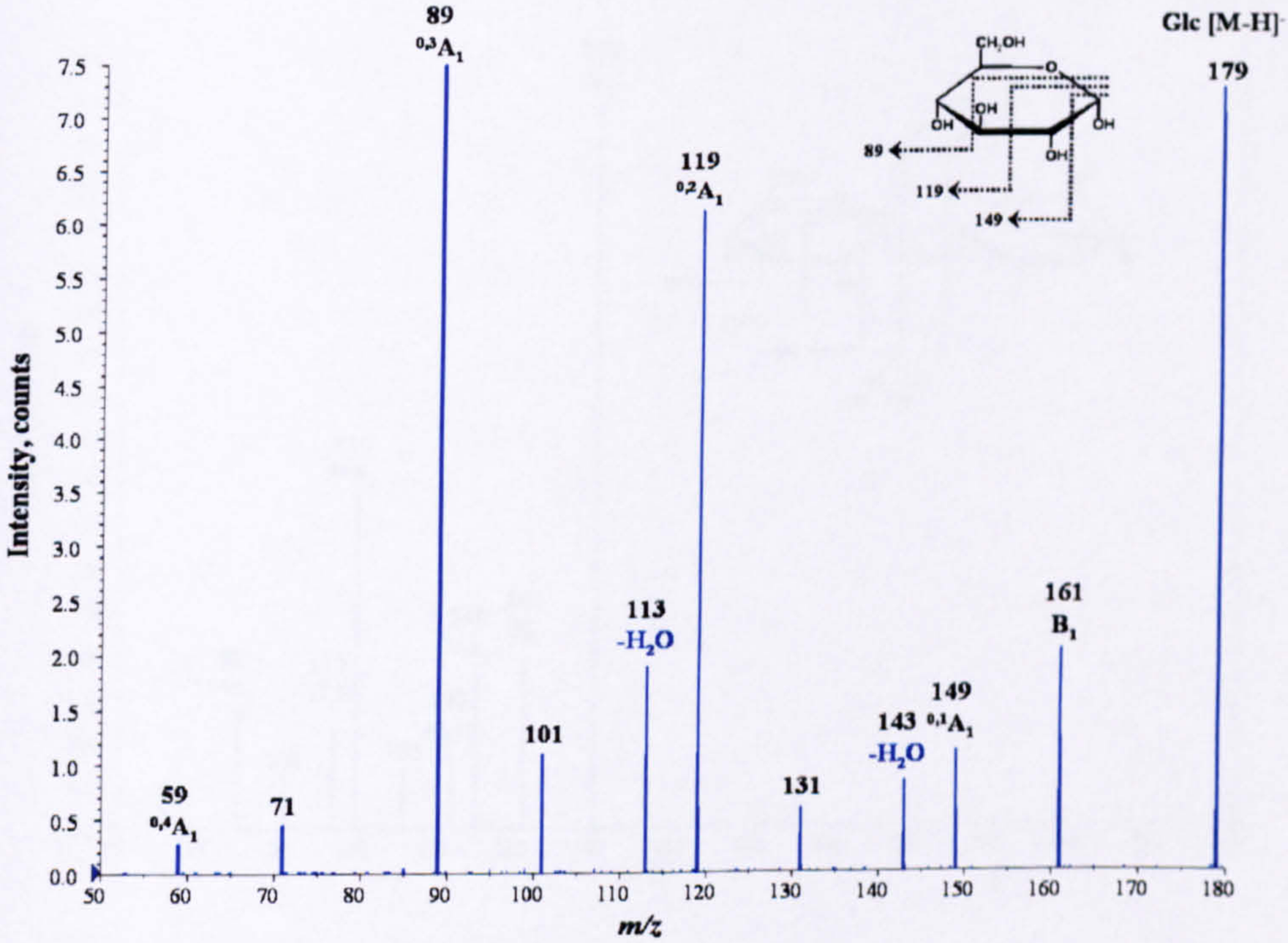

Figure 3.2 CID MS^2 product ion spectrum of Glc ($[M-H]^-$ at *m/z* 179).

The CID MS^2 product ion spectrum of Tre ($[M-H]^-$ at *m/z* 341) produced an intense ion at *m/z* 179 which corresponds to a Y_1 ion formed by cleavage of the glycoside bond and the loss of one hexose moiety $C_6H_{10}O_5$ (-162 Da), a B_1 ion at *m/z* 161 formed by the neutral loss of one monosaccharide $C_6H_{12}O_6$ (-180 Da), and multiple cross ring cleavages to form the A_1 ions at *m/z* 149 ($^{0,1}A_1$), *m/z* 119 ($^{0,2}A_1$), and *m/z* 89 ($^{0,3}A_1$) (March and Stadey, 2005; Taylor et al., 2005). Product ions at *m/z* 131, 101 and 71 correspond to the neutral loss of one monosaccharide $C_6H_{12}O_6$ (-180 Da) and a neutral loss of one, two and three molecules of CH_2O (-30 Da), respectively, as described by March and Stadey in a previous negative ion CID-MS/MS study disaccharides using ESI-qTOF-MS (March and Stadey, 2005) (Figure 3.3).

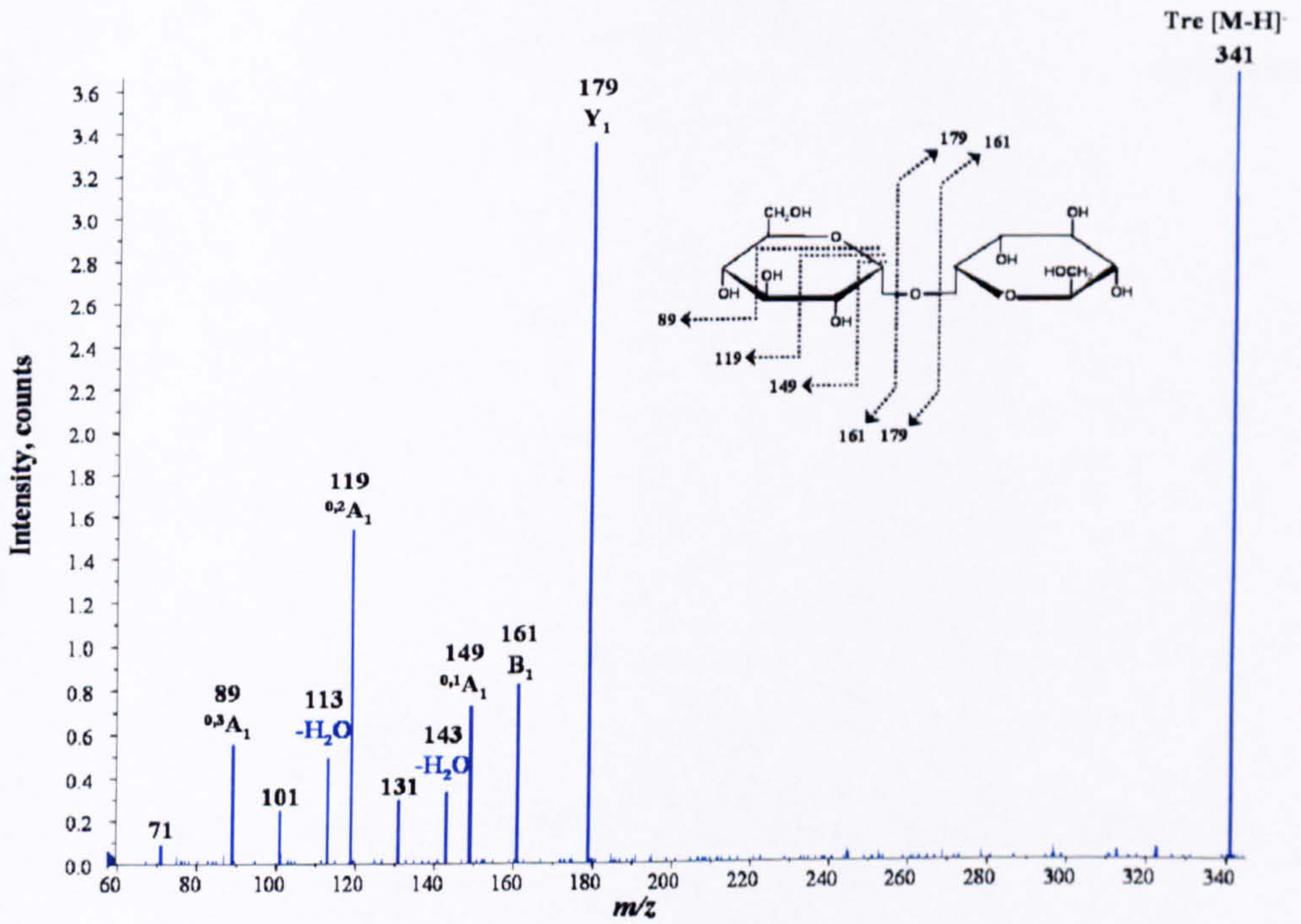

Figure 3.3 CID MS^2 product ion spectrum of Tre ($[M-H]^-$ at *m/z* 341).

The CID MS^2 product ion spectrum of Suc6P ($[M-H]^-$ at *m/z* 421) produced an intense ion at *m/z* 241 which corresponds to a B_1 ion formed by cleavage of the glycosidic bond and the neutral loss of one monosaccharide $C_6H_{12}O_6$ (-180 Da), and a C_1 ion at *m/z* 259 formed by cleavage of the glycoside bond and the loss of one hexose moiety $C_6H_{10}O_5$ (-162 Da). The product ion at *m/z* 181 is formed by the loss of $C_2H_4O_2$ (C_1-C_2, and ring O) from the B_1 ion at *m/z* 241, and the product ion at m/z 139 corresponds to the loss of C_1-C_4 from the B_1 ion at *m/z* 241. The phosphate group gives rise to the product ions at *m/z* 79 $[PO_3]^-$ and *m/z* 97 $[H_2PO_4]^-$ (Figure 3.4). No reports were found in the literature describing the CID-MS/MS analysis of phosphorylated disaccharides.

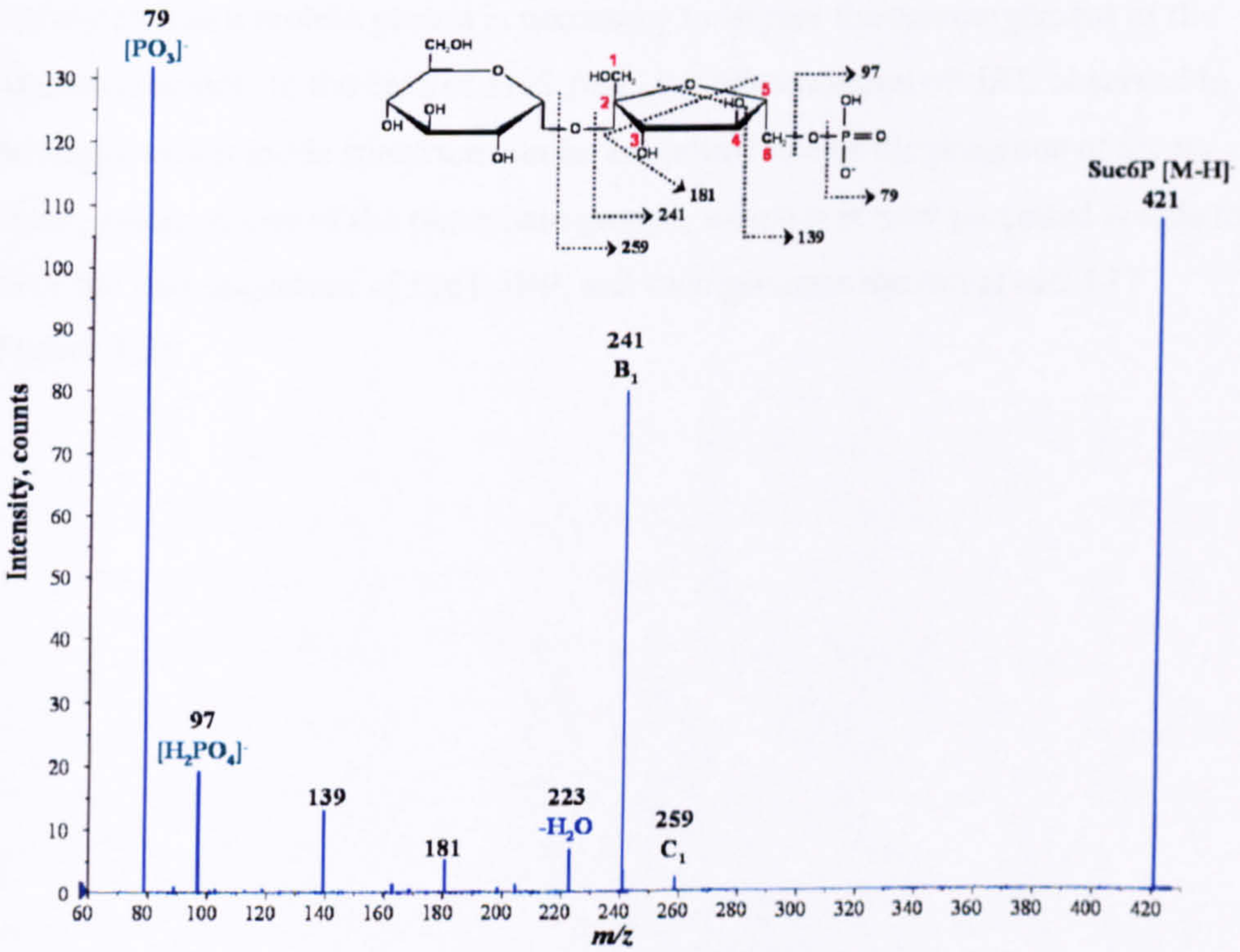

Figure 3.4 CID MS^2 product ion spectrum of Suc6P ($[M-H]^-$ at *m/z* 421).

The CID MS^2 product ion spectrum of Fru1,6BP ($[M-H]^-$ at *m/z* 339) produced an intense B_1 ion at *m/z* 241 which corresponds to the neutral loss of phosphoric acid H_3PO_4 (-98 Da). Product ions at *m/z* 181 and 139 are formed as described above. The product ion at *m/z* 169 corresponds to the loss of C_1-C_3 from the B_1 ion at *m/z* 241, and the product ion at m/z 143 corresponds to the neutral loss of phosphoric acid H_3PO_4 (-98 Da) from the B_1 ion at *m/z* 241. The phosphate groups give rise to the product ions at *m/z* 79 $[PO_3]^-$ and *m/z* 97 $[H_2PO_4]^-$. Curiously, the product ion at *m/z* 177 can be rationalised as arising by loss of a hexose moiety $C_6H_{10}O_5$ (-162 Da), by a process of 'internal residue loss' (IRL). Previous CID-MS/MS studies of oligosaccharides reported by Brüll and co-workers revealed that ions resulting from IRL are not observed in the spectra obtained in the negative ion mode (Brüll et al., 1998). In order to generate these specific ions, it was postulated that a mobile proton is necessary to trigger the rearrangement of the oligosaccharides. In the case of Fru1,6BP, the phenomenon of IRL observed in the negative ion mode spectrum can be explained due to the presence of a very labile proton on one of the phosphate groups, which it is now proposed is able to drive the rearrangement of Fru1,6BP, and thus generate the ion at *m/z* 177 (Figure 3.5).

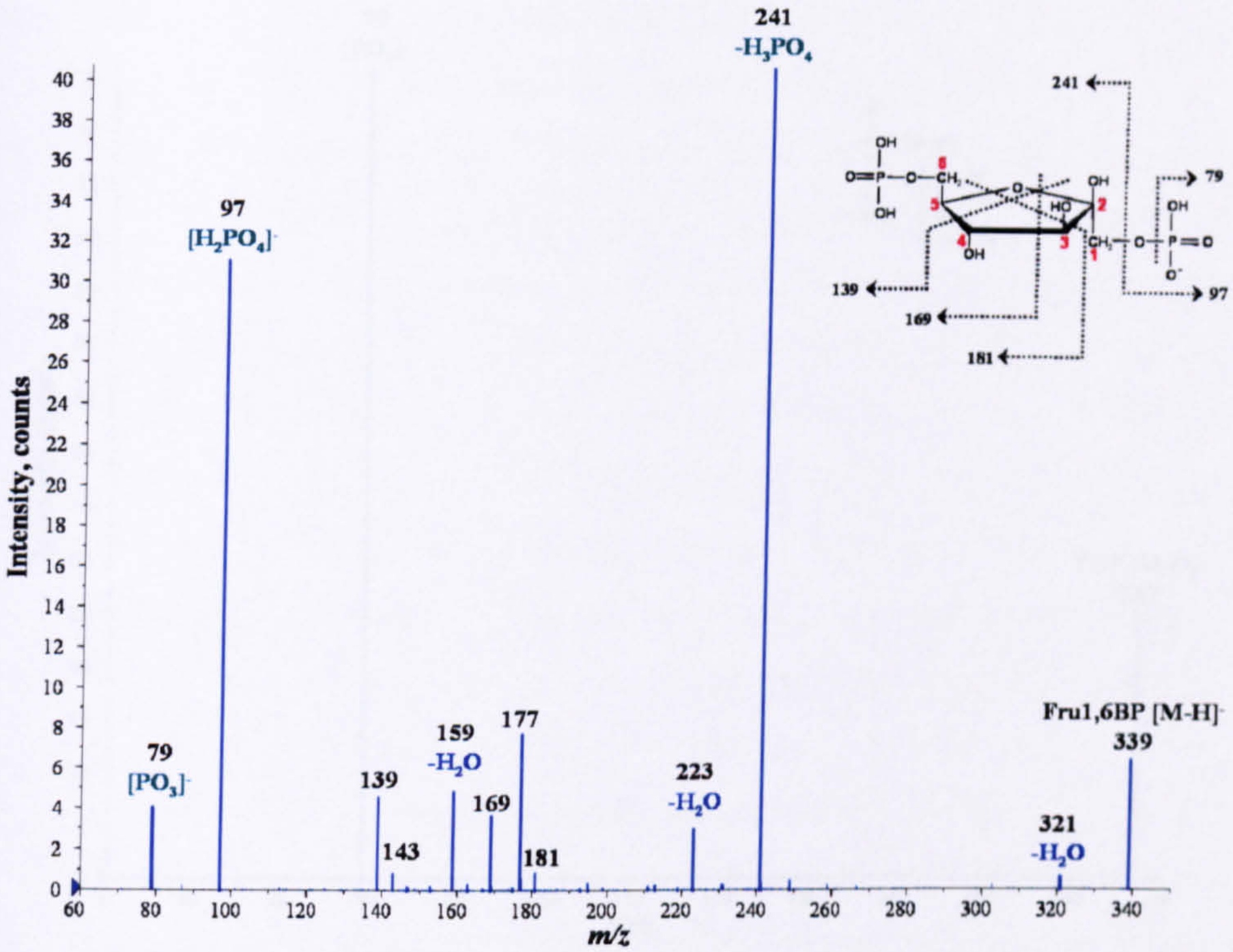

Figure 3.5 CID MS^2 product ion spectrum of Fru1,6BP ($[M-H]^-$ at *m/z* 339).

The CID MS^2 product ion spectrum of PEP ($[M-H]^-$ at *m/z* 167) produced an intense ion at *m/z* 79 due to the phosphate group $[PO_3]^-$ (Figure 3.6). The CID MS^2 product ion spectrum of Pyr ($[M-H]^-$ at *m/z* 87) produced an intense ion at *m/z* 43 due to the loss of CO_2 (- 44 Da) (Figure 3.7).

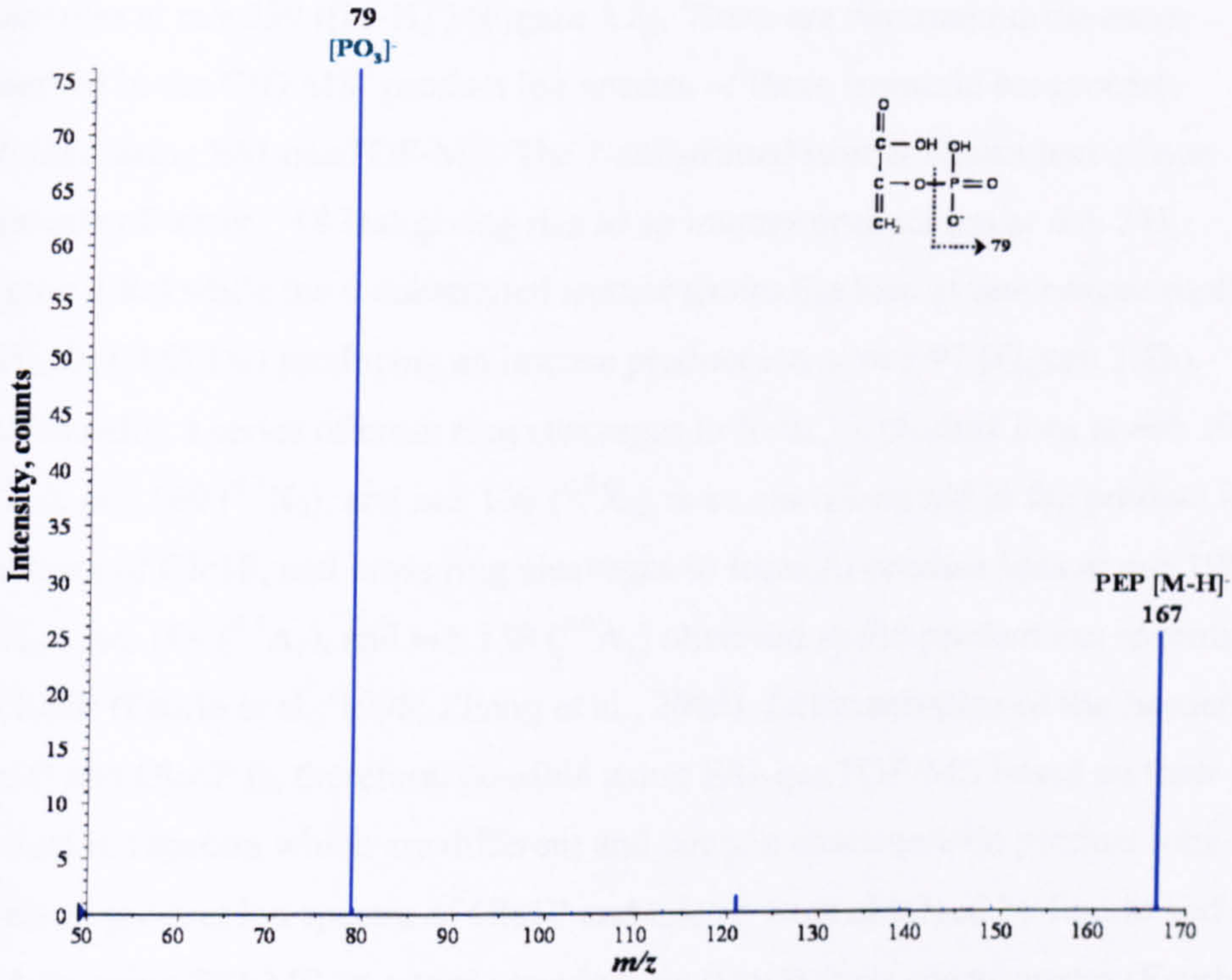

Figure 3.6 CID MS^2 product ion spectrum of PEP ([M-H]$^-$ at *m/z* 167).

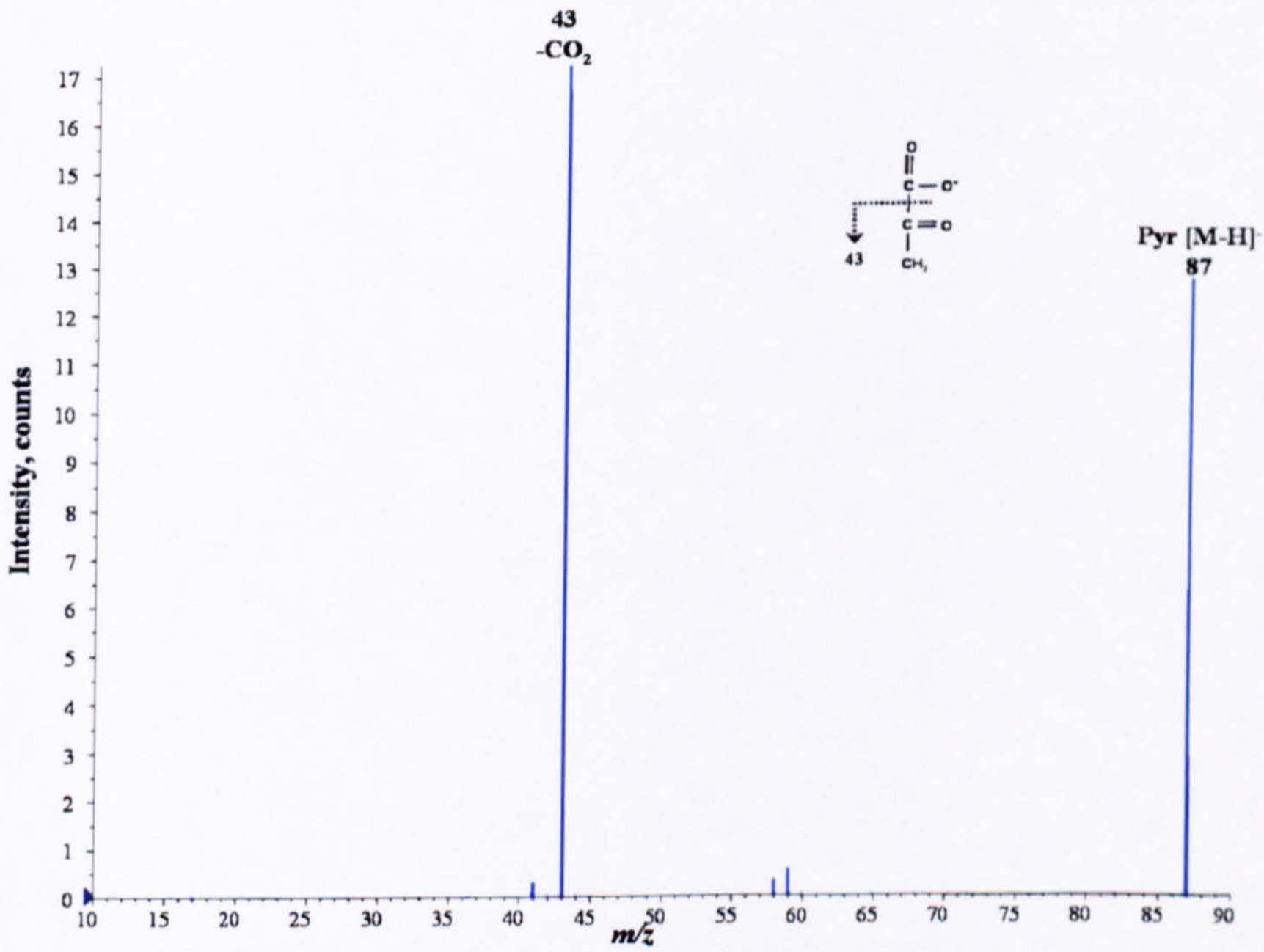

Figure 3.7 CID MS^2 product ion spectrum of Pyr ([M-H]$^-$ at *m/z* 87).

Glc1P and Glc6P are isomeric monosaccharides, detected as deprotonated molecules at *m/z* 259 ($[M-H]^-$) (Figure 3.8). There are two main differences observed in the CID MS^2 product ion spectra of these isomeric compounds obtained using ESI-qoaTOF-MS. The 1-substituted isomer shows loss of one molecule of water (-18 Da) giving rise to an intense product ion at *m/z* 241 (Figure 3.8a) while the 6-substituted isomer shows the loss of one hexose moiety $C_6H_{10}O_5$ (-162 Da) producing an intense product ion at *m/z* 97 (Figure 3.8b). Additionally, a series of cross ring cleavages to form X_0 product ions at *m/z* 199 ($^{0,4}X_0$), *m/z* 169 ($^{0,3}X_0$), and *m/z* 139 ($^{0,2}X_0$) were also observed in the product ion spectrum of Glc1P, and cross ring cleavages to form A_1 product ions at *m/z* 199 ($^{0,2}A_1$), *m/z* 169 ($^{0,3}A_1$), and *m/z* 139 ($^{0,4}A_1$) observed in the product ion spectrum of Glc6P (Feurle et al., 1998; Zhang et al., 2005). Differentiation of the isomers Glc1P and Glc6P is, therefore, possible using ESI-qoaTOF-MS based on their product ion spectra which are different and contain characteristic product ions. Identical product ion spectra of Glc1P and Glc6P were obtained by Feurle and co-workers using ESI-MS on a triple quadrupole (QqQ) mass spectrometer (Feurle et al., 1998).

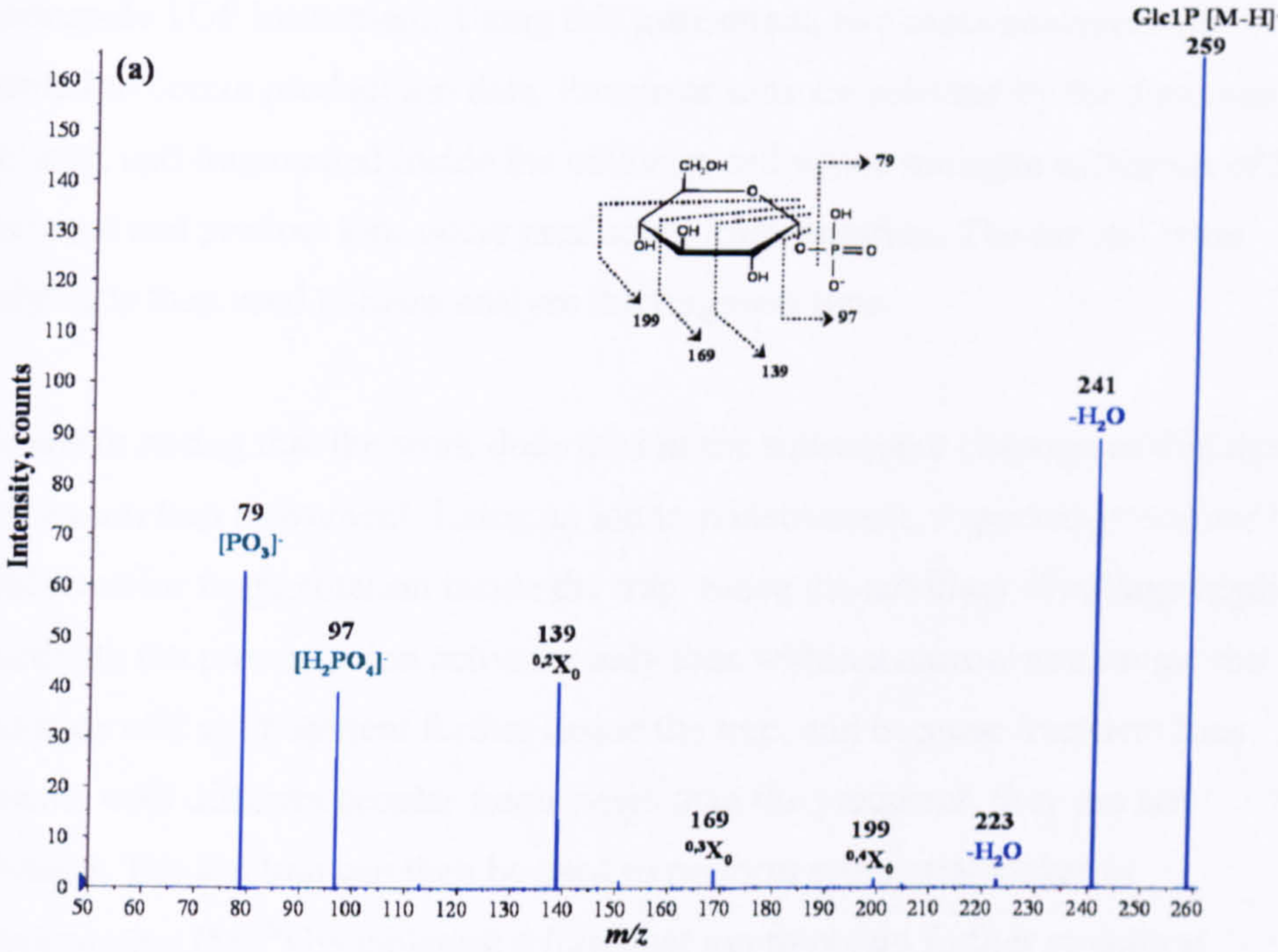

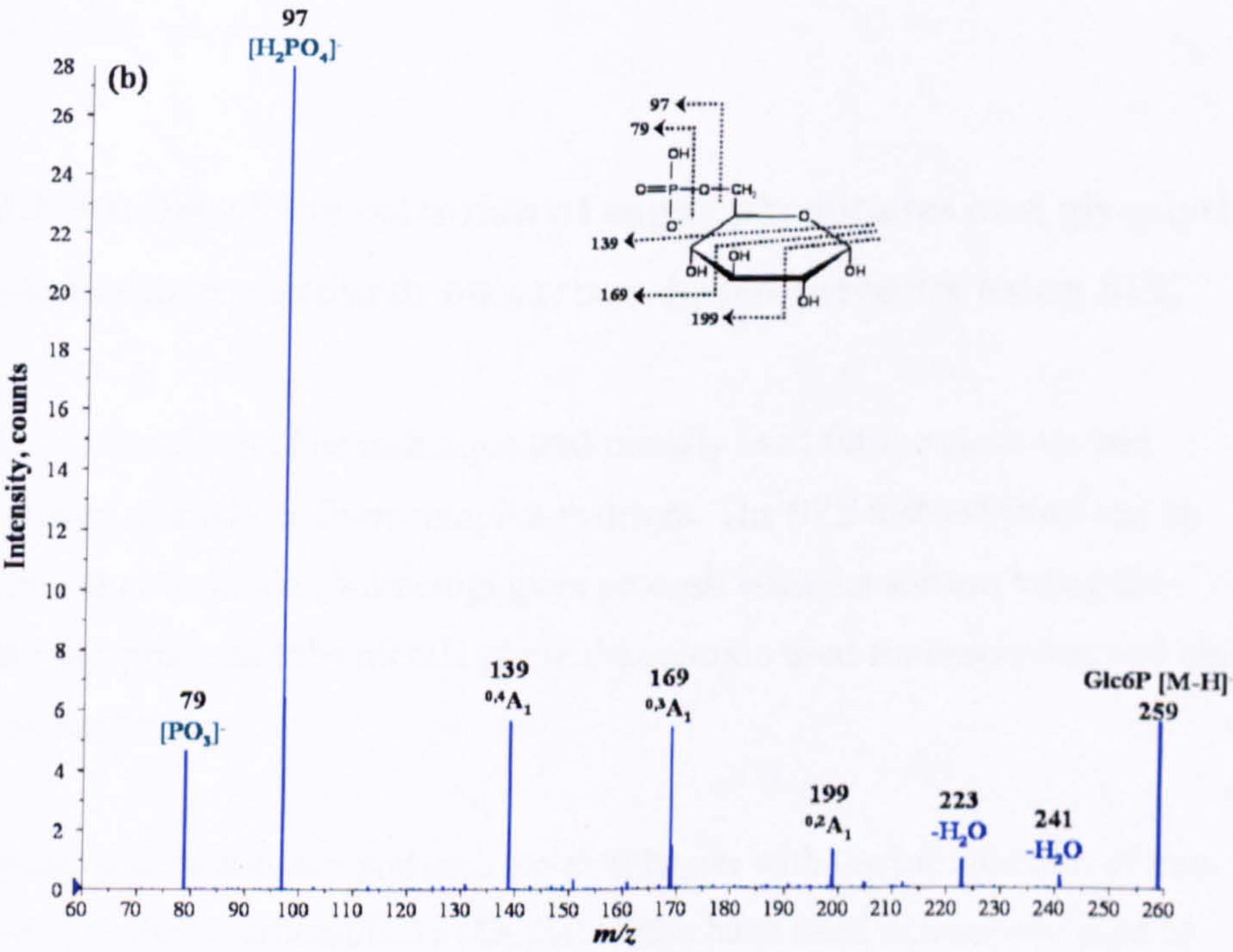

Figure 3.8 Differentiation of the isomeric compounds Glc1P and Glc6P (precursor ion $[M-H]^-$ at *m/z* 259) by ESI-qoaTOF-MS/MS: (a) CID MS^2 product ion spectrum of Glc1P; (b) CID MS^2 product ion spectrum of Glc6P.

All CID product ion spectra described in this section were obtained using a quadrupole TOF instrument. Using this instrument, two mass analysers are coupled to obtain product ion data. Precursor ions are selected by the first mass analyser, and fragmented inside the collision cell where multiple collisions of both precursor and product ions occur producing fragmentation. The second mass analyser is then used to mass analyse the fragment ions.

It is worth noting that the work described in the subsequent chapters of this thesis used an ion trap instrument. Using an ion trap instrument, a specific precursor ion is selected for fragmentation inside the trap. Since the auxiliary rf voltage applied to activate the precursor ion activates only ions within a narrow m/z range, the precursor will not fragment further inside the trap, and because fragment ions resonate with different secular frequencies than the precursor, they are not activated. The ion trap can then be used to perform sequential stages of fragmentation (MS^n) by isolating a fragment ion to obtain further structural information; the same mass analyser is used to carry out the successive stages of analysis.

3.2.2 Studies of the retention of sugar phosphates and glycolytic intermediate standards on carbon-based sorbents using SPE

SPE is a simple and fast technique traditionally used for the clean-up and extraction of analytes from complex matrices. The SPE method itself can be described as a simple chromatographic process, with the sorbent being the stationary phase and the mobile phase the solution used for desorption and elution of the analytes.

The use of carbon-based sorbents for SPE began with the introduction of non-porous graphitic carbon blacks (GCBs) which have been extensively used to extract polar pesticides and other organic pollutants from water (Borra et al., 1986; Di Corcia and Marchetti, 1991). However, non-porous GCB materials have

poor mechanical strength, being too fragile to be used in HPLC. Attempts to improve the structure of these materials led to changes to their preparation process to form a new material which was then called porous graphitic carbon (PGC) (Gilbert et al., 1982; Knox et al., 1986). PGC displayed the mechanical strength required for HPLC, and since then has been successfully used as an HPLC stationary phase under the trade name Hypercarb.

Non-porous GCB sorbents for SPE are commercially available under the trade name Envicarb (Supelco) or Carbograph (Alltech). PGC sorbents for SPE are commercially available under the trade name Hypersep, which is a packing material similar to the HPLC-grade Hypercarb. The use of off-line SPE non-porous GCB (Carbograph) has been previously reported in the literature for the fractionation and purification of oligosaccharides released from glycoproteins (Packer et al., 1998). In that study, it was shown that phosphorylated monosaccharides (Glc6P) and other charged species were retained on a graphitic carbon SPE column, and their elution required at least (25:75, v/v) acetonitrile:water plus the addition of a small amount (0.05%) of dilute acid. In a different study by Redmond and Packer (Redmond and Packer, 1999), SPE non-porous GCB (Carbograph) was used for the separation of different groups of sugar standards, and it was shown that neutral monosaccharides (Glc) were not retained on the graphitic carbon SPE column and were eluted with the water wash; neutral di- (maltose) and trisaccharides (raffinose) and other neutral glycans were successfully retained and eluted with increased ratios of acetonitrile:water.

The use of PGC Hypercarb HPLC columns has been reported in the literature for the separation of a wide range of different mono-, di- and oligosaccharides (Koizumi et al., 1991; Davies et al., 1993; Fan et al., 1994; Koizumi, 1996; Robinson et al., 2007). However, their use for the separation of phosphorylated carbohydrates and glycolytic intermediates has been restricted to only a few compounds, such as Glc6P, Fru6P, 2-phosphoglycerate (2PG) and 3-phosphoglycerate (3PG) (Buchholz et al., 2001).

In this section, the use of off-line PGC Hypersep and non-porous GCB Envicarb SPE columns is described as a quick and cheap approach to investigate the retention of the less documented sugar phosphates and glycolytic intermediate compounds on carbon-based packing materials. These experiments were preliminary to the development of an on-line PGC-LC-MS method for the analysis of these compounds from plant leaf extracts (see Chapter 4).

The sample used in the first SPE experiment designed to test this, was an aqueous standard mixture containing: a monosaccharide (Glc), a disaccharide (Tre), a monosaccharide phosphate (Glc1P), and a glycolytic intermediate (Pyr) at a concentration of 50 μg/mL per compound. This standard mixture was applied to both porous and non-porous SPE columns and allowed to run into the graphitic carbon material. The columns were then rinsed with water (water wash) and elution of the compounds was achieved by applying gradients composed of different ratios of acetonitrile:water and acetonitrile:water containing 0.1% (v/v) of formic acid (FA) (see Chapter 2). The elution of the various components was determined by collection of the different fractions and their analysis using negative ion mode ESI-qoaTOF-MS.

On both porous and non-porous graphitic carbon SPE columns Glc ($[M-H]^-$ at *m/z* 179; $[M+HCOO]^-$ at *m/z* 225) was not retained and appeared in the water wash (Figure 3.9). The disaccharide Tre ($[M-H]^-$ at *m/z* 341; $[M+HCOO]^-$ at *m/z* 387) eluted with 4:96 (v/v) acetonitrile:water (Figure 3.10). The monosaccharide phosphate Glc1P ($[M-H]^-$ at *m/z* 259) eluted only when the organic content was 25:75 (v/v) acetonitrile:water and in the presence of 0.1% FA (Figure 3.11). These results are consistent with previous studies reported in the literature (Packer et al., 1998; Redmond and Packer, 1999). Pyr was strongly retained on both porous and non-porous graphitic carbon materials, and its elution was not observed using the elution conditions tested.

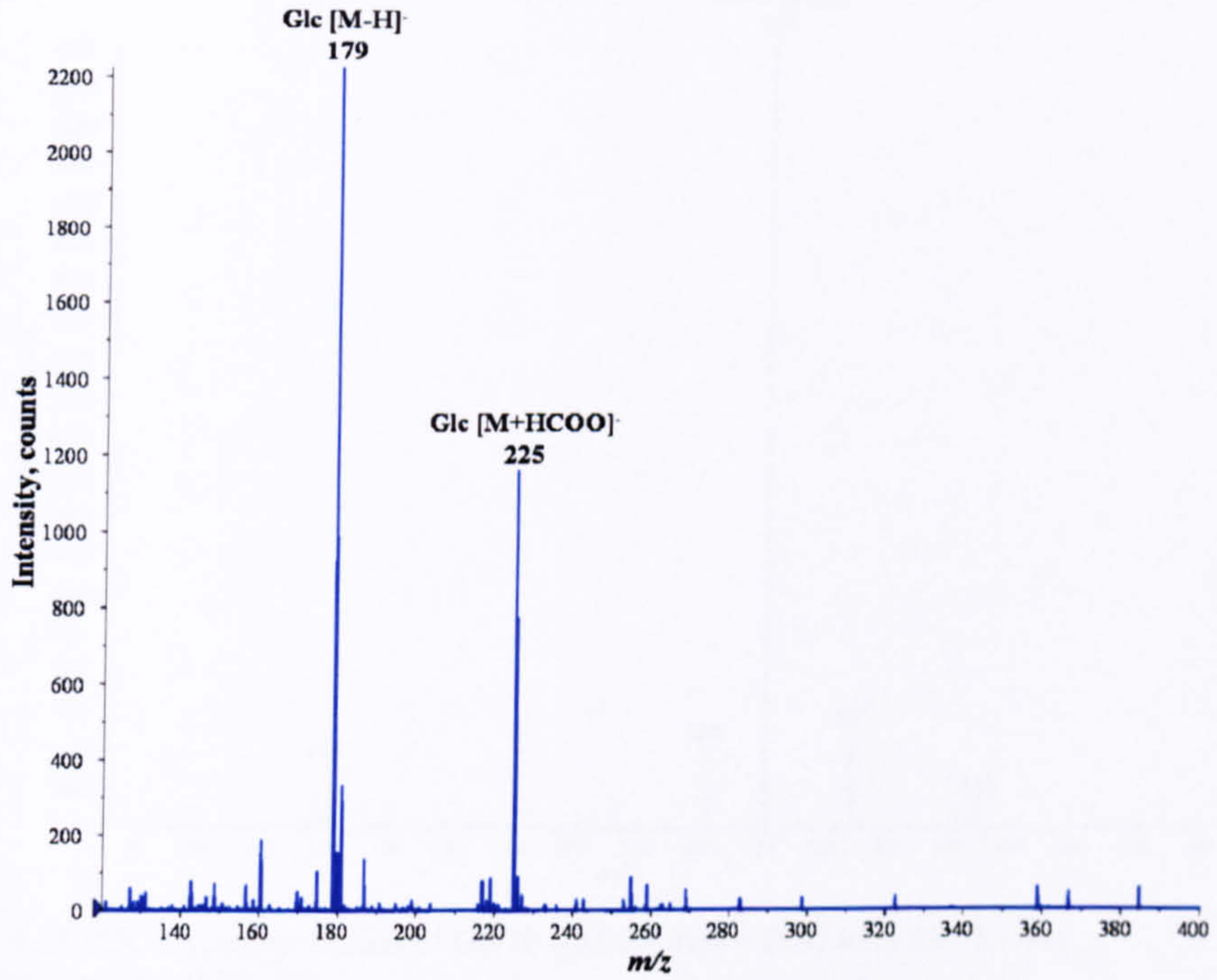

Figure 3.9 PGC Hypersep did not retain Glc ($[M-H]^-$ at *m/z* 179; $[M+HCOO]^-$ at *m/z* 225) which was washed through with the water wash.

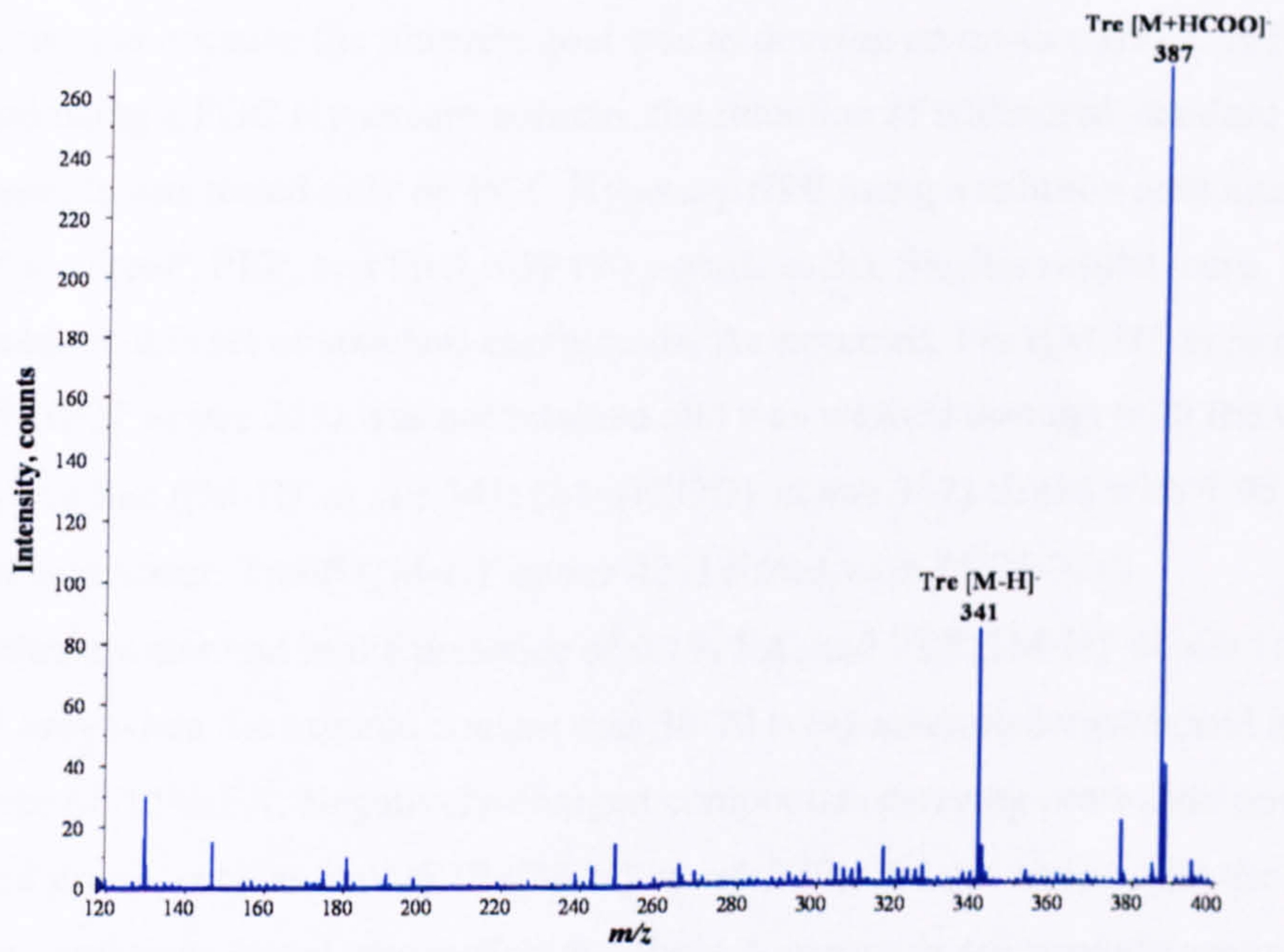

Figure 3.10 PGC Hypersep elution of Tre ($[M-H]^-$ at *m/z* 341; $[M+HCOO]^-$ at *m/z* 387) with 4:96 (v/v) acetonitrile:water.

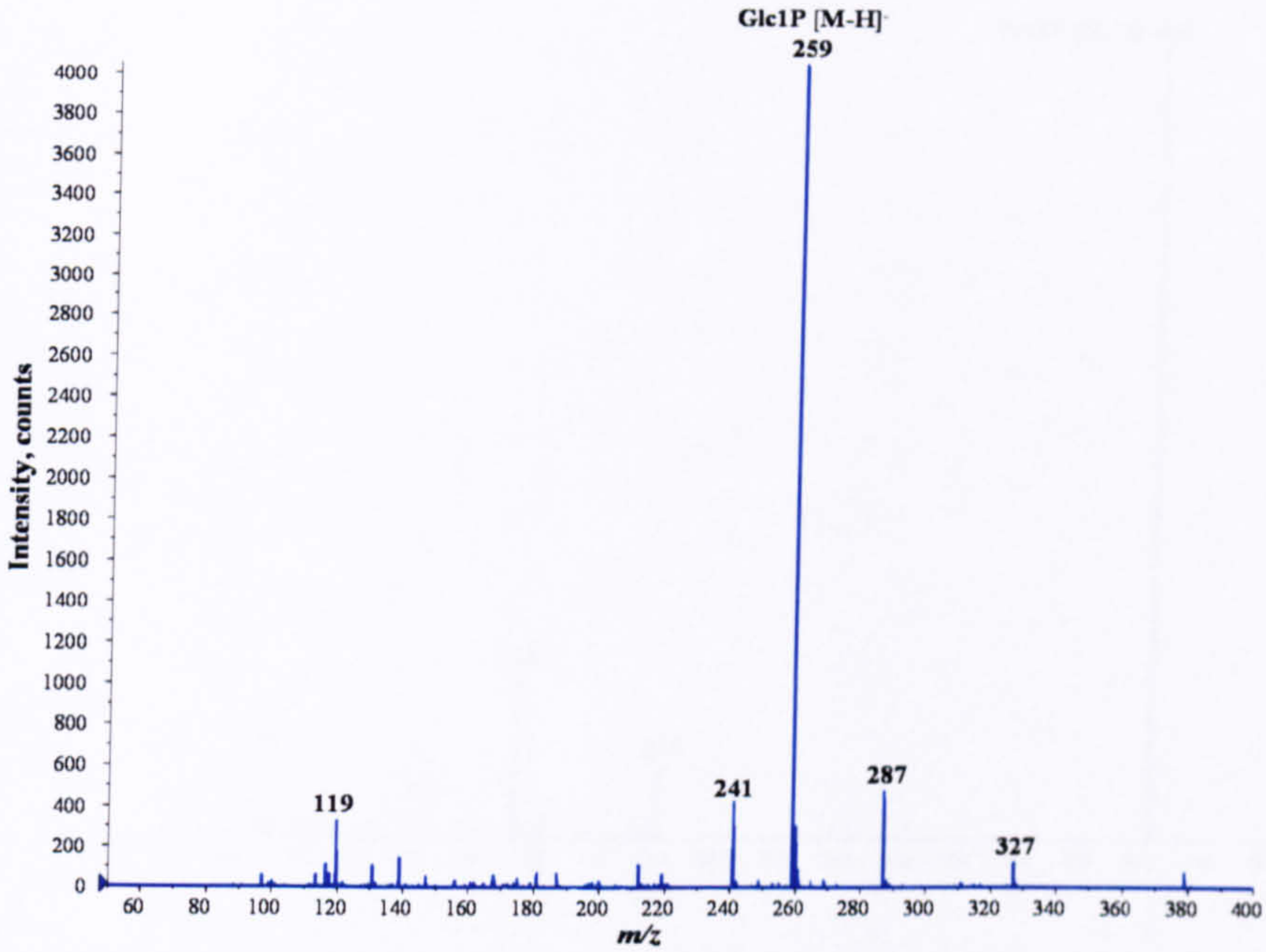

Figure 3.11 PGC Hypersep elution of Glc1P ([M-H]$^-$ at *m/z* 259) with 25:75 (v/v) acetonitrile:water + 0.1% FA.

Non-porous GCBs are not commercially available as HPLC-grade analytical columns, and because the ultimate goal was to develop an on-line HPLC-MS method using a PGC Hypercarb column, the retention of additional standard compounds was tested only on PGC Hypersep SPE using a solution containing: Fru, Suc, Tre6P, PEP, and Fru1,6BP (50 µg/mL each). Similar results were obtained for this set of standard compounds. As expected, Fru ([M-H]$^-$ at *m/z* 179; [M+HCOO]$^-$ at *m/z* 225) was not retained and was washed through with the water wash, and Suc ([M-H]$^-$ at *m/z* 341; [M+HCOO]$^-$ at *m/z* 387) eluted with 4:96 (v/v) acetonitrile:water. Tre6P ([M-H]$^-$ at *m/z* 421) eluted with 25:75 (v/v) acetonitrile:water and in the presence of 0.1% FA, and PEP ([M-H]$^-$ at *m/z* 167) eluted only when the organic content was 30:70 (v/v) acetonitrile:water and in the presence of 0.1% FA. Negatively-charged compounds carrying more than one charged group, such as Fru1,6BP ([M-H]$^-$ at *m/z* 339), did not elute under the elution conditions tested, suggesting that these compounds are strongly retained on both porous and non-porous graphitic carbon materials.

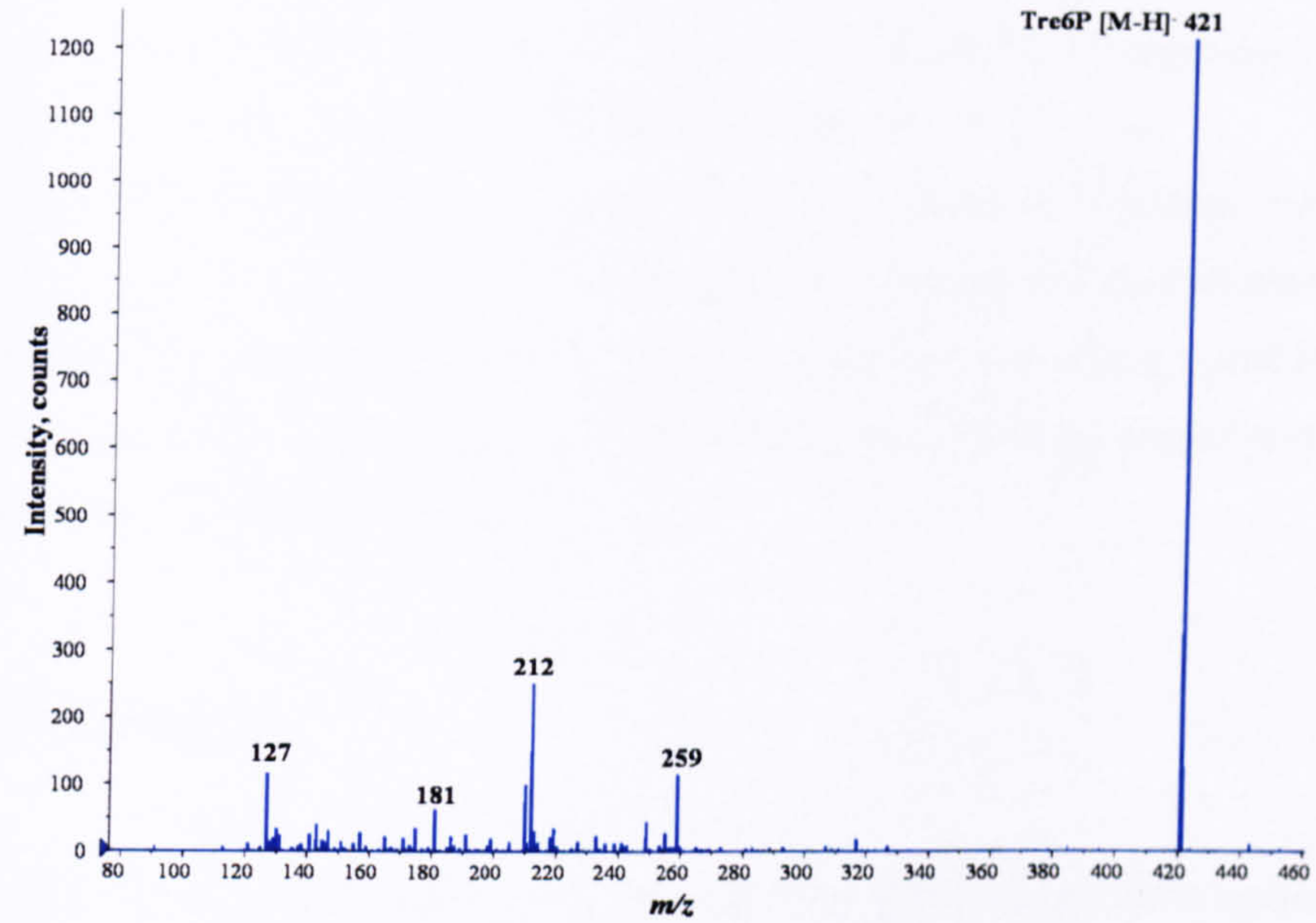

Figure 3.12 PGC Hypersep elution of Tre6P ($[M-H]^-$ at *m/z* 421) with 25:75 (v/v) acetonitrile:water + 0.1% FA.

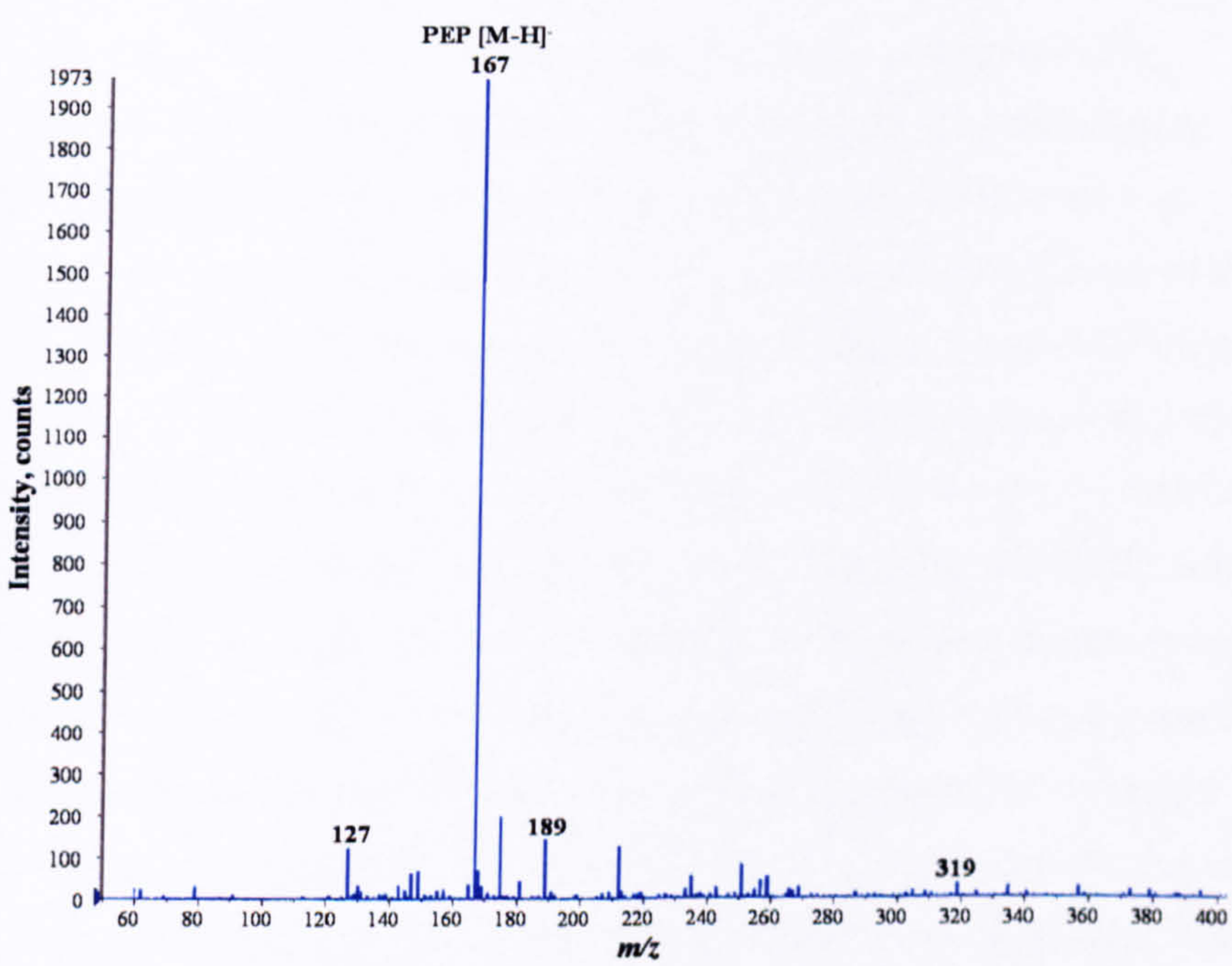

Figure 3.13 PGC Hypersep elution of PEP ($[M-H]^-$ at *m/z* 167) with 30:70 (v/v) acetonitrile:water + 0.1% FA.

From these SPE experiments, an elution order can be drawn up: neutral monosaccharides (Glc, Fru) < neutral disaccharides (Suc, Tre) < monosaccharide phosphates (Glc1P) < disaccharide phosphates (Tre6P) < PEP. The monosaccharide bisphosphate Fru1,6BP and the glycolytic intermediate Pyr were strongly retained on these graphitic carbon-based materials and their elution was not observed, suggesting that elution conditions stronger than those tested in these SPE experiments may be needed to elute these compounds (e.g., proportion of acid modifier higher than 0.1%).

3.3 Conclusions

No signals for negatively charged compounds were obtained on direct infusion positive ion mode ESI-qoaTOF-MS analyses of a mixture containing Glc, Suc, Tre6P, Glc1P, Fru1,6BP, PEP and Pyr. In the negative ion mode, signals for all seven components were obtained. Therefore, negative ion mode was selected for further collision induced dissociation (CID) tandem mass spectrometry experiments. CID-MS/MS experiments were performed on each authentic standard compound and their characteristic fragmentation behaviour was determined. The results obtained from the SPE experiments demonstrated that neutral disaccharides and phosphorylated carbohydrates are successfully retained on both porous and non-porous graphitic carbons. It was also shown that mobile phases composed of different ratios of acetonitrile:water proved too weak to elute the negatively-charged compounds (Glc1P, Tre6P, PEP, and Fru1,6BP), and only neutral disaccharides were successfully eluted from the porous and non-porous graphitic carbons. The presence of small amounts of formic acid in the mobile phase was necessary to elute the more strongly retained negatively-charged compounds Glc1P, Tre6P, and PEP from both porous and non-porous graphitic carbons. Disadvantages associated with the use of carbon-based packing materials is their poor retention of small monosaccharides (Glc, Fru), and strong retention of more highly charged species (e.g., Fru1,6BP), which require the use of high concentrations of acid modifier to elute.

Chapter 4

Porous graphitic carbon liquid chromatography electrospray ion trap mass spectrometry for the analysis of sugars, sugar phosphates, and glycolytic intermediates from *Arabidopsis thaliana* leaf tissues

The work described in this chapter has been published in:

Journal of Chromatography A, 1172 (2007) 170-178

Carla Antonio[a], Tony Larson[b], Alison Gilday[b], Ian Graham[b], Ed Bergström[a] and Jane Thomas-Oates[a]

[a] Department of Chemistry,
University of York,
UK

[b] Centre for Novel Agricultural Products,
Department of Biology,
University of York,
UK

Chapter 4. Porous graphitic carbon liquid chromatography electrospray quadrupole ion trap tandem mass spectrometry for the analysis of sugars, sugar phosphates, and glycolytic intermediates from *Arabidopsis thaliana* leaf tissues (PGC-LC-ESI-QIT-MS^n)

4.1 Introduction

Glycolytic intermediates and sugar phosphates are central compounds in metabolism and signalling pathways. They are important intermediates of cellular energy metabolic pathways, such as glycolysis, the pentose phosphate pathway, and starch and sucrose synthesis in plants. However, due to their high polarity, low *in vivo* concentrations, structural variety, poor UV absorbance, and rapid metabolic turnover (de Koning and van Dam, 1992), these compounds are a particularly challenging class of compounds within the plant metabolome to analyse. Glycolytic intermediates and sugar phosphates in plants have been traditionally measured using highly sensitive techniques such as enzymatic assays (Stitt et al., 1989). Such assays offer the advantage of being very specific, which at the same time is their primary disadvantage; it is not possible to perform parallel determinations of different metabolites in the same sample. To overcome this, mass spectrometry (MS), combined with on-line separations, typically liquid chromatography (LC) and gas chromatography (GC), has been widely applied in metabolome analysis allowing the detection and identification of a wide range of metabolites in a single run (Sumner et al., 1996; Fiehn et al., 2000; Roessner et al., 2000; Roessner et al., 2001a; Fiehn, 2002; Huhman and Sumner, 2002; Fiehn, 2003; Roessner-Tunali et al., 2003; Desbrosses et al., 2005). Moreover, the low limits of detection and the ability to perform tandem MS experiments providing structural information from unknowns (compounds for which standards are not run) separated from plant extracts has made MS a popular choice. Glycolytic

intermediates and sugar phosphates are non-volatile and unstable compounds, and to analyse this class of metabolites by gas chromatography coupled to MS (GC-MS), derivatisation is required. The main disadvantage associated with derivatisation protocols is the time and sample losses associated with the additional step in sample handling; in many cases, LC-MS methods are used to avoid the derivatization step. However, in LC-MS applications, the column chemistry most widely used is reversed-phase (RP) C_{18}, and highly polar metabolites, such as carbohydrates, sugar phosphates and intermediary metabolites, are poorly retained or completely unretained on these columns, and generally elute close to the void volume without chromatographic separation (Dunn and Ellis, 2005; Sumner, 2006).

One suitable approach for the analysis of underivatised carbohydrate-related compounds is high performance anion-exchange liquid chromatography (HPAEC) with pulsed amperometric detection (PAD) (Townsend et al., 1989; Lee, 1990, 1996). HPAEC-PAD has been widely used for the analysis of sugar phosphates and other intermediary metabolites from animal tissues (Swezey, 1995), *Escherichia coli* cell extracts (Bhattacharya et al., 1995), yeast (Smits et al., 1998; Groussac et al., 2000), potato (de Bruijn et al., 1999), and more recently from *Arabidopsis thaliana* tissues (Sekiguchi et al., 2004). Nonetheless, the mobile phases used with commercial HPAEC systems (Dionex) contain high concentrations of sodium hydroxide and sodium acetate, and therefore are not directly MS compatible. The high ionic strength suppresses sample ionisation and causes ion source contamination, thus compromising sensitivity (Barroso et al., 2002). Post-column membrane suppressors were developed by Dionex that were designed to remove the salt from the mobile phase following separation (Niessen et al., 1993; Wunschel et al., 1997). Although using this approach on-line coupling of HPAEC with MS has been reported for the analysis of glycolytic intermediates in yeast (van Dam et al., 2002) and more recently, for the sensitive measurement of trehalose-6-phosphate (Tre6P) from *A. thaliana* tissues using HPAEC coupled to a triple quadrupole MS (Lunn et al., 2006), this coupling is not effective and robust enough to make on-line coupling with ESI-MS routinely

applicable, especially for highthroughput analyses. Alternative LC-MS methods have been reported for the analysis of these polar compounds based on new column chemistries and efficient on-line coupling with electrospray ionisation mass spectrometry. A β-cyclodextrin-bonded stationary phase was used for the separation of various commercially available sugar phosphates by LC-ESI-MS (Feurle et al., 1998). Although chromatographic resolution of the isomeric compounds glucose-1-phosphate (Glc1P) and glucose-6-phosphate (Glc6P) was not achieved, these compounds could be differentiated by tandem MS based on their characteristic product ion spectra. Hydrophilic interaction liquid chromatography (HILIC) coupled to ESI-MS was used for the analysis of highly polar compounds, such as oligosaccharides and sugar nucleotides, from *Cucurbita maxima* phloem tissues (Tolstikov and Fiehn, 2002), and a C_{18} silica-based monolithic capillary column coupled to ESI-MS was applied for plant metabolomics using *A. thaliana* tissues (Tolstikov et al., 2003). Although these LC-MS methods have proven to be powerful tools for the analysis of highly polar compounds, their application to the targeted analysis of glycolytic intermediates and sugar phosphates from plant tissues has yet to be tested (see Chapter 6).

Porous graphitic carbon (PGC) was developed as an alternative to the commonly used RP silica packings (Gilbert et al., 1982; Knox et al., 1986). PGC stationary phases have advantages over classical silica-based columns of stability over the entire pH range 0-14*, and over HPAEC columns of using 'MS friendly' mobile phases without ion-pairing reagents. Knox and Ross defined the retention mechanism as the polar retention effect on graphite (PREG), determined by hydrophobic eluent-analyte interactions, and electronic interactions of polarizable (or polarized) functional groups in the analyte with the delocalized π-electrons of the graphite surface (Knox and Ross, 1997). Due to this retention mechanism, carboxylic acids are commonly used as additives in the mobile phase to provide adequate anions for electronic interaction with the π-electrons of PGC, and therefore elute more retained compounds (Lim, 1989; Elfakir et al., 1998; Mercier

* pH range for silica-based columns stability 2-7.

et al., 1999; Xing et al., 2004). Elfakir and co-workers investigated the behaviour of different carboxylic acids for the separation of inorganic ions on a PGC column and they found that the elution strength decreased in the following order: heptafluorobutyric acid> trifluoroacetic acid (TFA)> formic acid> acetic acid (Elfakir and Dreux, 1996). The use of PGC columns has been reported for the separation of mono-, di- and oligosaccharides (Koizumi et al., 1991; Davies et al., 1993; Fan et al., 1994; Koizumi, 1996; Barroso et al., 2002), polar compounds (Hennion et al., 1995), positional isomers (Wan et al., 1995), oligosaccharide branch isomers (Lipniunas et al., 1996), some pairs of isomeric glycolytic intermediates such as Glc6P/Fru6P, and 2-phosphoglycerate and 3-phosphoglycerate (2PG/3PG) from *E. coli* cell extracts (Buchholz et al., 2001), conjugated estrogen isomers (Reepmeyer et al., 2005), and more recently for the study of endogenous underivatised water-soluble oligosaccharides extracted from *Triticum aestivum* stems (Robinson et al., 2007).

4.1.1 Aim

The work described in this chapter is part of a collaborative project entitled 'CHEMCELL, Chemical Biology in Reactors and cells', and was carried out in collaboration with Prof. Ian Graham's group, in the Centre for Novel Agricultural Products (CNAP), Department of Biology, University of York. This project was funded by a Marie Curie Early Stage Research Training Fellowship of the European Community's Sixth Framework Programme under contract number MEST-CT-2004-504345. This chapter describes the development of a robust on-line PGC-LC-ESI-MS^n method using a quadrupole ion trap instrument for the simultaneous targeted quantitation of glycolytic intermediates, soluble sugars and sugar phosphates from *A. thaliana* leaf tissues and an MS compatible mobile phase. *A. thaliana* was used as a model system (The Arabidopsis Genome Initiative, 2000) for establishing and optimising the PGC-LC-MS-based method and demonstrating its utility for the analysis not only of commercial standards but also of complex biological samples.

4.2 Results and discussion

4.2.1 PGC-LC-ESI-QIT-MS^n method development

Standard compounds were separated on a PGC column without derivatization and detected using negative ion mode electrospray quadrupole ion trap mass spectrometry. The negative ion mode was chosen because in preliminary investigations (Chapter 3), in the positive ion mode ESI-qoaTOF-MS analysis of a standard mixture containing glucose (Glc), Suc, Tre6P, Glc1P, fructose-1,6-bisphosphate (Fru1,6BP), phospho*enol*pyruvate (PEP) and pyruvate, only Glc and Suc were observed to ionise, both giving sodiated molecules $[M+Na]^+$; in the negative ion mode analysis of this same standard mixture, all seven compounds were observed to ionise as deprotonated molecules $[M-H]^-$ and formylated molecules $[M+HCOO]^-$ (neutral sugars).

LC separation was optimised using mobile phases composed of different ratios of acetonitrile:water and a standard solution containing a mixture of some of the intermediary metabolites that commonly occur in plants. This mixture was constituted in order to contain representatives of the main compound types: neutral monosaccharide (Glc), neutral disaccharide (Suc), a monosaccharide monophosphate (Glc6P), a disaccharide monophosphate (Tre6P), a monosaccharide bisphosphate (Fru1,6BP), and a glycolytic intermediate (PEP).

Using a mobile phase composed only of acetonitrile and water proved too weak to elute the negatively-charged compounds (Glc6P, Tre6P, Fru1,6BP, and PEP), and only Glc and Suc were successfully eluted from the PGC column. These results were in accordance with those obtained on our preliminary experiments using graphitic carbon-based SPE columns (Chapter 3). To elute the strongly retained compounds, it was found to be essential to include anionic modifiers in the aqueous mobile phase for competitive interaction with the negatively-charged

phosphate groups for the π-electrons of PGC (Lim, 1989; Packer et al., 1998; Redmond and Packer, 1999). The effect of anionic modifiers was investigated by adding increasing amounts of formic acid or acetic acid to the aqueous mobile phase until satisfactory separation for all compounds was achieved.

Figure 4.1 shows the extracted ion chromatograms obtained on negative ion mode PGC-LC-ESI-QIT-MS of a standard solution containing Glc, Suc, Glc6P, Tre6P, Fru1,6BP, and PEP (50 µg/mL each), using a mobile phase composed of acetonitrile and water modified with 10% of acetic acid (Figure 4.1a), and using a mobile phase composed of acetonitrile containing the equivalent proportion of formic acid (Figure 4.1b). Negatively-charged compounds were detected as deprotonated molecules $[M-H]^-$, and neutral sugars were detected as acetylated $[M+CH_3COO]^-$ or formylated $[M+HCOO]^-$ molecules depending on whether acetic acid or formic acid was present in the mobile phase, respectively.

Formic acid has been reported to have higher elution strength than acetic acid (Elfakir and Dreux, 1996). The presence of formate anions in the mobile phase provided better MS responses and better peak shapes for all compounds than a mobile phase containing the equivalent proportion of acetate anions (Figure 4.1). Therefore, formic acid was used for further mobile phase optimisations. TFA was not evaluated due to its well documented incompatibility with ESI-MS (Apffel et al., 1995; Kuhlmann et al., 1995; Gustavsson et al., 2001).

It was observed that the negatively-charged diphosphate compounds interacted so strongly with the PGC surface that the addition of 10% of formic acid was still not enough to elute these compounds from the PGC column (Figure 4.1b). Elution of all the negatively charged compounds was achieved only when the proportion of formic acid added to the aqueous mobile phase was 15% (Figure 4.2).

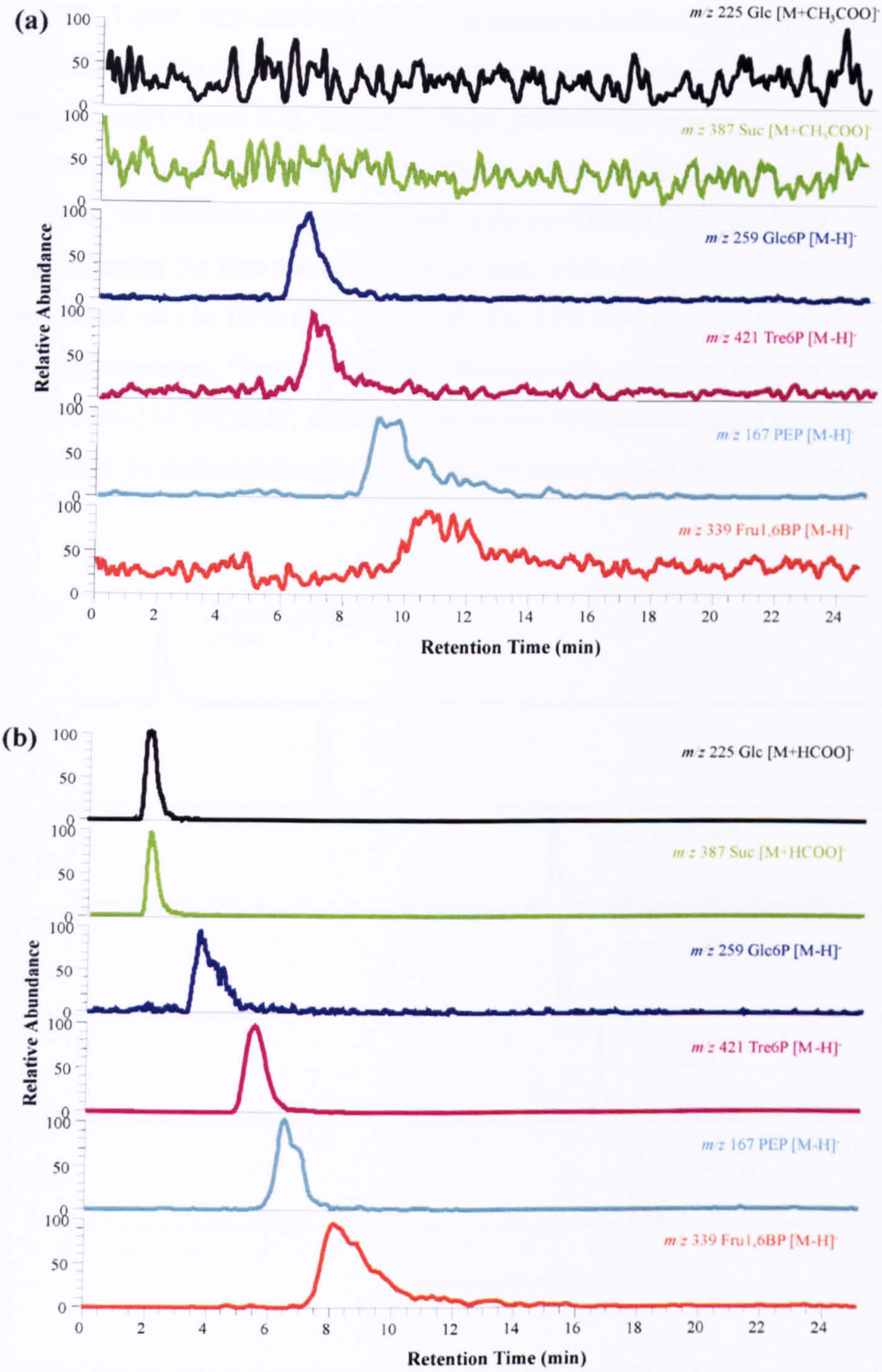

Figure 4.1 Extracted ion chromatograms obtained on PGC-LC-ESI-QIT-MS separation of a 50 µg/mL standard solution of a mixture of intermediary metabolites. HPLC conditions: PGC column (100 mm x 4.6 mm i.d.), 600 µL/min, 20 µL injection, mobile phase composed of (a) acetonitrile and 10% aqueous acetic acid; (b) acetonitrile and 10% aqueous formic acid.

Good LC separation and identification for all standard compounds (Glc, Suc, Glc6P, Tre6P, PEP and Fru1,6BP) was achieved in less than 20 min using an optimised triple stage gradient composed of water, acetonitrile, and 15% aqueous formic acid (Figure 4.2). The triple stage gradient was required in order to allow retention and separation of the neutral, the mono- and the diphosphorylated species; the neutrals were unretained in the presence of acid modifier, necessitating the first acetonitrile/water step, while the monophosphates were separable only in 10 % (not 15%) acid. The 15% acid step was needed to separate the diphosphates. Neutral mono- and disaccharides, detected as formylated molecules $[M+HCOO]^-$, eluted first from the PGC column, then monophosphates followed by diphosphates, both detected as deprotonated molecules $[M-H]^-$.

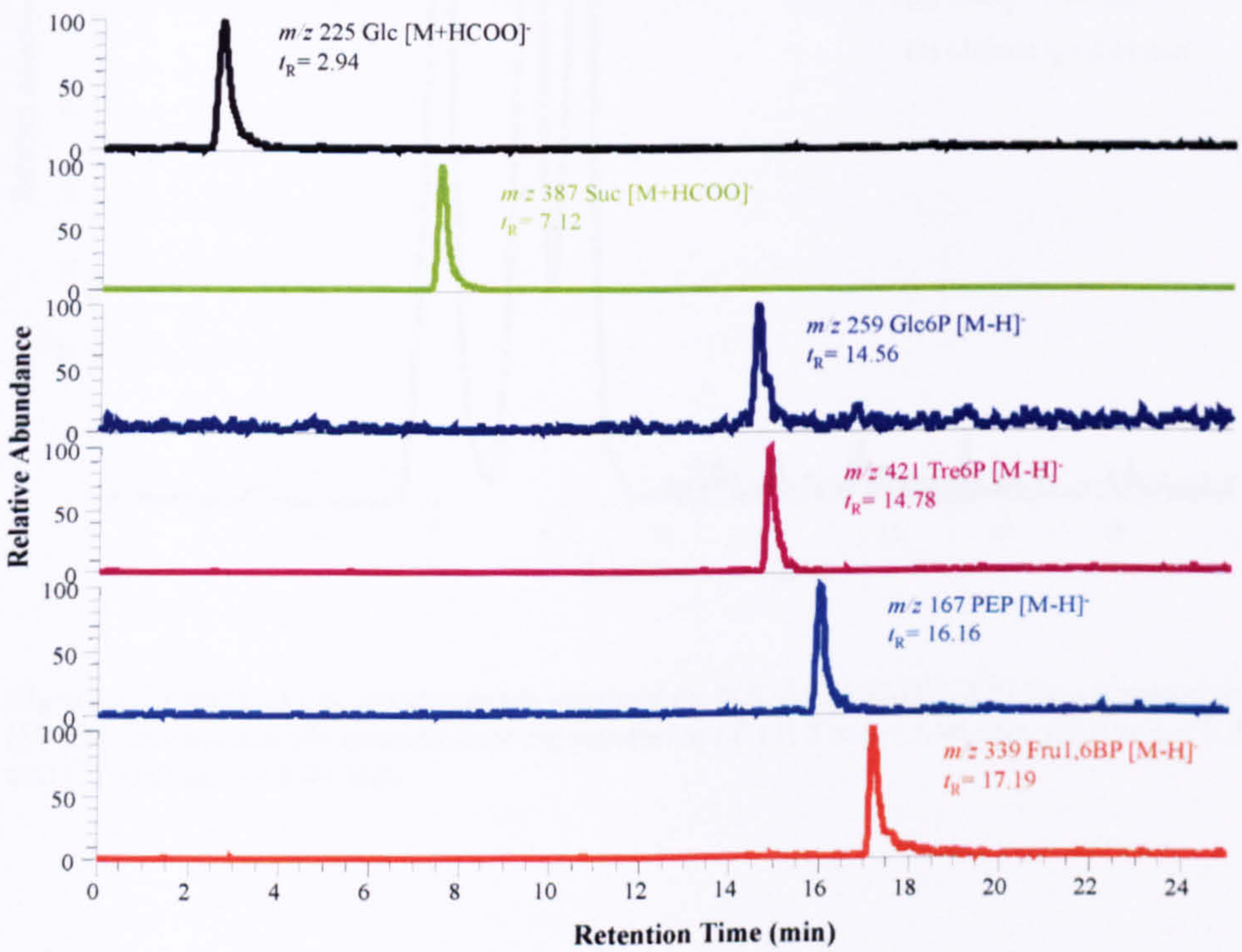

Figure 4.2 Extracted ion chromatograms obtained on PGC-LC-ESI-QIT-MS separation of a 50 µg/mL standard solution of a mixture of intermediary metabolites. HPLC conditions: PGC column (100 mm x 4.6 mm i.d.), 600 µL/min, 20 µL injection, optimised triple stage gradient.

PGC is known to be excellent for the separation of isomers or structurally related compounds (Wan et al., 1995; Reepmeyer et al., 2005; Robinson et al., 2007). This PGC-based LC-MS method showed separation of the isomeric disaccharides trehalose (Tre), sucrose (Suc) and maltose, detected at *m/z* 387 as formylated molecules ($[M+HCOO]^-$) (Figure 4.3).

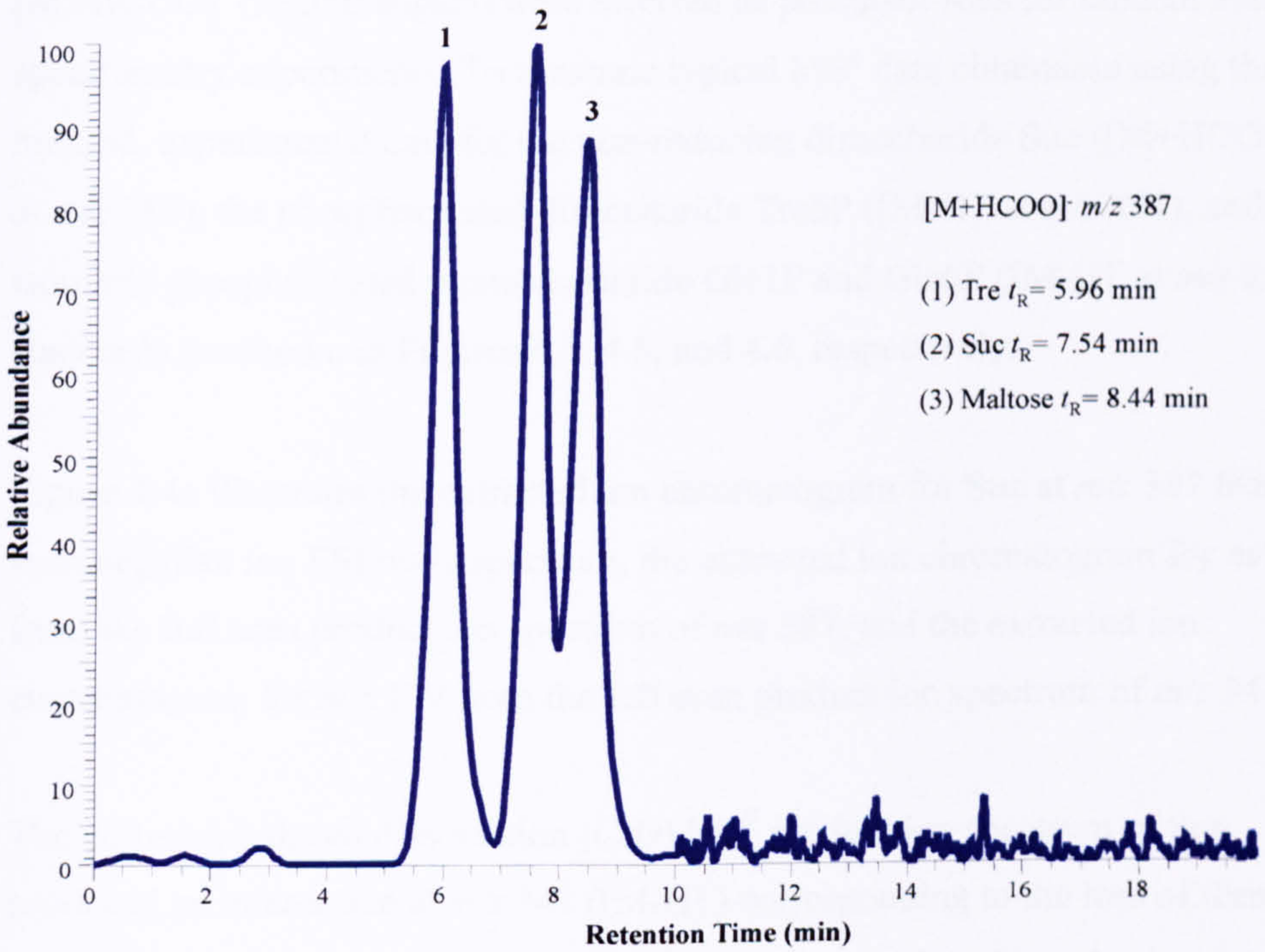

Figure 4.3 Extracted ion chromatogram obtained on PGC-LC-ESI-QIT-MS for a standard solution (10 μM) of disaccharide isomers showing separation of: (1) Tre t_R= 5.96 min, (2) Suc t_R= 7.54 min and (3) Maltose t_R= 8.44 min.

4.2.2 Negative ion CID behaviour of standard compounds using PGC-LC-ESI-QIT-MS^n

PGC-LC-IT-tandem mass spectrometry (MS^n) of authentic standard compounds was performed to aid in the identification of metabolites based on their retention times, masses, and characteristic mass spectrometric fragmentation behaviour. Deprotonated $[M-H]^-$ (negatively-charged compounds) or formylated molecules $[M+HCOO]^-$ (neutral sugars) were selected as precursor ions for tandem mass spectrometry experiments. To illustrate typical MS^n data obtainable using this method, experimental data for the non-reducing disaccharide Suc ($[M+HCOO]^-$ at *m/z* 387), the phosphorylated disaccharide Tre6P ($[M-H]^-$ at *m/z* 421), and the isomeric phosphorylated monosaccharide Glc1P and Glc6P ($[M-H]^-$ at *m/z* 259) standards are shown in Figures 4.4, 4.5, and 4.6, respectively.

Figure 4.4a illustrates the extracted ion chromatogram for Suc at *m/z* 387 from full scan negative ion ESI mass spectrum, the extracted ion chromatogram for *m/z* 341 from the full scan product ion spectrum of *m/z* 387, and the extracted ion chromatogram for *m/z* 179 from the full scan product ion spectrum of *m/z* 341.

The collision induced dissociation (CID) MS^2 product ion spectrum of Suc produced an intense ion at *m/z* 341 ($[M-H]^-$) corresponding to the loss of formic acid (Figure 4.4b). Subsequent CID MS^3 analysis, readily achieved using ion trap MS, of the $[M-H]^-$ ion at *m/z* 341 produced intense ions at *m/z* 179 and at *m/z* 161, which, according to the nomenclature for carbohydrate fragmentation of Domon and Costello (Domon and Costello, 1988) correspond to a Y_1 ion formed by cleavage of the glycoside bond with the loss of a hexose moiety $C_6H_{10}O_5$ (-162 Da), and a B_1 ion arising by the neutral loss of one monosaccharide $C_6H_{12}O_6$ (-180 Da) (Figure 4.4c).

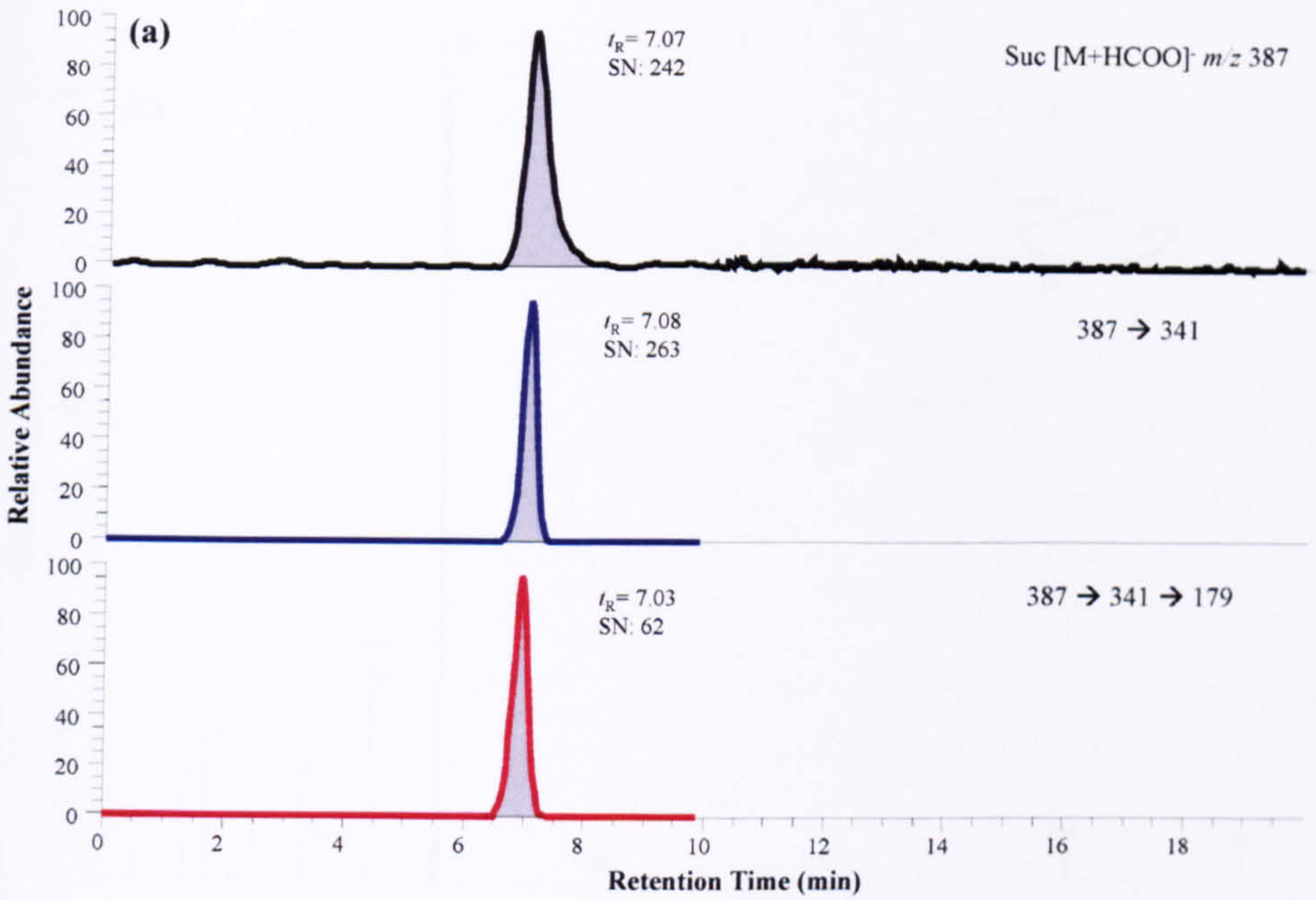

Figure 4.4 (a) Extracted ion chromatograms obtained on PGC-LC-ESI-QIT-MS^n showing the specificity of detection provided by CID MS^n for a standard solution (10 μM) of Suc; (b) CID MS^2 product ion spectrum of Suc (precursor ion $[M+HCOO]^-$ *m/z* 387); (c) CID MS^3 spectrum of Suc (precursor ion *m/z* 341).

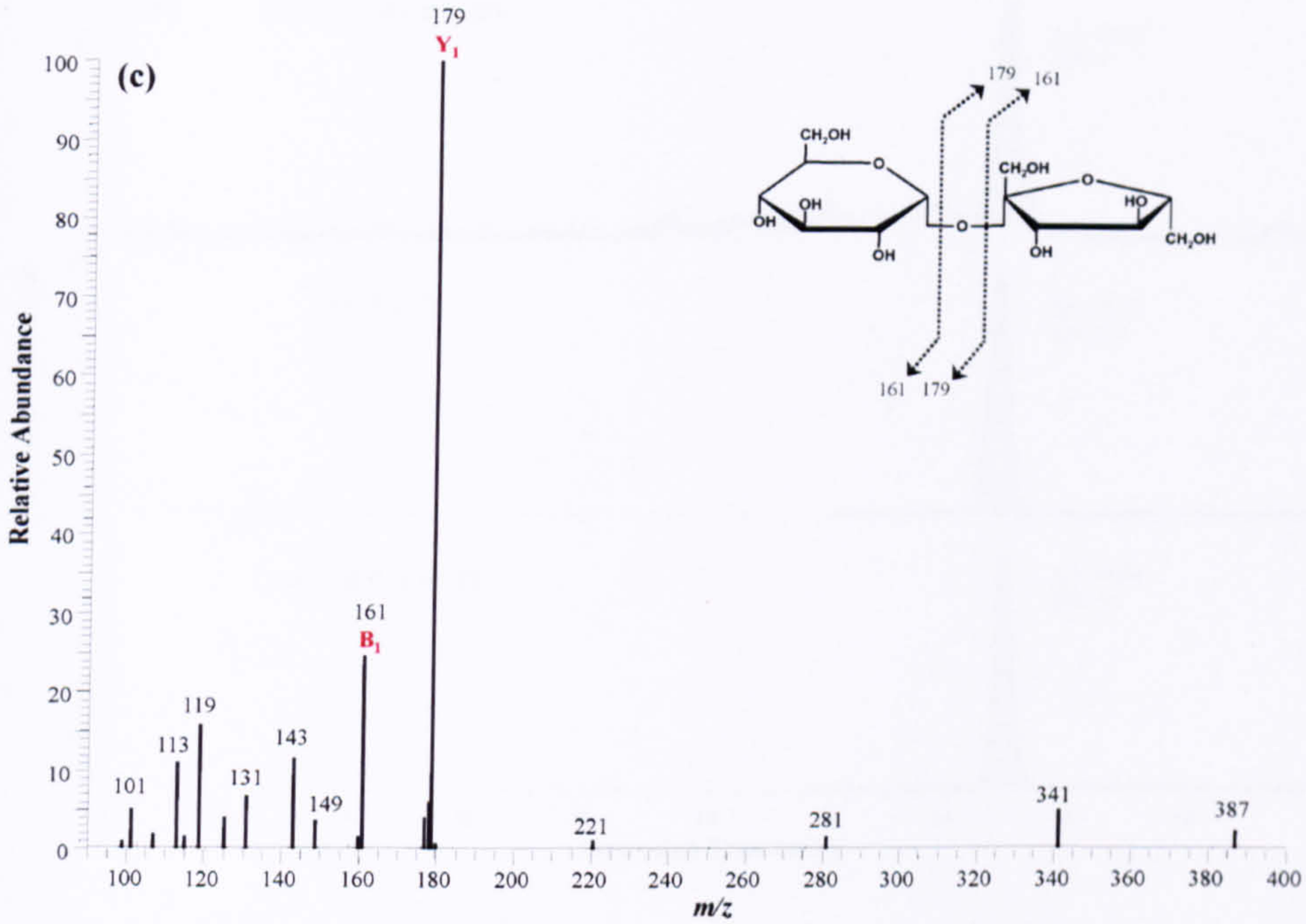

Figure 4.4 *(Continued).*

Figure 4.5a illustrates the extracted ion chromatogram for Tre6P at *m/z* 421 from full scan negative ion ESI mass spectrum, the extracted ion chromatogram for *m/z* 241 from the full scan product ion spectrum of *m/z* 421, and the extracted ion chromatogram for *m/z* 97 from the full scan product ion spectrum of *m/z* 241.

The CID MS^2 product ion spectrum of Tre6P ($[M-H]^-$ at *m/z* 421) contains an intense B_1 ion at *m/z* 241 formed by cleavage of the glycoside bond corresponding to the neutral loss of one monosaccharide $C_6H_{12}O_6$ (-180 Da) (Figure 4.5b). The presence of the phosphate group is clear from the product ions at *m/z* 79 $[PO_3]^-$ and *m/z* 97 $[H_2PO_4]^-$ in the MS^3 spectrum obtained on CID of *m/z* 241 (Figure 4.5c).

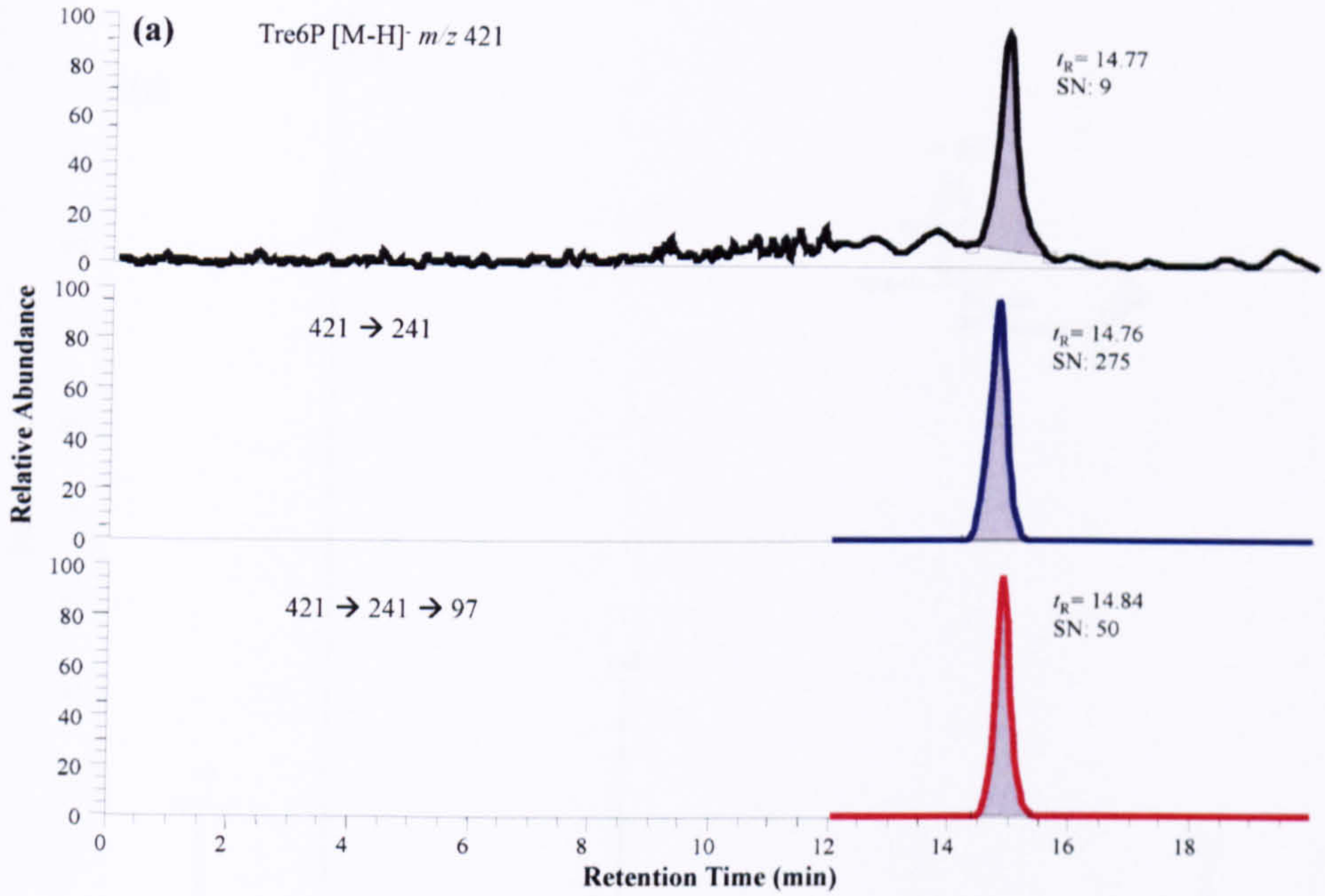

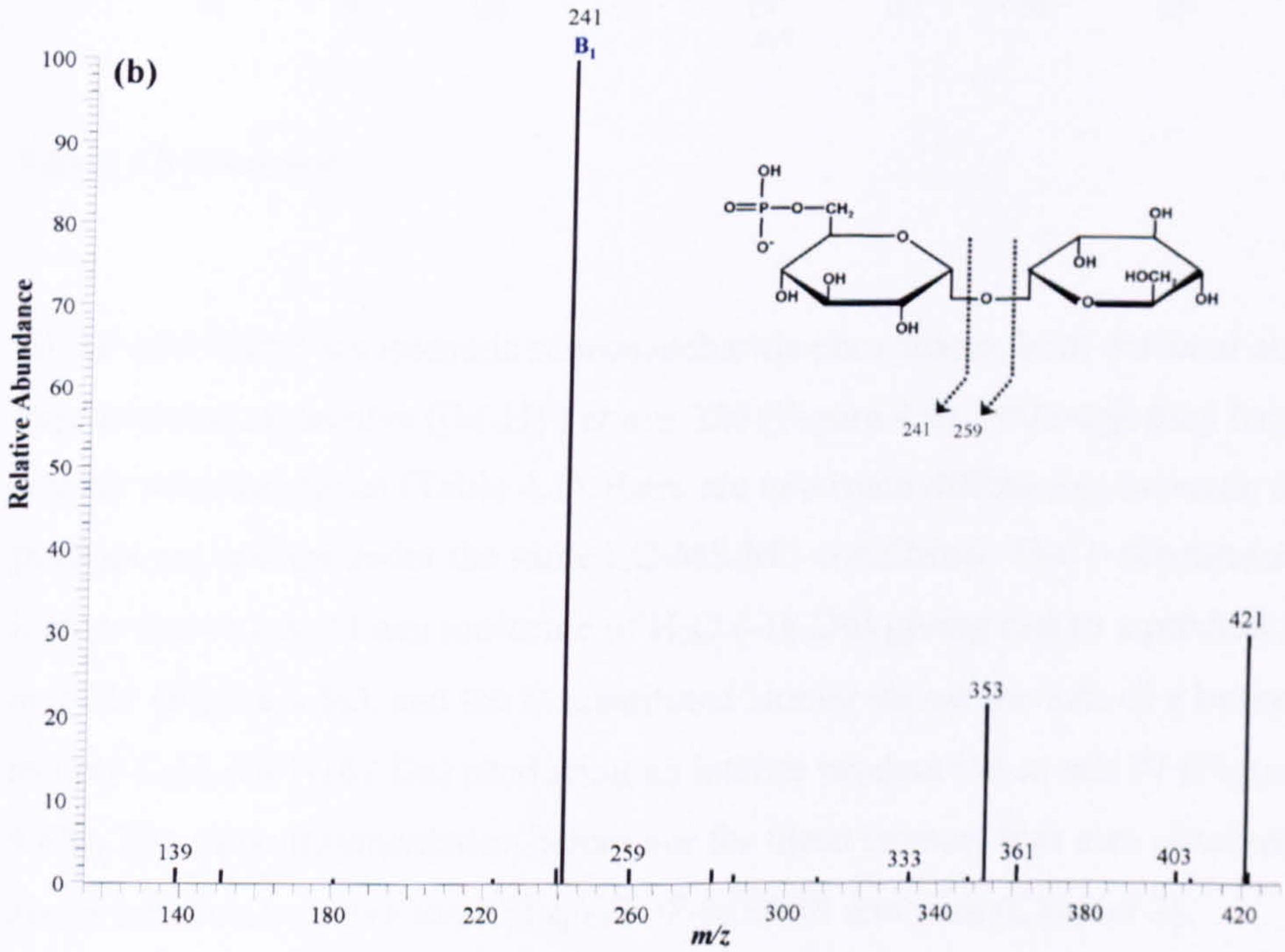

Figure 4.5 (a) Extracted ion chromatograms obtained on PGC-LC-ESI-QIT-MS^n showing the specificity of detection provided by CID MS^n for a standard solution (10 μM) of Tre6P; (b) CID MS^2 product ion spectrum of Tre6P (precursor ion $[M-H]^-$ *m/z* 421); (c) CID MS^3 spectrum of Tre6P (precursor ion *m/z* 241).

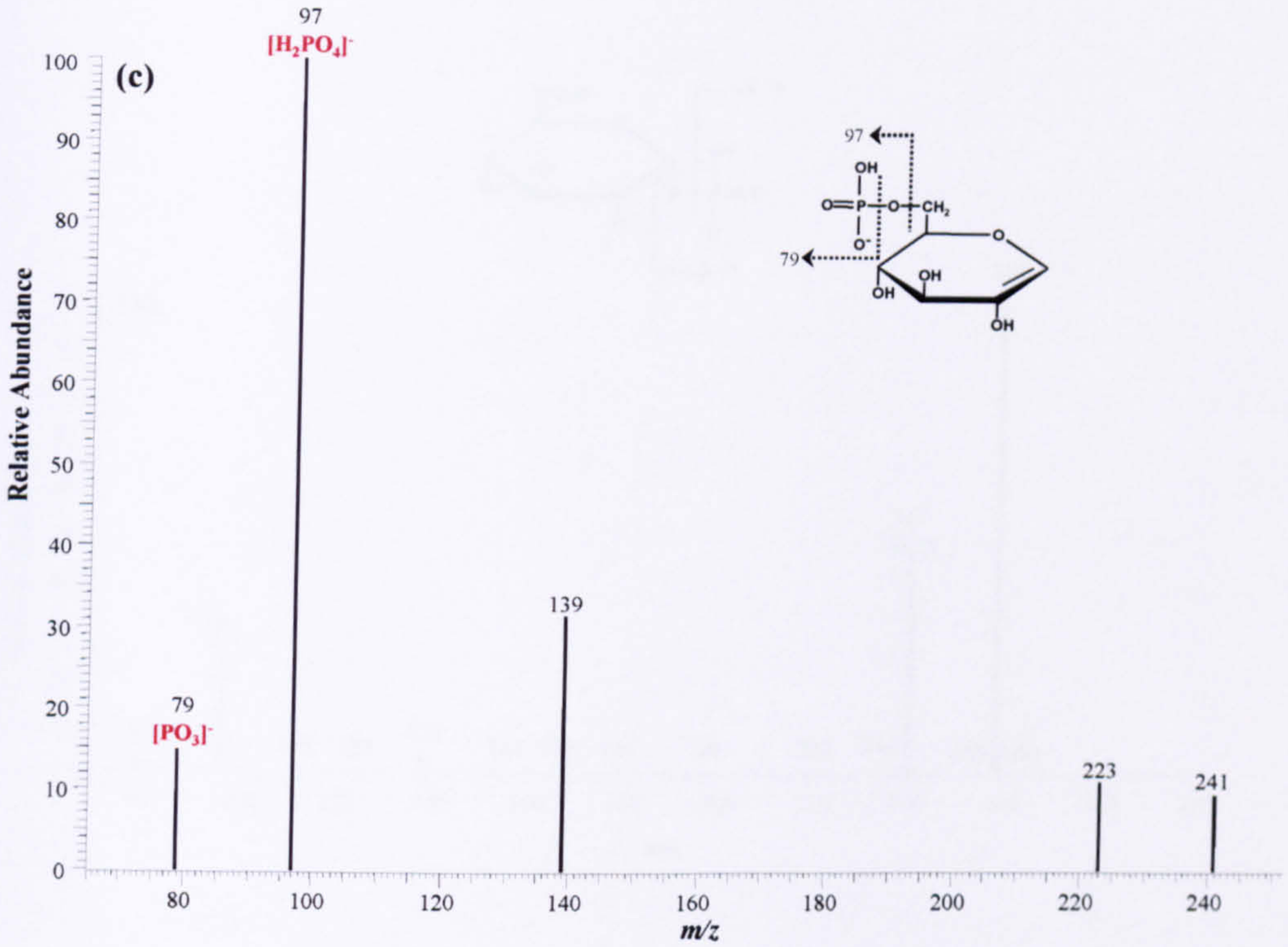

Figure 4.5 *(Continued).*

Glc1P and Glc6P are isomeric monosaccharide phosphates, both detected as deprotonated molecules ($[M-H]^-$) at *m/z* 259 (Figure 4.6). Although they have similar retention times (Table 4.1), there are two main differences between their product ion spectra under the same LC-MS/MS conditions. The 1-substituted isomer shows loss of one molecule of H_2O (-18 Da) giving rise to a product ion at *m/z* 241 (Figure 4.6a), and the 6-substituted isomer shows the loss of a hexose moiety $C_6H_{10}O_5$ (-162 Da) producing an intense product ion at *m/z* 97 (Figure 4.6b). The same fragmentation behaviour for these isomers was also obtained on direct infusion negative ion ESI-qoaTOF-MS/MS analyses (Chapter 3). Identification and differentiation of the isomers Glc1P and Glc6P is therefore possible based on a consideration of both their retention times and their product ion spectra which are different and contain characteristic product ions (Feurle et al., 1998).

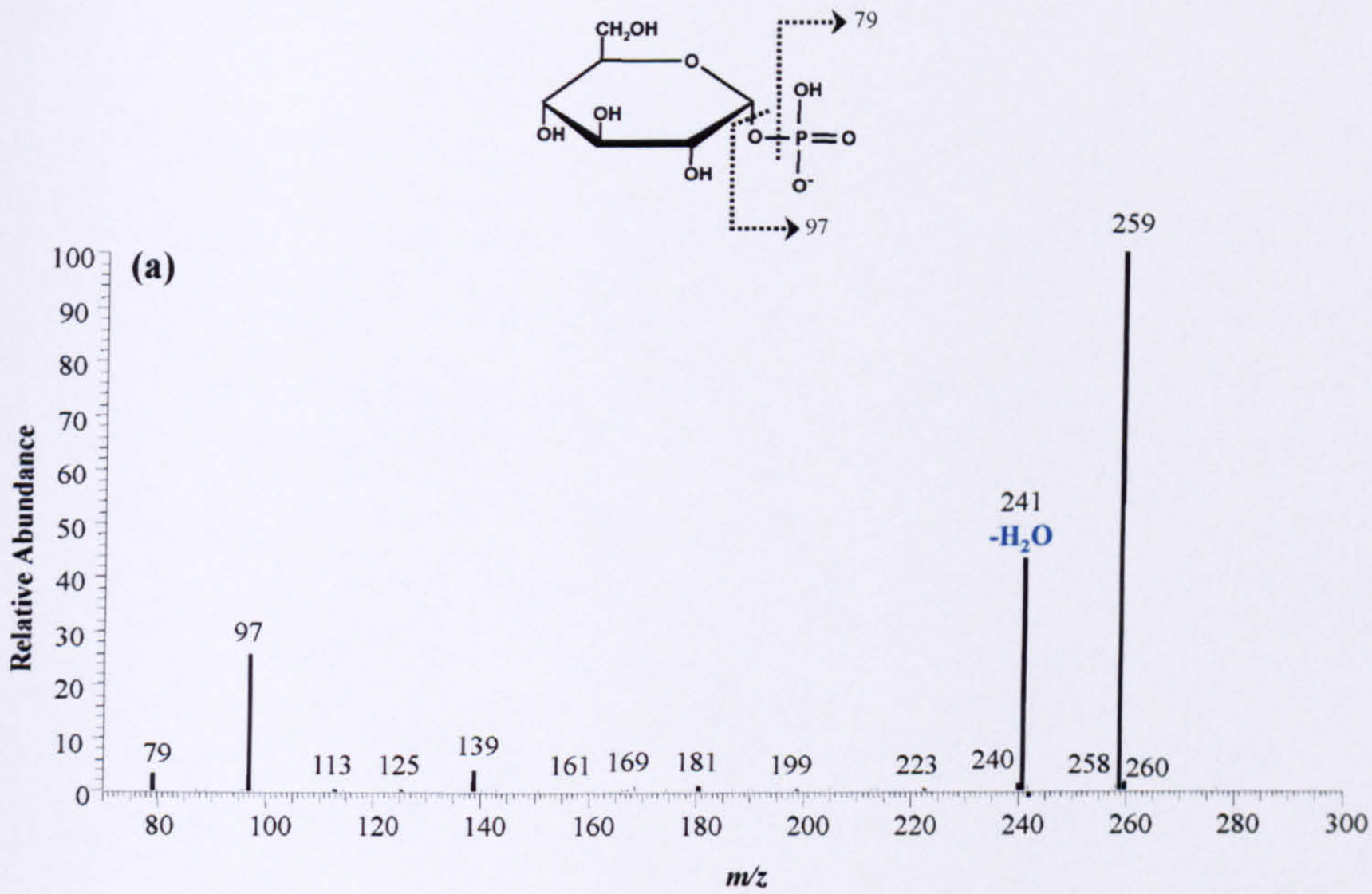

Figure 4.6 Differentiation of the isomeric compounds Glc1P and Glc6P by ion trap tandem MS: (a) CID MS^2 product ion spectrum of Glc1P *m/z* 259; (b) CID MS^2 product ion spectrum of Glc6P *m/z* 259.

4.2.3 Linearity, limits of detection (LOD), and limits of quantification (LOQ) of the PGC-LC-ESI-QIT-MS method

To evaluate the potential of the method for quantitative analysis of soluble sugars and sugar phosphates from plant tissues, intra- and inter-day repeatability of retention times, and linearity of the PGC-LC-ESI-QIT-MS method were tested. Intra-day repeatability was measured by injecting the same standard solution three times in a single day. Inter-day repeatability was measured by analysing the same standard solution over six different days. Intra- and inter-day repeatability of retention times using our method gave relative standard deviations (RSD) of less than 2% (Table 4.1). The linearity of the PGC-LC-ESI-QIT-MS response was measured for each compound by recording the responses at different concentrations over the range 0-100 μM. Five-point standard curves were established by plotting integrated peak areas versus concentration. Each point on the calibration curve was the mean value of three independent measurements using the PGC-LC-ESI-QIT-MS method. The LOD for each compound was calculated as the minimum amount injected which gave a detector response higher than three times the signal-to-noise ratio (S/N). The on-line PGC-LC-ESI-QIT-MS method showed good linearity over the concentration range 0-100 μM for all compounds with estimated LODs of 0.5 μM obtained for Glc, 0.1 μM for disaccharides (Tre, Suc, and maltose), 0.3 μM for Tre6P, and 1.5 μM for hexose phosphates (Fru6P, Glc1P, Glc6P) and PEP. The LOQ was also determined for each compound at an S/N ratio of 10 (Table 4.1).

Table 4.1 Nominal *m/z* values, retention times, intra- and inter-day repeatabilities of retention times, LOD, LOQ, and linearity of calibration curves obtained for standard compounds using negative ion PGC-LC-ESI-QIT-MS.

Standard compounds	Diagnostic ion (*m/z*)	t_R (min)	t_R (intra RSD)[a] (%, n=3)	t_R (inter RSD)[b] (%, n=6)	LOD[c] (μM)	LOQ[d] (μM)	Amout LOD[e] (pmol)	$R^{2,f}$
Fru	225 $[M+HCOO]^-$	2.87	0.70	0.75	2.0	6.7	40	0.9956
Glc	225 $[M+HCOO]^-$	2.93	0.20	1.15	0.5	1.6	9	0.9969
Tre	387 $[M+HCOO]^-$	5.62	1.46	1.64	0.1	0.3	2	0.9988
Suc	387 $[M+HCOO]^-$	7.12	0.41	0.59	0.1	0.3	2	0.9958
Maltose	387 $[M+HCOO]^-$	8.32	0.35	0.64	0.1	0.4	2	0.9929
Glc1P	259 $[M-H]^-$	14.37	0.26	0.87	1.5	5.0	30	0.9991
Fru6P	259 $[M-H]^-$	14.42	0.16	0.82	1.5	5.0	30	0.9913
Glc6P	259 $[M-H]^-$	14.56	0.07	0.26	1.5	5.0	30	0.9979
Tre6P	421 $[M-H]^-$	15.15	0.04	0.68	0.3	2.5	6	0.9939
Suc6P	421 $[M-H]^-$	15.33	0.11	0.12	0.8	2.5	15	0.9917
PEP	167 $[M-H]^-$	16.20	0.07	0.12	1.5	5.0	30	0.9947

HPLC conditions: Hypercarb PGC column (100 mm x 4.6 mm i.d.), triple stage gradient , 20 μL injection, flow rate 600 μL/min. [a] Intra-day RSD of retention times (n=3 independent measurements); [b] Inter-day RSD of retention times (n=6 independent measurements); [c] Concentration LOD calculated at an S/N of 3; [d] LOQ calculated at an S/N of 10; [e] LOD of the amount loaded onto column calculated at an S/N of 3; [f] Correlation coefficients for the standard curves (five points) of relative peak areas against concentration (0-100μM).

4.2.4 Analytical recoveries of standards added to *A. thaliana* tissue extracts

The efficiency of the extraction methods used in this work was investigated by determining the analytical recoveries of phosphate standards spiked into *A. thaliana* tissue extracts (Figure 4.7). The recovery of different phosphate standards (Glc1P, Glc6P, Fru6P, Tre6P, Fru1, 6BP, and PEP) was tested using two extraction methods: extraction in trichloroacetic acid (TCA)/ether using approximately 50 mg of leaf material, and extraction in chloroform/methanol using approximately 10 mg of leaf material (Chapter 2). Recovery experiments were carried out in triplicate by adding known amounts of authentic standards into accurately weighed pooled *A. thaliana* Col-0 frozen plant samples at the beginning of the extraction procedure.

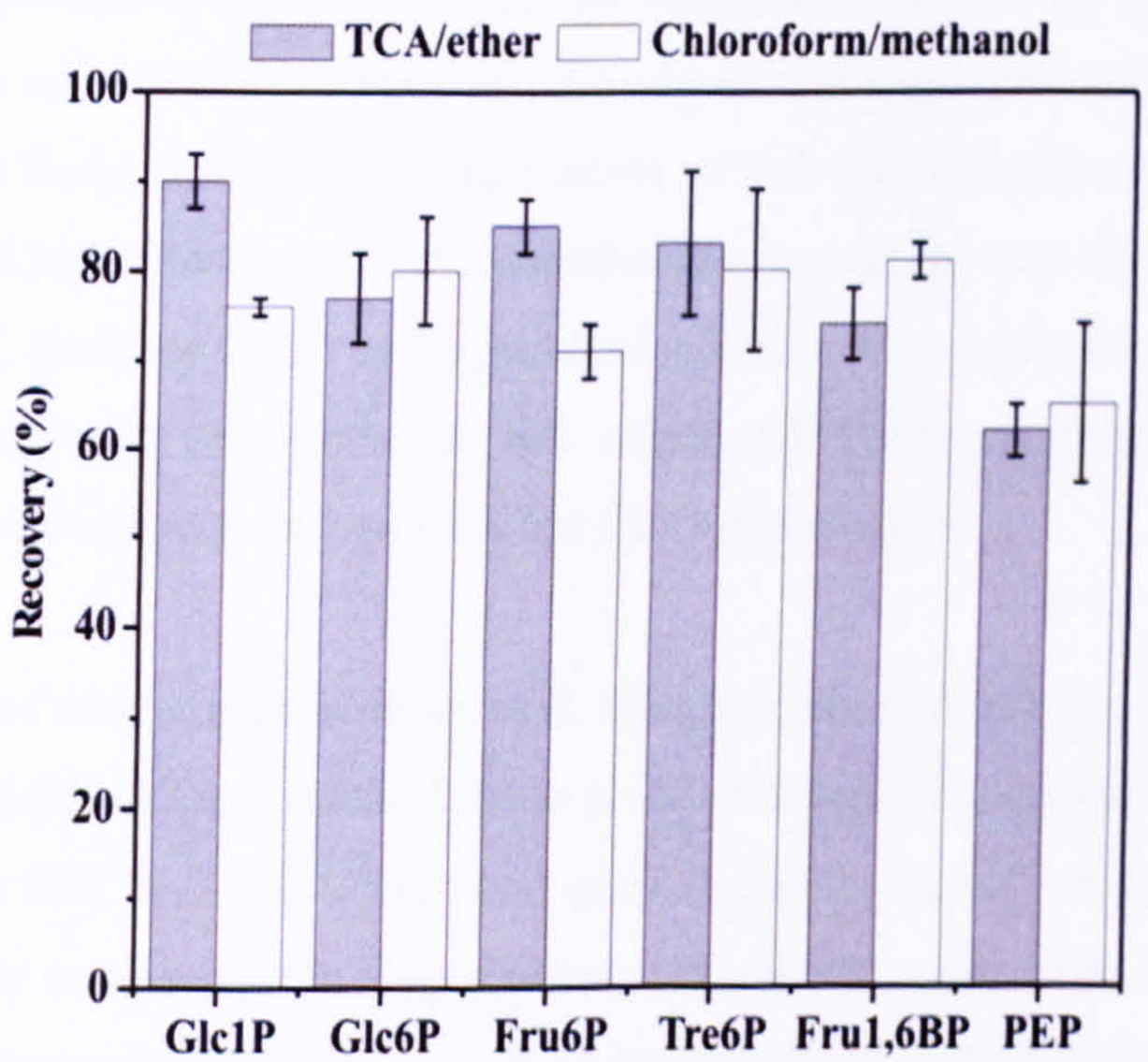

Figure 4.7 Recoveries of different phosphate standards added to accurately weighed *A. thaliana* Col-0 leaf extracts using two extraction methods: TCA/ether and chloroform/methanol. Values are mean ± SD (n=3 biological replicates, each containing leaves from three rosettes). Each biological replicate is the mean value of n=3-4 independent PGC-LC-ESI-QIT-MS measurements.

Standards were identified in plant extracts using retention time, *m/z* value, and characteristic product ion spectra. The estimated recoveries of phosphate standards were found to be approximately 70-80% using both extraction methods, which is satisfactory for a complex matrix. The chloroform/methanol extraction method was chosen for further experiments because it is less laborious than the TCA/ether extraction method.

4.2.5 Application of the PGC-LC-ESI-QIT-MS method to the analysis of metabolic intermediates from *A. thaliana* wild-type Col-0 and *pgm1* plants growing in a 16 h light/ 8 h dark photoperiod

The value of this on-line analytical PGC-LC-ESI-QIT-MS method for the analysis of target compounds in complex biological samples was tested by applying it for the separation and identification of soluble sugars and sugar phosphates from *A. thaliana* plant tissue extracts. The application of this method allowed the separation and identification of three metabolites in a single-run: Glc, Suc, and Glc6P from *A. thaliana* Col-0 and *pgm1* leaf extracts. Metabolites were identified in plant extracts using retention time, *m/z* value, and characteristic product ion spectra of specific precursor ions selected for fragmentation.

The presence of matrix interferences in *A. thaliana* leaf extracts was investigated using the standard addition method. Five-point standard addition curves were established for Glc, Suc, and Glc6P, and good linearity was shown for all compounds. By comparing the slopes obtained by linear regression, e.g. for Glc6P, using the standard addition method (y=2517846x+109023882) and the aqueous standard calibration (y=2534211x-6511278), the values for the gradients of the curves differed by less than 1% demonstrating that no significant matrix-derived interferences were present in the *A. thaliana* tissue extract. Therefore, Glc,

Suc and Glc6P present in *A. thaliana* Col-0 and *pgm1* leaf extracts were quantified by PGC-LC-ESI-MS using aqueous standard calibration curves, using the ions at *m/z* 225 for Glc ($[M+HCOO]^-$), *m/z* 387 for Suc ($[M+HCOO]^-$), and *m/z* 259 for Glc6P ($[M-H]^-$) (Table 4.1).

There are known to be significant differences in the amounts of extractable soluble sugars (Glc and Suc) and glycolytic intermediates between *A. thaliana* wild-type Col-0 and *pgm1* plants, which are well characterised model organisms. In most studies, soluble sugars and glycolytic intermediates, including Glc6P, have been measured in *A. thaliana* Col-0 and *pgm1* plants using enzymatic assays (Gibon et al., 2002; Gibon et al., 2004; Bläsing et al., 2005).

A. thaliana pgm1 mutant plants are deficient in plastidial phosphoglucomutase (pPGM) activity, an enzyme which catalyzes the interconversion of Glc6P and Glc1P. Plastidial PGM is essential for starch synthesis in the leaf during the day, and therefore plants carrying the *pgm1* mutation are unable to synthesize starch (Caspar et al., 1985; Caspar et al., 1991). As a result, high levels of soluble sugars accumulate in their leaves during the day, instead of starch.

Figure 4.8 shows the quantitative results obtained using PGC-LC-ESI-QIT-MS for extracts of *A. thaliana* Col-0 and starchless *pgm1* plants, grown under a 16 h light/ 8 h dark photoperiod and harvested during the day at developmental stage 6.0 (Boyes et al., 2001). Using this method, levels of 5.87±1.22 $\mu mol.g^{-1}$ of fresh weight (FW) for Glc, 1.97±0.36 $\mu mol.g^{-1}$ FW for Suc, and 0.31±0.04 $\mu mol.g^{-1}$ FW for Glc6P were determined in the leaves of the starchless *pgm1*. The levels of soluble sugars found in *A. thaliana* wild-type Col-0 leaves were, as expected, much lower at 0.87±0.09 $\mu mol.g^{-1}$ FW for Glc, 0.71±0.11 $\mu mol.g^{-1}$ FW for Suc, and 0.11±0.01 $\mu mol.g^{-1}$ FW for Glc6P.

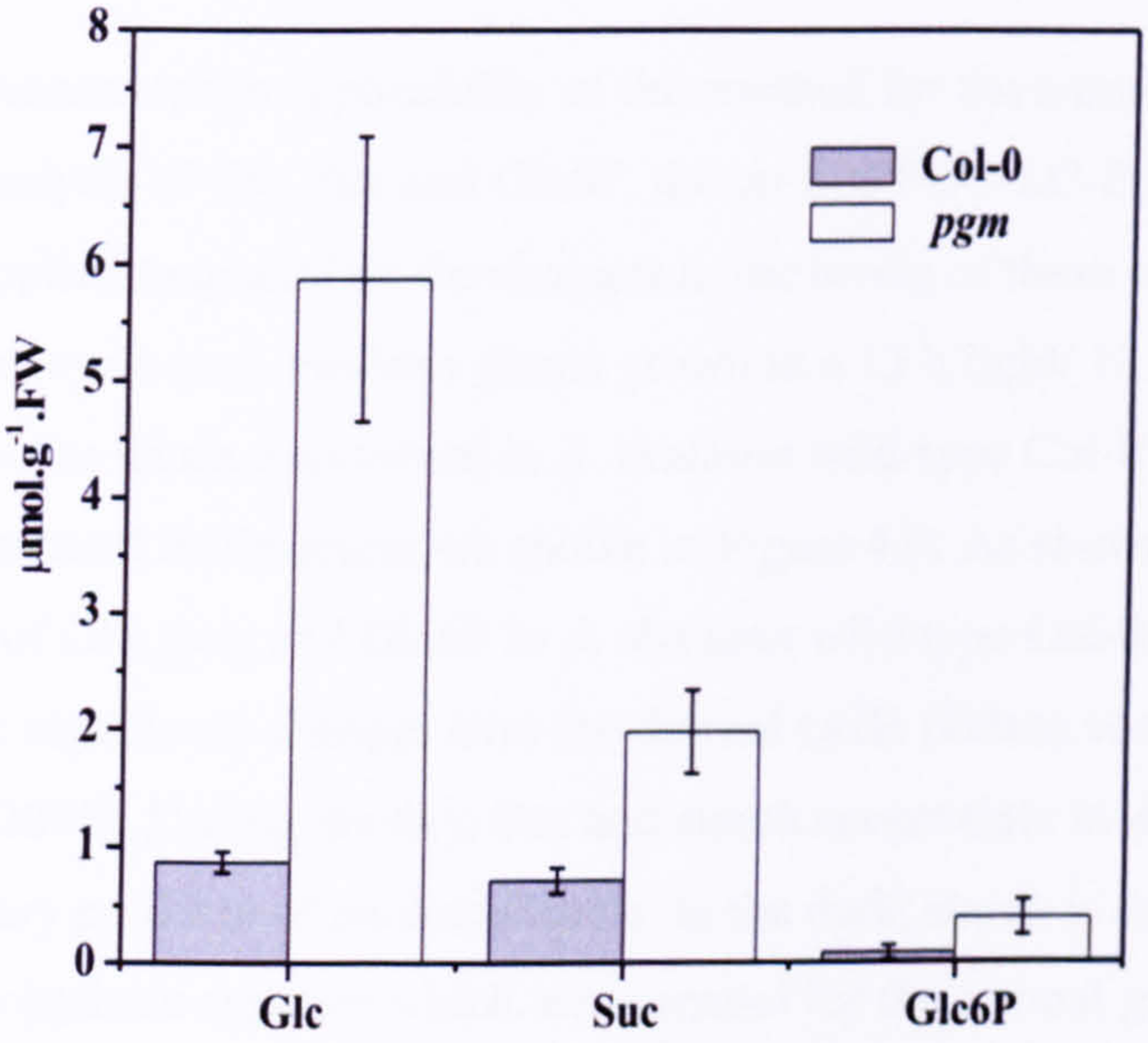

Figure 4.8 Metabolite levels (Glc, Suc and Glc6P) determined in *A. thaliana* Col-0 and starchless *pgm1* chloroform/methanol leaf extracts using PGC-LC-ESI-QIT-MS. Plants were grown under a 16 h light/ 8 h dark photoperiod and harvested at developmental stage 6.0. Values are mean ± SD (n=3 biological replicates, each containing leaves from three rosettes). Each biological replicate is the mean value of n=3-4 independent measurements. FW, fresh weight.

4.2.6 Application of the PGC-LC-ESI-QIT-MS method to the analysis of metabolite level changes during the diurnal cycle in *A. thaliana* wild-type Col-0 and *pgm1* plants growing in a 12 h light/ 12 h dark regime

To further demonstrate the applicability of this method for the simultaneous quantitative analysis of Glc, Suc and Glc6P, the on-line PGC-LC-ESI-QIT-MS method was applied to quantitate the changes in the levels of these metabolites over the diurnal cycle in *A. thaliana* plants grown in a 12 h light/ 12 h dark regime. Metabolite levels determined in *A. thaliana* wild-type Col-0 and *pgm1* chloroform/methanol leaf extracts are shown in Figure 4.9. As shown in Figure 4.9, the levels of Glc, Suc, and Glc6P in *A. thaliana* wild-type Col-0 and *pgm1* leaves undergo significant changes over the diurnal cycle (Gibon et al., 2004; Bläsing et al., 2005). During the day, Suc and starch accumulate in *A. thaliana* leaves as primary products of photosynthesis. In the dark, starch is degraded providing carbohydrate supplies which are essential for the normal growth of the plant in the dark (Zeeman et al., 2004; Smith et al., 2005; Zeeman et al., 2007). *A. thaliana* wild-type Col-0 leaves accumulated low levels of Glc, Suc and Glc6P during the light period as these are converted to starch for storage. In contrast, in *pgm1* leaves, high levels of these sugars accumulated during the light period (starch is not synthesized), and during the dark these sugars dramatically decreased because these carbon supplies are being used for plant growth and metabolism in the dark. These results are in accordance with those reported by Bläsing *et al.* (Bläsing et al., 2005) in a similar study of metabolite changes over the diurnal cycle in *A. thaliana* wild-type Col-0 and *pgm1* plants grown in a 12 h light/ 12 h dark regime. In that study, metabolite measurements (including Glc, Suc, and Glc6P) were determined using enzymatic assays, in which only one compound could be determined per assay. This PGC-LC-ESI-QIT-MS method offers the advantage of being able to simultaneously measure these soluble sugars in a single run.

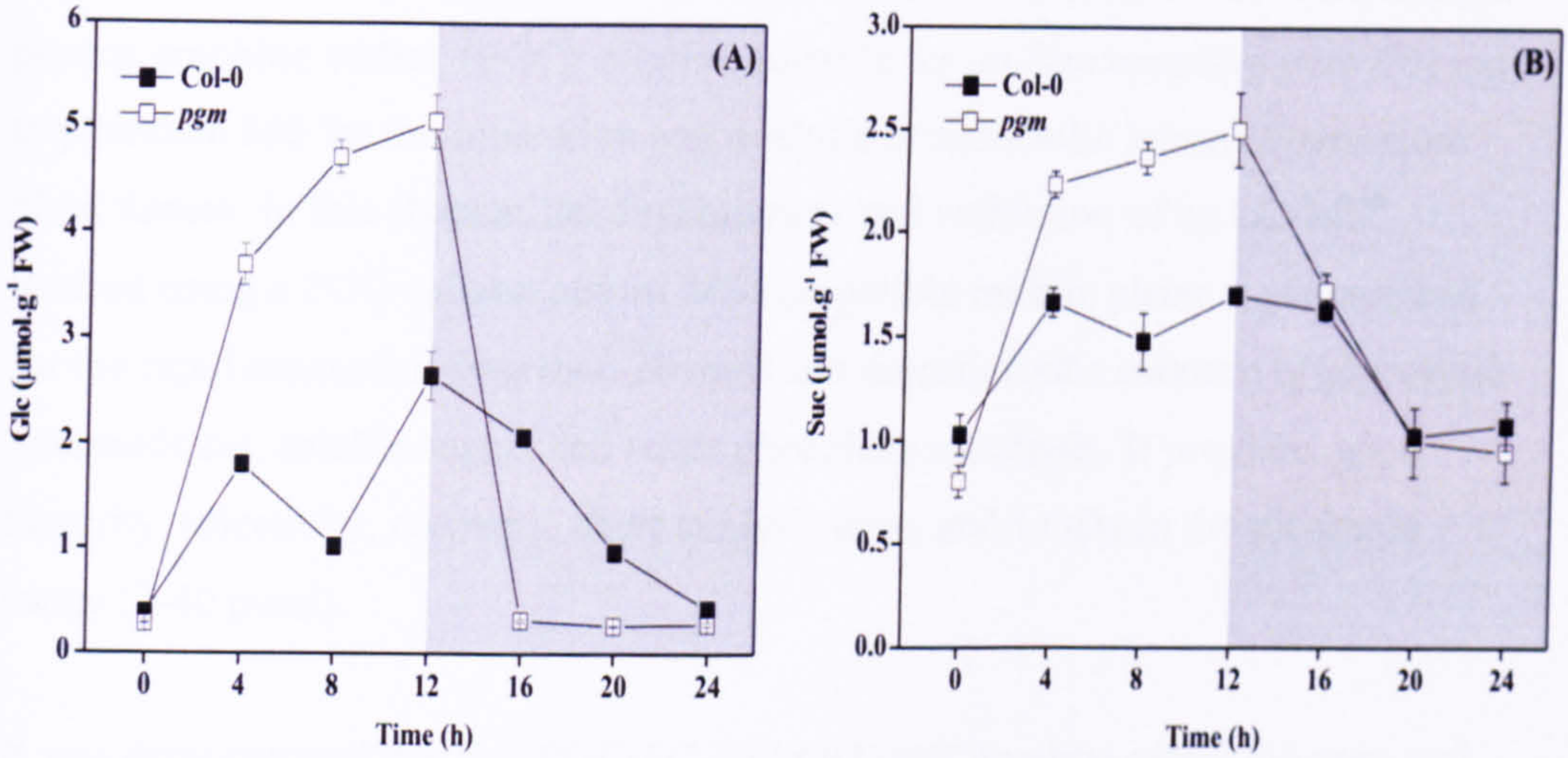

Figure 4.9 Metabolite level changes observed over a 12 h light/ 12 h dark cycle in *A. thaliana* wild-type Col-0 (■) and starchless *pgm1* (□) chloroform/methanol leaf extracts using PGC-LC-ESI-MS: (A) Glc, (B) Suc and (C) Glc6P. Rosettes were harvested at the end of the night, 4 h, 8 h, 12 h into the light period, 4 h, 8 h, and again 12 h into the dark period. Values are mean ± SD (n=3 biological replicates, each containing leaves from three rosettes). Each biological replicate is the mean value of n=3-4 independent measurements. FW, fresh weight.

4.3 Conclusions

The aim of this study was to develop and optimise a robust HPLC system, using a porous graphitic carbon (PGC) column, suitable for on-line coupling with ESI ion trap tandem MS for the separation and analysis of metabolic intermediates from plant tissues. In this chapter, the development and validation of an LC-MS^n method using a PGC column and an MS compatible mobile phase was described for the rapid separation (less than 20 min) and detection of a mixture of glycolytic intermediates, soluble sugars and sugar phosphate standards. It provides good linearity, selectivity, recovery, short analysis time, and LODs in the picomole range (2-40 pmol).

It was demonstrated that this PGC-LC-ESI-QIT-MS^n method offers the very real advantage over traditional enzymatic assays of being able to simultaneously separate, detect and quantitate soluble sugars (Glc, Suc) in the concentration range 0.26-6.0 $\mu mol.g^{-1}$ FW and sugar phosphates (Glc6P) in the concentration range 25-300 $nmol.g^{-1}$ FW in a single extract of 10 mg of plant material, and in a single LC-MS separation that takes only 20 minutes.

Lunn and co-workers (Lunn et al., 2006) reported a method using HPAEC coupled to a triple quadrupole MS operated in the highly selective multiple reaction monitoring mode, with a detection limit in the femtomole range for the measurement of trehalose-6-phosphate (Tre6P) in *A. thaliana*. Using this approach, Tre6P was measured at very low concentrations, ranging from 23-298 $pmol.g^{-1}$ FW in wild-type Col-0 rosette leaves, and 380 $pmol.g^{-1}$ FW in the *pgm1* mutant. This triple quadrupole MS method offers better concentration sensitivity, and therefore lower limits of detection for specific, targeted analytes. However, the method described in this chapter, using an ion trap instrument, offers a great potential to detect unknown compounds in plant extracts in an untargeted 'open' way; full-scan LC-MS data were recorded and are thus available for further data mining.

Chapter 5

Porous graphitic carbon liquid chromatography electrospray ion trap mass spectrometry for the analysis of carbohydrates in *Lupinus albus* stems in response to water deficit

The work described in this chapter has been published in:

Journal of Chromatography A, 1187 (2008) 111-118

Carla Antonio[a], Carla Pinheiro[b], Maria Manuela Chaves[b,c], Cândido Pinto Ricardo[b], Maria Fernanda Ortuño[b,d], and Jane Thomas-Oates[a]

[a] Department of Chemistry,
University of York,
UK

[b] Instituto de Tecnologia Química e Biológica,
Oeiras, Portugal

[c] Instituto Superior de Agronomia,
Lisboa, Portugal

[d] Centro de Edafología y Biología Aplicada del Segura,
Murcia, Spain

Chapter 5. Porous graphitic carbon liquid chromatography electrospray quadrupole ion trap tandem mass spectrometry for the analysis of carbohydrates in Lupinus albus stems in response to water deficit (PGC-LC-ESI-QIT-MS^n)

5.1 Introduction

Lupinus albus L. (white lupin) is an important seed legume crop widely cultivated throughout the Mediterranean region (Gladstones, 1998). Fully developed lupin seeds are of great nutritional value, primarily due to their unique carbohydrate properties, characterised by negligible levels of starch, and high levels of proteins, and are widely used in animal feed and for human consumption (Petterson, 1998). Lupins are also known for their beneficial soil properties; they are used as a source of nitrogen in farming systems and increase the percentage of phosphorus in the soil (Huyghe, 1997).

A feature of Mediterranean climates is the high rainfall during winter with increasing water shortage during spring and early summer, and so *L. albus* crops are frequently subjected to periods of water deficit (WD), especially during late spring. Abiotic stresses such as drought are one of the major constraints on crop productivity, leading to huge reductions in the reproductive development and crop yield (Dracup et al., 1998; Chaves and Oliveira, 2004). From a commercial and agronomic point of view, crop WD survival is thus vital.

L. albus is one such crop that is able to survive severe drought conditions. It has been previously reported that it can withstand WD during both vegetative and reproductive growth (Rodrigues et al., 1995; Pinheiro et al., 2001). When occurring during vegetative growth, WD affects a range of organs in different ways.

Despite the loss of its leaves, *L. albus* plants recover upon rewatering (RW), the stems being the fundamental structures that allow the plant to survive (Pinheiro et al., 2001; Chaves et al., 2002; Pinheiro et al., 2004). Furthermore, the metabolism in the two stem components (cortex and stele) is differently affected by WD, suggesting that these two components are important systems for studying the biochemical alterations that allow the plant to survive this stress.

Carbohydrate metabolism is very sensitive to changes in the plant water status. It has been generally proposed that the alterations in the carbohydrate content of a plant under WD act as a metabolic signal in response to stress; carbohydrates (mainly soluble sugars and sugar alcohols) are also known to act as compatible solutes (or compatible osmolytes), and osmoprotectants during dehydration (Chaves and Oliveira, 2004; Seki et al., 2007).

Although they are thus important analytes for understanding the biochemical processes underlying drought resistance, carbohydrates are difficult compounds to analyse due to their high polarity, poor UV absorbance, and the structural variety of isomeric structures. Highly polar compounds are poorly or completely unretained on reversed-phase (RP) silica columns and generally elute at or close to the void volume without chromatographic separation (Dunn and Ellis, 2005). High performance anion-exchange liquid chromatography with pulsed amperometric detection (HPAEC-PAD) has been widely used for the analysis of carbohydrates; however, the high salt content in the mobile phase is not compatible for a robust direct coupling with ESI-MS (see Section 4.1). One suitable approach for the analysis of such polar compounds is the use of porous graphitic carbon (PGC) LC stationary phases, developed as an alternative to RP columns for the analysis of polar compounds (Gilbert et al., 1982; Knox et al., 1986; Knox and Ross, 1997). PGC-LC columns have been widely used for the separation of many different types of carbohydrate compounds, including mono-, di- and oligosaccharides (Koizumi et al., 1991; Davies et al., 1993; Fan et al., 1994; Koizumi, 1996).

In addition, the aqueous/organic mobile phases used with PGC are MS compatible, hence allowing robust direct coupling with ESI, and recently, new PGC-LC-ESI-MS-based methods have been reported for the analysis of water soluble oligosaccharides present in *Triticum aestivum* stems (Robinson et al., 2007), and water soluble neutral and phosphorylated carbohydrates extracted from *Arabidopsis thaliana* leaves (Antonio et al., 2007) (Chapter 4).

5.1.1 Aim

The work described in this chapter is part of a collaborative project entitled 'Screening for stress responsive metabolites in *Lupinus albus*' and was carried out in collaboration with the Plant Sciences Division, Instituto de Tecnologia Química e Biológica (ITQB, Oeiras, Portugal). This project is funded by the British Council under the Treaty of Windsor Anglo-Portuguese Joint Research Programme.

This chapter focuses on the development and application of a new on-line negative ion mode PGC-LC-ESI-QIT-MS^n method for the analysis of carbohydrates extracted from *L. albus* stem tissues that have been subjected to periods of drought. Quantitative changes of water deficit-responsive carbohydrates in *L. albus* stems (cortex and stele) induced by gradual imposition of dehydration, followed by a rewatering period are described.

5.2 Results and discussion

5.2.1 PGC-LC-ESI-QIT-MS^n method development

Separation of mono-, di-, and oligosaccharides on PGC columns have been reported by several different groups to be successful using mobile phases composed mainly of acetonitrile and water (Koizumi et al., 1991; Koizumi, 1996; Antonio et al., 2007; Robinson et al., 2007). In the light of this consideration, the PGC-LC separation was first optimised by using mobile phases composed of different ratios of water and acetonitrile (mobile phase 1), and making use of a solution containing a mixture of authentic standard neutral soluble sugars and sugar alcohols that are known to act as osmolytes in plants during dehydration. The standard mixture was constituted in order to contain representatives of the main compound types in this category: neutral monosaccharide glucose (Glc), neutral disaccharide sucrose (Suc), neutral trisaccharide (raffinose), neutral tetrasaccharide (stachyose), neutral pentasaccharide (verbascose), and the sugar alcohols mannitol (monosaccharide alcohol), and maltitol (disaccharide alcohol).

This mixture was separated on a PGC column without derivatisation and all standard compounds were detected in the negative ion mode as formylated molecules $[M+HCOO]^-$ using electrospray ion trap MS (Figure 5.1). Neutral carbohydrates were also observed to ionise as formylated molecules on direct infusion negative ion mode ESI-qoaTOF-MS analyses of standard solutions in 50:50 (v/v) methanol:water (Chapter 3), thus showing their affinity for low levels of background formate anions present in the instrument.

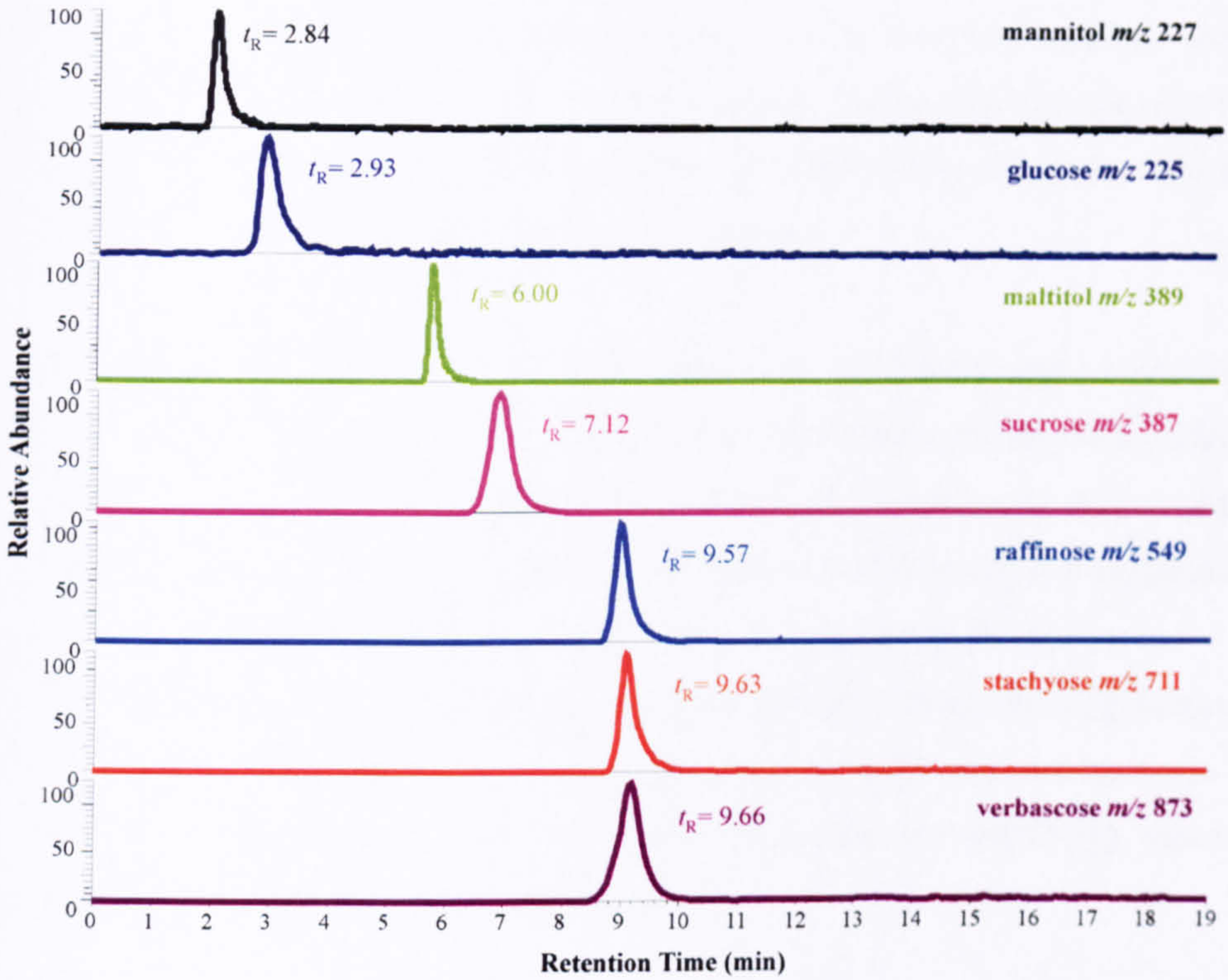

Figure 5.1 Extracted ion chromatograms obtained using mobile phase 1 and negative ion mode PGC-LC-ESI-QIT-MS for the separation of a 50 µg/mL standard mixture of neutral sugars and sugar alcohols. All compounds were detected as formylated molecules $[M+HCOO]^-$.

In order to ensure that these data would be reproducible in other laboratories using other LC-systems (where formate anions may not be present in the background) the effect of addition of small amounts (0.1%) of formate to the mobile phase was therefore tested (mobile phase 2). In this experiment, solvent (A) was water modified with 0.1% formic acid (FA) and (B) acetonitrile modified with 0.1% FA, to ensure that formate anions are present. To test the effect on the chromatography of this modification to the eluents, the same standard mixture as in Figure 5.1 was used and separated on the PGC column using these new eluents. It was verified that the same elution profile as in Figure 5.1 was obtained (when no formic acid was present in the mobile phase), as well as that the retention times remained unchanged (Table 5.1) (all were the same within the standard deviation). The LODs for all the standard compounds listed in Table 5.1 were also determined

using mobile phase 2, and it was verified that they too remained unchanged. Since good PGC-LC separation and identification of all standard compounds was achieved in approximately 10 min using a binary gradient composed of water and acetonitrile (without the need for addition of formate), the remainder of the experiments were carried out using mobile phase 1.

Although raffinose (t_R= 9.57 min), stachyose (t_R= 9.63 min), and verbascose (t_R= 9.66 min) elute very close together, since these compounds have different masses it was decided not to attempt to separate them further, as this would have required extending the gradient and thus the run time. Instead, it was decided to make use of the conveniently short run time, by exploiting the ability to differentiate these compounds mass spectrometrically. Conversely, galactinol (t_R= 4.35 min), Suc (t_R= 7.49 min) and maltose (t_R= 8.37 min) are isomeric compounds detected at *m/z* 387 (formylated molecules $[M+HCOO]^-$); these were resolved using this PGC method (Figure 5.2).

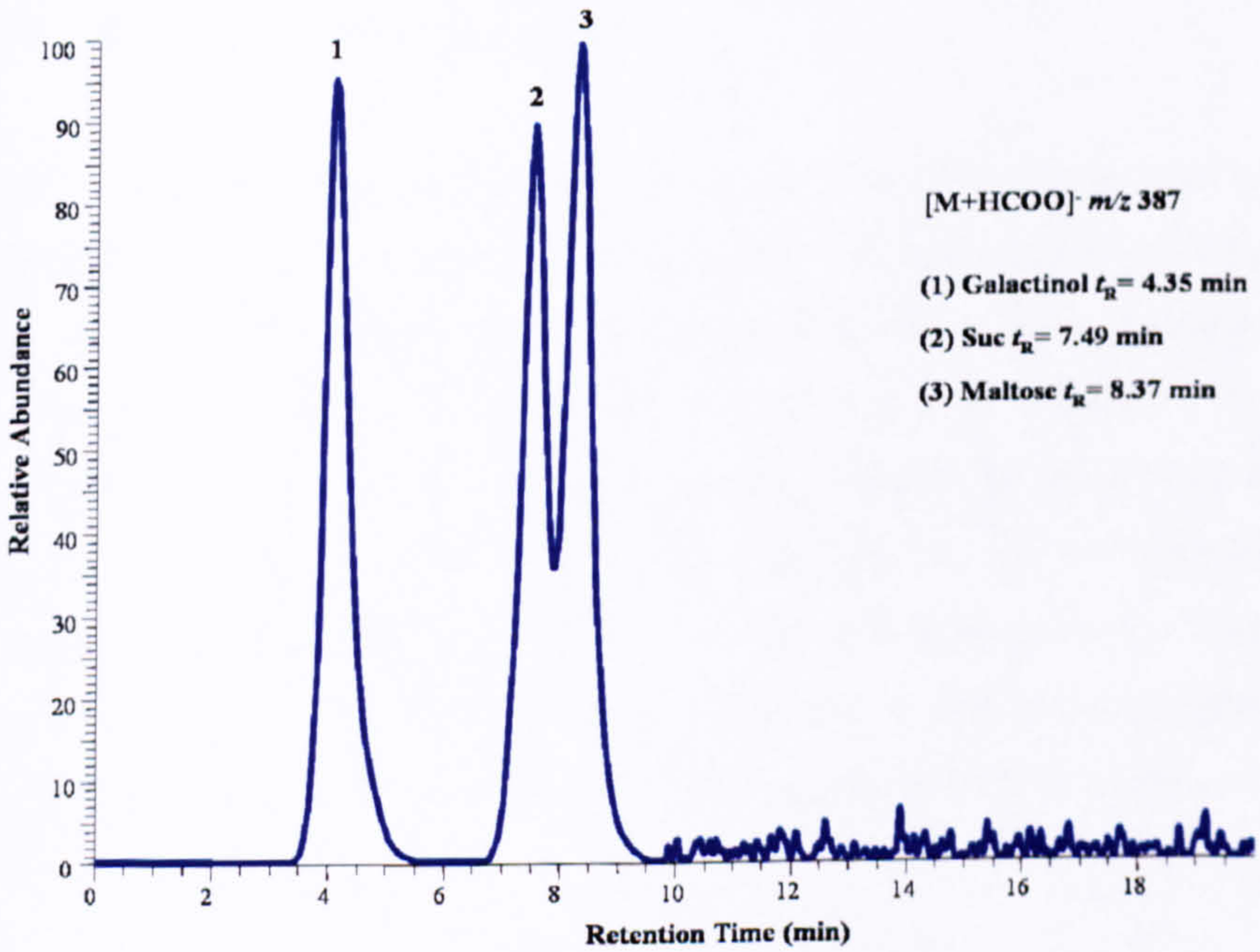

Figure 5.2 Extracted ion chromatogram obtained on PGC-LC-ESI-QIT-MS for a standard solution (10 μM) of the isomeric compounds: (1) Galactinol t_R= 4.31 min, (2) Suc t_R= 7.12 min and (3) Maltose t_R= 8.34 min, all detected at *m/z* 387 (formylated molecules $[M+HCOO]^-$).

Following the optimisation of the PGC-LC separation, the PGC method was further developed by performing LC-IT-tandem mass spectrometry experiments (MS^n) on the individual authentic standard compounds listed in Table 5.1 to record their characteristic ion trap mass spectrometric fragmentation behaviour. Specific ions (formylated molecules $[M+HCOO]^-$) were selected as precursors for fragmentation in order to collect MS^2 and MS^3 data.

To illustrate typical MS^n data obtainable using this PGC-based method, experimental data are described for the non-reducing trisaccharide raffinose ($[M+HCOO]^-$ at *m/z* 549) (Figure 5.3). Raffinose is a member of the raffinose family oligosaccharides (RFOs), which are non-reducing carbohydrates, consisting of galactose (Gal) units linked to Suc via α-1,6 glycosidic linkages.

Figure 5.3a illustrates the extracted ion chromatogram for raffinose at *m/z* 549 from the full scan negative ion ESI mass spectrum, the extracted ion chromatogram for *m/z* 503 from the full scan product ion spectrum of *m/z* 549, and the extracted ion chromatogram for *m/z* 179 from the full scan product ion spectrum of *m/z* 503 (Figure 5.3a).

The collision induced dissociation (CID) MS^2 product ion spectrum of raffinose produced an intense ion at *m/z* 503 ($[M-H]^-$) corresponding to the loss of formic acid [HCOOH] (Figure 5.3b). Subsequent CID MS^3 analysis, readily achieved using ion trap MS, of the $[M-H]^-$ ion at *m/z* 503 produced intense ions at *m/z* 341 and at *m/z* 179, which are formed by cleavage of the glycoside bond with the loss of one hexose moiety $C_6H_{10}O_5$ (-162 Da), and the loss of two hexose moieties $C_6H_{10}O_5$ (-324 Da), respectively, and produced A-type cross-ring fragment ions at *m/z* 221, 251, 281, and 311 which are formed by multiple neutral losses of CH_2O (-30 Da) (Figure 5.3c). For a detailed discussion of the MS behaviour of the RFOs, see Chapter 6.

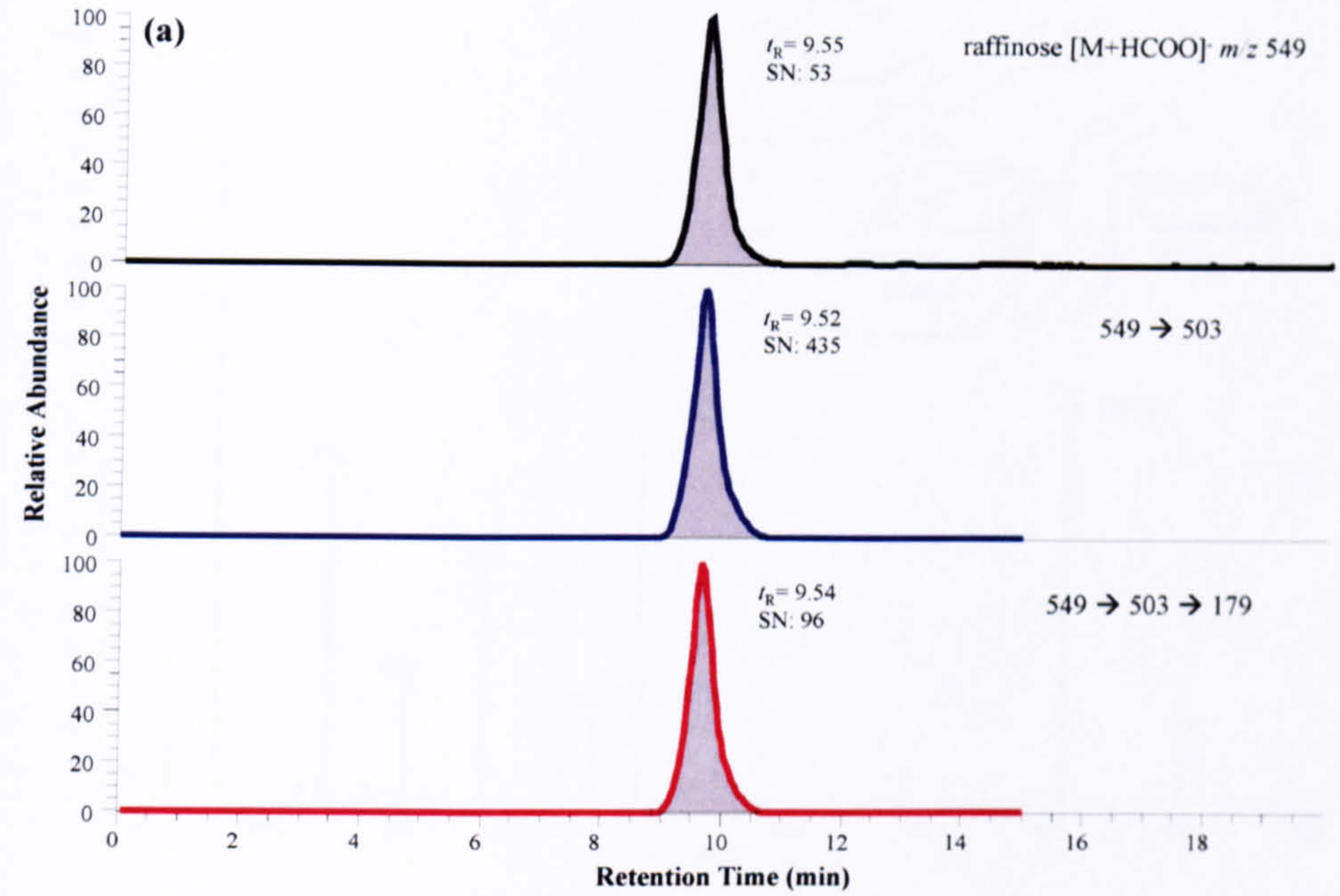

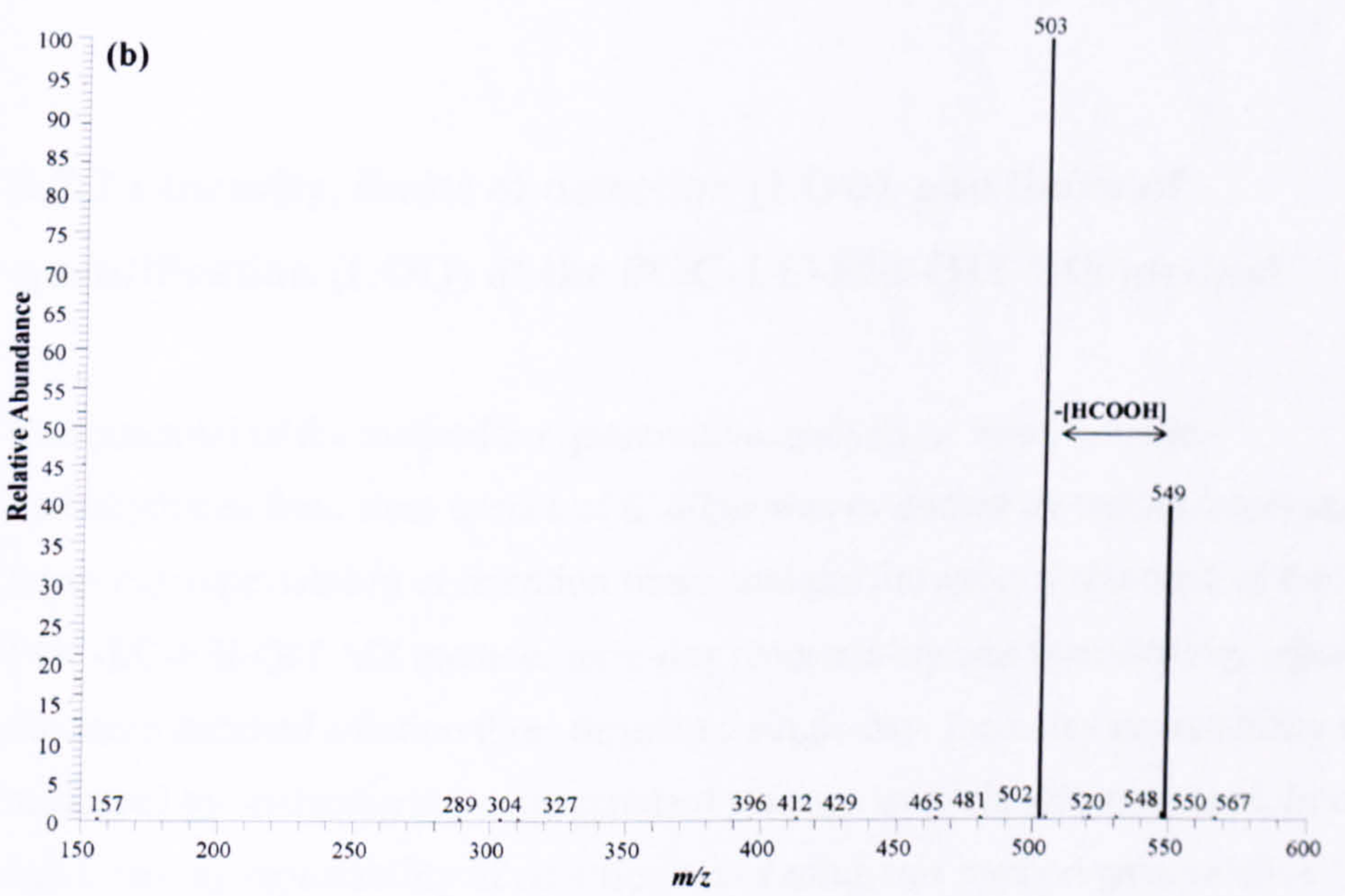

Figure 5.3 (a) Extracted ion chromatograms (mobile phase 1) obtained using negative ion mode PGC-LC-ESI-QIT-MS showing the specificity of detection provided by CID MS^n for a standard solution (10 μM) of raffinose, detected at *m/z* 549 ($[M+HCOO]^-$); (c) CID MS^3 spectrum of raffinose (precursor ion $[M-H]^-$ at *m/z* 503).

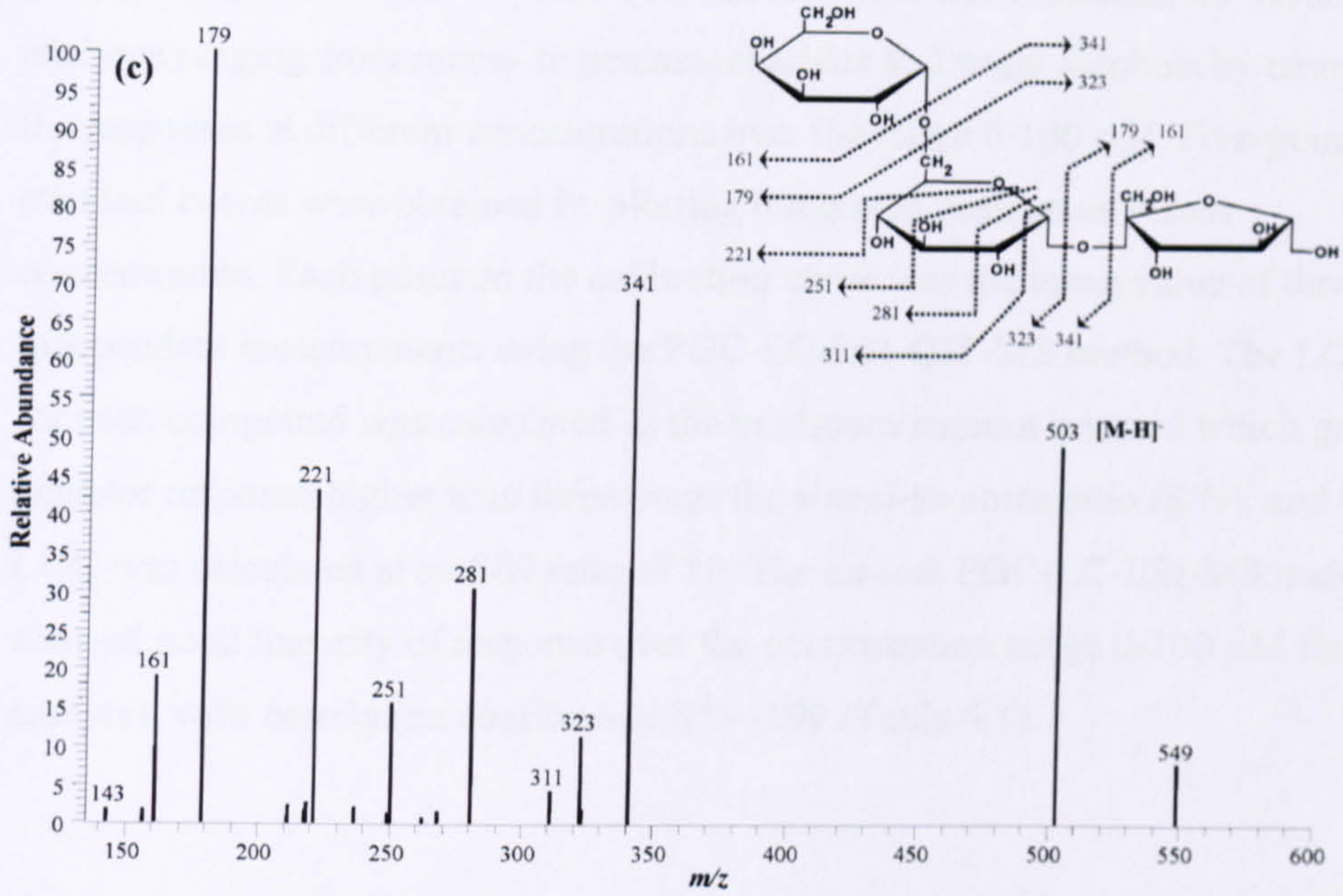

Figure 5.3 *(Continued).*

5.2.2 Linearity, limits of detection (LOD), and limits of quantification (LOQ) of the PGC-LC-ESI-QIT-MS method

The potential of the method for quantitative analysis of water soluble carbohydrates from stem tissues of *L. albus* was evaluated by testing intra- and inter- day repeatability of retention times, and the linearity of response of the PGC-LC-ESI-QIT-MS method. Intra-day repeatability was measured by injecting the same standard solution three times in a single day. Inter-day repeatability was measured by analysing the same standard solution over six different days. Intra- and inter-day repeatability of retention times using this method gave relative standard deviations (RSD) of less than 2% (Table 5.1).

The linearity of the PGC-LC-ESI-QIT-MS response was measured for several analytes ranging from mono- to pentasaccharides and sugar alcohols by recording the responses at different concentrations over the range 0-100 μM. Five-point standard curves were obtained by plotting integrated peak areas versus concentration. Each point on the calibration curve was the mean value of three independent measurements using the PGC-LC-ESI-QIT-MS method. The LOD for each compound was calculated as the minimum amount injected which gave a detector response higher than three times the signal-to-noise ratio (S/N), and the LOQ was calculated at an S/N ratio of 10. The on-line PGC-LC-ESI-MS method showed good linearity of response over the concentration range 0-100 μM for all analytes, with correlation coefficients $R^2 > 0.99$ (Table 5.1).

Table 5.1 Nominal *m/z* values, retention times, intra- and inter-day repeatabilities of retention times, LOD, LOQ, and linearity of calibration curves obtained for standard compounds using negative ion PGC-LC-ESI-QIT-MS.

Standard compounds	Diagnostic ion (*m/z*)	t_R 1[a] (min)	t_R 2[b] (min)	t_R (intra RSD)[c] (%, n=3)	t_R (inter RSD)[d] (%, n=6)	LOD [e] (μM)	LOQ [f] (μM)	Amout LOD [g] (pmol)	R [2,h]
Inositol	225 $[M+HCOO]^-$	2.44	2.49	0.47	1.48	0.60	2.00	12	0.9981
Mannitol	227 $[M+HCOO]^-$	2.84	2.87	0.54	0.96	1.00	3.33	20	0.9985
Fru	225 $[M+HCOO]^-$	2.86	2.91	0.68	0.77	2.00	6.70	40	0.9958
Glc	225 $[M+HCOO]^-$	2.93	2.98	0.20	1.15	0.45	1.60	9	0.9956
Sorbitol	227 $[M+HCOO]^-$	2.95	2.99	0.78	1.47	1.00	3.33	20	0.9989
Galactinol	387 $[M+HCOO]^-$	4.31	4.35	0.48	0.50	0.08	0.25	2	0.9958
Maltitol	389 $[M+HCOO]^-$	6.00	6.07	0.35	1.11	0.08	0.25	2	0.9991
Suc	387 $[M+HCOO]^-$	7.12	7.19	0.41	0.59	0.08	0.25	2	0.9995
Maltose	387 $[M+HCOO]^-$	8.34	8.40	0.37	0.71	0.08	0.25	2	0.9931
Raffinose	549 $[M+HCOO]^-$	9.57	9.59	0.12	0.50	0.10	0.33	2	0.9966
Stachyose	711 $[M+HCOO]^-$	9.63	9.65	0.21	0.41	0.06	0.20	1	0.9970
Verbascose	873 $[M+HCOO]^-$	9.66	9.70	0.26	0.42	0.02	0.07	0.4	0.9997

HPLC conditions: Hypercarb PGC column (100 mm x 4.6 mm i.d.), 20 μL injection, flow rate 600 μL/min. [a] Retention times obtained using mobile phase 1; [b] Retention times obtained using mobile phase 2; [c] Intra-day RSD of retention times (mobile phase 1, n=3 independent measurements); [d] Inter-day RSD of retention times (mobile phase 1, n=6 independent measurements); [e] Concentration LOD calculated at an S/N of 3 (mobile phase 1); [f] LOQ calculated at an S/N of 10 (mobile phase 1); [g] LOD of the amount loaded onto column calculated at an S/N of 3 (mobile phase 1); [h] Correlation coefficients for the standard curves (five points) of relative peak areas against concentration (0-100μM) (mobile phase 1).

5.2.3 Characterisation of the *L. albus* water status during early/mild/severe water deficit, and recovery conditions

The characterisation of the *L. albus* plant water status during development and stress imposition was monitored by means of soil water content, predawn leaf water potential (Ψ_{leafpd}), and tissue relative water content (RWC) (Table 5.2). These results were obtained by collaborators at the Plant Sciences Division, ITBQ, Oeiras, Portugal.

At 4 days after withholding water (DAW), soil water content had decreased by approximately 40-45% when compared to that of well watered (WW) control plants, but the plant water status was barely affected, as the leaf and stem RWCs decreased by only around 5%. Although there was a clear soil water shortage at 4 DAW the stress on the plant can be considered as mild.

At 13 DAW, soil water content was dramatically reduced (by approximately 85%) when compared to WW control plants, and this was significantly reflected in the plant water status: Ψ_{leafpd} decreased by about 5 fold (down to -1.7 MPa), leaf RWC decreased by approximately 50%, and stem RWC decreased by around 15%. It was clear from these results that at 13 DAW the plant is under severe water deficit. However, the stem components (cortex and stele) were much less affected during the WD period than leaves, as they showed a higher capacity to retain water (only 15% reduction). It was also clear that *L. albus* can withstand severe WD, since upon rewatering (RW) the plant water status was rapidly restored (Table 5.2). In fact, 6 h after water reintroduction the RWC of leaves and stems was restored and after 26 h of rewatering the plant water status was similar to that of the control plants.

Table 5.2 Soil water content (%), pre-dawn leaf water potential (Ψ_{leafpd}) and leaf, stem stele and stem cortex relative water content (RWC) during the period of water deficit (WD) imposition and rewatering (RW). WW, well watered plants (control).

	soil water content (%)		Ψ_{leafpd}(MPa)		leaf RWC (%)		stem stele RWC (%)		stem cortex RWC (%)	
DAW	WW	WD	WW	WD	WW	WD	WW	WD	WW	WD
4 d	27.6 ± 0.8	15.3 ± 0.5	-0.23 ± 0.01	-0.28 ± 0.01	90 ± 1.7	87 ± 0.8	91 ± 1.0	92 ± 0.1	68 ± 4.6	64 ± 0.5
13 d	18.3 ± 0.3	2.2 ± 0.1	-0.33 ± 0.02	-1.74 ± 0.05	86 ± 2.7	46 ± 4.7	91 ± 0.5	77 ± 0.7	66 ± 3.7	55 ± 2.9
6 h RW	22.0 ± 0.5	20.1 ± 1.5	-	-	-	84 ± 2.1	-	91 ± 1.0	-	67 ± 0.3
26 h RW	19.5 ± 0.2	16.9 ± 1.4	-0.31 ± 0.03	-0.35 ± 0.04	88 ± 4.2	86 ± 1.7	94 ± 5.3	90 ± 3.0	67 ± 1.7	71 ± 0.3

5.2.4 PGC-LC-ESI-QIT-MS^n analysis of water soluble carbohydrates from *L. albus* stem extracts

The results described in the previous section (Section 5.2.3) indicate that two very distinct water deficit phases can be studied in *L. albus* plants corresponding to early stress (4 DAW), and severe stress (13 DAW), and it was previously shown that the stems are fundamental systems that allow *L. albus* plants to survive such WD (Pinheiro et al., 2001; Pinheiro et al., 2004). This on-line PGC-LC-ESI-QIT-MS system was, thus, applied as a sensitive method to study the effect of water deficit on the water soluble carbohydrate components of *L. albus* stem tissues (cortex and stele) at 4 DAW and 13 DAW, and 6 and 26 h after rewatering.

The application of this on-line PGC-LC-ESI-QIT-MS method allowed the separation and identification in a single run of three water deficit responsive metabolites from *L. albus* stem extracts: the water soluble carbohydrates Glc, Suc, and raffinose. The presence of Glc, Suc, and raffinose in stem extracts was demonstrated based on the retention times, masses, and characteristic fragmentation patterns (MS^2 and MS^3) of peaks obtained on analysis of the stem extracts, and their comparison with those obtained for authentic standard compounds (Table 5.1). Glc, Suc, and raffinose were quantified by PGC-LC-ESI-QIT-MS using the aqueous calibration curves (Table 5.1), and the ions at *m/z* 225 for Glc ($[M+HCOO]^-$), *m/z* 387 for Suc ($[M+HCOO]^-$), and *m/z* 549 for raffinose ($[M+HCOO]^-$).

Figure 5.4 shows the quantitative results obtained using PGC-LC-ESI-QIT-MS for *L. albus* stems (cortex and stele) at 4 DAW (early/mild stress), 13 DAW (severe stress), and subsequent rewatering (RW) for 6 and 26 h for Glc (Figure 5.4a), Suc (Figure 5.4b), and raffinose (Figure 5.4c). Quantitative values for the control plants (well watered) at 4 and 13 d are also shown.

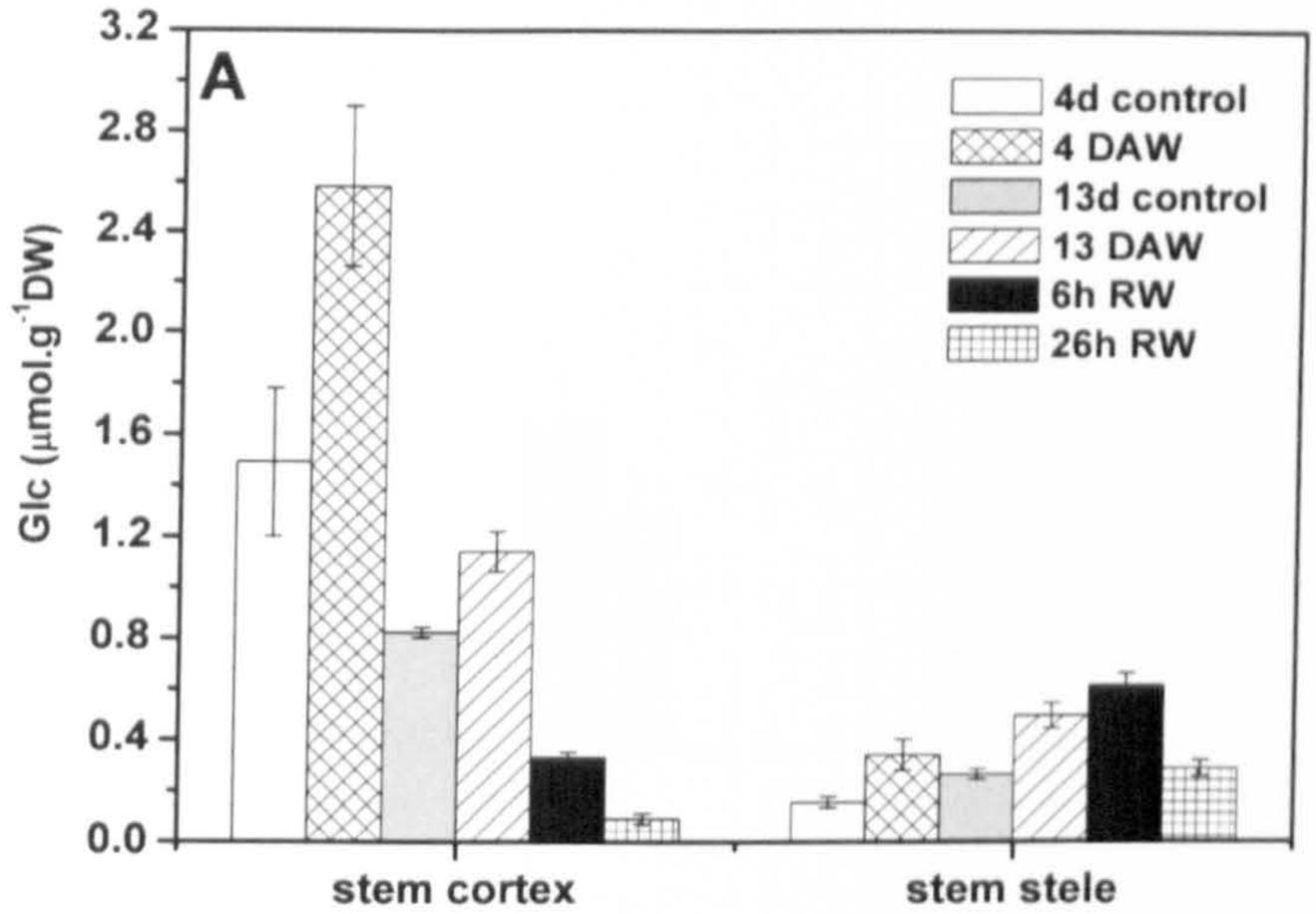

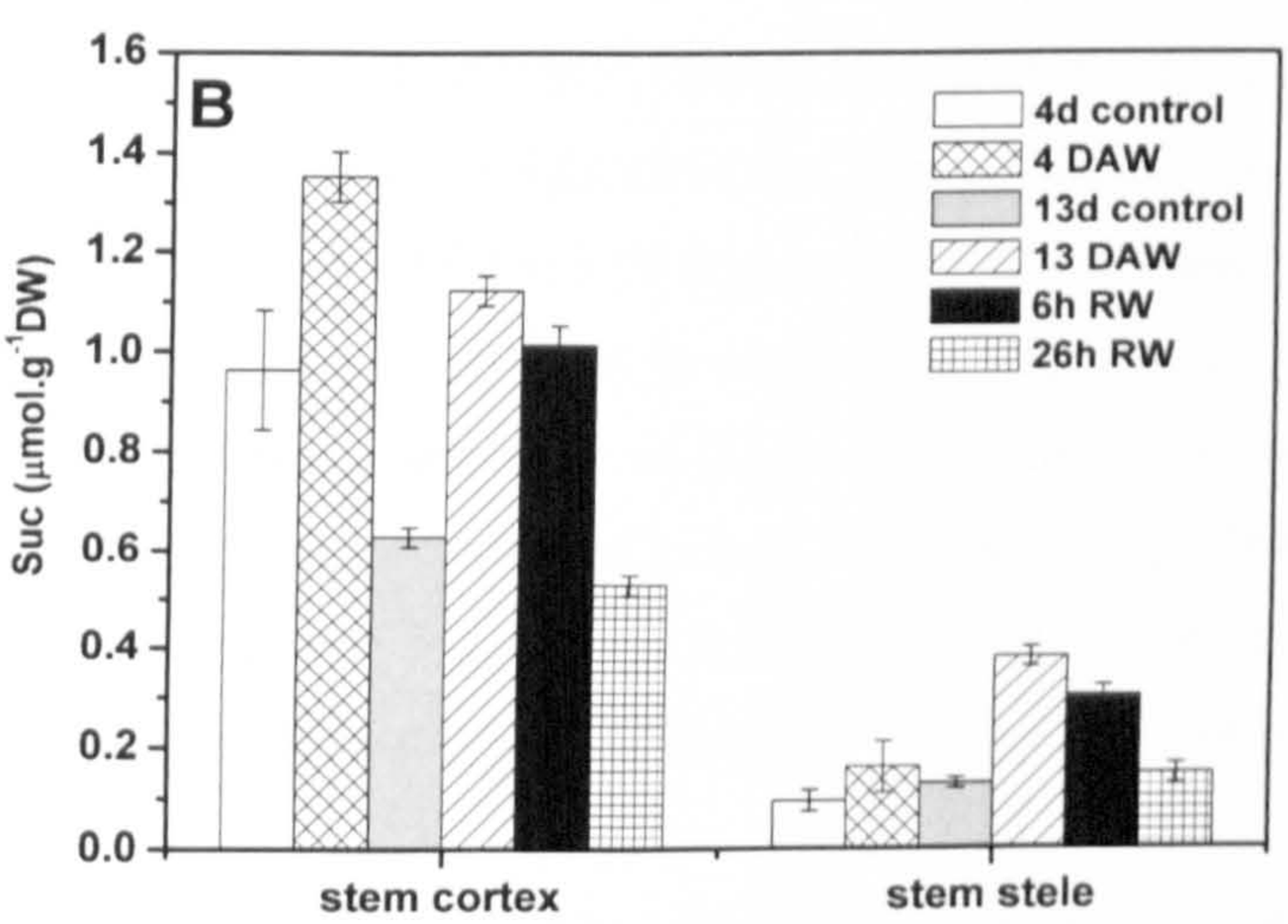

Figure 5.4 Water soluble carbohydrate levels in *Lupinus albus* stems obtained by PGC-LC-ESI-QIT-MS at 4 days after withholding water (DAW; early water stress), 13 DAW (severe water stress), 6 and 26 h after rewatering (RW). (A) Glc, (B) Suc, and (C) raffinose. Data are mean ± SD of n=2-3 biological replicates. Each biological replicate is the mean value of n=2-3 independent PGC-LC-ESI-QIT-MS measurements. DW, dry weight. Control, well watered plants. nd, not detected.

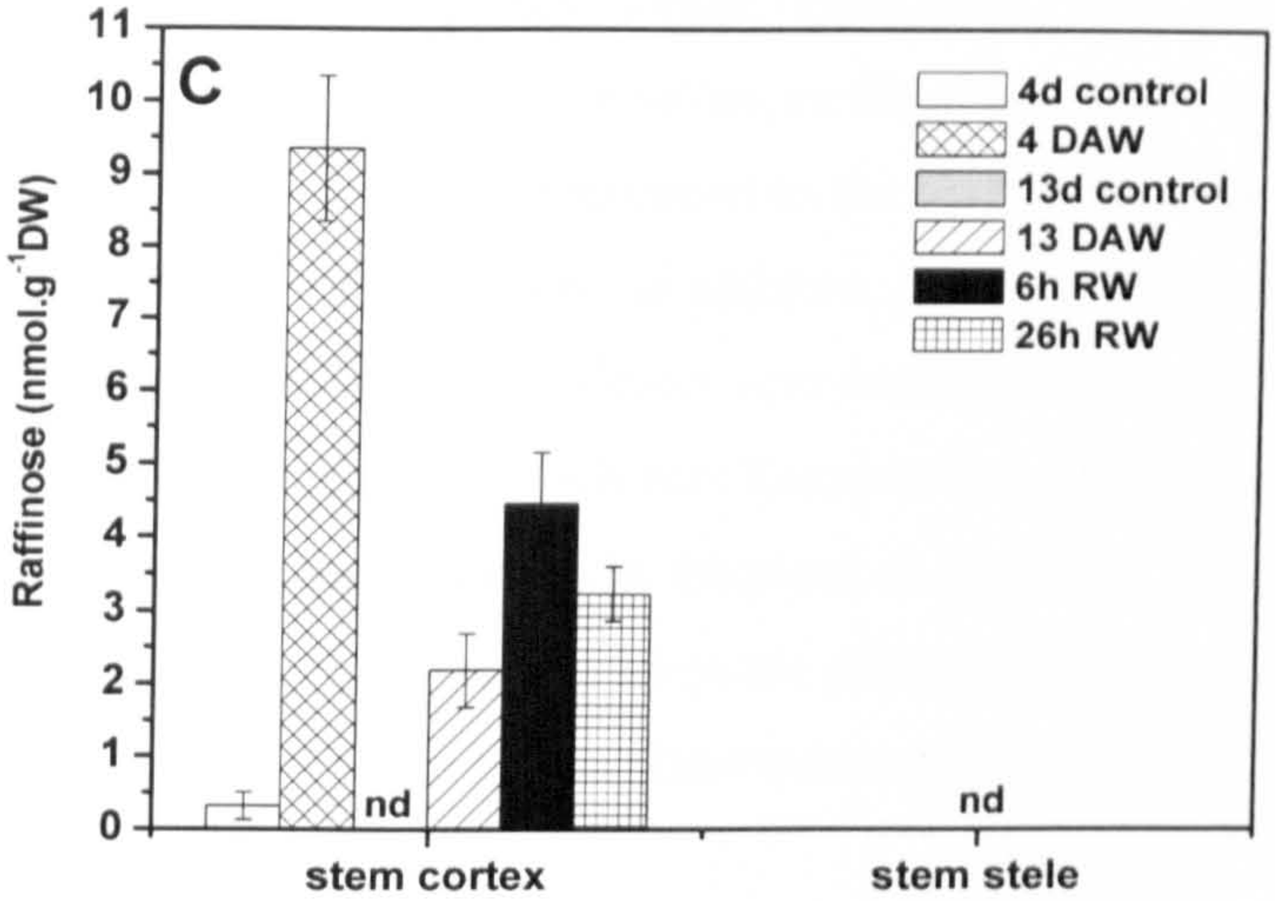

Figure 5.4 *(Continued).*

Using this PGC-LC-ESI-QIT-MS method, at 4 DAW (early stress), levels of 2.58±0.32 μmol.g^{-1} of dry weight (DW) for Glc, 1.35±0.05 μmol.g^{-1} DW for Suc, and much lower levels of 9.34±1.00 nmol.g^{-1} DW for raffinose were determined in stem cortex extracts of *L. albus*. In comparison with the early stress, a decrease in sugar amounts was observed at 13 DAW (severe stress) in stem cortex extracts of *L. albus*, with levels determined to be 1.14±0.08 μmol.g^{-1} DW for Glc, 1.12±0.03 μmol.g^{-1} DW for Suc, and 2.18±0.50 nmol.g^{-1} DW for raffinose. RW caused a subsequent decrease in the levels of Glc and Suc, but not raffinose.

In the stem stele extracts of *L. albus*, the levels of these water soluble carbohydrates were found to be much lower than those in the stem cortex; 4 DAW stele levels of 0.34±0.06 μmol.g^{-1} DW for Glc, and 0.16±0.05 μmol.g^{-1} DW for Suc were obtained (raffinose was not detected). In contrast to what is observed in stem cortex tissues, an increase in sugar amounts was observed at 13 DAW (severe stress) in stem stele extracts when compared to early stress, with levels of 0.49±0.05 μmol.g^{-1} DW for Glc, and 0.38±0.01 μmol.g^{-1} DW for Suc determined. RW caused a steady decrease in glucose and sucrose. It was observed that *L. albus*

stems accumulate water soluble sugars (Glc, Suc, and raffinose) during WD suggesting a role as a temporary storage organ during dehydration. Despite the small variations in the plant water status, or the small variations in the stem RWC (Table 5.2), WD causes large alterations in the carbohydrate content of *L. albus* stems both 4 DAW and 13 DAW. In addition, by using PGC coupled to ESI-MS, we could separate, identify, and detect very small amounts of raffinose (nmol.g^{-1} DW) in stem cortex tissues, which was found to be highly responsive to WD, reacting rapidly to small changes in the plant water status. Interestingly, its response is higher in early stress (when the plant water status is still largely unaffected) and on RW (when the plant water status is re-established).

Raffinose is a member of the RFOs, and it has been proposed that the primary roles of RFOs in seeds and vegetative tissues are to function as storage reserves for use during seed maturation, transport carbohydrates in the phloem, and also to function as osmoprotection molecules against abiotic stresses, such as drought, salinity or cold (Taji et al., 2002; Zuther et al., 2004). The accumulation of raffinose during seed maturation has also been associated with the development of desiccation tolerance in mature seeds (Koster and Leopold, 1988; Taji et al., 2002).

The presence of raffinose has been previously detected in vegetative tissues of different plant systems exposed to WD (mainly using HPLC with refractive index detection or HPAEC-PAD). In coleus leaves, raffinose levels remained unchanged in response to WD, and were found to vary between 0.1-0.2 μmol.g^{-1} FW (Pattanagul and Madore, 1999). In perennial ryegrass leaves, raffinose levels decreased in response to WD, leaf bases being less affected (from 0.7 to 0.2 μmol.g^{-1} DW) than leaf blades (from 3.1 to 0.7 μmol.g^{-1} DW) (Amiard et al., 2003). On the other hand, in *Arabidopsis thaliana* plants, raffinose was found to be highly responsive to progressive WD, accumulating up to 0.4 μmol.g^{-1} FW (Taji et al., 2002). A similar response was found recently in the leaves of the angiosperm resurrection plant *Xerophyta viscosa*, where raffinose accumulated up to 35 μmol.g^{-1} DW (Peters et al., 2007).

In *L. albus* stem cortex tissues, not only were much lower levels of raffinose determined (nmol.g^{-1} DW) than those cited above for the leaves of other plants, but it was also shown that raffinose does not increase steadily under progressive WD (i.e., a transient accumulation of raffinose is observed between early and severe stress) which brings into question the role of raffinose in desiccation tolerance in stems. Taking into account that the separation occurred at the vascular cambium level*, the stele includes both the parenchymatous pith tissue and the xylem while the cortex includes parenchymatous tissue and the phloem, these results are in agreement with the hypothesis that raffinose is more effectively retained in the phloem, leading to higher transport efficiency (Hannah et al., 2006).

5.3 Conclusions

The aim of this study was to develop a robust LC-MS system using a PGC Hypercarb column, suitable for on-line coupling with ESI-QIT-MS^n, for the sensitive analysis of water soluble carbohydrates extracted from the stem tissues of *L. albus* plants subjected to early and severe water deficit conditions, followed by a rewatering period. This PGC-LC-ESI-QIT-MS method provides good linearity, selectivity, short analysis times (approximately 10 min), and LODs in the low picomole range (0.4-20 pmol) for a wide variety of sugars and sugar alcohols.

In this study, raffinose was found to be highly responsive to WD in stem cortex tissues, reacting rapidly at a very early stage of dehydration when only small changes in the plant water status occur. Such an early stress study requires a sensitive technique that can measure small amounts of water deficit-responsive metabolites as well as tissue specific responses in *L. albus* plants, induced by mild

* The vascular cambium is the lateral embryonic tissue region that forms the vascular tissues (phloem and xylem) in the stem and root. Is located between those two tissues, and gives cells towards both tissues (Evert, 2006).

drought. It was demonstrated that this PGC-LC-ESI-QIT-MS^n method is capable of separating, detecting and measuring in a single run, water soluble sugars (Glc, Suc and raffinose) from *L. albus* stem tissue extracts, down to nmol.g^{-1} DW levels. This method is sensitive, and combines the separation power of the LC system with an ion trap instrument that can perform multistage tandem MS, thus, providing useful structural identification of metabolites from a single sample analysis.

In order to further understand a possible physiological role of raffinose in desiccation tolerance in *L. albus* plants, a new study is now being set up as part of the collaborative project entitled 'Screening for stress responsive metabolites in *Lupinus albus*'. The PGC-LC-ESI-QIT-MS^n described in this chapter will be used primarily to study the effects of early stress WD imposition not only in *L. albus* stems but also in other organs (young leaves and roots).

Chapter 6

Hydrophilic interaction chromatography electrospray ion trap mass spectrometry for the analysis of carbohydrate-related metabolites from *Arabidopsis thaliana* leaf tissues

The work described in this chapter has been published in:

Rapid Communications in Mass Spectrometry 22 (2008) 1399-1407

Carla Antonio[a], Tony Larson[b], Alison Gilday[b], Ian Graham[b], Ed Bergström[a] and Jane Thomas-Oates[a]

[a] Department of Chemistry,
University of York,
UK

[b] Centre for Novel Agricultural Products,
Department of Biology,
University of York,
UK

Chapter 6. Hydrophilic interaction chromatography electrospray quadrupole ion trap tandem mass spectrometry for the analysis of carbohydrate-related metabolites from *Arabidopsis thaliana* leaf tissues (HILIC-ESI-QIT-MS^n)

6.1 Introduction

The column chemistry most widely used in LC-MS applications is reversed-phase (RP) C_{18}. However, polar carbohydrate-related metabolites, such as neutral sugars, sugar alcohols, and sugar phosphates, are poorly retained or completely unretained on typical RP columns (Dunn and Ellis, 2005).The development of appropriate LC-MS methods based on other column chemistries, using ESI-MS compatible mobile phase compositions for the analysis of such compounds is thus required.

Porous graphitic carbon (PGC) stationary phases are one suitable alternative to RP columns for the analysis of polar compounds (Gilbert et al., 1982; Knox et al., 1986; Knox and Ross, 1997), and new PGC-LC-ESI-MS-based methods have been reported and are described in this thesis for the analysis of plant metabolites, including water soluble carbohydrates present in *Triticum aestivum* stems (Robinson et al., 2007), water soluble neutral and phosphorylated carbohydrates extracted from *Arabidopsis thaliana* leaves (Antonio et al., 2007) (Chapter 4), and more recently, water soluble carbohydrates extracted from *Lupinus albus* stems exposed to a gradual imposition of water deficit (Antonio et al., 2008b) (Chapter 5).

These methods offer the advantage of robust and rapid separations of carbohydrate compounds from plant tissues using MS-friendly eluents. However, elution from PGC of highly polar compounds often requires extensive method

development and the inclusion of significant amounts of carboxylic acids (formic or acetic acid) in the mobile phase to provide anions (formate or acetate) for electronic interaction with the PGC surface, in order to elute the more retained compounds (Antonio et al., 2007) (Chapter 4). This has prompted the investigation of alternative column chemistries for these applications.

Another suitable approach for the separation of very polar compounds is hydrophilic interaction chromatography (HILIC). HILIC columns contain a stationary phase that is hydrophilic, and the separation is achieved by partitioning of the analytes into this hydrophilic environment (Alpert, 1990; Alpert et al., 1994). HILIC performance is orthogonal to RP-LC, and similar to that of normal-phase liquid chromatography (NP-LC), but the non-aqueous mobile phase used in NP-LC is replaced by an aqueous-organic mixture (typically acetonitrile in water or volatile buffer) making this technique also well suited for on-line coupling with ESI-MS. HILIC coupled to ESI-MS has been reported for the analysis of food samples (Schlichtherle-Cerny et al., 2003), separation and quantitation of water soluble metabolites extracted from *Escherichia coli* (Bajad et al., 2006), and recently applied in metabonomic studies of urine (Cubbon et al., 2007).

In plant metabolomic studies, the use of HILIC-ESI-MS was introduced by Tolstikov and Fiehn (Tolstikov and Fiehn, 2002) for the analysis of *Cucurbita maxima* phloem tissues. This species is believed to mainly transport raffinose family oligosaccharides (RFOs), such as raffinose, stachyose, and verbascose, and in that study, sucrose, RFOs, uridine diphosphate glucose (UDPGlc), amino acids, and other larger oligosaccharides could be detected in *C. maxima* phloem tissues using HILIC-ESI-MS. The method was used to quantify stachyose, which was found to be present in the range 1-7 mM. Although these few studies have proven that HILIC-ESI-MS is an important tool for the analysis of polar compounds in complex mixtures, its potential for studying the plant metabolome needs to be further developed.

6.1.1 Aim

The work described in this chapter is part of the collaborative project entitled 'CHEMCELL' and was carried out in collaboration with Prof. Ian Graham's group, in CNAP, Department of Biology, at the University of York. This project was funded by a Marie Curie Early Stage Research Training Fellowship of the European Community's Sixth Framework Programme under contract number MEST-CT-2004-504345.

This chapter focuses on the development of a robust on-line HILIC-ESI-MS^n method using negative ion mode and a quadrupole ion trap instrument for the analysis of a range of hydrophilic compounds (neutral sugars, sugar alcohols, and sugar phosphates) commonly found in the plant metabolome, which are generally very difficult to retain on traditional RP-LC, and may be difficult to resolve in a single dimension PGC elution. This HILIC-ESI-QIT-MS method was applied for the analysis of *A. thaliana* wild-type Columbia-0 (Col-0) and its starchless phosphoglucomutase mutant (*pgm1*) leaf extracts, and was used to quantify Glc, Suc, raffinose, and Glc6P in *A. thaliana* extracts. Data obtained using this HILIC-ESI-QIT-MS method were compared with those obtained using a comparable porous graphitic carbon-based LC-ESI-QIT-MS method (Antonio et al., 2007) (Chapter 4). The ion trap negative ion collision induced dissociation (CID) fragmentation behaviour of non-reducing RFOs raffinose, stachyose, and verbascose was also studied and is described in this chapter.

6.2 Results and discussion

6.2.1 HILIC-ESI-QIT-MS^n method development

Typical gradients used for HILIC consist of organic solvents (60-95%) in water or a volatile buffer, with acetonitrile being the most popular choice as it provides better retention of analytes than methanol (Alpert, 1990; Alpert et al., 1994; Schlichtherle-Cerny et al., 2003; Bajad et al., 2006). Buffers used for HILIC are typically ammonium salts of acetate and formate (5-20 mM) due to their solubility at such high percentages of organic solvent. A suitable pH range for HILIC is pH 3-8 (Guo and Gaiki, 2005).

Optimisation of the HILIC separations was carried out using different solutions containing mixtures of authentic standards and a mobile phase composed of acetonitrile and 5 mM ammonium acetate, adjusted to pH 4 with the addition of 0.1% (v/v) of formic acid (FA), adapted from Cubbon *et al.* (Cubbon et al., 2007). The standard mixtures were constituted in order to contain representatives of different polar compound types commonly found in plants: soluble neutral sugars, sugar alcohols, and phosphorylated sugars. In a first step, HILIC separations were optimised using a standard mixture of soluble neutral sugars containing the monosaccharide glucose (Glc), disaccharide sucrose (Suc), trisaccharide (raffinose), tetrasaccharide (stachyose), and pentasaccharide (verbascose) (Figure 6.1).

Good separation, sharp peaks, and retention of all neutral sugars, detected as formylated molecules $[M+HCOO]^-$, were achieved using negative ion mode HILIC-ESI-QIT-MS. The analytes were eluted in the order mono- < di- < tri- < tetra- < pentasaccharide, with the most polar and hydrophilic compound (the pentasaccharide verbascose) being retained longest on the HILIC column.

These results are in agreement with those reported by Tolstikov and Fiehn (Tolstikov and Fiehn, 2002) using HILIC coupled to an ion trap instrument, and a solution containing the following authentic standard compounds: di- (Suc) < tri- (raffinose) < tetra- (stachyose) < heptasaccharide (heptaose).

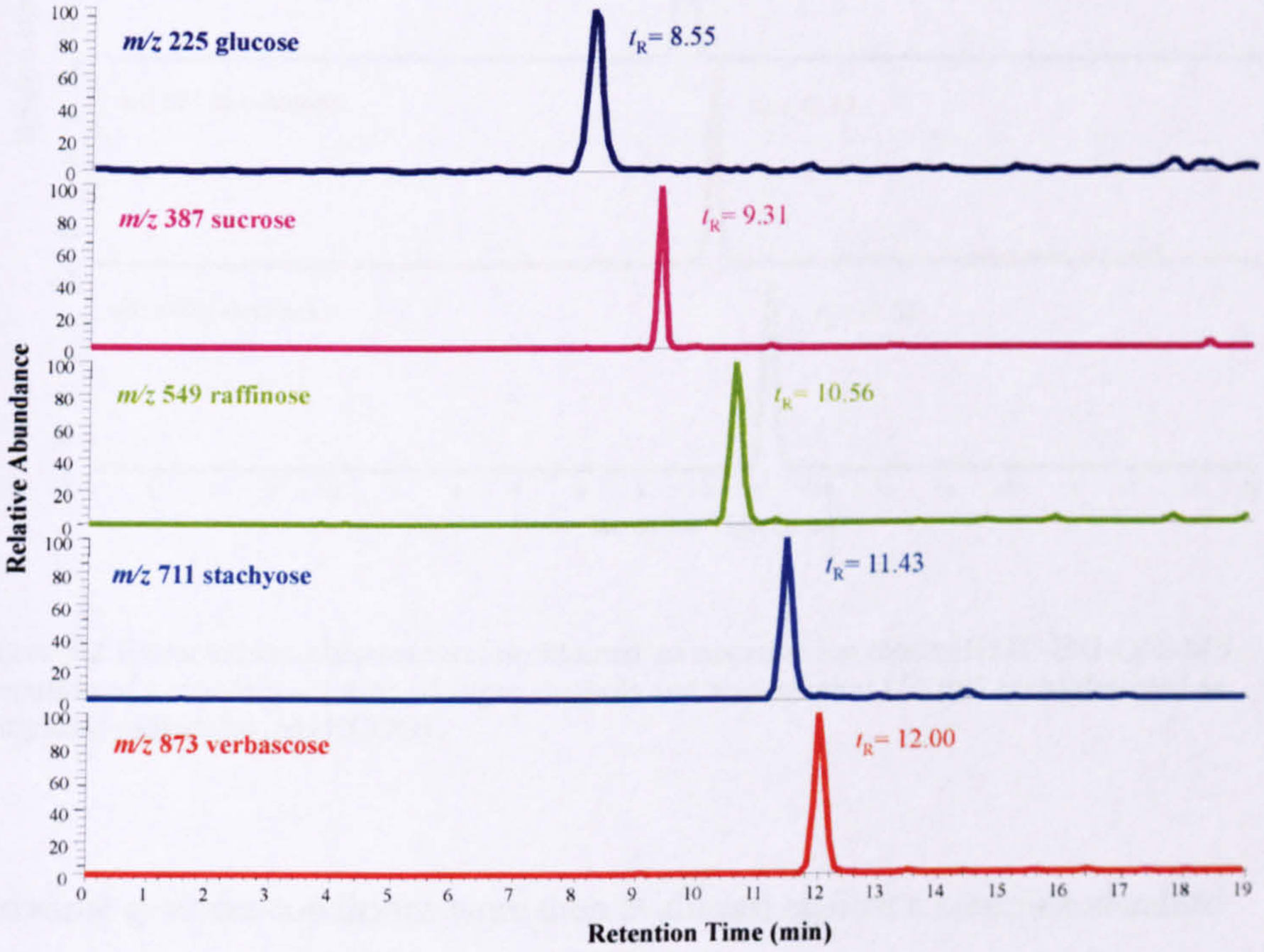

Figure 6.1 Extracted ion chromatograms obtained on negative ion mode HILIC-ESI-QIT-MS separation of a standard solution of neutral sugars (50 μM each) detected as formylated molecules $[M+HCOO]^-$.

In order to assess the suitability of this gradient method for the separation of other polar compounds, we tested the separation of a standard solution of sugar alcohols containing: mannitol (monosaccharide alcohol), maltitol and galactinol (disaccharide alcohols) plus *myo*-inositol. Good separation and retention for all compounds were achieved using HILIC, and these alcohols were also detected as formylated molecules $[M+HCOO]^-$ (Figure 6.2).

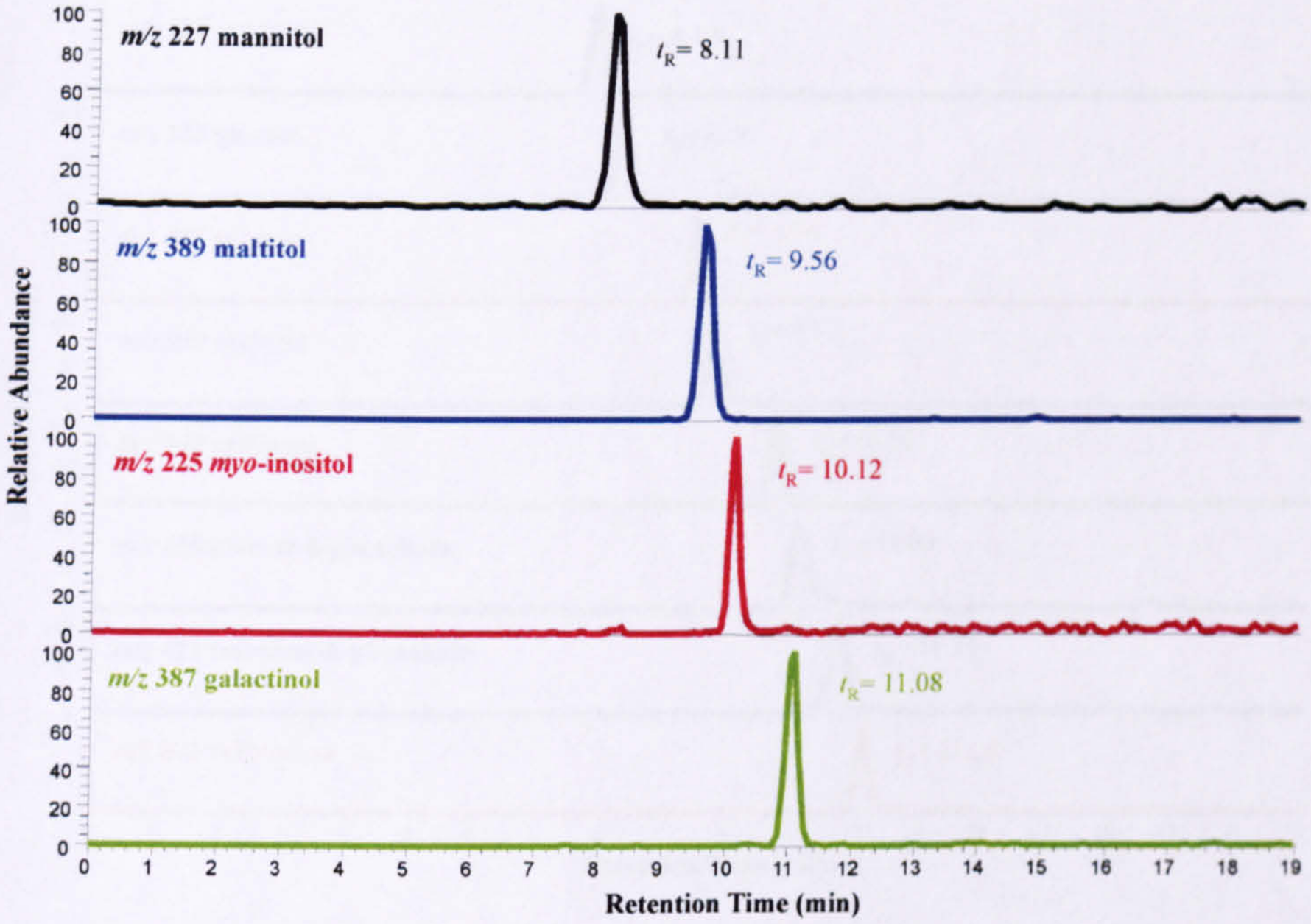

Figure 6.2 Extracted ion chromatograms obtained on negative ion mode HILIC-ESI-QIT-MS separation of a standard solution of sugar alcohols and *myo*-inositol (50 µM each) detected as formylated molecules $[M+HCOO]^-$.

The same gradient conditions were then evaluated against a complex standard mixture containing representatives of different polar compound types found in plants, ranging from neutral soluble sugars (Glc, Suc, raffinose and verbascose), to sugar alcohols (mannitol and maltitol), and negatively charged sugar phosphates, such as glucose-6-phosphate (Glc6P) (phosphorylated monosaccharide) and trehalose-6-phosphate (Tre6P) (phosphorylated disaccharide) (Figure 6.3). Figure 6.3 shows that the same mobile phase has also proven to be successful for the separation of this complex standard mixture containing a wide range of highly polar compounds; therefore, these experimental conditions were selected for further experiments.

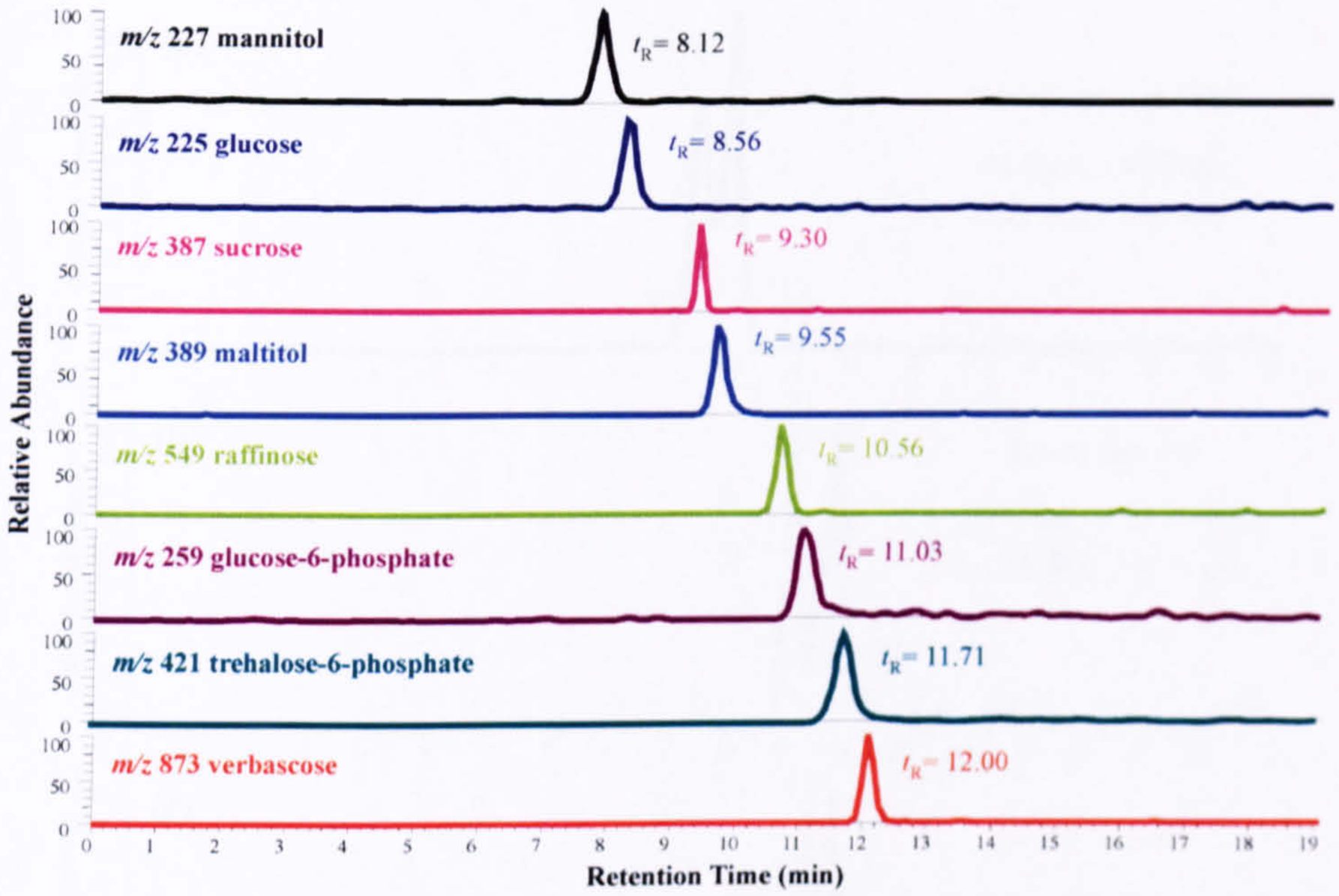

Figure 6.3 Extracted ion chromatograms obtained on negative ion mode HILIC-ESI-QIT-MS separation of a standard solution containing neutral sugars (formylated molecules $[M+HCOO]^-$), sugar alcohols (formylated molecules $[M+HCOO]^-$), and sugar phosphates (deprotonated molecules $[M-H]^-$) (50 μM each).

HILIC was also tested for the separation of isomeric compounds. Figure 6.4 depicts the extracted ion chromatograms obtained using negative ion mode HILIC-ESI-QIT-MS of different standard solutions (50 μM each) containing the isomeric disaccharides Suc and trehalose (Tre), detected as formylated molecules $[M+HCOO]^-$ at m/z 387 (Figure 6.4a), the isomeric monosaccharide phosphates glucose-1-phosphate (Glc1P) and Glc6P, detected as deprotonated molecules $[M-H]^-$ at m/z 259 (Figure 6.4b), and the isomeric disaccharide phosphates sucrose-6-phosphate (Suc6P) and Tre6P, detected as deprotonated molecules $[M-H]^-$ at m/z 421 (Figure 6.4c).

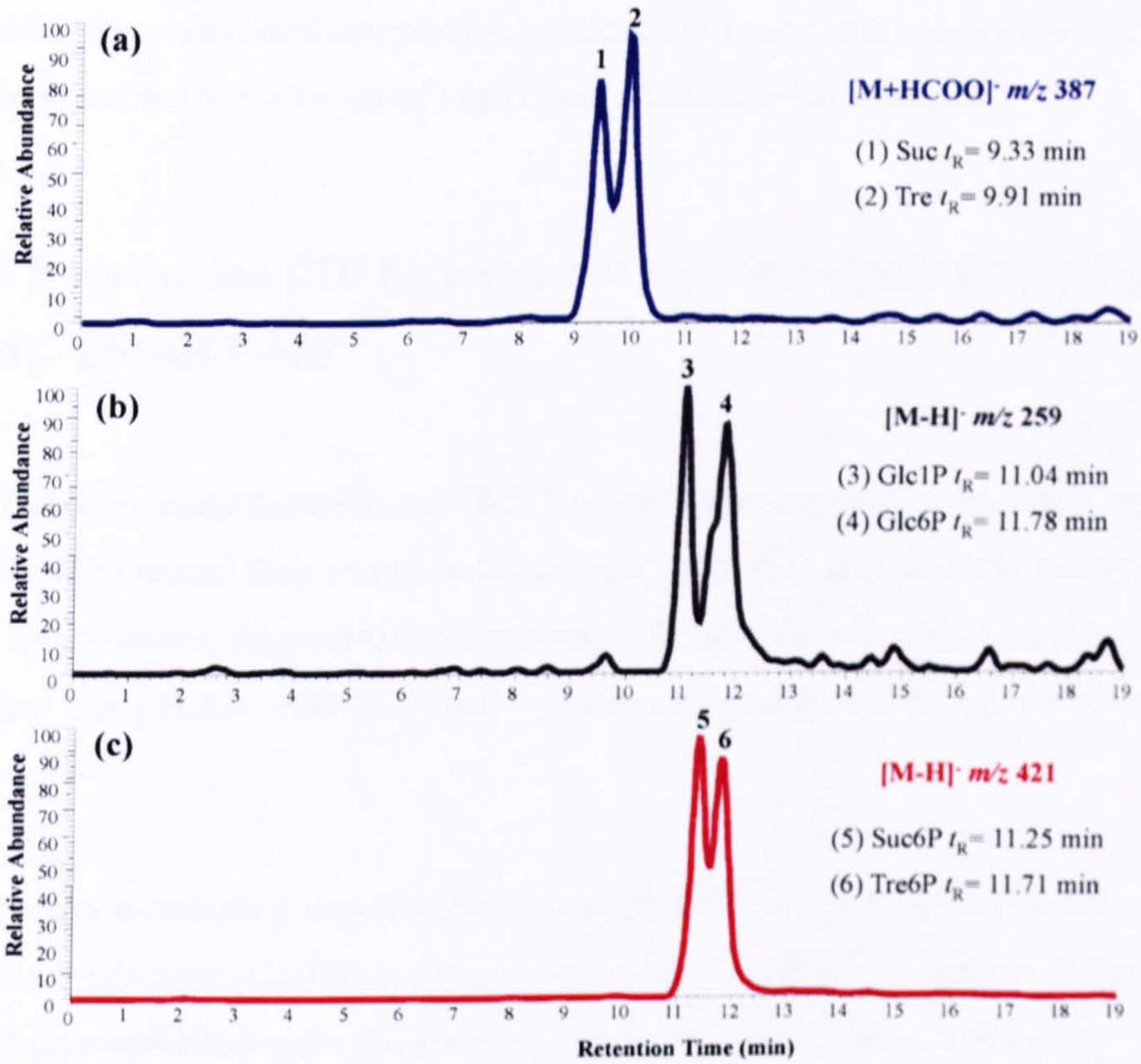

Figure 6.4 Extracted ion chromatograms obtained on HILIC-ESI-QIT-MS separation of different standard solutions containing (a) isomeric disaccharides Suc t_{R1}=9.33 min and Tre t_{R2}= 9.91 min; (b) isomeric monosaccharide phosphates Glc1P t_{R3}=11.04 min and Glc6P t_{R4}= 11.78 min; (c) isomeric disaccharide phosphates Suc6P t_{R5}=11.25 min and Tre6P t_{R6}=11.71 min (50 μM each).

Using HILIC-ESI-QIT-MS, satisfactory chromatographic separation was achieved for these isomeric compounds, and identification and differentiation is possible based on their retention times. Moreover, under the same HILIC-ESI-QIT-MS conditions, the product ion spectra of Glc1P and Glc6P are different and show characteristic product ions that can also be used for unambiguous identification (Chapter 3) (Feurle et al., 1998; Antonio et al., 2007). Better chromatographic separation of the isomeric disaccharides Suc and Tre was recently reported using a porous graphitic carbon (PGC)-LC-ESI-QIT-MS method (Antonio et al., 2007) (Chapter 4). However, the isomeric phosphorylated sugars Glc1P/Glc6P and Suc6P/Tre6P could not be resolved using PGC-LC-ESI-QIT-MS. Using this

HILIC-ESI-QIT-MS, better chromatographic separation was achieved for these isomeric phosphorylated compounds, without the need for extensive method development or the inclusion of high concentrations of formic acid.

6.2.2 Negative ion CID behaviour of non-reducing RFOs using HILIC-ESI-QIT-MS^n

LC-IT-tandem mass spectrometry (MS^n) of authentic standard compounds was performed to record their retention times (t_R) (Table 6.1) and their characteristic mass spectrometric fragmentation behaviour. Typical negative ion CID data obtained using HILIC-ESI-QIT-MS^n are presented and described for non-reducing RFOs.

RFOs are non-reducing sugars widely distributed in the plant kingdom, and consist of galactose (Gal) units linked to the glucose moiety of sucrose via α-(1→6) glycosidic linkages. Diagram 6.1 represents the structure of these carbohydrates showing the nomenclature for carbohydrate fragmentation of Domon and Costello (Domon and Costello, 1988). In the case of these non-reducing glycans, the galactose-containing portion of the molecule is taken as the classical non-reducing terminus, so that its B ion fragments are labelled sequentially from B_1; the 'reducing' terminus is thus attributed to the fructose residue of the sucrose moiety, and its fragments are thus labelled B_n and Y_1, respectively (this extension of the Domon and Costello nomenclature was proposed by B. Domon (Domon, 2008; personal communication).

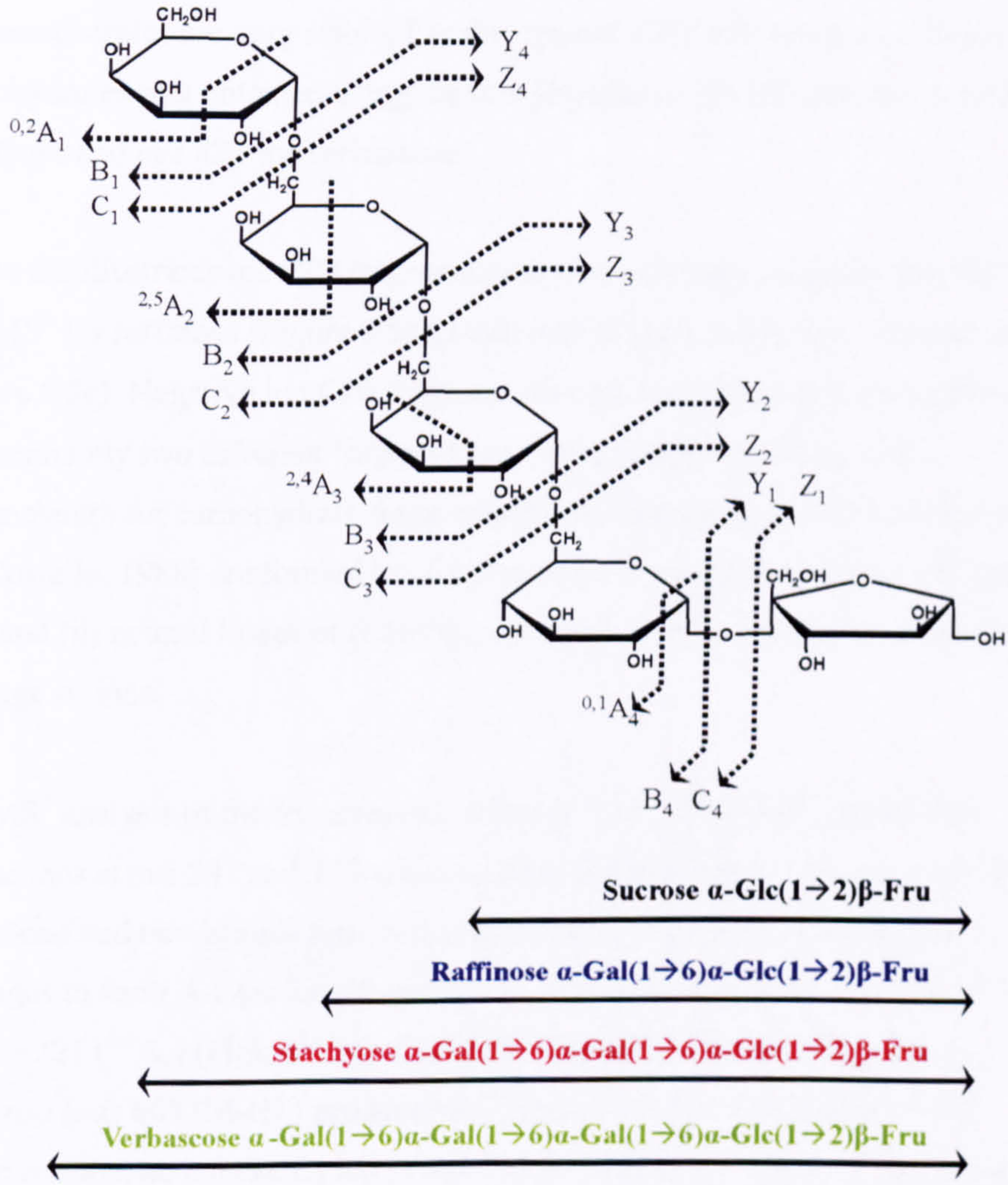

Diagram 6.1 Structure of non-reducing RFOs showing carbohydrate fragmentation according to the nomenclature of Domon and Costello (Domon and Costello, 1988; Domon, 2008; personal communication).

The negative ion CID MS^2 product ion spectrum of the trisaccharide raffinose (*m/z* 549 $[M+HCOO]^-$) produced an intense ion at *m/z* 503 $[M-H]^-$, formed by the loss of formic acid. Subsequent CID MS^3 analysis of the $[M-H]^-$ ion at *m/z* 503 produced characteristic mass spectrometric fragmentation. However, negative ion CID MS^2 analysis of the tetrasaccharide stachyose (*m/z* 711 $[M+HCOO]^-$) and pentasaccharide verbascose (*m/z* 873 $[M+HCOO]^-$) did not produce fragment ions, even when the normalized collision energy was varied between 30-40%,

presumably because the formylated molecules $[M+HCOO]^-$ of these tetra- and pentasaccharides are very stable. For this reason, CID MS^2 analysis of these carbohydrates was obtained using the low abundance $[M-H]^-$ ions at *m/z* 665 for stachyose and *m/z* 827 for verbascose.

Figure 6.5 illustrates the CID fragmentation obtained using negative ion HILIC-ESI-MS^n for raffinose (Figure 6.5a), stachyose (Figure 6.5b), and verbascose (Figure 6.5c). Negative ion CID fragmentation of non-reducing sugars gave predominantly two different fragment ion types, which according to the nomenclature for carbohydrate fragmentation of Domon and Costello (Domon and Costello, 1988) are formed by: (i) glycosidic bond cleavages to give C_i and B_i ions, and (ii) neutral losses of $(CH_2O)_n$, where n= 1, 2,3, or 4 to give cross-ring cleavage A_i ions.

CID MS^3 analysis of the trisaccharide raffinose (*m/z* 503 $[M-H]^-$) produced intense ions at *m/z* 341 and 179 which correspond to C_2 and C_1 ions formed by the loss of one and two hexose residues, respectively, and multiple cross-ring cleavages to form A-type ions at *m/z* 311 ($^{0,1}A_2$), *m/z* 281 ($^{0,2}A_2$), *m/z* 251 ($^{0,3}A_2$), and *m/z* 221 ($^{0,4}A_2$) (Figure 6.5a). CID MS^2 analysis of the tetrasaccharide stachyose (*m/z* 665 $[M-H]^-$) produced a C_3 ion at *m/z* 503 due to loss of one hexose residue, an intense C_2 ion at *m/z* 341 formed by the loss of two hexose residues, and multiple cross-ring cleavages to form the A_2 ions and A_3 ions at *m/z* 443 ($^{0,2}A_3$), *m/z* 413 ($^{0,3}A_3$), and *m/z* 383 ($^{0,4}A_3$) (Figure 6.5b). An identical CID MS^2 spectrum for stachyose was obtained by Tolstikov and Fiehn also using a quadrupole ion trap instrument (Tolstikov and Fiehn, 2002). CID MS^2 analysis of the pentasaccharide verbascose (*m/z* 827 $[M-H]^-$) produced a weak C_4 ion at *m/z* 665 from loss of one hexose residue, an intense C_3 ion at *m/z* 503 formed by the loss of two hexose residues, and multiple cross-ring cleavages to form the A_2 and A_3 ions and A_4 ions at *m/z* 605 ($^{0,2}A_4$), and *m/z* 545 ($^{0,4}A_4$) (Figure 6.5c).

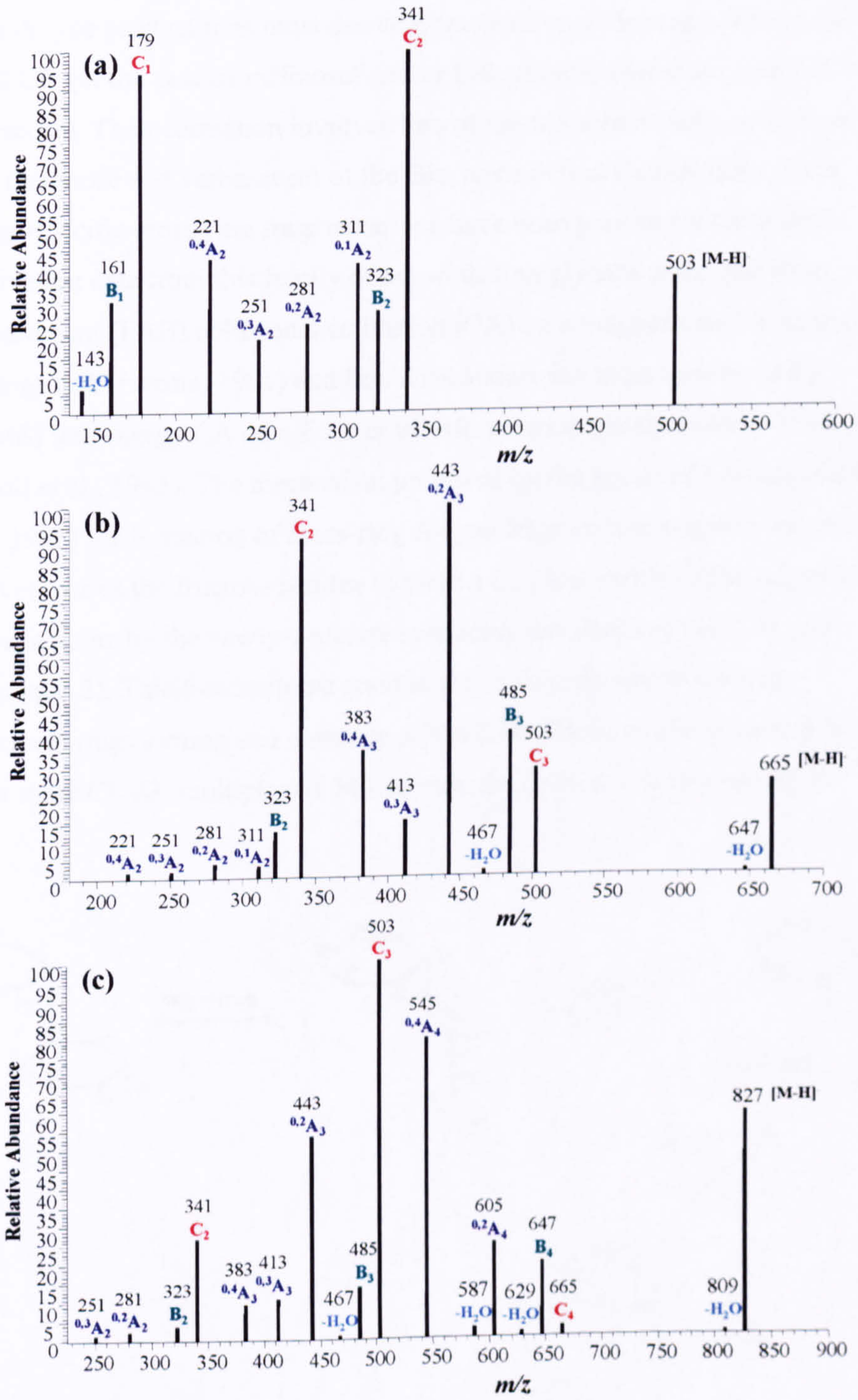

Figure 6.5 Negative ion CID spectra of non-reducing RFOs obtained by HILIC-ESI-QIT-MS^n showing nomenclature of Domon and Costello (Domon and Costello, 1988; Domon, 2008; personal communication). (a) CID MS^3 spectrum of raffinose (precursor ion $[M-H]^-$ *m/z* 503); (b) CID MS^2 spectrum of stachyose (precursor ion $[M-H]^-$ *m/z* 665); (c) CID MS^2 spectrum of verbascose (precursor ion $[M-H]^-$ *m/z* 827).

These A-type product ions must derive from cross-ring cleavage of the α-(1→6) linked Glc (in the case of raffinose) and/or Gal residues (for stachyose and verbascose). Their formation involves loss of the fructose moiety, as well as parts or all (raffinose and verbascose) of the Glc, and internal Gal residues. Such linkage-specific cross-ring fragmentations have been previously reported in negative ion data from this family of non-reducing glycans using fast atom bombardment (FAB) collisional activation (CA) on a magnetic sector instrument (Dallinga and Heerma, 1991) and liquid secondary ion mass spectrometry (LSIMS) low energy CA on a Fourier transform mass spectrometer (FT-MS) (Carroll et al., 1995). The mechanism proposed by the group of Lebrilla (Carroll et al., 1995) for formation of cross-ring A-type fragments in negative ion mode involves loss of the fructose residue to yield a C_{n-1} ion, in which the negative charge is borne by the newly-generated reducing terminal anomeric oxygen (Diagram 6.2). This 6-substituted residue was then proposed to undergo subsequent ring opening and cleavage of the C-backbone to allow neutral loss of one or more CH_2O (multiples of 30 Da) moieties from the monosaccharide.

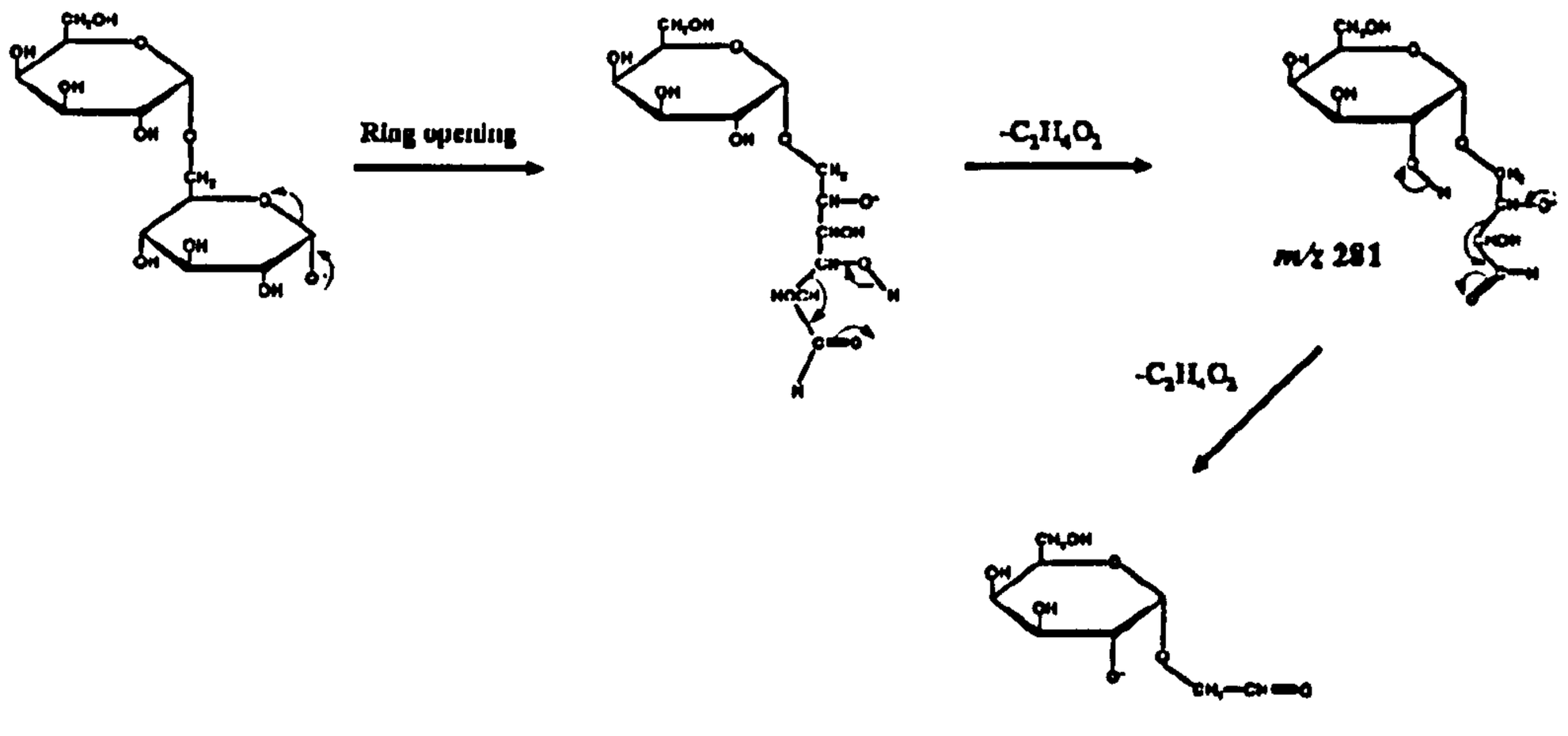

Diagram 6.2 Mechanism proposed by the group of Lebrilla (Carroll et al., 1995) for the formation of the cross-ring A-type fragment ions at *m/z* 281 and 221 from the deprotonated anomeric oxygen, after the loss of the fructose moiety by the $[M-H]^-$ ion of the non-reducing trisaccharide raffinose.

Interestingly, this mechanism cannot explain the formation of the A-type ions observed in the experiments described in this chapter, since these were carried out in a quadrupole ion trap. If cleavage of the α-(1→2) Glc-Fru bond occurred to yield the C_{n-1} ion, this would not fragment further in an ion trap, since the auxiliary rf voltage applied to activate the precursor ion activates only ions within a narrow m/z range. Fragment ions resonate with different secular frequencies than the precursor and thus are not activated; the C_{n-1} product ion would thus not fragment further. A concerted mechanism such as those proposed by Dallinga and Heerma (Dallinga and Heerma, 1991) in which fragmentation takes place in a single step must therefore be postulated for the cleavages observed in the ion trap (Diagram 6.3).

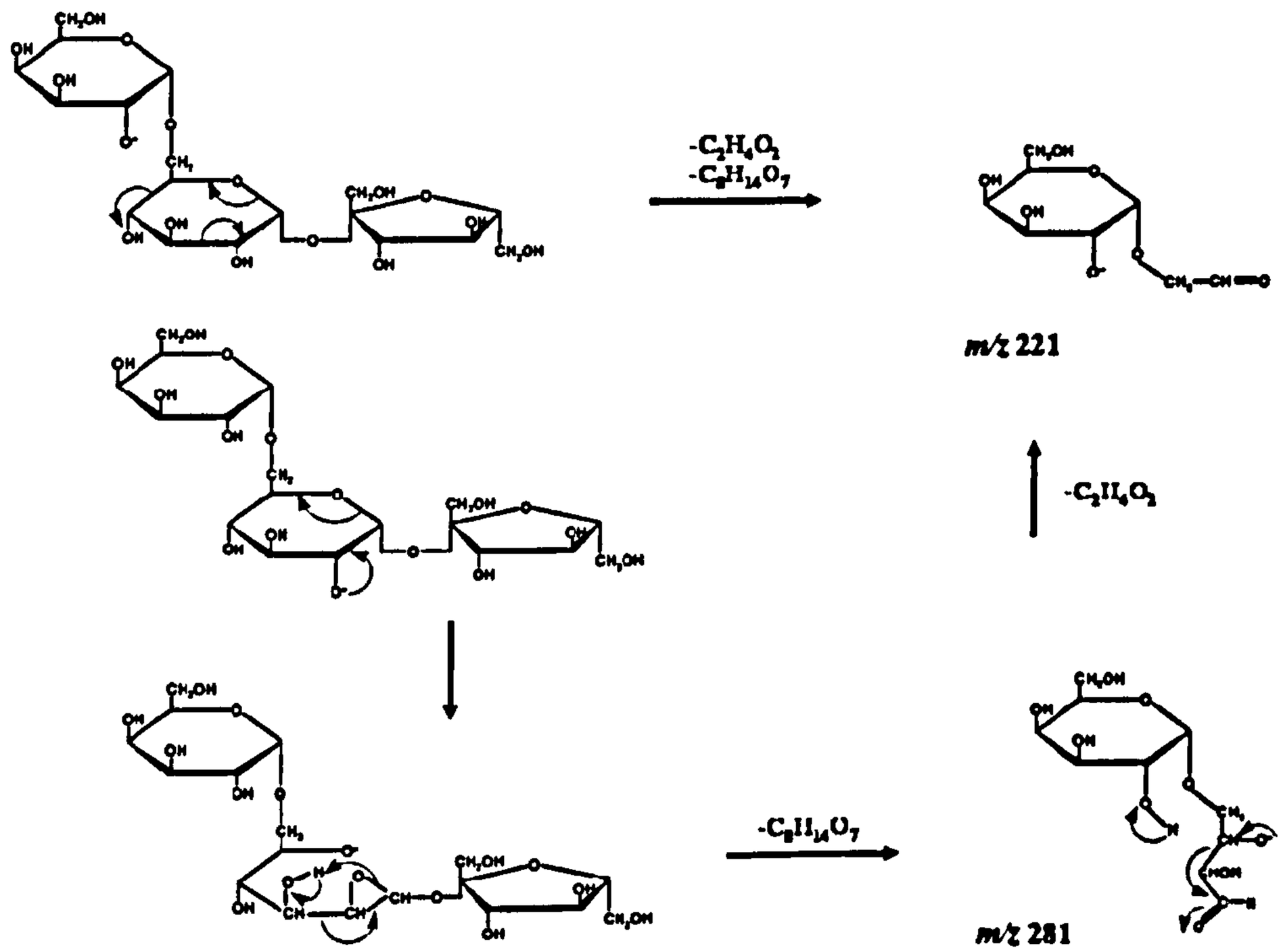

Diagram 6.3 Concerted mechanism proposed by Dallinga and Heerma (Dallinga and Heerma, 1991) for the formation of the cross-ring A-type fragment ions at *m/z* 281 and 221 from the $[M-H]^-$ ion of the non-reducing trisaccharide raffinose.

6.2.3 Repeatability, limits of detection (LOD), and limits of quantification (LOQ) of the HILIC-ESI-QIT-MS method

Intra-day repeatability was measured by injecting the same standard solution three times in a single day. Inter-day repeatability was measured by analysing the same standard solution over five different days. Intra- and inter-day repeatability of retention times using the HILIC-ESI-QIT-MS method gave relative standard deviations (RSD) of less than 2% (Table 6.1). The LOD for each compound was calculated as the minimum amount injected which gave a detector response higher than three times the signal-to-noise ratio (S/N), and the LOQ was calculated at an S/N ratio of 10. The method gave LODs ranging from 0.2 μM obtained for neutral sugars, and 1.0 μM obtained for sugar alcohols and *myo*-inositol, to 2.0 μM obtained for the sugar phosphates, which are very comparable to those reported for these compounds using PGC-LC-ESI-QIT-MS (Antonio et al., 2007) (Chapter 4).

Table 6.1 Nominal *m/z* values, retention times, intra- and inter-day repeatabilities of retention times, LOD, and LOQ obtained for *myo*-inositol, sugars, sugar alcohols, and sugar phosphate standard compounds using negative ion HILIC-ESI-QIT-MS.

Standard compounds	Diagnostic ion (*m/z*)	t_R (min)	t_R (intra RSD)[a] (%, n=3)	t_R (inter RSD)[b] (%, n=5)	LOD[c] (μM)	LOQ[d] (μM)	Amout LOD[e] (pmol)
myo-inositol	225 $[M+HCOO]^-$	10.08	1.00	1.25	1.0	3.0	0.5
Sugars:							
Fru	225 $[M+HCOO]^-$	7.50	1.53	1.93	1.0	3.0	0.5
Glc	225 $[M+HCOO]^-$	8.55	0.95	1.15	1.0	3.0	0.5
Suc	387 $[M+HCOO]^-$	9.33	0.70	1.12	0.2	0.7	0.1
Tre	387 $[M+HCOO]^-$	9.93	1.43	1.78	0.2	0.7	0.1
Raffinose	549 $[M+HCOO]^-$	10.55	0.70	1.67	0.2	0.7	0.1
Stachyose	711 $[M+HCOO]^-$	11.44	1.46	1.89	0.2	0.7	0.1
Verbascose	873 $[M+HCOO]^-$	12.01	1.00	1.12	0.2	0.7	0.1
Sugar alcohols:							
Sorbitol	227 $[M+HCOO]^-$	8.00	1.00	1.72	1.0	3.0	0.5
Mannitol	227 $[M+HCOO]^-$	8.11	0.82	1.58	1.0	3.0	0.5
Maltitol	389 $[M+HCOO]^-$	9.55	1.53	1.94	1.0	3.0	0.5
Galactinol	387 $[M+HCOO]^-$	11.04	0.87	1.65	1.0	3.0	0.5
Sugar phosphates:							
Glc1P	259 $[M-H]^-$	11.03	1.00	1.12	2.0	6.7	1.0
Fru6P	259 $[M-H]^-$	11.09	0.58	1.11	2.0	6.7	1.0
Suc6P	421 $[M-H]^-$	11.28	0.58	1.73	1.0	3.0	0.5
Tre6P	421 $[M-H]^-$	11.69	1.15	1.83	1.0	3.0	0.5
Glc6P	259 $[M-H]^-$	11.81	0.58	0.95	2.0	6.7	1.0
Fru1,6BP	339 $[M-H]^-$	13.73	0.94	1.92	2.0	6.7	1.0

HPLC conditions: ZIC-HILIC column (150 mm x 2.1 mm i.d.), 0.5 μL injection, flow rate 200 μL/min. [a] Intra-day RSD of retention times (n=3 independent measurements); [b] Inter-day RSD of retention times (n=5 independent measurements); [c] Concentration LOD calculated at an S/N of 3; [d] LOQ calculated at an S/N of 10; [e] LOD of the amount loaded onto column calculated at an S/N of 3.

6.2.4 Quantification of carbohydrate-related metabolites in *A. thaliana* wild-type Col-0 and *pgm1* leaf extracts using HILIC-ESI-QIT-MS

To evaluate the potential of this on-line HILIC-ESI-QIT-MS method as a tool for the separation and characterisation of carbohydrate-related metabolites present in the complex biological matrices typically encountered in plant metabolomics studies, we have applied it for the analysis of *A. thaliana* wild-type Col-0 and *pgm1* chloroform/methanol leaf extracts. *A. thaliana pgm1* plants lack plastidial phosphoglucomutase (pPGM) activity, essential for starch synthesis (Caspar et al., 1985; Caspar et al., 1991), and so high levels of the soluble sugars Glc and Suc accumulate in their leaves during the day, as they are not converted to starch for storage.

The application of this HILIC-ESI-QIT-MS method allowed the separation and identification of four metabolites present in *A. thaliana* Col-0 and *pgm1* chloroform/methanol leaf extracts: Glc, Suc, raffinose, and Glc6P. Metabolite identification was based on the comparison of retention times, masses, and ion trap tandem mass spectra with those obtained for standard compounds (Table 6.1). Figure 6.6a depicts the typical negative ion base peak chromatogram obtained on the analysis of a leaf extract of *A. thaliana* wild-type Col-0 and Figure 6.6b illustrates the extracted ion chromatograms for Glc ($[M+HCOO]^-$ at *m/z* 225), Suc ($[M+HCOO]^-$ at *m/z* 387), raffinose ($[M+HCOO]^-$ at *m/z* 549), and Glc6P ($[M-H]^-$ at *m/z* 259) obtained using HILIC-ESI-QIT-MS; for comparison, Figure 6.6c and Figure 6.6d show the separation and identification of these metabolites using PGC-LC-ESI-QIT-MS of an equivalent but separate set of Col-0 and *pgm1* preparations (Antonio et al., 2007) (Chapter 4). It can be observed that HILIC separations afford narrower peaks than those obtained using PGC.

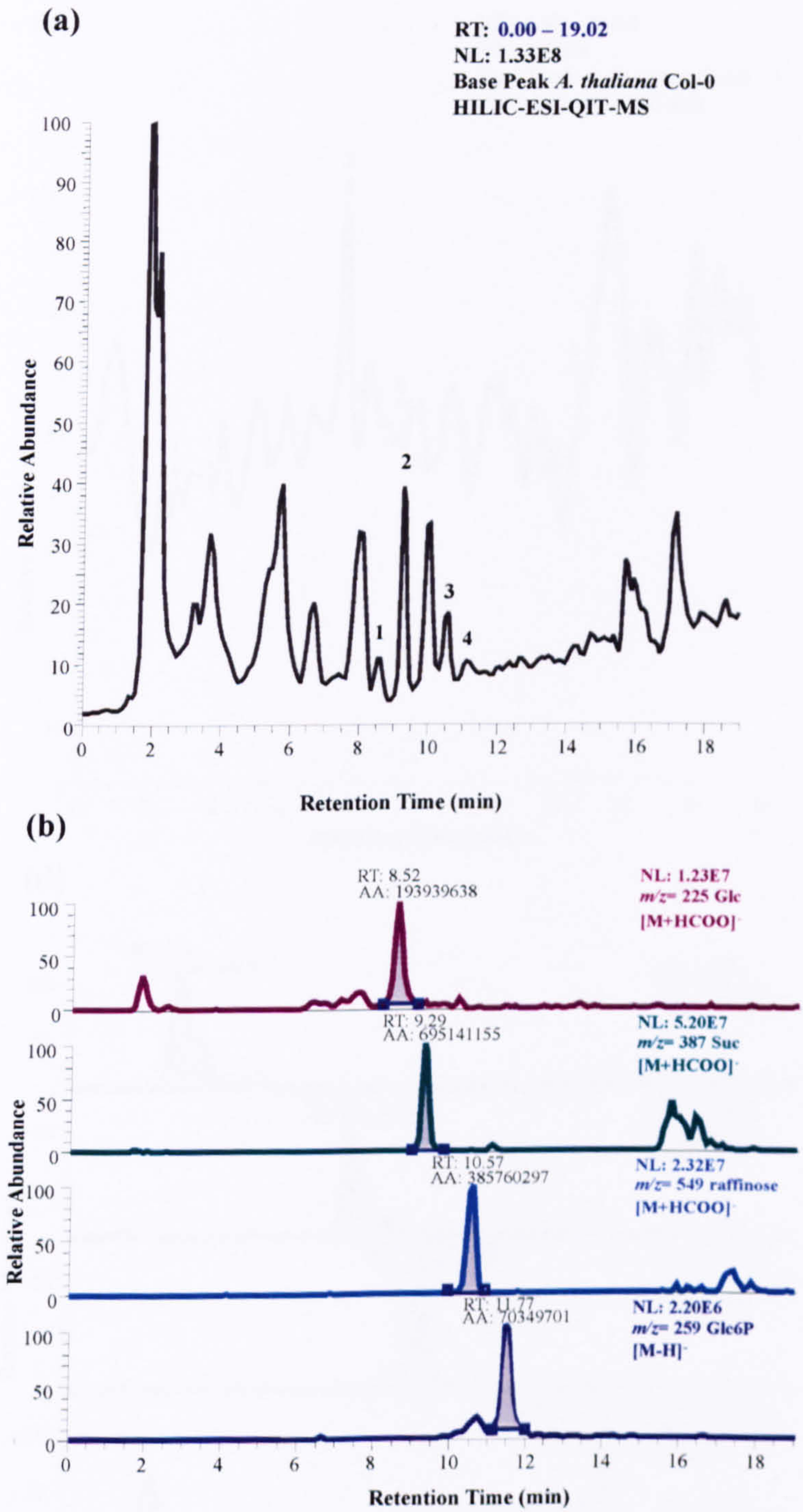

Figure 6.6 Typical negative ion base peak chromatogram obtained on separation of an *A. thaliana* Col-0 chloroform/methanol leaf extract (16 h light/8 h dark photoperiod) using (a) HILIC-ESI-QIT-MS and (c) PGC-LC-QIT-MS. The extracted ion chromatograms for Glc ($[M+HCOO]^-$ at *m/z* 225), Suc ($[M+HCOO]^-$ at *m/z* 387), raffinose ($[M+HCOO]^-$ at *m/z* 549), and Glc6P ($[M-H]^-$ at *m/z* 259) obtained using (b) HILIC-ESI-QIT-MS and (d) PGC-LC-ESI-QIT-MS are shown. HPLC conditions: ZIC-HILIC column (150 mm x 2.1 mm i.d.), 0.5 µL injection, flow rate 200 µL/min; Hypercarb PGC column (100 mm x 4.6 mm i.d.), 20 µL injection, flow rate 600 µL/min.

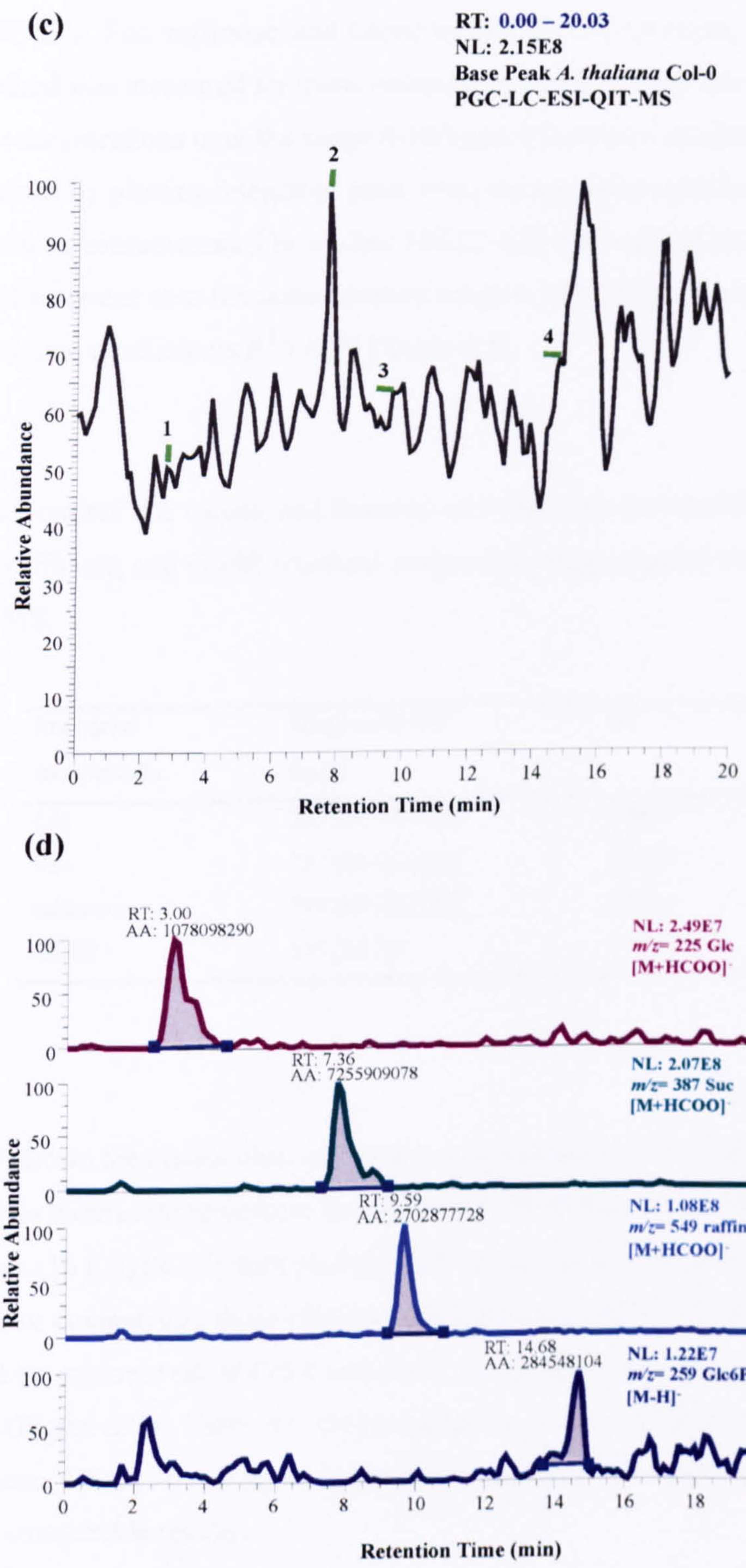

Figure 6.6 (*Continued*).

To quantify Glc, Suc, raffinose, and Glc6P by HILIC-ESI-QIT-MS, the linearity of the method was measured for these compounds by recording their responses at different concentrations over the range 0-100 µM. Five-point standard curves were obtained by plotting integrated peak areas versus concentration (n=3 independent measurements). The on-line HILIC-ESI-MS method showed good linearity of response over the concentration range 0-100 µM for these analytes, with correlation coefficients $R^2 > 0.99$ (Table 6.2).

Table 6.2 Nominal *m/z* values, and linearity of calibration curves obtained for Glc, Suc, raffinose, and Glc6P standard compounds using negative ion HILIC-ESI-QIT-MS.

Standard compounds	Diagnostic ion (m/z)	R^2
Glc	225 $[M+HCOO]^-$	0.9975
Suc	387 $[M+HCOO]^-$	0.9968
raffinose	549 $[M+HCOO]^-$	0.9985
Glc6P	259 $[M-H]^-$	0.9981

Figure 6.7 shows the results obtained for the quantification of Glc, Suc, raffinose and Glc6P in methanol/chloroform leaf extracts of *A. thaliana* WT Col-0 and *pgm1* plants (16 h light/ 8 h dark photoperiod) using HILIC-ESI-QIT-MS (Figure 6.7a), and for comparison, those obtained using PGC-LC-ESI-QIT-MS of an equivalent but separate set of Col-0 and *pgm1* preparations as described in Chapter 4 (Figure 6.7b). Table 6.3 shows the levels of these soluble sugars found in *A. thaliana* WT Col-0 and *pgm1* leaf extracts using the two methods, which gave very comparable results.

Table 6.3 Metabolite levels (Glc, Suc, raffinose, and Glc6P) determined in *A. thaliana* WT Col-0 and *pgm1* leaf extracts using negative ion mode HILIC-ESI-QIT-MS and PGC-LC-ESI-QIT-MS.

Metabolites	HILIC-ESI-QIT-MS[a]		PGC-LC-ESI-QIT-MS[b]	
(µmol.g^{-1} FW)	WT Col-0	*pgm1*	WT Col-0	*pgm1*
Glc	1.30±0.10	6.26±0.50	0.87±0.09	5.87±1.22
Suc	1.60±0.20	2.92±0.30	0.71±0.11	1.97±0.36
raffinose	0.35±0.17	0.85±0.20	0.28±0.09	0.57±0.22
Glc6P	0.22±0.09	0.53±0.09	0.11±0.01	0.31±0.04

HPLC conditions: [a] ZIC-HILIC column (150 mm x 2.1 mm i.d.), 200 µL/min, 0.5 µL injection; [b] Hypercarb PGC column (100 mm x 4.6 mm i.d.), 600 µL/min, 20 µL injection. Plants were grown under a 16 h light/8 h dark photoperiod and harvested at developmental stage 6.0. Values are mean ± SD (n= 3 biological replicates, each containing leaves from three rosettes). Each biological replicate is the mean value of n=3 independent LC-MS measurements. FW, fresh weight.

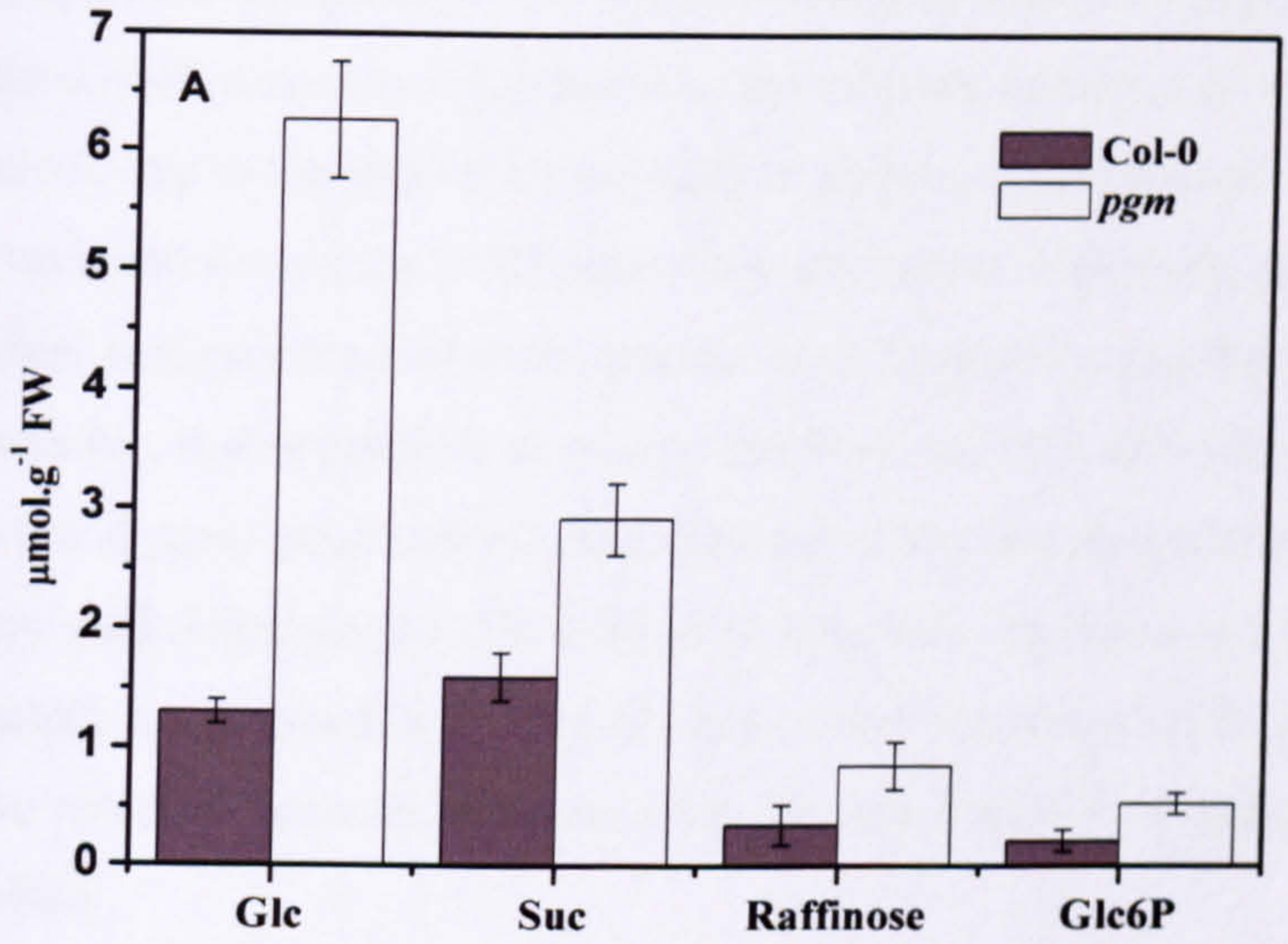

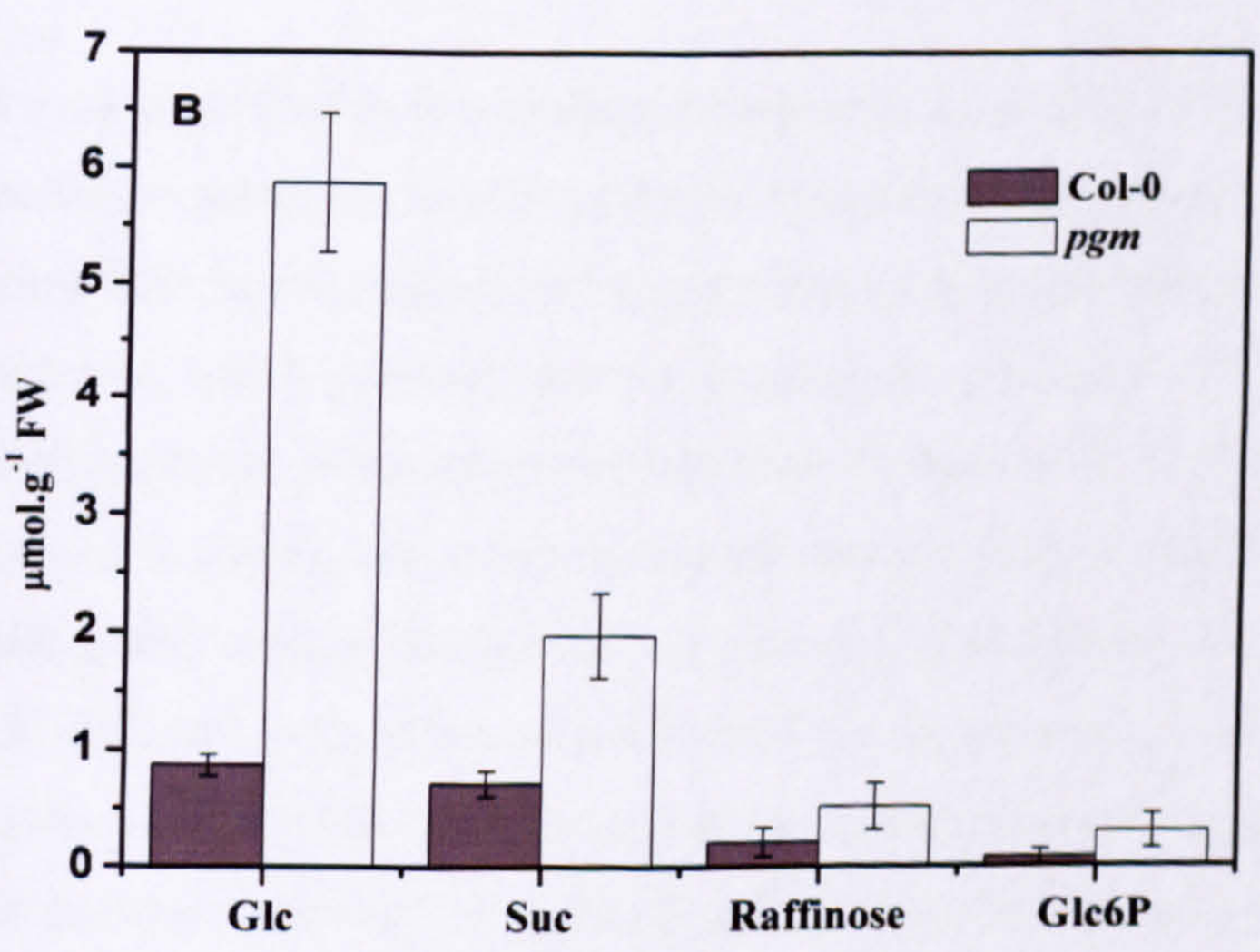

Figure 6.7 Metabolite levels (Glc, Suc, raffinose, and Glc6P) determined in *Arabidopsis thaliana* Col-0 and *pgm1* chloroform/methanol leaf extracts using (A) HILIC-ESI-QIT-MS and (B) PGC-LC-ESI-QIT-MS. Plants were grown under a 16 h light/8 h dark photoperiod and harvested at developmental stage 6.0. Values are mean ± SD (n= 3 biological replicates, each containing leaves from three rosettes). Each biological replicate is the mean value of n=3 independent LC-MS measurements. FW, fresh weight.

The detection and identification of raffinose in *A. thaliana* Col-0 and *pgm1* chloroform/methanol leaf extracts using HILIC prompted the re-analysis of the data obtained using PGC-LC-ESI-QIT-MS (described in Chapter 4). Using that method, raffinose was not detected in the original analyses of *A. thaliana* leaf extracts, due to the lack of an authentic standard, which meant that raffinose was not included during the PGC method development. However, since during the original analyses the ESI mass spectra were recorded using the ion trap in full-scan mode, it was possible to re-visit the PGC-LC-MS data obtained for that set of Col-0 and *pgm1* preparations, and determine whether an ion at *m/z* 549 (raffinose formylated molecule $[M+HCOO]^-$) was detected. An ion at *m/z* 549 was in fact detected; it was possible to identify this as deriving from raffinose by comparison of the retention time for this peak with that obtained for an authentic raffinose standard.

6.3 Conclusions

The work described in this chapter demonstrates the use of HILIC coupled to negative ion mode ion trap ESI-MS for the analysis of several polar metabolites, ranging from neutral sugars and sugar alcohols to negatively-charged sugar phosphates, which generally are not retained on typical RP-LC columns. This method is robust, selective, rapid (less than 15 min), with LODs in the low μM range (0.2-2.0 μM), and uses MS-friendly mobile phases, enabling efficient coupling with on-line ESI-MS. It was demonstrated that this newly developed HILIC-ESI-MS method is a powerful tool for the separation, identification, and quantification of polar compounds, ranging from mono- (Glc), di- (Suc), and trisaccharides (raffinose) to sugar phosphates (Glc6P) from *A. thaliana* plant tissues.

Little work has been published in the literature on the negative ion fragmentation of non-reducing sugars, such as RFOs. HILIC coupled to ion trap multistage MS was used to produce negative ion CID spectra of RFOs, which were dominated by

fragment ions formed by C_i and B_i glycosidic cleavages and A_i cross-ring cleavages; the cross-ring fragments are characteristic of the α-(1→6) linkage of the hexopyranose residues in these glycans.

The use of HILIC and PGC columns are two alternatives to traditional RP-LC methods for the analysis of very polar metabolites. The results described in Chapter 4, and those described in this chapter, demonstrate that PGC-ESI-MS and HILIC-ESI-MS afford robust, repeatable, and comparable quantitative results (and LODs) for the analysis of plant metabolites. However, the fact that PGC gradient separations require extensive method development and strong conditions for elution of highly polar compounds makes HILIC a very suitable and more convenient approach for analysis of these compounds in routine plant metabolomic studies.

Tolstikov and Fiehn (Tolstikov and Fiehn, 2002) have previously reported a HILIC-ESI-MS method for the analysis of oligosaccharides and sugar nucleotides from plant tissues. That method used a 60 min gradient elution, which was necessary for separating the complex and diverse mixture of analytes in those experiments. The retention times obtained for the standards Suc, raffinose and stachyose were t_R= 29.57 min, t_R= 35.57 min, and t_R= 40.21 min, respectively. The LOD reported for stachyose was 0.5 ng. Using this HILIC method, aimed at separation of carbohydrate-related metabolites, separation of these compounds was achieved in significantly less time (around 10 min, Table 6.1). In addition, a better LOD was obtained for stachyose (0.1 pmol, i.e. 66 pg), which represents a distinct improvement for these analytes over the more broadly targeted method of Tolstikov and Fiehn.

Chapter 7

Concluding remarks and future work

Chapter 7. Concluding remarks and future work

7.1 Concluding remarks

The aim of the work described in this thesis was to develop and implement new LC-MS approaches for studying key plant primary metabolites, using *A. thaliana* as the model system. The methods development aspects described were driven by the need to develop sensitive LC-MS-based methods, able to separate and identify sugars, sugar phosphates, and some glycolytic intermediates, that are predominantly polar compounds. The LC-MS methods described proved to be efficient for the identification and determination of some of these metabolites in complex biological samples such as extracts of plant tissues. The structural complexity and variety of carbohydrate-related metabolites is a challenge to any analytical technology used for the identification and differentiation of the wide range of isomeric structures. The challenge in LC-MS applications for plant metabolome analysis lies in the development of appropriate LC-MS methods based on new column chemistries and MS compatible mobile phases in order to achieve efficient and robust on-line coupling with ESI-MS.

7.2 Future work

Although the LC-MS analyses described in this thesis were targeted at particular analytes (neutral and phosphorylated sugars and sugar alcohols), full-scan LC-MS data were recorded and are thus available for further data mining. LC-MS data-sets are available from two studies, one using wild-type *Arabidopsis thaliana* Col-0 and *pgm1* mutant leaf tissues, and the other using *Lupinus albus* stem tissues subjected to water deficit. This has prompted the investigation of the use of multivariate statistical methods to analyse these LC-MS data sets, which may uncover other metabolites, the levels of which change either over the light/dark

cycle or between the WT and mutant, or in response to water stress or recovery from it. These studies are now being planned with informatics experts at the University of York.

As part of the collaborative project entitled 'Screening for stress responsive metabolites in *Lupinus albus*', a new study is now being set up where the PGC-LC-ESI-QIT-MS method described in Chapter 5 will be used primarily to study the effects of early stress WD imposition in different *L. albus* organs (young leaves and roots); the use of HILIC columns will also be considered. These experimental studies are aimed at understanding a possible physiological role of raffinose in desiccation tolerance in *L. albus* plants. Data obtained from these studies, together with photosynthetic studies to be carried out by collaborators at ITQB, will be prepared for publication in *Journal of Experimental Biology*. This collaboration is funded by the British Council under the Treaty of Windsor Anglo-Portuguese Joint Research Programme, and will have a further year's funding, in which the author will continue closely involved.

Although not yet widely explored within the metabolomics field, hydrophilic interaction chromatography proved to be one suitable LC approach for the analysis of highly polar metabolites typically found in plant extracts. The results obtained using HILIC-MS correlated well with those obtained using PGC-LC-MS. Within the JTO group, the recent use of HILIC-ESI-MS has resulted in two publications, one applied to metabonomics studies of urine (Cubbon et al., 2007) and the other, described in this thesis, of its application to plant metabolomics studies (Antonio et al., 2008a). The authors have been invited to collaborate in writing a review of the application of HILIC-MS in metabolomics studies. The title of this review is 'Metabolomic applications of HILIC-LC-MS', and the starting date for writing this review has been scheduled for Summer 2008; it will be published in *Mass Spectrometry Reviews*.

Chapter 8

References

Chapter 8. References

Aharoni A, Ric de Vos CH, Verhoeven HA, Maliepaard CA, Kruppa G, Bino R, Goodenowe DB (2002) Nontargeted metabolome analysis by use of Fourier transform ion cyclotron mass spectrometry. Omics 6: 217-234

Alpert AJ (1990) Hydrophilic-interaction chromatography for the separation of peptides, nucleic acids and other polar compounds. J. Chromatogr. 499: 177-196

Alpert AJ, Shukla M, Shukla AK, Zieske LR, Yuen SW, Ferguson MAJ, Mehlert A, Pauly M, Orlando R (1994) Hydrophilic-interaction chromatography of complex carbohydrates. J. Chromatogr. A 676: 191-202

Alvarez S, Marsh EL, Schroeder SG, Schachtman DP (2008) Metabolomic and proteomic changes in the xylem sap of maize under drought. Plant Cell Environ. 31: 325-340

Amiard V, Morvan-Bertrand A, Billard J-P, Huault C, Keller F, Prud'homme M-P (2003) Fructans, but not the sucrosyl-galactosides, raffinose and loliose, are affected by drought stress in *Perennial Ryegrass*. Plant Physiol. 132: 2218-2229

Antonio C, Larson T, Gilday A, Graham I, Bergström E, Thomas-Oates J (2007) Quantification of sugars and sugar phosphates from *Arabidopsis thaliana* tissues using porous graphitic carbon liquid chromatography-electrospray ionization mass spectrometry. J. Chromatogr. A 1172: 170-178

Antonio C, Larson T, Gilday A, Graham I, Bergström E, Thomas-Oates J (2008a) Hydrophilic interaction chromatography/electrospray mass spectrometry analysis of carbohydrate-related metabolites from *Arabidopsis thaliana* leaf tissue. Rapid Commun. Mass Spectrom. 22: 1399-1407

Antonio C, Pinheiro C, Chaves MM, Ricardo CP, Ortuño MF, Thomas-Oates J (2008b) Analysis of carbohydrates in *Lupinus albus* stems on imposition of water deficit, using porous graphitic carbon liquid chromatography-electrospray ionization mass spectrometry. J. Chromatogr. A **1187: 111-118**

Apffel A, Fisher S, Goldberg G, Goodley PC, Kuhlmann FE (1995) Enhanced sensitivity for peptide mapping with electrospray liquid chromatography-mass spectrometry in the presence of signal suppression due to trifluoroacetic acid-containing mobile phases. J. Chromatogr. A **712: 177-190**

Bahr U, Pfenninger A, Karas M (1997) High-sensitivity analysis of neutral underivatized oligosaccharides by nanoelectrospray mass spectrometry. Anal. Chem. **69: 4530-4535**

Bajad SU, Lu W, Kimball EH, Yuan J, Peterson C, Rabinowitz JD (2006) Separation and quantitation of water soluble cellular metabolites by hydrophilic interaction chromatography-tandem mass spectrometry. J. Chromatogr. A **1125: 76-88**

Balogh MP (2004) Debating resolution and mass accuracy. LC GC Europe **17: 152-159**

Barrett DA, Pawula M, Knaggs RD, Shaw PN (1998) Retention behaviour of morphine and its metabolites on porous graphitic carbon column. Chromatographia **47: 667-672**

Barroso B, Dijkstra R, Geerts M, Lagewerf F, van Veelen P, de Ru A (2002) On-line high-performance liquid chromatography/mass spectrometric characterization of native oligosaccharides from glycoproteins. Rapid Commun. Mass Spectrom. **16: 1320-1329**

Bhattacharya M, Fuhrman L, Ingram A, Nickerson KW, Conway T (1995) Single-run separation and detection of multiple metabolic intermediates by anion-exchange high-performance liquid chromatography and application to cell pool extracts prepared from *Escherichia coli*. Anal. Biochem. **232:** 98-106

Bino RJ, Hall RD, Fiehn O, Kopka J, Saito K, Draper J, Nikolau BJ, Mendes P, Roessner-Tunali U, et al. (2004) Potential of metabolomics as a functional genomics tool. Trends Plant Sci. **9:** 418–425

Bläsing OE, Gibon Y, Günther M, Höhne M, Morcuende R, Osuna D, Thimm O, Usadel B, Scheible W-R, Stitt M (2005) Sugars and circadian regulation make major contributions to the global regulation of diurnal gene expression in *Arabidopsis*. Plant Cell **17:** 3257-3281

Borra C, Di Corcia A, Marchetti M, Samperi R (1986) Evaluation of graphitized carbon black cartridges for rapid organic trace enrichment from water: application to priority pollutant phenols. Anal. Chem. **58:** 2048-2052

Boyes DC, Zayed AM, Ascenzi R, McCaskill AJ, Hoffman NE, Davis KR (2001) Growth stage-based phenotypic analysis of *Arabidopsis*: a model for high throughput functional genomics in plants. Plant Cell **13:** 1499-1510

Bray EA, Bailey-Serres J, Weretilnyk E (2000) Responses to Abiotic Stresses. *In* BB Buchanan, W Gruissem, RL Jones, eds, Biochemistry and Molecular Biology of Plants. American Society of Plant Physiologists, pp 1158-1203

Breitling R, Pitt AR, Barrett MP (2006) Precision mapping of the metabolome. Trends Biotech. **24:** 543-548

Brown M, Dunn WB, Ellis DI, Goodacre R, Handl J, Knowles JD, O'Hagan S, Spasić I, Kell DB (2005a) A metabolome pipeline: from concept to data knowledge. Metabolomics **1:** 39-51

Brown SC, Kruppa G, Dasseux J-L (2005b) Metabolomics applications of FT-ICR mass spectrometry. Mass Spectrom. Rev. 24: 223-231

Brüll LP, Kovácik V, Thomas-Oates JE, Heerma W, Haverkamp J (1998) Sodium-cationized Oligosaccharides Do Not Appear to Undergo 'Internal Residue Loss' Rearrangement Processes on Tandem Mass Spectrometry. Rapid Commun. Mass Spectrom. 12: 1520-1532

Buchholz A, Takors R, Wandrey C (2001) Quantification of intracellular metabolites in *Escherichia coli* K12 using liquid chromatographic-electrospray ionization tandem mass spectrometric techniques. Anal. Biochem. 295: 129-137

Carroll JA, Willard D, Lebrilla CB (1995) Energetics of cross-ring cleavages and their relevance to the linkage determination of oligosaccharides. Anal. Chim. Acta 307: 431-447

Caspar T, Huber SC, Somerville C (1985) Alterations in growth, photosynthesis, and respiration in a starchless mutant of *Arabidopsis thaliana* (L.) deficient in chloroplast phosphoglucomutase activity. Plant Physiol. 79: 11-17

Caspar T, Lin T-P, Kakefuda G, Benbow L, Preiss J, Somerville C (1991) Mutants of *Arabidopsis* with altered regulation of starch degradation. Plant Physiol. 95: 1181-1188

Chaves MM, Oliveira MM (2004) Mechanisms underlying plant resilience to water deficits: prospects for water-saving agriculture. J. Exp. Bot. 55: 2365-2384

Chaves MM, Pereira JS, Maroco JP, Rodrigues ML, Ricardo CP, Osório ML, Carvalho I, Faria T, Pinheiro C (2002) How plants cope with water stress in the field. Photosynthesis and growth. Annals Bot. 89: 907-916

Chernushevich IV, Loboda AV, Thomson BA (2001) An introduction to quadrupole-time-of-flight mass spectrometry. J. Mass Spectrom. **36:** 849-865

Chia T, Thorneycroft D, Chapple A, Messerli G, Chen J, Zeeman SC, Smith SM, Smith AM (2004) A cytosolic glucosyltransferase is required for conversion of starch to sucrose in *Arabidopsis* leaves at night. Plant J. **37:** 853-863

Choi BK, Hercules DM, Gusev AI (2001) Effect of liquid chromatogaphy separation of complex matrices on liquid chromatography-tandem mass spectrometry signal suppression. J. Chromatogr. A **907:** 337-342

Coles J, Guilhaus M (1993) Orthogonal acceleration - a new direction for time-of-flight mass spectrometry: fast, sensitive mass analysis for continuous ion sources. Trends Anal. Chem. **12:** 203-213

Cotter R (1992) Time-of-flight mass spectrometry for the structural analysis of biological molecules. Anal. Chem. **64:** 1037A-1039A

Critchley J, Zeeman S, Takaha T, Smith AM, Smith SM (2001) A critical role for disproportionating enzyme in starch breakdown is revealed by a knockout mutation in *Arabidopsis thaliana*. Plant J. **26:** 89-100

Croteau R, Kutchan TM, Lewis NG (2000) Natural Products. *In* BB Buchanan, W Gruissem, RL Jones, eds, Biochemistry and Molecular Biology of Plants. American Society of Plant Physiologists, pp 1250-1318

Cubbon S, Bradbury T, Wilson J, Thomas-Oates J (2007) Hydrophilic interaction chromatography for mass spectrometric metabonomic studies of urine. Anal. Chem. **79:** 8911-8918

Dallinga JW, Heerma W (1991) Reaction mechanism and fragment ion structure determination of deprotonated small oligosaccharides, studied by negative ion fast

atom bombardment (tandem) mass spectrometry. Biol. Mass Spectrom. **20:** 215-231

Davies MJ, Smith KD, Carrunthers RA, Chai W, Lawson AM, Hounsell EF (1993) Use of porous graphitised carbon column for the high-performance liquid chromatography of oligosaccharides, alditols and glycopeptides with subsequent mass spectrometry analysis. J. Chromatogr. **646:** 317-326

Dawson JHJ, Guilhaus M (1989) Orthogonal-acceleration time-of-flight mass spectrometer. Rapid Commun. Mass Spectrom. **3:** 155-159

de Bruijn SM, Visser RG, Vreugdenhil D (1999) Simultaneous analysis of a series of phosphorylated sugars in small tissue samples by anion exchange chromatography and pulsed amperometric detection. Phytochem. Anal. **10:** 107-112

de Koning W, van Dam K (1992) A method for the determination of changes of glycolytic metabolites in yeast on a subsecond time scale using extraction at neutral pH. Anal. Biochem. **204:** 118-123

Desbrosses GG, Kopka J, Udvardi MK (2005) *Lotus japonicus* metabolic profiling. Development of gas chromatography-mass spectrometry resources for the study of plant-microbe interactions. Plant Physiol. **137:** 1302-1318

Di Corcia A, Marchetti M (1991) Multiresidue method for pesticides in drinking water using a graphitized carbon black cartridge extraction and liquid chromatographic analysis. Anal. Chem. **63:** 580-585

Dole M, Mack LL, Hines RL, Mobley RC, Ferguson LD, Alice MB (1968) Molecular beams of macroions. J. Chem. Phys. **49:** 2240-2249

Domon B (2008) personal communication.

Domon B, Costello CE (1988) A systematic nomenclature for carbohydrate fragmentations in FAB-MS/MS spectra of glycoconjugates. Glycoconjugate J. **5:** 397-409

Dracup M, Turner NC, Tang C, Reader M, Palta J (1998) Responses to Abiotic Stresses. *In* JS Gladstones, CA Atkins, J Hamblin, eds, Lupin as Crop Plants: Biology, Production and Utilization. CAB International, pp 227-262

Dunn WB, Ellis DI (2005) Metabolomics: current analytical platforms and methodologies. Trends Anal. Chem. **24:** 285-294

Elfakir C, Chaimbault P, Dreux M (1998) Determination of inorganic anions on porous graphitic carbon using evaporative light scattering detection. Use of carboxylic acids as electronic competitors. J. Chromatogr. A **829:** 193-199

Elfakir C, Dreux M (1996) Simultaneous analysis of intact and desulfated glucosinolates with porous graphitized carbon column. J. Chromatogr. A **727:** 71-82

Emery MF, Lim CK (1989) Separation of cationic technetium-99m amine complexes on porous graphitic carbon. J. Chromatogr. **479:** 212-215

Evert RF (2006) Esau's Plant Anatomy - meristems, cells, and tissues of the plant body: their structure, function, and development, Ed 3. John Wiley & Sons, Inc., Hoboken, New Jersey

Fan J-Q, Kondo A, Kato I, Lee YC (1994) High-performance liquid chromatography of glycopeptides and oligosaccharides on graphitized carbon columns. Anal. Biochem. **219:** 224-229

Fenn JB, Mann M, Meng CK, Wong SF, Whitehouse CM (1989) Electrospray ionization mass spectrometry of large biomolecules. Science **246:** 64-71

Fernie A (2003) Metabolome characterisation in plant system analysis. Funct. Plant Biol. **30: 111-120**

Fernie AR, Roessner U, Trethewey RN, Willmitzer L (2001) The contribution of plastidial phosphoglucomutase to the control of starch synthesis within the potato tuber. Planta **213: 418-426**

Fernie AR, Trethewey RN, Krotzky AJ, Willmitzer L (2004) Metabolite profiling: from diagnostics to systems biology. Nat. Rev. Mol. Cell Biol. **5:** 763-769

Feurle J, Jomaa H, Wilhelm M, Gutsche B, Herderich M (1998) Analysis of phosphorylated carbohydrates by high-performance liquid chromatography-electrospray ionization tandem mass spectrometry utilising a β-cyclodextrin bonded stationary phase. J. Chromatogr. A **803: 111-119**

Fiehn O (2001) Combining genomics, metabolome analysis and biochemical modelling to understand metabolic networks. Comp. Funct. Genomics **2:** 155-168

Fiehn O (2002) Metabolomics - the link between genotypes and phenotypes. Plant Mol. Biol. **48: 155-171**

Fiehn O (2003) Metabolic networks of *Cucurbita maxima* phloem. Phytochem. **62:** 875-886

Fiehn O (2006) Metabolite profiling in *Arabidopsis*. *In* HP Inc., ed, Methods in Molecular Biology: Arabidopsis protocols, Vol 323, Totowa, NJ, pp 439-447

Fiehn O, Kopka J, Dörmann P, Altmann T, Trethewey RN, Willmitzer L (2000a) Metabolite profiling for plant functional genomics. Nature Biotechnol. **18: 1157-1161**

Fiehn O, Kopka J, Trethewey RN, Willmitzer L (2000b) Identification of uncommon plant metabolites based on calculation of elemental compositions using gas chromatography and quadrupole mass spectrometry. Anal. Chem. **72:** 3573-3580

Gibon Y, Bläsing OE, Palacios-Rojas N, Pankovic D, Hendriks JH, Fisahn J, Hohne M, Gunther M, Stitt M (2004) Adjustment of diurnal starch turnover to short days: depletion of sugar during the night leads to a temporary inhibition of carbohydrate utilization, accumulation of sugars and post-translational activation of ADP-glucose pyrophosphorylase in the following light period. Plant J. **39:** 847-862

Gibon Y, Vigeolas H, Tiessen A, Geigenberger P, Stitt M (2002) Sensitive and high throughput metabolite assays for inorganic pyrophosphate, ADPGlc, nucleotide phosphates, and glycolytic intermediates based on a novel enzymatic cycling system. Plant J. **30:** 221-235

Gilbert MT, Knox JH, Kaur B (1982) Porous glassy carbon, a new columns packing material for gas chromatography and high performance liquid chromatography. Chromatographia **16:** 138-146

Gladstones JS (1998) Distribution, Origin, Taxonomy, History and Importance. *In* JS Gladstones, CA Atkins, J Hamblin, eds, Lupin as Crop Plants: Biology, Production and Utilization. CAB International, pp 1-39

Goodacre R, Vaidyanathan S, Dunn WB, Harrigan GG, Kell DB (2004) Metabolomics by numbers: acquiring and understanding global metabolite data. Trends Biotechnol. **22:** 245-252

Groussac E, Ortiz M, François J (2000) Improved protocols for quantitative determination of metabolites from biological samples using high performance

ionic-exchange chromatography with conductimetric and pulsed amperometric detection. Enzyme Microb. Technol. **26: 715-723**

Gu G, Lim CK (1990) Separation of anionic and cationic compounds of biomedical interest by high-performance liquid chromatography on porous graphitic carbon. J. Chromatogr. **515:** 183-192

Guilhaus M, Selby D, Mlynski V (2000) Orthogonal acceleration time-of-flight mass spectrometry. Mass Spectrom. Rev. **19: 65-107**

Gullberg J, Jonsson P, Nordström A, Sjöström M, Moritz T (2004) Design of experiments: an efficient strategy to identify factors influencing extraction and derivatization of *Arabidopsis thaliana* samples in metabolomic studies with gas chromatography/mass spectrometry. Anal. Biochem. **331:** 283-295

Guo Y, Gaiki S (2005) Retention behaviour of small polar compounds on polar stationary phases in hydrophilic interaction chromatography. J. Chromatogr. A **1074: 71-80**

Gustavsson SÅ, Samskog J, Markides KE, Långström B (2001) Studies of signal suppression in liquid chromatography-electrospray ionization mass spectrometry using volatile ion-pairing reagents. J. Chromatogr. A **937:** 41-47

Hall R, Beale M, Fiehn O, Hardy N, Sumner L, Bino R (2002) Plant metabolomics: the missing link in functional genomics strategies. Plant Cell **14:** 1437-1440

Hall RD (2006) Plant metabolomics: from holistic hope, to hype, to hot topic. New Phytol. **169: 453-468**

Hammond-Kosak K, Jones JDG (2000) Responses to Plant Pathogens. *In* BB Buchanan, W Gruissem, RL Jones, eds, Biochemistry and Molecular Biology of Plants. American Society of Plant Physiologists, pp 1102-1156

Hanai T (2003) Separation of polar compounds using carbon columns. J. Chromatogr. A **989:** 183-196

Hannah MA, Zuther E, Buchel K, Heyer AG (2006) Transport and metabolism of raffinose family oligosaccharides in transgenic potato. J. Exp. Bot. **57:** 3801-3811

Harvey DJ, Horning MG (1973) Characterization of the trimethylsilyl derivatives of sugar phosphates and related compounds by gas chromatography and gas chromatography-mass spectrometry. J. Chromatogr. **76:** 51-62

Havlová M, Dobrev PI, Motyka V, Štorchová H, Libus J, Dobrá J, Malbeck J, Gaudinová A, Vanková R (2008) The role of cytokinins in responses to water deficit in tobacco plants over-expressing *trans*-zeatin O-glucosyltransferase gene under *35S* or *SAG12* promoters. Plant Cell Environ. **31:** 341-353

Hennion M-C, Coquart V, Guenu S, Sella C (1995) Retention behaviour of polar compounds using porous graphitic carbon with water-rich mobile phases. J. Chromatogr. A **712:** 287-301

Hermström P, Irgum K (2006) Hydrophilic interaction chromatography. J. Sep. Sci. **29:** 1784-1821

Hirai MY, Klein M, Fujikawa Y, Yano M, Goodenowe DB, Yamazaki Y, Kanaya S, Nakamura Y, Kitayama M, et al. (2005) Elucidation of gene-to-gene and metabolite-to-gene networks in *Arabidopsis* by integration of metabolomics and transcriptomics. J. Biol. Chem. **280:** 25590-25595

Huhman DV, Sumner LW (2002) Metabolic profiling of saponins in *Medicago sativa* and *Medicago truncatula* using HPLC coupled to an electrospray ion-trap mass spectrometer. Phytochem. **59:** 347-360

Huyghe C (1997) White lupin (*Lupinus albus* L.). Field Crops Res. **53:** 147-160

International Rice Genome Sequencing Project (2005) The map-based sequence of the rice genome. Nature **436:** 793-800

Iribarne J, Thomson B (1976) On the evaporation of small ions from charged droplets. J. Chem. Phys. **64:** 2287-2294

Jelitto T, Sonnewald U, Willmitzer L, Hajirezeai M, Stitt M (1992) Inorganic pyrophosphate content and metabolites in potato and tobacco plants expressing *E. coli* pyrophosphatase in their cytosol. Planta **188:** 238-244

Jonscher KR, Yates JR, III (1997) The quadrupole ion trap mass spectrometer - a small solution to a big challenge. Anal. Biochem. **244:** 1-15

Juraschek R, Dülcks T, Karas M (1999) Nanoelectrospray - More than just a minimized-flow electrospray ionization source. J. Am. Soc. Mass Spectrom. **10:** 300-308

Knox JH, Kaur B, Millward GR (1986) Structure and performance of porous graphitic carbon in liquid chromatography. J. Chromatogr. **352:** 3-25

Knox JH, Ross P (1997) Carbon-based packing materials for liquid chromatography: structure, performance, and retention mechanisms. Adv. Chromatogr. **37:** 73-119

Koizumi K (1996) High-performance liquid chromatographic separation of carbohydrates on graphitized carbon columns. J. Chromatogr. A **720:** 119-126

Koizumi K, Okada Y, Fukuda M (1991) High-performance liquid chromatography of mono- and oligo-saccharides on a graphitized carbon column. Carbohydr. Res. **215:** 67-80

Kopka J (2006a) Current challenges and developments in GC-MS based metabolite profiling technology. J. Biotechnol. **124:** 312-322

Kopka J (2006b) Gas chromatography mass spectrometry. *In* K Saito, RA Dixon, L Willmitzer, eds, Biotechnology in agriculture and forestry: Plant metabolomics, Vol 57. Springer-Verlag Berlin Heidelberg, pp 3-20

Kopka J, Fernie A, Weckwerth W, Gibon Y, Stitt M (2004) Metabolite profiling in plant biology: platforms and destinations. Genome Biol. **5:** 109

Koster KL, Leopold AC (1988) Sugars and desiccation tolerance in seeds. Plant Physiol. **88:** 829-832

Krishnan P, Kruger NJ, Ratcliffe RG (2005) Metabolite fingerprinting and profiling in plants using NMR. J. Exp. Bot. **56:** 255-265

Kuhlmann FE, Apffel A, Fisher S, Goldberg G, Goodley PC (1995) Signal enhancement for gradient reverse-phase high-performance liquid chromatography-electrospray ionization mass spectrometry analysis with trifluoroacetic and other strong acid modifiers by postcolumn addition of propionic acid and isopropanol. J. Am. Soc. Mass Spectrom. **6:** 1221-1225

Lee YC (1990) High-performance anion-exchange chromatography for carbohydrate analysis. Anal. Biochem. **189:** 151-162

Lee YC (1996) Carbohydrate analyses with high-performance anion-exchange chromatography. J. Chromatogr. A **720:** 137-149

Lim CK (1989) Electronic interaction chromatography on porous graphitic carbon. Separation of [^{99m}Tc]Pertechnetate and Perrhenate anions. Biomed. Chromatogr. **3:** 92-93

Lin X, Kaul S, Rounsley S, Shea TP, Benito M-I, Town CD, Fujii CY, Mason T, Bowman CL, et al. (1999) Sequence and analysis of chromosome 2 of the plant *Arabidopsis thaliana*. Nature **402:** 761-768

Lindon JC, Holmes E, Nicholson JK (2003) So what's the deal with metabonomics? Anal. Chem. **75:** 384A-391A

Lipniunas PH, Neville DCA, Trimble RB, Townsend RR (1996) Separation of biosynthetic oligosaccharide branch isomers using high-performance liquid chromatography on a porous two-dimensional graphite stationary phase. Anal. Biochem. **243:** 203-209

Lloyd JR, Kossmann J, Ritte G (2005) Leaf starch degradation comes out of the shadows. Trends Plant Sci. **10:** 130-137

Lunn JE, Feil R, Hendriks JH, Gibon Y, Morcuende R, Osuna D, Scheible WR, Carillo P, Hajirezaei MR, et al. (2006) Sugar-induced increases in trehalose 6-phosphate are correlated with redox activation of ADPglucose pyrophosphorylase and higher rates of starch synthesis in *Arabidopsis thaliana*. Biochem. J. **397:** 139-148

Lunn JE, MacRae E (2003) Nem complexities in the synthesis of sucrose. Curr. Opin. Plant Biol. **6:** 208-214

Lytovchenko A, Fernie A (2003) Photosynthetic metabolism is severely impaired on the parallel reduction of plastidial and cytosolic isoforms of phosphoglucomutase. Plant Physiol. Biochem. **41:** 193-200

Mamyrin BA, Karatajev VJ, Shmikk DV, Zagulin VA (1973) The mass-reflectron, a new non magnetic time-of-flight mass spectrometer with high resolution. Sov. Phys. JETP **37:** 45-48

March R (1997) An introduction to quadrupole ion trap mass spectrometry. J. Mass Spectrom. **32:** 351-369

March RE, Stadey CJ (2005) A tandem mass spectrometric study of saccharides at high mass resolution. Rapid Commun. Mass Spectrom. **19:** 805-812

Matuszewski BK, Constanzer ML, Chavez-Eng CM (2003) Strategies for the assessment of matrix effect in quantitative bioanalytical methods based on HPLC-MS/MS. Anal. Chem. **75:** 3019-3030

Mayer K, Schuller C, Wambutt R, Murphy G, Volckaert G, Pohl T, Dusterhoft A, Stiekema W, Entian K-D, et al. (1999) Sequence and analysis of chromosome 4 of the plant *Arabidopsis thaliana*. Nature **402:** 769-777

Mehrotra B, Mendes P (2006) Bioinformatics approaches to integrate metabolomics and other systems biology data. *In* K Saito, RA Dixon, L Willmitzer, eds, Biotechnology in agriculture and forestry: Plant metabolomics, Vol 57. Springer-Verlag Berlin Heidelberg, pp 105-115

Meinke DW, Cherry JM, Dean C, Rounsley SD, Koornneef M (1998) *Arabidopsis thaliana*: A model plant for genome analysis. Science **282:** 662-682

Mercier J-P, Morin P, Dreux M, Tambuté A (1999) Liquid chromatography analysis of phosphonic acids in porous graphitic carbon stationary phase with evaporative light-scattering and mass spectrometry detection. J. Chromatogr. A **849:** 197-207

Moing A, Maucourt M, Renaud C, Graudillere M, Brougisse R, Leboutellier B, Gousset-Dupont A, Vidal J, Granot D, et al. (2004) Quantitative metabolic profiling by 1-dimensional H-1-NMR analyses: application to plant genetics and functional genomics. Funct. Plant Biol. **31:** 889-902

Monton MRN, Soga T (2007) Metabolome analysis by capillary electrophoresis-mass spectrometry. J. Chromatogr. A **1168:** 237-246

Moritz T, Johansson AI (2008) Plant metabolomics. *In* WJ Griffiths, ed, Metabolomics, Metabonomics and Metabolite Profiling. RSC Publishing, pp 254-272

Murashige T, Skoog F (1962) A revised medium for rapid growth and bio assays with tobacco tissue cultures. Physiol. Plant. **15:** 473-497

Nicholson JK, Lindon JC, Holmes E (1999) 'Metabonomics': understanding the metabolic responses of living systems to pathophysiological stimuli via multivariate statistical analysis of biological NMR spectroscopic data. Xenobiotica **29:** 1181-1189

Niessen WMA, van der Hoeven RAM, van der Greef J, Schols HA, Voragen AGJ (1993) Recent progress in high-performance anion-exchange chromatography-thermospray mass spectrometry of oligosaccharides. J. Chromatogr. **647:** 319-327

Niittylä T, Messerli G, Trevisan M, Chen J, Smith AM, Zeeman SC (2004) A previously unknown maltose transporter essential for starch degradation in leaves. Science **303:** 87-89

Ohta D, Shibata D, Kanaya S (2007) Metabolic profiling using Fourier-transform ion-cyclotron-resonance mass spectrometry. Anal. Bioanal. Chem. **389:** 1469-1475

Oikawa A, Nakamura Y, Ogura T, Kimura A, Suzuki H, Sakurai N, Shinbo Y, Shibata D, Kanaya S, et al. (2006) Clarification of pathway-specific inhibition by Fourier transform ion cyclotron resonance/mass spectrometry-based metabolic phenotyping studies. Plant Physiol. **142:** 398-413

Oliver SG, Winson MK, Kell DB, Baganz F (1998) Systematic functional analysis of the yeast genome. Trends Biotechnol. **16:** 373-378

Ott K-H, Aranibar N, Singh B, Stockton GW (2003) Metabonomics classifies pathways affected by bioactive compounds. Artificial neural network classification of NMR spectra of plant extracts. Phytochem. **62:** 971-985

Packer NH, Lawson MA, Jardine DR, Redmond JW (1998) A general approach to desalting oligosaccharides released from glycoproteins. Glycoconjugate J. **15:** 737-747

Pattanagul W, Madore MA (1999) Water deficit effects on raffinose family oligosaccharide metabolism in coleus. Plant Physiol. **121:** 987-993

Periappuram C, Steinhauer L, Barton DL, Taylor DC, Chatson B, Zou J (2000) The plastidic phosphoglucomutase from Arabidopsis. A reversible enzyme reaction with an important role in metabolic control. Plant Physiol. **122:** 1193-1199

Peters S, Mundree SG, Thomson JA, Farrant JM, Keller F (2007) Protection mechanisms in the resurrection plant *Xerophyta viscosa* (Baker): both sucrose and raffinose family oligosaccharides (RFOs) accumulate in leaves in response to water deficit. J. Exp. Bot. **58:** 1947-1956

Petterson DS (1998) Composition and food uses of lupins. *In* JS Gladstones, CA Atkins, J Hamblin, eds, Lupin as Crop Plants: Biology, Production and Utilization. CAB International, pp 353–384

Pinheiro C, Chaves MM, Ricardo CP (2001) Alterations in carbon and nitrogen metabolism induced by water deficit in the stems and leaves of Lupinus albus L. J. Exp. Bot. **52:** 1063-1070

Pinheiro C, Passarinho JA, Ricardo CP (2004) Effect of drought and rewatering on the metabolism of *Lupinus albus* organs. J. Plant Physiol. **161:** 1203-1210

Pinheiro C, Cruz de Carvalho MH, Bartels D, Ricardo CP, Chaves MM (2008) Dehydrins in Lupinus albus: pattern of protein accumulation in response to drought. Funct. Plant Biol. **35:** 85-91

Ramautar R, Demirci A, de Jong GJ (2006) Capillary electrophoresis in metabolomics. Trends Anal. Chem. **25:** 455-466

Ratcliffe RG, Shachar-Hill Y (2001) Probing plant metabolism with NMR. Annu. Rev. Plant Physiol. Plant Mol. Biol. **52:** 499-526

Ratcliffe RG, Shachar-Hill Y (2005) Revealing metabolic phenotypes in plants: inputs from NMR analysis. Biol. Rev. **80:** 27-43

Redmond JW, Packer NH (1999) The use of solid-phase extraction with graphitised carbon for the fractionation and purification of sugars. Carbohydr. Res. **319:** 74-79

Reepmeyer JC, Brower JF, Ye H (2005) Separation and detection of the isomeric equine conjugated estrogens, equilin sulfate and $\Delta^{8,9}$-dehydroestrone sulfate, by liquid chromatography-electrospray-mass spectrometry using carbon-coated zirconia and porous graphitic carbon stationary phases. J. Chromatogr. A **1083:** 42-51

Robinson S, Bergström E, Seymour M, Thomas-Oates J (2007) Screening of underivatized oligosaccharides extracted from the stems of *Triticum aestivum* using porous graphitized carbon liquid chromatography-mass spectrometry. Anal. Chem. **79:** 2437-2445

Rodrigues JA, Taylor AM, Sumpton DP, Reynolds JC, Pickford R, Thomas-Oates J (2008) Mass spectrometry of carbohydrates: newer aspects. Adv. Carbohydr. Chem. Biochem. **61:** 59-141

Rodrigues ML, Pacheco CMA, Chaves MM (1995) Soil-plant water relations, root distribution and biomass partitioning in *Lupinus albus* L. under drought conditions. J. Exp. Bot. **46:** 947-956

Roessner-Tunali U, Hegemann B, Lytovchenko A, Carrari F, Bruedigam C, Granot D, Fernie AR (2003) Metabolic profiling of transgenic tomato plants overexpressing hexokinase reveals that the influence of hexose phosphorylation diminishes during fruit development. Plant Physiol. **133:** 84-99

Roessner U, Luedemann A, Brust D, Fiehn O, Linke T, Willmitzer L, Fernie AR (2001a) Metabolic profiling allows comprehensive phenotyping of genetically or environmentally modified plant systems. Plant Cell **13:** 11-29

Roessner U, Wagner C, Kopka J, Trethewey RN, Willmitzer L (2000) Simultaneous analysis of metabolites in potato tuber by gas chromatography–mass spectrometry. Plant J. **23:** 131-142

Roessner U, Willmitzer L, Fernie AR (2001b) High-resolution metabolic phenotyping of genetically and environmentally diverse potato tuber systems. Identification of phenocopies. Plant Physiol. **127:** 749-764

Ryan D, Robards K (2006) Analytical chemistry considerations in plant metabolomics. Sep. & Purif. Rev. **35:** 319-356

Salanoubat M, Lemcke K, Rieger M, Ansorge W, Unseld M, Fartmann B, Valle G, Blocker H, Perez-Alonso M, et al. (2000) Sequence and analysis of chromosome 3 of the plant *Arabidopsis thaliana*. Nature **408:** 820-822

Sato S, Soga T, Nishioka T, Tomita M (2004) Simultaneous determination of the main metabolites in rice leaves using capillary electrophoresis mass spectrometry and capillary electrophoresis diode array detection. Plant J. **40:** 151-163

Schlichtherle-Cerny H, Affolter M, Cerny C (2003) Hydrophilic interaction liquid chromatography coupled to electrospray mass spectrometry of small polar compounds in food analysis. Anal. Chem. **75:** 2349-2354

Sekiguchi Y, Mitsuhashi N, Inoue Y, Yagisawa H, Mimura T (2004) Analysis of sugar phosphates in plants by ion chromatography on a titanium dioxide column with pulsed amperometric detection. J. Chromatogr. A **1039:** 71-76

Seki M, Umezawa T, Urano K, Shinozaki K (2007) Regulatory metabolic networks in drought stress responses. Curr. Opinion Plant Biol. **10:** 296-302

SeQuant (2006) A practical guide to HILIC: a tutorial and application book, Ed 1. SeQuant AB, Umeå, Sweden

Shauer N, Fernie AR (2006) Plant metabolomics: towards biological function and mechanism. Trends Plant Sci. **11:** 508-516

Smith AM, Zeeman SC, Smith SM (2005) Starch Degradation. Annu. Rev. Plant Biol. **56:** 73-98

Smith AM, Zeeman SC, Thorneycroft D, Smith SM (2003) Starch mobilization in leaves. J. Exp. Bot. **54:** 577-583

Smits HP, Cohen A, Buttler T, Nielsen J, Olsson L (1998) Cleanup and analysis of sugar phosphates in biological extracts by using solid-phase extraction and anion-exchange chromatography with pulsed amperometric detection. Anal. Biochem. **261:** 36-42

Soga T, Ueno Y, Naraoka H, Ohashi Y, Tomita M, Nishioka T (2002) Simultaneous determination of anionic intermediates for *Bacillus subtilis* metabolic pathways by capillary electrophoresis electrospray ionization mass spectrometry. Anal. Chem. **74:** 2233-2239

Stafford GC, Kelley PE, Syka JEP, Reynolds WE, Todd JFJ (1984) Recent improvements in and analytical applications of advanced ion trap technology. Int. J. Mass Spectrom. Ion Processes **60:** 85-98

Stitt M, Fernie AR (2003) From measurements of metabolites to metabolomics: an 'on the fly' perspective illustrated by recent studies of carbon-nitrogen interactions. Curr. Opinion Biotechnol. **14:** 136-144

Stitt M, Lilley RM, Gerhardt R, Heldt HW (1989) Determination of metabolite levels in specific cells and subcellular compartments of plant leaves. Methods Enzymol. **174:** 518-552

Sumner LW (2006) Current status and forward looking thoughts on LC/MS metabolomics. *In* K Saito, RA Dixon, L Willmitzer, eds, Biotechnology in agriculture and forestry: Plant metabolomics, Vol 57. Berlin Heidelberg: Springer-Verlag, pp 21-32

Sumner LW, Mendes P, Dixon RA (2003) Plant metabolomics: large-scale phytochemistry in the functional genomics era. Phytochem. **62:** 817-836

Sumner LW, Paiva NL, Dixon RA, Geno PW (1996) High performance liquid chromatography continuous-flow liquid secondary ion mass spectrometry of flavonoid glycosides in leguminous plant extracts. J. Mass Spectrom. **31:** 472-485

Swezey RR (1995) High-performance liquid chromatographic system for separating sugar phosphates and other intermediary metabolites. J. Chromatogr. B **669:** 171-176

Tabata S, Kaneko T, Nakamura Y, Kotani H, Kato T, Asamizu E, Miyajima N, Sasamoto S, Kimura T, et al. (2000) Sequence and analysis of chromosome 5 of the plant *Arabidopsis thaliana*. Nature **408:** 823-826

Taji T, Ohsumi C, Luchi S, Seki M, Kasuga M, Kobayashi M, Yamaguchi-Shinozaki K, Shinozaki K (2002) Important roles of drought- and cold-inducible genes for galactinol synthase in stress tolerance in *Arabidopsis thaliana*. Plant J. **29:** 417-426

Taylor VF, MArch RE, Longerich HP, Stadey CJ (2005) A mass spectrometric study of glucose, sucrose, and fructose using an inductively coupled plasma and electrospray ionization. Int. J. Mass Spectrom. **243:** 71-84

The Arabidopsis Genome Initiative (2000) Analysis of the genome sequence of the flowering plant *Arabidopsis thaliana*. Nature **408:** 796-815

Theologis A, Ecker JR, Palm CJ, Federspiel NA, Kaul S, White O, Alonso J, Alta H, Araujo R, et al. (2000) Sequence and analysis of chromosome 1 of the plant *Arabidopsis thaliana*. Nature **408:** 816-820

Thorneycroft D, Sherson SM, Smith SM (2001) Using gene knockouts to investigate plant metabolism. J. Exp. Bot. **52:** 1593-1601

Tohge T, Nishiyama Y, Hirai MY, Yano M, Nakajima J, Awazuhara M, Inoue E, Takahashi H, Goodenowe DB, et al. (2005) Functional genomics by integrated analysis of metabolome and transcriptome of *Arabidopsis* plants over-expressing an MYB transcript factor. Plant J. **42:** 218-235

Tolstikov V, Fiehn O (2002) Analysis of highly polar compounds of plant origin: combination of hydrophilic interaction chromatography and electrospray ion trap mass spectrometry. Anal. Biochem. **301:** 298-307

Tolstikov V, Lommen A, Nakanishi K, Tanaka N, Fiehn O (2003) Monolithic silica-based capillary reversed-phase liquid chromatography/electrospray mass spectrometry for plant metabolomics. Anal. Chem. **75:** 6737-6740

Townsend RR, Hardy MR, Lee YC (1989) Separation of oligosaccharides using high-performance anion-exchange chromatography with pulsed amperometric detection. Methods Enzymol. **179:** 65-76

Trygg J, Gullberg J, Johansson AI, Jonsson P, Moritz T (2006) Chemometrics in metabolomics - an introduction. *In* K Saito, RA Dixon, L Willmitzer, eds, Biotechnology in agriculture and forestry: Plant metabolomics, Vol 57. Springer-Verlag Berlin Heidelberg, pp 117-128

Valliyodan B, Nguyen HT (2006) Understanding regulatory networks and engineering for enhanced drought tolerance in plants. Curr. Opin. Plant Biol. **9:** 189-195

van Dam JC, Eman M, Frank J, Lange HC, van Dedem GWK, Heijnen SJ (2002) Analysis of glycolytic intermediates in *Saccharomyces cerevisae* using anion exchange chromatography and electrospray ionization with tandem mass spectrometric detection. Anal. Chim. Acta **460:** 209-218

Wan QH, Shaw PN, Davies MC, Barrett DA (1995) Chromatographic behaviour of positional isomers on porous graphitic carbon. J. Chromatogr. A **697:** 219-227

Wang W, Vinocur B, Altman A (2003) Plant responses to drought, salinity, and extreme temperatures: Towards genetic engineering for stress tolerance. Planta **218:** 1-14

Wang Y, Griffiths WJ (2008) Mass spectrometry for metabolite identification. *In* WJ Griffiths, ed, Metabolomics, Metabonomics and Metabolite Profiling. RSC Publishing, pp 1-43

Ward JL, Beale MH (2006) NMR spectroscopy in plant metabolomics. *In* K Saito, RA Dixon, L Willmitzer, eds, Biotechnology in agriculture and forestry: Plant metabolomics, Vol 57. Springer-Verlag Berlin Heidelberg, pp 81-91

Ward JL, Harris C, Lewis J, Beale MH (2003) Assessment of ^{1}H NMR spectroscopy and multivariate analysis as a technique for metabolite fingerprinting of *Arabidopsis thaliana*. Phytochem. **62:** 949-957

Weckwerth W (2003) Metabolomics in systems biology. Annu. Rev. Plant Biol. **54:** 669-689

Weiner H, Stitt M, Heldt HW (1987) Subcellular compartmentation of pyrophosphate and alkaline pyrophosphate in leaves. Biochim. Biophys. Acta **893:** 13-21

Wilm M, Mann M (1994) Electrospray and Taylor-cone theory, Dole's beam of macromolecules at last? Int. J. Mass Spectrom. Ion Processes **136:** 167-180

Wilm M, Mann M (1996) Analytical properties of the nanoelectrospray ion source Anal. Chem. **68:** 1-8

Wilson ID, Brinkman UAT (2003) Hyphenation and hypernation - The practice and prospects of multiple hyphenation. J. Chromatogr. A **1000:** 325-356

Wunschel DS, Fox KF, Fox A, Nagpal ML, Kim K, Stewart GC, Shahgholi M (1997) Quantitative analysis of neutral and acidic sugars in whole bacterial cell hydrolysates using high-performance anion-exchange liquid chromatography-electrospray ionization tandem mass spectrometry. J. Chromatogr. A **776:** 205-219

Xing J, Apedo A, Tymiak A, Zhao N (2004) Liquid chromatographic analysis of nucleosides and their mono-, di- and triphosphates using porous graphitic carbon stationary phase coupled with electrospray mass spectrometry. Rapid Commun. Mass Spectrom. **18:** 1599-1606

Yamashita M, Fenn JB (1984) Electrospray ion source. Another variation on the free-jet theme. J. Phys.Chem. **88:** 4451-4459

Yu T-S, Kofler H, Häusler RE, Hille D, Függle U-I, Zeeman SC, Smith AM, Kossmann J, Lloyd J, et al. (2001) The *Arabidopsis sex1* mutant is defective in the R1 protein, a general regulator of starch degradation in plants, and not in the chloroplast hexose transporter. Plant Cell **13:** 1907-1918

Zeeman SC, Smith SM, Smith AM (2004) The breakdown of starch in leaves. New Phytol. **163:** 247–261

Zeeman SC, Smith SM, Smith AM (2007) The diurnal metabolism of leaf starch. Biochem. J. **401:** 13-28

Zhang Y, Go EP, Jiang H, Desaire H (2005) A novel mass spectrometric method to distinguish isobaric mnosaccharides that are phosphorylated or sulfated using ion-pairing reagents. J. Am. Soc. Mass Spectrom. **16:** 1827-1839

Zuther E, Büchel K, Hundertmark M, Stitt M, Hincha DK, Heyer AG (2004) The role of raffinose in the cold acclimation response of *Arabidopsis thaliana*. FEBS Letters **576:** 169-173

Chapter 9

Outcomes of this PhD

Chapter 9. Outcomes of this PhD

9.1 Publications

9.1.1 Conference Proceedings

1. **Carla Antonio**, Tony Larson, Alison Gilday, Ian Graham, Ed Bergström, and Jane Thomas-Oates **(2006)**. LC–MS-based system for the analysis of glycolytic intermediates and sugar phosphates from *Arabidopsis thaliana*. Proceedings from the 4th International Plant Metabolomics Conference, *Metabolomics*, **2**, 299p.

9.1.2 Original Papers in Peer-Reviewed Journals

1. **Carla Antonio**, Tony Larson, Alison Gilday, Ian Graham, Ed Bergström, and Jane Thomas-Oates **(2007)**. Quantification of sugars and sugar phosphates in *Arabidopsis thaliana* tissues using porous graphitic carbon liquid chromatography-electrospray ionization mass spectrometry, *J. Chromatogr. A*, **1172**, 170-178.

2. **Carla Antonio**, Carla Pinheiro, Maria Manuela Chaves, Cândido Pinto Ricardo, Maria Fernanda Ortuño, and Jane Thomas-Oates **(2008)**. Analysis of carbohydrates in *Lupinus albus* stems using porous graphitic carbon liquid chromatography-electrospray ionization mass spectrometry, on imposition of water deficit, *J. Chromatogr. A.*, **1187**, 111-118.

3. **Carla Antonio**, Tony Larson, Alison Gilday, Ian Graham, Ed Bergström, and Jane Thomas-Oates **(2008)**. Hydrophilic interaction liquid chromatography-electrospray ionization mass spectrometry analysis of carbohydrate-related metabolites in *Arabidopsis thaliana* leaf tissue, *Rapid Comm. Mass Spectrom.*, **22**, 1399-1407.

9.1.3 Book Chapters (co-author)

1. João Rodrigues, **Carla Antonio**, Sarah Robinson, and Jane Thomas-Oates **(2008)**. Metabolomics, Metabonomics and Metabolite Profiling. *RSC Biomolecular Science Series*, ed. W. Griffiths, UK (ISBN 978-0-85404-299-9). Chapter 8, Mass Spectrometry in Glycobiology, 215-239p.

9.2 Oral Presentations

1. **Carla Antonio**, Tony Larson, Alison Gilday, Ian Graham, Ed Bergström, and Jane Thomas-Oates **(December 2005)**. LC-MS-based method for the determination of phosphorylated intermediates from plant tissues. *4° Encontro Nacional de Cromatografia, Évora, Portugal.*

2. **Carla Antonio**, Tony Larson, Alison Gilday, Ian Graham, Ed Bergström, and Jane Thomas-Oates **(September 2006)**. Development of an LC-MS method for the analysis of sugars and sugar phosphates from plant tissues. *CHEMCELL Science Day, Dept of Biology, University of York, UK.*

3. **Carla Antonio**, Tony Larson, Alison Gilday, Ian Graham, Ed Bergström, and Jane Thomas-Oates **(March 2007)**. LC-MS method for the analysis of sugars and sugar phosphates from plant tissues. *Prof. Manuela Chaves Research Group, Instituto de Tecnologia Química e Biológica (ITQB), Oeiras, Portugal.*

4. **Carla Antonio**, Tony Larson, Alison Gilday, Ian Graham, Ed Bergström, and Jane Thomas-Oates **(May 2007)**. Analysis of sugars and sugar phosphates by LC-ESI-MS using a porous graphitic carbon stationary phase. *Prof. Mike Ferguson Research Group, Division of Biological Chemistry & Molecular Microbiology, Wellcome Trust Biocentre, Dundee, Scotland, UK.*

5. **Carla Antonio**, Tony Larson, Alison Gilday, Ian Graham, Ed Bergström, and Jane Thomas-Oates **(July 2007)**. LC-MS-based system for the analysis of glycolytic intermediates and sugar phosphates from plant tissues. *Analytical Research Forum 2007, Glasgow, Scotland, UK.*

6. **Carla Antonio**, Tony Larson, Alison Gilday, Ian Graham, Ed Bergström, and Jane Thomas-Oates **(October 2007)**. Development and application of LC-MS approaches for studying the plant primary metabolome. *CHEMCELL Science Day, Dept of Biology, University of York, UK.*

9.3 Selected Poster Presentations

1. **Carla Antonio**, Tony Larson, Alison Gilday, Ian Graham, Ed Bergström, and Jane Thomas-Oates **(September 2005)**. Development of an LC-MS system for the analysis of phosphorylated carbohydrates from plant tissues. *28th Annual Meeting British Mass Spectrometry Society (BMSS), University of York, UK.*

2. **Carla Antonio**, Tony Larson, Alison Gilday, Ian Graham, Ed Bergström, and Jane Thomas-Oates **(April 2006)**. LC-MS-based system for the analysis of glycolytic intermediates and sugar phosphates from plant tissues. *4th International Plant Metabolomics Conference, Wokefield Park, Berkshire, Reading, UK.*

3. **Carla Antonio**, Tony Larson, Alison Gilday, Ian Graham, Ed Bergström, and Jane Thomas-Oates **(June 2006)**. Development of an LC-MS method for the

analysis of sugars and sugar phosphates from *Arabidopsis thaliana*. *2nd International Conference of the Metabolomics Society, Boston, MA, USA.*

4. **Carla Antonio**, Tony Larson, Alison Gilday, Ian Graham, Ed Bergström, and Jane Thomas-Oates **(June 2007)**. LC-MS-based system for the analysis of glycolytic intermediates and sugar phosphates from plant tissues. *3rd International Conference of the Metabolomics Society, Manchester, UK.*

9.4 Collaborations

1. Collaborative project entitle **'Screening for stress responsive metabolites'** between The University of York, and Prof. Manuela Chaves & Dr Carla Pinheiro at Instituto de Tecnologia Química e Biológica (ITQB, Oeiras, Portugal). This project is funded by the Treaty of Windsor Anglo-Portuguese Joint Research Programme, British Council, Lisboa, Portugal, and the author contributed to the grant proposal writing and submission which was successfully approved by the British Council.

Appendix I

Quantification of sugars and sugar phosphates in *Arabidopsis thaliana* tissues using porous graphitic carbon liquid chromatography-electrospray ionization mass spectrometry

Carla Antonio[a], Tony Larson[b], Alison Gilday[b], Ian Graham[b], Ed Bergström[a] and Jane Thomas-Oates[a]

[a] Department of Chemistry,
University of York,
UK

[b] Centre for Novel Agricultural Products,
Department of Biology,
University of York,
UK

Journal of Chromatography A, 1172 (2007) 170-178

Available online at www.sciencedirect.com
ScienceDirect
Journal of Chromatography A, 1172 (2007) 170–178
JOURNAL OF CHROMATOGRAPHY A
www.elsevier.com/locate/chroma

Quantification of sugars and sugar phosphates in *Arabidopsis thaliana* tissues using porous graphitic carbon liquid chromatography-electrospray ionization mass spectrometry

Carla Antonio [a], Tony Larson [b], Alison Gilday [b], Ian Graham [b], Ed Bergström [a], Jane Thomas-Oates [a,*]

[a] *Department of Chemistry, University of York, Heslington, York YO10 5DD, UK*
[b] *Centre for Novel Agricultural Products, Department of Biology, University of York, York YO10 5YW, UK*

Received 14 August 2007; received in revised form 2 October 2007; accepted 4 October 2007
Available online 10 October 2007

Abstract

This work reports the development and optimisation of a negative ion mode on-line LC-ESI-MS/MS method for the sensitive targeted analysis of the key glycolytic intermediates, sugars and sugar phosphates from plants, using a porous graphitic carbon (PGC) stationary phase and an MS compatible mobile phase. Using this newly developed method, separation and detection of a solution of standard compounds is achieved in less than 20 min. Target metabolite compounds were identified in plant extracts from their characteristic retention times, and product ion spectra. This on-line PGC-ESI-MS/MS method shows good linearity over the concentration range 0–100 μM, selectivity, short analysis time, and limits of detection of 0.1 μM for disaccharides trehalose (Tre), sucrose (Suc), and maltose, and 1.5 μM for hexose phosphates fructose-6-phosphate (Fru6P), glucose-1-phosphate (Glc1P), and glucose-6-phosphate (Glc6P), and phosphoenolpyruvate (PEP). This paper describes details of our method and its application to the simultaneous quantitative analysis of soluble sugars and sugar phosphates from *Arabidopsis thaliana* tissues. We have demonstrated the utility of our method for the analysis of biological samples by applying it to the simultaneous quantitation of changes in soluble sugars and sugar phosphates in *A. thaliana* Columbia-0 (Col-0) and its starchless phosphoglucomutase (*pgm*) mutant over a 12-h light/12-h dark growth cycle.

Keywords: Glycolytic intermediates; Sugar phosphates; Porous graphitic carbon; HPLC–MS/MS; *Arabidopsis thaliana*; *pgm1* Mutant

1. Introduction

Glycolytic intermediates and sugar phosphates are central compounds in metabolism and signalling pathways. They are important intermediates of cellular energy metabolic pathways, such as glycolysis, the pentose phosphate pathway, and starch and sucrose synthesis in plants. However, due to their high polarity, low *in vivo* concentrations, rapid metabolic turnover, structural variety, instability and poor UV absorbance, these compounds are a particularly challenging subclass of the metabolome to analyse.

Glycolytic intermediates and sugar phosphates in plants have been traditionally measured using highly sensitive techniques such as enzyme assays [1,2]. Such assays offer the advantage of being very specific, which at the same time is their primary disadvantage; it is not possible to perform parallel determinations of different metabolites in the same sample. To overcome this, mass spectrometry (MS), combined with on-line separations, has been widely applied in metabolome analysis allowing the detection and identification of a wide range of metabolites in a single run. Moreover, the low limits of detection and the ability to perform multistage tandem MS experiments has made MS a popular choice.

Glycolytic intermediates and sugar phosphates are non-volatile and unstable compounds, and to analyse this class of metabolite by GC–MS, derivatization is required. The main disadvantage associated with derivatization protocols is the time and sample losses associated with the additional step in sample

* Corresponding author. Tel.: +44 1904 43 4459; fax: +44 1904 43 2516.
E-mail addresses: cipa500@york.ac.uk (C. Antonio), trl1@york.ac.uk (T. Larson), adg5@york.ac.uk (A. Gilday), iag1@york.ac.uk (I. Graham), etb2@york.ac.uk (E. Bergström), jeto1@york.ac.uk (J. Thomas-Oates).

0021-9673/$ – see front matter © 2007 Elsevier B.V. All rights reserved.
doi:10.1016/j.chroma.2007.10.011

handling; in many cases, LC–MS methods are used to avoid the derivatization step. MS is also highly desirable because it provides structural information from unknowns (compounds for which standards are not run) separated from plant extracts. In LC–MS applications, the column chemistry most commonly used is reversed-phase C_{18}. However, highly polar metabolites such as glycolytic intermediates and sugar phosphates, show minimal retention on RP-columns and generally elute close to the void volume without chromatographic separation.

High performance anion-exchange liquid chromatography (HPAEC) with electrochemical detection has been widely used for the analysis of sugar phosphates and other intermediary metabolites from animal tissues [3], *Escherichia coli* cell extracts [4], yeast [5,6], potato [7], and more recently from *Arabidopsis thaliana* tissues [8]. Nonetheless, the mobile phases used with commercial HPAEC systems (Dionex) contain high concentrations of sodium hydroxide and sodium acetate, and therefore are not MS compatible. The high ionic strength suppresses sample ionization [9,10] and causes ion source contamination, thus compromising sensitivity. Post-column membrane suppressors were developed by Dionex that were designed to remove the salt from the mobile phase following separation [11]. Although using this approach on-line coupling of HPAEC with MS has been reported for the analysis of glycolytic intermediates in yeast [12] and more recently, for the sensitive measurement of trehalose-6-phosphate (Tre6P) from *A. thaliana* tissues using HPAEC coupled to a triple quadrupole MS [13], this coupling does not appear to have been widely adopted.

Alternative LC–MS methods have been reported for the analysis of polar compounds based on new column chemistries and efficient on-line coupling with electrospray ionization mass spectrometry. A β-cyclodextrin bonded stationary phase was used for the separation of various commercially available sugar phosphates by LC-ESI-MS [14]. Although chromatographic resolution of the isomeric compounds glucose-1-phosphate (Glc1P) and glucose-6-phosphate (Glc6P) was not achieved, these compounds could be differentiated by tandem MS based on their characteristic product ion spectra. Hydrophilic interaction liquid chromatography (HILIC) coupled to ESI-MS was used for the analysis of highly polar compounds, such as oligosaccharides and sugar nucleotides, from *Cucurbita maxima* phloem tissues [15], and a C_{18} silica-based monolithic capillary column coupled to ESI-MS was applied for plant metabolomics using *A. thaliana* tissues [16]. Although these LC–MS methods have proven to be powerful tools for the analysis of highly polar compounds, their application to the targeted analysis of glycolytic intermediates and sugar phosphates from plant tissues has yet to be tested.

Porous graphitic carbon (PGC) was developed as an alternative to the commonly used RP-silica packings and became commercially available under the trade name Hypercarb™ [17,18]. It has advantages over classical RP-, NP- and HPAEC columns of stability over the entire pH range and the use of 'MS friendly' mobile phases with no ion-pairing reagents. In contrast to what is observed on RP materials, the retention of analytes on PGC increases with polarity. Knox and Ross defined the retention mechanism as the polar retention effect on graphite (PREG), determined by hydrophobic eluent–analyte interactions, and electronic interactions of polarizable (or polarized) functional groups in the analyte with the delocalized π-electrons of the graphite surface [19]. Due to the retention mechanism, carboxylic acids are commonly used as additives in the mobile phase to provide adequate anions for electronic interaction with the π-electrons of PGC, and therefore, elute more retained compounds [20–23]. Elfakir and Dreux investigated the behaviour of different carboxylic acids for the separation of inorganic ions on a PGC column and they found that the elution strength decreased in the following order: heptafluorobutyric acid > TFA > formic acid > acetic acid [24]. The use of PGC columns has been reported for the separation of mono- and oligosaccharides [25], polar compounds [26], some pairs of isomeric glycolytic intermediates such as glucose-6-phosphate and fructose-6-phosphate (Glc6P/Fru6P), and 2-phosphoglycerate and 3-phosphoglycerate (2PG/3PG) from *E. coli* cell extracts [27], positional isomers [28], conjugated estrogen isomers [29], and more recently for the study of endogenous underivatised water-soluble oligosaccharides extracted from *Triticum aestivum* stems [30].

Here we report the development of a robust on-line LC-ESI-MS/MS method using an ion trap instrument for the simultaneous targeted quantitation of glycolytic intermediates, soluble sugars and sugar phosphates from *A. thaliana* tissues on a PGC (Hypercarb™) column using an MS compatible mobile phase with formic acid as electronic competitor. We have used *A. thaliana* as a model system [31] for establishing and optimising our LC–MS-based method and demonstrating its utility for the analysis not only of commercial standards but also of complex biological samples. However, the method clearly also has applicability for the analysis of these central metabolites in other biological systems.

2. Experimental

2.1. Chemicals

All standards were purchased from Sigma (Poole, UK). Water and solvents used for chromatography were of HPLC grade and purchased from Fisher. Standard stock solutions were prepared in water at the concentration of 1.0 mg mL^{-1} and stored at −20 °C prior to use. Further dilutions were prepared in water.

2.2. Liquid chromatography–mass spectrometry

LC–MS method development was carried out on a Thermo Finnigan Surveyor HPLC coupled to an ion trap mass spectrometer (LCQ DECA XP Plus, Thermo Electron, San Jose, CA, USA), equipped with a Thermo Finnigan orthogonal electrospray interface. Chromatographic separation was performed on a Hypercarb column (5 μm, 100 mm × 4.6 mm; Thermo Electron, Cheshire, UK). The flow rate was 600 μL/min, the sample injection volume was 20 μL and the PGC column was used at ambient temperature (25 °C). The triple stage mobile phase was composed of (A) water, (B) acetonitrile, and (C) 15% aqueous

formic acid (Sigma). The LC run time was 20 min using the gradient elution profile: 0–5 min, 96% A 4% B to 92% A 8% B; 5–7 min, 92% A 8% B to 75% A 25% B and maintained for 3 min; 10–20 min, 75% A 25% B to 25% B 75% C followed by column re-equilibration: 20–22 min, 25% B 75% C to 50% A 50% B and maintained for 5 min; 27–30 min, 50% A 50% B to 96% A 4% B and maintained for 10 min. The ion trap mass spectrometer was operated in the negative ion mode with the ion source voltage set to −3.0 kV, capillary voltage −20 V, tube lens offset −60 V, capillary temperature 300 °C, sheath gas 40 (arbitrary units) and auxiliary gas 30 (arbitrary units). Mass spectra were acquired over the scan range *m/z* 50–800. Precursor ions were selected with an isolation width of 2 Th and activated for 30 ms. Collision induced dissociation (CID) experiments used helium as the collision gas and normalized collision energy settings were in the range 20–30%, depending on the compound. Data were processed using Xcalibur 1.3 software (Thermo Finnigan, San Jose, CA, USA). Optimum negative ion ESI-MS/MS parameters were determined for each standard compound using a solution of 50 μg/mL in methanol:water (50:50, v/v) by direct infusion with a syringe pump at a flow rate of 3 μL/min into solvent flow from the LC at a flow rate of 600 μL/min, over the scan range *m/z* 50–800.

2.3. Plant material

A. thaliana wild-type (WT) Columbia (Col-0) and starchless *pgm1* [32] mutant seeds were cold-treated at 4 °C and imbibed in the dark for 4 days on plates with 1/2-strength Murashige and Skoog medium [33]. Plants were grown in controlled-environment growth chambers under long-day photoperiod 16-h light/8-h dark (22/17 °C, 150 μmol photons m^{-2} s^{-1} light intensity, 70/60% humidity, day/night regime). Rosettes were harvested at developmental growth stage 6.0 [34], quenched by immediately freezing in the light at the temperature of liquid nitrogen, and stored at −80 °C prior to extraction and analysis. For the analysis of metabolite changes over the diurnal cycle, plants were grown in controlled-environment growth chambers under a 12-h light/12-h dark cycle (22/17 °C, 150 μmol photons m^{-2} s^{-1} light intensity, 70/60% humidity, day/night regime). Five-week-old rosettes were harvested at the end of the night period, 4, 8, and 12 h into the light period, 4, 8 h into the dark period, and again at the end of the night. Plant material was quenched by immediately freezing in liquid nitrogen, and stored at −80 °C prior to extraction and analysis.

2.4. Extraction of metabolites from A. thaliana tissues

Metabolites were extracted from *A. thaliana* plant tissues in trichloroacetic acid (TCA)/ether using a method adapted from Weiner et al. [35] and Jelitto et al. [36]. Leaf material was ground to a fine powder in liquid nitrogen in a pre-cooled mortar and pestle. Approximately 50 mg frozen plant material was transferred to a polypropylene microfuge tube (2.0 mL) containing 500 μL ice-cold 16% (v/v) TCA in diethylether, vortex-mixed and stored on ice for 30 min. To the tube was added 500 μL 16% (v/v) aqueous TCA containing 5 mM ethylene glycol-bis(2-aminoethylether)-*N*,*N*,*N*′,*N*′-tetraacetic acid (EGTA) and the mixture was homogenised and stored on ice for 2 h to achieve a complete inactivation of the enzymes and extraction of metabolites. The extract was then centrifuged for 4 min at 17,900 × *g* at 4 °C and the upper phase discarded. The water phase was washed with 800 μL diethylether saturated with water, centrifuged as above, and the upper phase discarded. The ether washing step was repeated three times. The extract was then neutralised with 1 μL 2.5 M KOH aliquots until the pH reached 5–6. The final neutralised extract was frozen in liquid nitrogen and stored at −80 °C prior to analysis. All plant extracts were centrifuged for 10 min at 17,900 × *g* at 4 °C and filtered through 0.22 μm Cameo syringe filters (Sigma, Poole, UK) prior to LC–mass spectrometric analysis.

Alternatively, metabolites were extracted from *A. thaliana* plant tissues in chloroform/methanol using a method adapted from Lunn et al. [13]. Leaf material was ground to a fine powder in liquid nitrogen in a pre-cooled mortar and pestle. Approximately 10 mg frozen plant material was transferred to a polypropylene microfuge tube (2.0 mL) containing 250 μL ice-cold chloroform:methanol (3:7, v/v), vortex-mixed, and the frozen mixture was incubated at −20 °C for 2 h to stop metabolism and extract water-soluble metabolites, including sugars and sugar phosphates. To the tube was added 200 μL ice-cold water and the tube was warmed to 4 °C with repeated shaking. The extract was then centrifuged for 10 min at 17,900 × *g* at 4 °C. The upper aqueous-methanol phase was transferred to a new polypropylene microfuge tube (1.5 mL) and kept at 4 °C. The lower chloroform phase was re-extracted by adding 200 μL ice-cold water, centrifuged as described above and the second aqueous-methanol phase was added to the first. The combined extract was evaporated to dryness using a centrifugal concentrator (Savant SpeedVac system, Thermo Electron Corporation, Runcorn, UK). Samples were reconstituted in 100 μL water and centrifuged for 30 min at 6800 × *g* at 20 °C followed by LC–mass spectrometric analysis.

3. Results and discussion

3.1. LC–MS/MS method development for the analysis of glycolytic intermediates and sugar phosphates

Standard compounds were separated on a PGC column without derivatization and detected in the negative ion mode as deprotonated $[M-H]^-$ (negatively charged compounds) or formylated molecules $[M+HCOO]^-$ (neutral sugars) using negative ion mode electrospray ion trap mass spectrometry. The negative ion mode was chosen because in preliminary investigations (data not shown), no signals for negatively charged compounds were obtained on direct infusion positive ion mode ESI analyses of a mixture containing glucose (Glc), Suc, Tre6P, Glc1P, fructose-1,6-bisphosphate (Fru1,6BP), phosphoenolpyruvate (PEP) and pyruvate. In the negative ion mode, signals for all seven components were obtained. LC separation was optimised using mobile phases composed of different ratios of acetonitrile/water and a standard solution containing a mixture of some of the intermediary metabolites that com-

monly occur in plants. This mixture was constituted in order to contain representatives of the main compound types: neutral monosaccharide (Glc), neutral disaccharide (Suc), a monosaccharide monophosphate (Glc6P), a disaccharide monophosphate (Tre6P), a monosaccharide bisphosphate (Fru1, 6BP), and a glycolytic intermediate (PEP). Using a mobile phase composed only of acetonitrile and water proved too weak to elute the negatively charged compounds (Glc6P, Tre6P, PEP, and Fru1, 6BP), and only Glc and Suc were successfully eluted from the PGC column (data not shown).

To elute the strongly retained compounds, it was found to be essential to include anionic modifiers in the aqueous mobile phase for competitive interaction with the negatively charged phosphate groups for the π-electrons of PGC [21]. The effect of anionic modifiers was investigated by adding increasing amounts of formic acid or acetic acid to the aqueous mobile phase until satisfactory separation for all compounds was achieved.

Formic acid has been reported to have a higher elution strength than acetic acid [24]. Additionally, the presence of formate anions in the mobile phase provided better MS responses and better peak shapes for all compounds than a mobile phase containing the equivalent concentration of acetate anions (data not shown). TFA was not evaluated, due to its well-documented incompatibility with ESI-MS. Therefore, formic acid was used for further mobile phase optimisations. It was observed that the negatively charged diphosphate compounds interacted so strongly with the PGC surface that the addition of 10% of formic acid was still not enough to elute these compounds from the PGC column. Elution of all the negatively charged compounds was achieved only when the proportion of formic acid added to the aqueous mobile phase was 15%. Because sugars and sugar phosphates are structurally similar compounds, in contrast to what is observed on RP materials, the retention of these compounds on PGC increases with polarity, and therefore follows PREG principles. Neutral mono- and disaccharides, detected as formylated molecules $[M+HCOO]^-$, eluted first from the PGC column, then monophosphates followed by diphosphates, detected as deprotonated molecules $[M-H]^-$. Good LC separation and identification for all standard compounds (Glc, Suc, Glc6P, Tre6P, PEP and Fru1, 6BP) was achieved in less than 20 min using a triple stage gradient composed of water, acetonitrile, and 15% aqueous formic acid as described in Section 2 (Fig. 1). The triple stage gradient was required in order to allow retention and separation of the neutral, the mono- and the di-phosphorylated species; the neutrals were unretained in the presence of acid modifier, necessitating the first acetonitrile/water step, while the monophosphates were separable only in 10% (not 15%) acid. The 15% acid step was needed to separate the diphosphates.

LC–MS/MS experiments on standard compounds were performed to aid in the identification of metabolites based on their retention times, masses, and product ion spectra. Deprotonated $[M-H]^-$ or formylated molecules $[M+HCOO]^-$ (neutral sugars) were selected as precursor ions for tandem

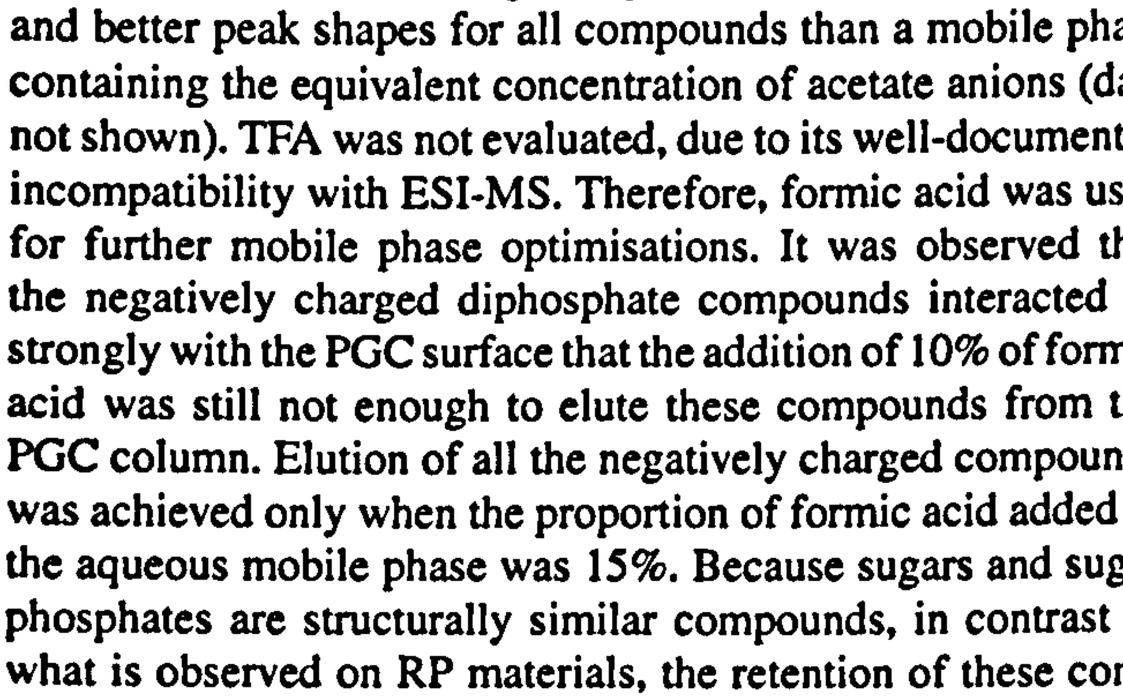

Fig. 1. Extracted ion chromatograms obtained on porous graphitic carbon (PGC) LC-ESI-MS separation of a 50 μg/mL standard solution of a mixture of intermediary metabolites. HPLC conditions: Hypercarb™ PGC (4.6 mm × 100 mm) column, 600 μL/min, 20 μL injection, optimised gradient (details in Section 2).

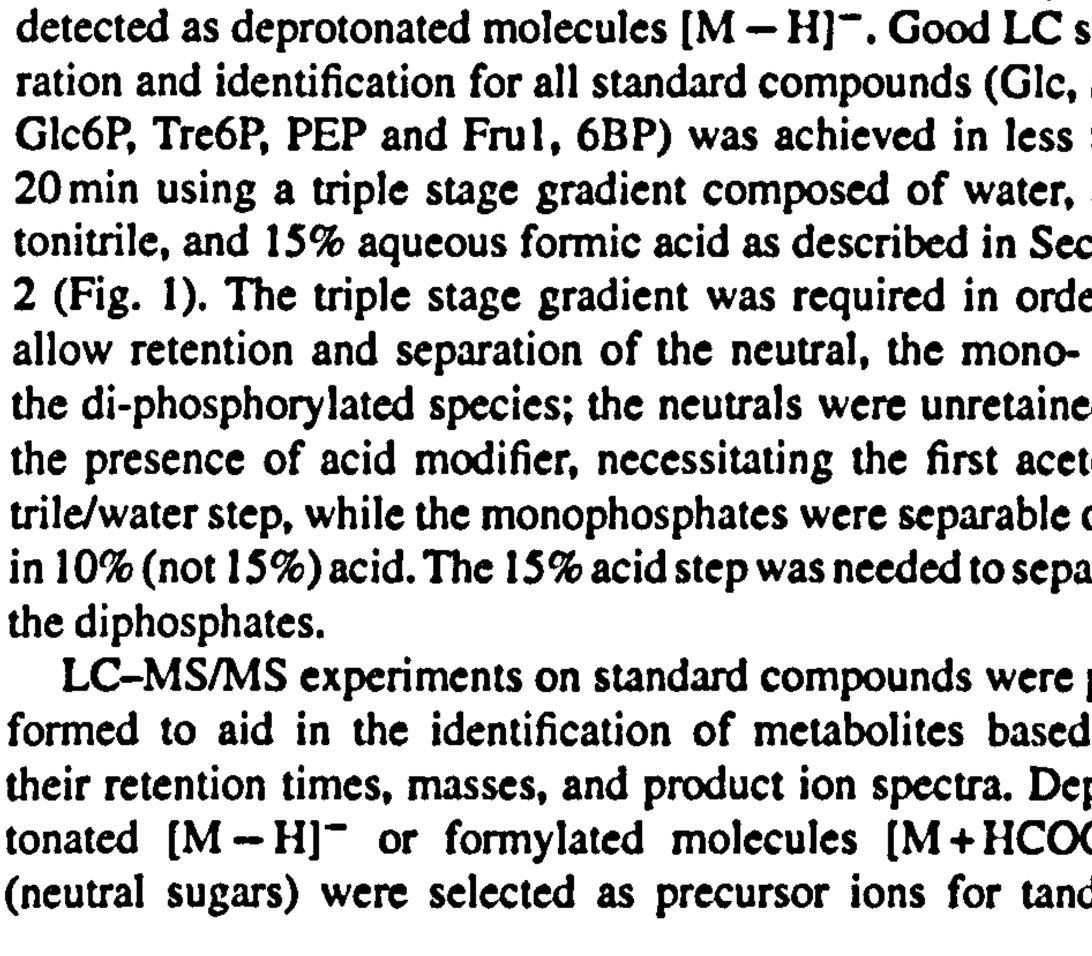

Fig. 2. (a) CID MS^2 product ion spectrum for a standard solution (10 μM) of Tre6P (precursor ion $[M-H]^-$ *m/z* 421); (b) CID MS^3 spectrum of Tre6P (precursor ion *m/z* 241).

mass spectrometry experiments. To illustrate typical MS^n data obtainable using our method, we describe experimental data for the non-reducing disaccharide sucrose ($[M+HCOO]^-$ at *m/z* 387) and the phosphorylated disaccharide trehalose-6-phosphate ($[M-H]^-$ at *m/z* 421) standards.

The collision induced dissociation MS^2 product ion spectrum of Suc produced an intense ion at *m/z* 341 ($[M-H]^-$) corresponding to the loss of formic acid. Subsequent CID MS^3 analysis, readily achieved using ion trap MS, of the $[M-H]^-$ ion at *m/z* 341 produced intense ions at *m/z* 179 and at *m/z* 161, which, according to the nomenclature for carbohydrate fragmentation of Domon and Costello [37], correspond to a Y_1 ion formed by cleavage of the glycoside bond with the loss of a hexose moiety $C_6H_{10}O_5$ (−162 Da), and a B_1 ion arising by the neutral loss of one monosaccharide $C_6H_{12}O_6$ (−180 Da).

The CID MS^2 product ion spectrum of Tre6P ($[M-H]^-$ at *m/z* 421) contains an intense B_1 ion at *m/z* 241 formed by cleavage of the glycoside bond corresponding to the neutral loss of one monosaccharide $C_6H_{12}O_6$ (−180 Da) (Fig. 2a). The presence of the phosphate group is clear from the product ions at *m/z* 79 $[PO_3]^-$ and *m/z* 97 $[H_2PO_4]^-$ in the MS^3 spectrum obtained on CID of *m/z* 241 (Fig. 2b).

PGC is known to be excellent for the separation of isomers or structurally related compounds [28–30]. Our PGC-based LC–MS method showed separation of the isomeric disaccharides trehalose (Tre), sucrose (Suc) and maltose, detected at *m/z* 387 as formylated molecules ($[M+HCOO]^-$) (Fig. 3).

Glucose-1-phosphate (Glc1P) and glucose-6-phosphate (Glc6P) are isomeric monosaccharides, detected as deprotonated molecules at *m/z* 259 ($[M-H]^-$) (Fig. 4). Although they have similar retention times (Table 1) there are two main differences between their product ion spectra under the same LC–MS/MS conditions. The 1-substituted isomer shows loss of H_2O (−18 Da) giving rise to the base peak at *m/z* 241 (Fig. 4a) and the 6-substituted isomer shows the loss of a hexose moiety $C_6H_{10}O_5$ (−162 Da) producing the base peak at *m/z* 97 (Fig. 4b). Identification and differentiation of the isomers Glc1P and Glc6P is, therefore, possible based on a consideration of both their retention times and their product ion spectra which are different and contain characteristic product ions [14].

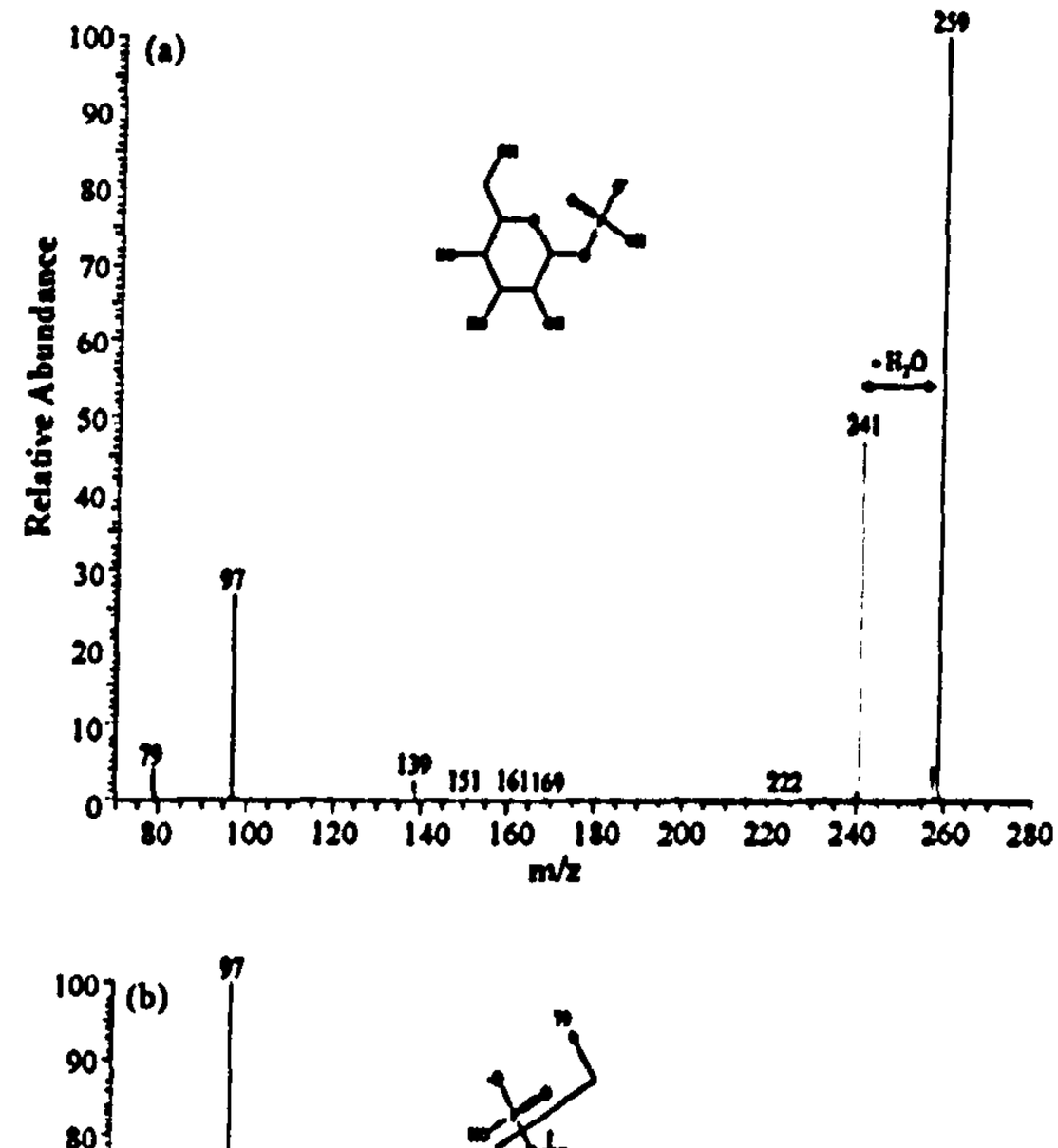

Fig. 4. Differentiation of the isomeric compounds Glc1P and Glc6P by ion trap tandem MS: (a) CID MS^2 product ion spectrum of Glc1P *m/z* 259; (b) CID MS^2 product ion spectrum of Glc6P *m/z* 259.

Fig. 3. Extracted ion chromatograms obtained on porous graphitic carbon (PGC) LC–MS for a standard solution (10 μM) of disaccharide isomers showing separation of: (1) Tre t_R = 5.96 min, (2) Suc t_R = 7.54 min and (3) maltose t_R = 8.44 min.

3.2. Linearity and limits of detection (LOD) of the PGC-LC-ESI-MS method

To evaluate the potential of the method for quantitative analysis of soluble sugars and sugar phosphates from plant tissues, intra- and inter-day repeatability of retention times, and linearity of the PGC-LC-ESI-MS method were tested. Intraday repeatability was measured by injecting the same standard solution three times in a single day. Inter-day repeatability was measured by analysing the same standard solution over 6 different

Table 1
Intra-day and inter-day repeatability of retention times, limits of detection (LOD), limits of quantification (LOQ), and linearity of calibration curves obtained for standard compounds using negative ion PGC-LC-ESI-MS

Standard compounds	Diagnostic ion (*m/z*)	t_R (min)	t_R (intra RSD)[a] (%, $n=3$)	t_R (inter RSD)[b] (%, $n=6$)	LOD[c] (μM)	LOQ[d] (μM)	Amount of LOD[e] (pmol)	R^{2f}
Fru	225 $[M+HCOO]^-$	2.87	0.70	0.75	2.0	6.7	40	0.9956
Glc	225 $[M+HCOO]^-$	2.93	0.20	1.15	0.5	1.6	9	0.9969
Tre	387 $[M+HCOO]^-$	5.62	1.46	1.64	0.1	0.3	2	0.9988
Suc	387 $[M+HCOO]^-$	7.12	0.41	0.59	0.1	0.3	2	0.9958
Maltose	387 $[M+HCOO]^-$	8.32	0.35	0.64	0.1	0.4	2	0.9929
Glc1P	259 $[M-H]^-$	14.37	0.26	0.87	1.5	5.0	30	0.9991
Fru6P	259 $[M-H]^-$	14.42	0.16	0.82	1.5	5.0	30	0.9913
Glc6P	259 $[M-H]^-$	14.56	0.07	0.26	1.5	5.0	30	0.9979
Tre6P	421 $[M-H]^-$	15.15	0.04	0.68	0.3	2.5	6	0.9939
Suc6P	421 $[M-H]^-$	15.33	0.11	0.12	0.8	2.5	15	0.9917
PEP	167 $[M-H]^-$	16.20	0.07	0.12	1.5	5.0	30	0.9947

HPLC conditions: Hypercarb PGC column (4.6 mm × 100 mm), 20 μL injection, triple stage gradient.
[a] Intra-day relative standard deviation (RSD) of retention times ($n=3$ independent measurements).
[b] Inter-day relative standard deviation (RSD) of retention times ($n=6$ independent measurements).
[c] Concentration limit of detection (LOD) calculated at a signal-to-noise ratio (S/N) of 3.
[d] Limit of quantification (LOQ) calculated at a signal-to-noise ratio (S/N) of 10.
[e] LOD of the amount loaded onto column calculated at a signal-to-noise ratio (S/N) of 3.
[f] Correlation coefficients for the standard curves (five-points) of relative peak areas against concentration (0–100 μM). Each point on the standard curve is the mean value of three independent measurements.

days. Intra-day and inter-day repeatability of retention times using our method gave relative standard deviations (RSD) of less than 2% (Table 1). The linearity of the PGC-LC-ESI-MS response was measured for each compound by recording the responses at different concentrations over the range 0–100 μM. Five-point standard curves were established by plotting integrated peak areas versus concentration. Each point on the calibration curve is the mean value of three independent measurements using the PGC-LC-ESI-MS method. The limit of detection for each compound was calculated as the minimum amount injected which gave a detector response higher than three times the signal-to-noise ratio (S/N). The on-line PGC-LC-ESI-MS method showed good linearity over the concentration range 0–100 μM for all compounds with estimated LODs of 0.5 μM obtained for Glc, 0.1 μM for disaccharides (Tre, Suc, and maltose), 0.3 μM for Tre6P, and 1.5 μM for hexose phosphates (Fru6P, Glc1P, Glc6P) and PEP. The limit of quantification (LOQ) was also determined for each compound at a S/N ratio of 10 (Table 1).

3.3. Analytical recoveries of standards from A. thaliana tissue extracts

The efficiency of the extraction methods used in this work was investigated by determining the analytical recoveries of phosphate standards spiked into *A. thaliana* tissue extracts. The recovery of different phosphate standards (Glc1P, Glc6P, Fru6P, Tre6P, Fru1, 6BP, and PEP) was tested using two extraction methods: extraction in trichloroacetic acid (TCA)/ether using approximately 50 mg of leaf material, and extraction in chloroform/methanol using approximately 10 mg of leaf material (details in Experimental Section). Recovery experiments were carried out in triplicate by adding known amounts of authentic standards into accurately weighed pooled *Arabidopsis* Col-0 frozen plant samples at the beginning of the extraction procedure. Standards were identified in plant extracts using retention time, *m/z* value, and characteristic product ion spectra. The estimated recoveries of phosphate standards were found to be approximately 70–80% using both extraction methods, which is satisfactory for a complex matrix (Fig. 5). The chloroform/methanol extraction method was chosen for further experiments because it is less laborious than the TCA/ether extraction method.

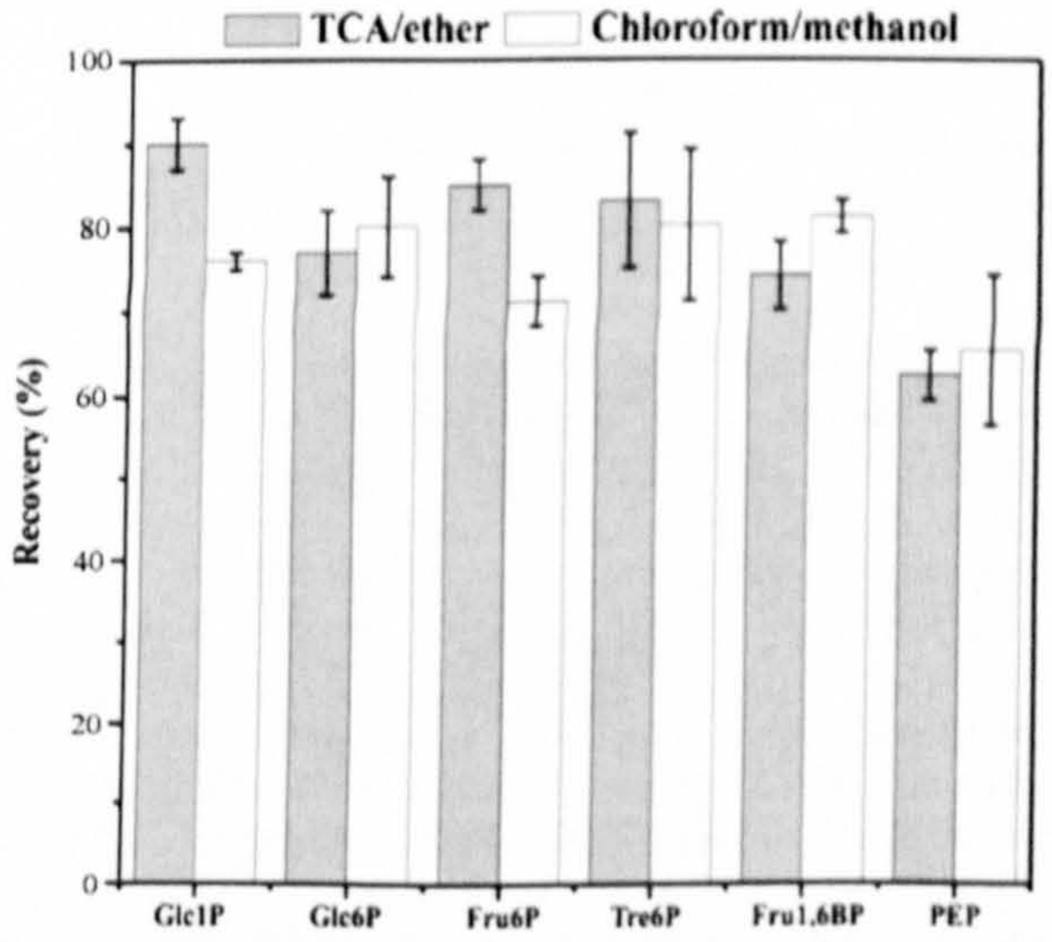

Fig. 5. Recoveries of different phosphate standards added to accurately weighed *Arabidopsis* Col-0 leaf extracts using two extraction methods: TCA/ether and chloroform/methanol. Values are mean ± SD ($n=3$ biological replicates, each containing leaves from three rosettes). Each biological replicate is the mean value of $n=3$–4 independent PGC-LC-ESI-MS measurements.

3.4. Analysis of metabolic intermediates from A. thaliana wild-type Col-0 and pgm1 plant extracts using PGC-LC-ESI-MS

The value of our on-line analytical PGC-LC-ESI-MS method for the analysis of our target compounds in complex biological samples was tested by applying it for the separation and identification of soluble sugars and sugar phosphates from *A. thaliana* plant tissue extracts.

The application of our on-line PGC-LC-ESI-MS method allowed the separation and identification of three metabolites in a single-run: Glc, Suc, and Glc6P from *Arabidopsis* Col-0 and *pgm1* leaf extracts. Metabolites were identified in plant extracts using retention time, *m/z* value, and characteristic product ion spectra of specific parent ions selected for fragmentation.

The presence of matrix-induced interferences in *Arabidopsis* leaf extracts was investigated using the standard addition method. Five-point standard addition curves were established for Glc, Suc, and Glc6P, and good linearity was shown for all compounds. By comparing the slopes obtained by linear regression using the standard addition method (data not shown) and the aqueous standard calibration (Table 1), the values for the gradients of the curves differed by less than 1%, demonstrating that no significant matrix-induced interferences were present in the *Arabidopsis* tissue extract. Therefore, Glc, Suc and Glc6P present in *Arabidopsis* Col-0 and *pgm1* leaf extracts were quantified by PGC-LC-ESI-MS using the aqueous standard calibration curves, using the ions at *m/z* 225 for Glc ($[M+HCOO]^-$), *m/z* 387 for Suc ($[M+HCOO]^-$), and *m/z* 259 for Glc6P ($[M-H]^-$) (Table 1). Fig. 6 shows the quantitative results obtained for *Arabidopsis* Col-0 and *pgm1* plants grown under a 16-h light/8-h dark photoperiod and harvested during the day at developmental stage 6.0 [34].

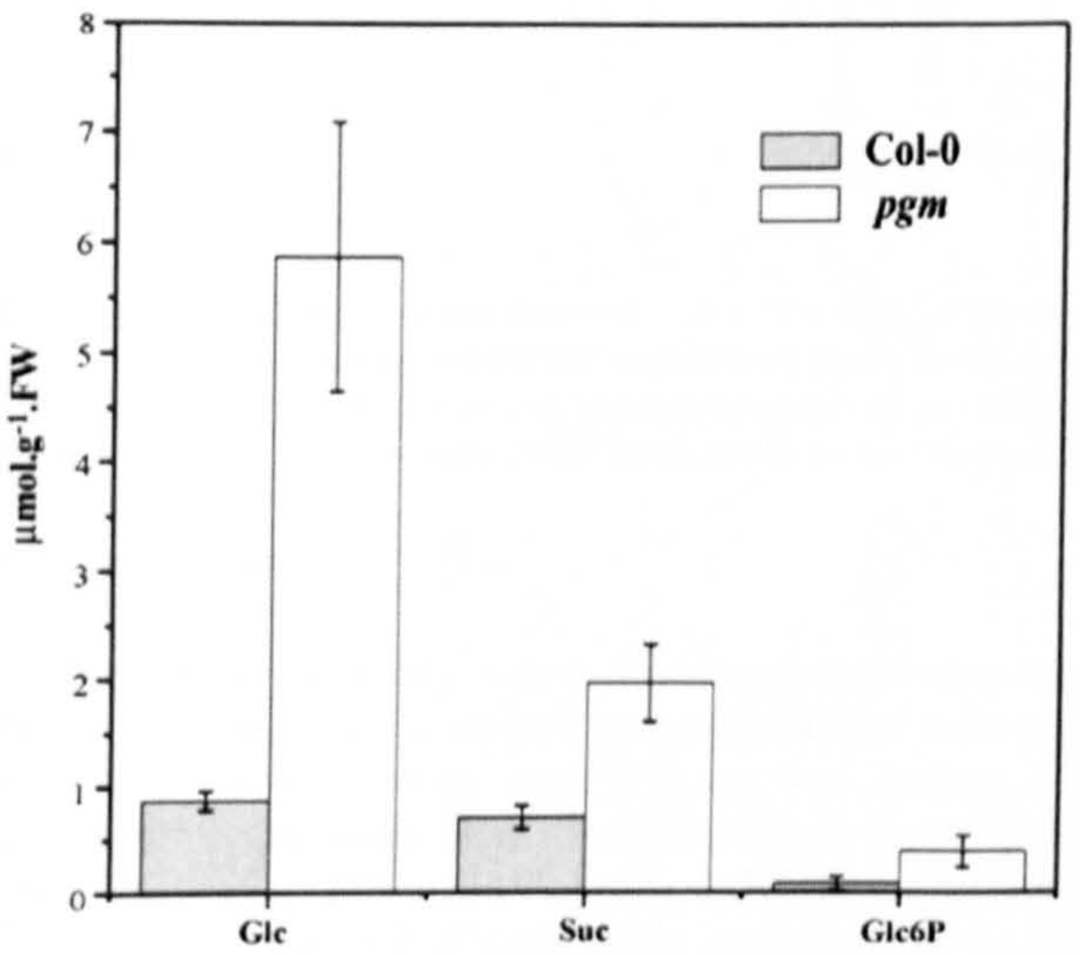

Fig. 6. Metabolite levels (Glc, Suc and Glc6P) determined in *Arabidopsis* Col-0 and *pgm1* chloroform/methanol leaf extracts using porous graphitic carbon (PGC) LC-ESI-MS. Plants were grown under a 16-h light/8-h dark photoperiod and harvested at developmental stage 6.0. Values are mean ± SD ($n = 3$ biological replicates, each containing leaves from three rosettes). Each biological replicate is the mean value of $n = 3$–4 independent PGC-LC-ESI-MS measurements. FW, fresh weight.

There are known to be significant differences in the amounts of extractable soluble sugars (Glc and Suc) between *Arabidopsis* WT and *pgm1* mutant plants, which are well characterised model organisms. In most studies, soluble sugars and glycolytic intermediates, including Glc6P, have been measured using enzymatic assays [38–40]. *Arabidopsis pgm1* plants are deficient in plastidic phosphoglucomutase (PGM) activity, an enzyme which catalyzes the interconversion of Glc6P and Glc1P. Plastidic PGM is essential for starch synthesis, and plants carrying the *pgm1* mutation are thus unable to synthesize starch [32,41]. As a result, *Arabidopsis pgm1* leaves accumulate high levels of soluble mono- and disaccharides during the light period.

Using our method, we determined levels of $5.87 \pm 1.22\ \mu mol\ g^{-1}$ of fresh weight (FW) for Glc and $1.97 \pm 0.36\ \mu mol\ g^{-1}$ FW for Suc in extracts of *Arabidopsis pgm1* leaves. The levels of soluble sugars found in wild-type Col-0 leaf extracts were much lower at $0.87 \pm 0.09\ \mu mol\ g^{-1}$ FW for Glc and $0.71 \pm 0.11\ \mu mol\ g^{-1}$ FW for Suc. In wild-type Col-0 leaves we found Glc6P levels of $0.11 \pm 0.01\ \mu mol\ g^{-1}$ FW, and in the starchless *pgm1* mutant of $0.31 \pm 0.04\ \mu mol\ g^{-1}$ FW.

3.5. Application to the analysis of metabolite level changes during the diurnal cycle in A. thaliana wild-type Col-0 and pgm1 in a 12-h light/12-h dark cycle

To further demonstrate the applicability of our on-line PGC-LC-ESI-MS method for the simultaneous quantitative analysis of Glc, Suc and Glc6P, we applied the method to quantitate the changes in the levels of these metabolites over the diurnal cycle in *Arabidopsis* Col-0 and *pgm1* plants grown in a 12-h light/12-h dark regime. Metabolite levels determined using our PGC-LC-ESI-MS method in wild-type Col-0 and *pgm1* chloroform/methanol extracts are shown in Fig. 7 for Glc (a), Suc (b), and Glc6P (c).

During the day, starch and sucrose are synthesized in wild-type *Arabidopsis* leaves as primary products of photosynthesis. During the night, starch is degraded providing carbohydrate supplies which are essential for the normal growth of the plant during the dark [42]. In contrast, wild-type *Arabidopsis* leaves accumulate much lower levels of Glc and Suc during the light period since these are converted to starch for storage. In *Arabidopsis pgm1* leaves, the levels of soluble sugars dramatically decrease during the dark period because these carbon supplies are being used for plant growth in the dark.

We have demonstrated that our method offers the very real advantage over traditional enzymatic assays of being able to simultaneously quantitate several targeted metabolites in a single extract of 10 mg of plant material, and in a single LC–MS separation that takes only 20 min.

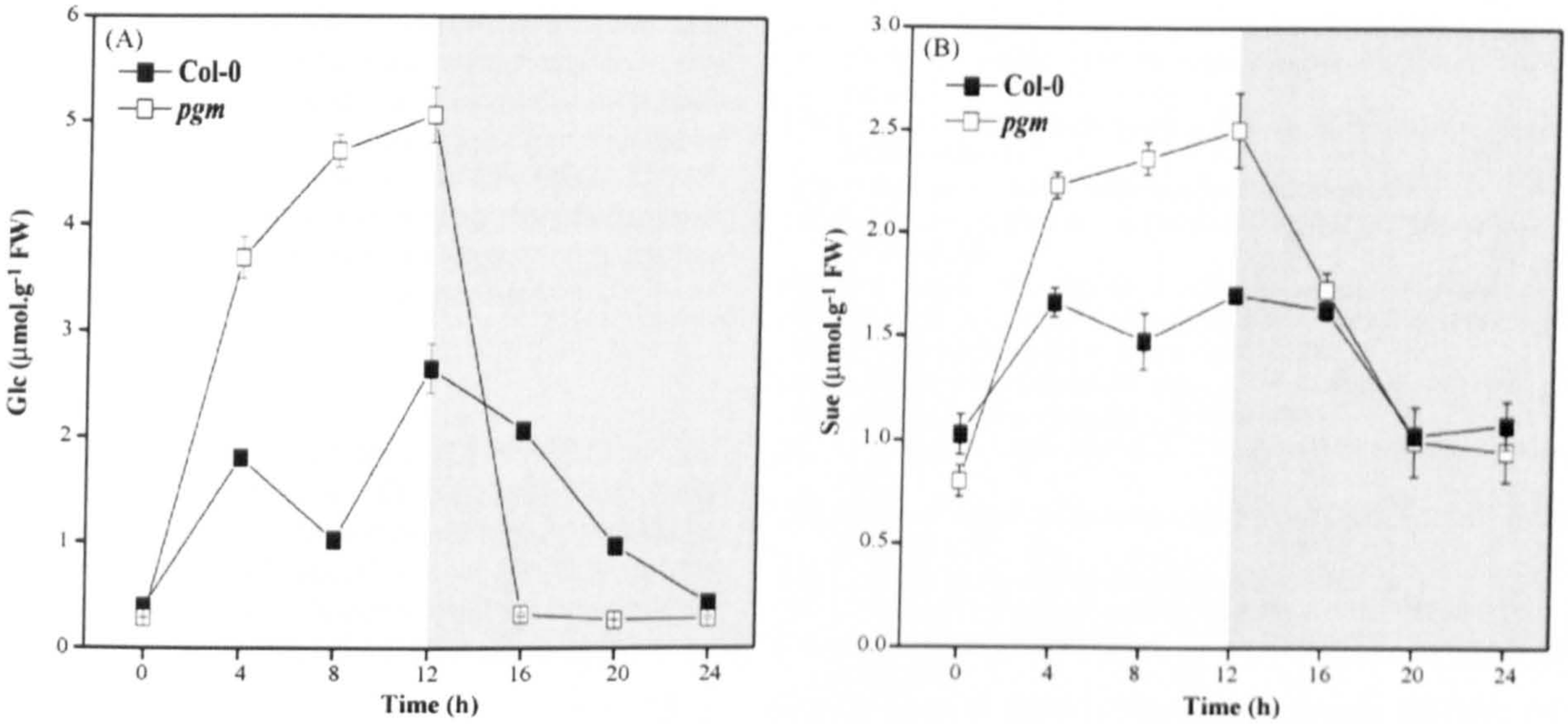

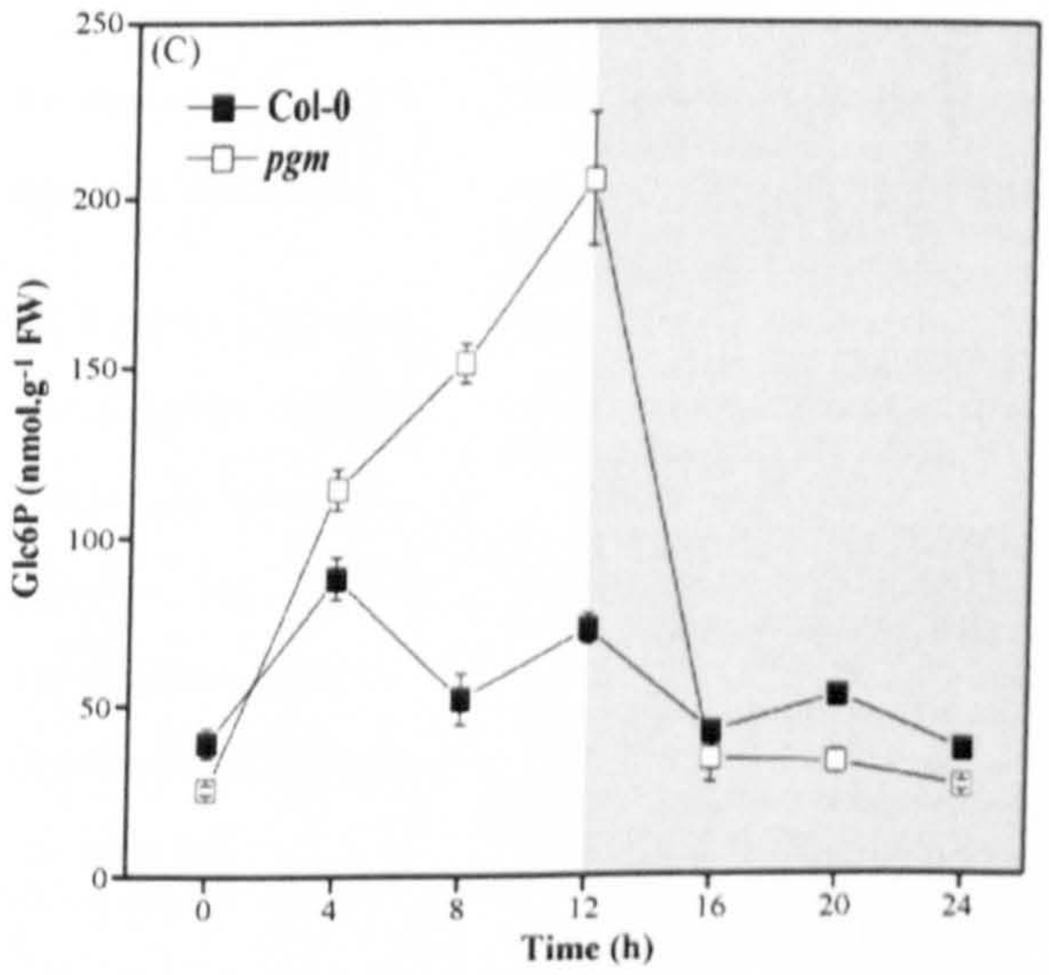

Fig. 7. Metabolite level changes observed over a 12-h light/12-h dark cycle in *A. thaliana* wild-type Col-0 (■) and *pgm1* (□) chloroform/methanol leaf extracts using porous graphitic carbon (PGC) LC-ESI-MS: (A) Glc, (B) Suc and (C) Glc6P. Rosettes were harvested at the end of the night, 4, 8, 12 h into the light period, 4, 8, and again 12 h into the dark period. Values are mean ± SD ($n = 3$ biological replicates, each containing leaves from three rosettes). Each biological replicate is the mean value of $n = 3$–4 independent PGC-LC-ESI-MS measurements. FW, fresh weight.

4. Conclusions

The aim of this study was to develop and optimise a robust HPLC system, using a porous graphitic carbon column, suitable for on-line coupling with ESI ion trap tandem MS for the separation and analysis of metabolic intermediates from plant tissues. In this paper, an LC–MS/MS method using a PGC column and an MS compatible mobile phase was developed and validated for the rapid separation (less than 20 min) and detection of a mixture of glycolytic intermediates, soluble sugars and sugar phosphate standards. It provides good linearity, selectivity, recovery, short analysis time, and LODs in the picomole range (2–40 pmol). We have demonstrated that our PGC-LC-ESI-MS/MS method is capable of separating, detecting and measuring in a single run soluble sugars (Glc, Suc) in the concentration range 0.26–6.0 µmol g^{-1} FW and sugar phosphates (Glc6P) in the concentration range 25–300 nmol g^{-1} FW from complex matrices such as *Arabidopsis* wild-type and *pgm1* plant tissue extracts. Lunn et al. [13] have recently reported a method using HPAEC coupled to a triple quadrupole MS operated in the highly selective multiple reaction monitoring mode, with a detection limit in the femtomole range for the measurement of trehalose-6-phosphate (Tre6P) in *A. thaliana*. Using this approach, Tre6P was measured at very low concentrations, ranging from 23 to 298 pmol g^{-1} FW in wild-type Col-0 rosette leaves, and 380 pmol g^{-1} FW in the *pgm* mutant. Although this triple quadrupole MS method offers better concentration sensitivity, and therefore lower limits of detection for specific,

targeted analytes, our method using an ion trap instrument offers a great potential to discover unknown compounds and other phosphorylated sugars in plant extracts by performing data-dependent MS/MS experiments, providing structure elucidation from a single sample analysis. Our new on-line PGC-LC–MS-based method using an ion trap instrument can be applied to other biological systems for the simultaneous separation, detection and quantitation of these metabolic intermediates.

Acknowledgements

The authors gratefully acknowledge the CHEMCELL project (Chemical Biology in Reactors and Cells), Marie Curie Early Stage Research Training at The University of York, Contract No. MEST-CT-2004-504345 for financial support. J.T.-O. gratefully acknowledges Thermo Finnigan's support and funding from the Analytical Chemistry Trust Fund, the RSC Analytical Division, and EPSRC.

References

[1] M. Stitt, R.M. Lilley, R. Gerhardt, H.W. Heldt, Methods Enzymol. 174 (1989) 518.
[2] Y. Gibon, H. Vigeolas, A. Tiessen, P. Geigenberger, M. Stitt, Plant J. 30 (2002) 221.
[3] R.R. Swezey, J. Chromatogr. B 669 (1995) 171.
[4] M. Bhattacharya, L. Fuhrman, A. Ingram, K.W. Nickerson, T. Conway, Anal. Biochem. 232 (1995) 98.
[5] E. Groussac, M. Ortiz, J. François, Enzyme Microb. Technol. 26 (2000) 715.
[6] H.P. Smits, A. Cohen, T. Buttler, J. Nielsen, L. Olsson, Anal. Biochem. 261 (1998) 36.
[7] S.M. de Bruijn, R.G. Visser, D. Vreugdenhil, Phytochem. Anal. 10 (1999) 107.
[8] Y. Sekiguchi, N. Mitsuhashi, Y. Inoue, H. Yagisawa, T. Mimura, J. Chromatogr. A 1039 (2004) 71.
[9] J.-P. Antignac, K. de Wasch, F. Monteau, H. De Brabander, F. Andre, B. Le Bizec, Anal. Chim. Acta 529 (2005) 129.
[10] L.L. Jessome, D.A. Volmer, LCGC North Am. 24 (2006) 498.
[11] W.M.A. Niessen, R.A.M. van der Hoeven, J. van der Greef, H.A. Schols, A.G.J. Voragen, J. Chromatogr. 647 (1993) 319.
[12] J.C. van Dam, M. Eman, J. Frank, H.C. Lange, G.W.K. van Dedem, S.J. Heijnen, Anal. Chim. Acta 460 (2002) 209.
[13] J.E. Lunn, R. Feil, J.H. Hendriks, Y. Gibon, R. Morcuende, D. Osuna, W.R. Scheible, P. Carillo, M.R. Hajirezaei, M. Stitt, Biochem. J. 397 (2006) 139.
[14] J. Feurle, H. Jomaa, M. Wilhelm, B. Gutsche, M. Herderich, J. Chromatogr. A 803 (1998) 111.
[15] V. Tolstikov, O. Fiehn, Anal. Biochem. 301 (2002) 298.
[16] V. Tolstikov, A. Lommen, K. Nakanishi, N. Tanaka, O. Fiehn, Anal. Chem. 75 (2003) 6737.
[17] M.T. Gilbert, J.H. Knox, B. Kaur, Chromatographia 16 (1982) 138.
[18] J.H. Knox, B. Kaur, G.R. Millward, J. Chromatogr. 352 (1986) 3.
[19] J.H. Knox, P. Ross, Adv. Chromatogr. 37 (1997) 73.
[20] C. Elfakir, P. Chaimbault, M. Dreux, J. Chromatogr. A 829 (1998) 193.
[21] C.K. Lim, Biomed. Chromatogr. 3 (1989) 92.
[22] J.-P. Mercier, P. Morin, M. Dreux, A. Tambuté, J. Chromatogr. A 849 (1999) 197.
[23] J. Xing, A. Apedo, A. Tymiak, N. Zhao, Rapid Commun. Mass Spectrom. 18 (2004) 1599.
[24] C. Elfakir, M. Dreux, J. Chromatogr. A 727 (1996) 71.
[25] K. Koizumi, Y. Okada, M. Fukuda, Carbohydr. Res. 215 (1991) 67.
[26] M.-C. Hennion, V. Coquart, S. Guenu, C. Sella, J. Chromatogr. A 712 (1995) 287.
[27] A. Buchholz, R. Takors, C. Wandrey, Anal. Biochem. 295 (2001) 129.
[28] Q.H. Wan, P.N. Shaw, M.C. Davies, D.A. Barrett, J. Chromatogr. A 697 (1995) 219.
[29] J.C. Reepmeyer, J.F. Brower, H. Ye, J. Chromatogr. A 1083 (2005) 42.
[30] S. Robinson, E. Bergstrom, M. Seymour, J. Thomas-Oates, Anal. Chem. 79 (2007) 2437.
[31] The Arabidopsis Genome Initiative, Nature 408 (2000) 796.
[32] T. Caspar, S.C. Huber, C. Somerville, Plant Physiol. 79 (1985) 11.
[33] T. Murashige, F. Skoog, Physiol. Plant. 15 (1962) 473.
[34] D.C. Boyes, A.M. Zayed, R. Ascenzi, A.J. McCaskill, N.E. Hoffman, K.R. Davis, Plant Cell 13 (2001) 1499.
[35] H. Weiner, M. Stitt, H.W. Heldt, Biochim. Biophys. Acta 893 (1987) 13.
[36] T. Jelitto, U. Sonnewald, L. Willmitzer, M. Hajirezeai, M. Stitt, Planta 188 (1992) 238.
[37] B. Domon, C.E. Costello, Glycoconjugate J. 5 (1988) 397.
[38] O.E. Bläsing, Y. Gibon, M. Günther, M. Höhne, R. Morcuende, D. Osuna, O. Thimm, B. Usadel, W.-R. Scheible, M. Stitt, Plant Cell 17 (2005) 3257.
[39] Y. Gibon, O.E. Bläsing, J. Hannemann, P. Carillo, M. Hohne, J.H. Hendriks, N. Palacios, J. Cross, J. Selbig, M. Stitt, Plant Cell 16 (2004) 3304.
[40] Y. Gibon, O.E. Bläsing, N. Palacios-Rojas, D. Pankovic, J.H. Hendriks, J. Fisahn, M. Hohne, M. Gunther, M. Stitt, Plant J. 39 (2004) 847.
[41] T. Caspar, T.-P. Lin, G. Kakefuda, L. Benbow, J. Preiss, C. Somerville, Plant Physiol. 95 (1991) 1181.
[42] S.C. Zeeman, S.M. Smith, A.M. Smith, Biochem. J. 401 (2007) 13.

Appendix II

Analysis of carbohydrates in *Lupinus albus* stems on imposition of water deficit, using porous graphitic carbon liquid chromatography-electrospray ionization mass spectrometry

Carla Antonio[a], Carla Pinheiro[b], Maria Manuela Chaves[b,c], Cândido Pinto Ricardo[b], Maria Fernanda Ortuño[b,d], and Jane Thomas-Oates[a]

[a] Department of Chemistry,
University of York,
UK

[b] Instituto de Tecnologia Química e Biológica (ITQB),
Oeiras, Portugal

[c] Instituto Superior de Agronomia (ISA),
Lisboa, Portugal

[d] Centro de Edafología y Biología Aplicada del Segura,
Murcia, Spain

Journal of Chromatography A, 1187 (2008) 111-118

Available online at www.sciencedirect.com
ScienceDirect
Journal of Chromatography A, 1187 (2008) 111–118
JOURNAL OF CHROMATOGRAPHY A
www.elsevier.com/locate/chroma

Analysis of carbohydrates in *Lupinus albus* stems on imposition of water deficit, using porous graphitic carbon liquid chromatography-electrospray ionization mass spectrometry

Carla Antonio [a], Carla Pinheiro [b], Maria Manuela Chaves [b,c], Cândido Pinto Ricardo [b], Maria Fernanda Ortuño [b,d], Jane Thomas-Oates [a,*]

[a] *Department of Chemistry, University of York, Heslington, York YO10 5DD, UK*
[b] *Instituto de Tecnologia Química e Biológica (ITQB), Av. Da República, Apartado 127, 2781-901 Oeiras, Portugal*
[c] *Instituto Superior de Agronomia (ISA), Universidade Técnica de Lisboa, Tapada da Ajuda, 1349-017 Lisboa, Portugal*
[d] *Centro de Edafología y Biología Aplicada del Segura, Campus Universitario de Espinardo, Apartado de Correos 164, Murcia E-30100, Spain*

Received 7 December 2007; received in revised form 25 January 2008; accepted 5 February 2008
Available online 8 February 2008

Abstract

This work reports the development and application of a negative ion mode online LC-ESI-MS method for studying the effect of water deficit on the carbohydrate content of *Lupinus albus* stems, using a porous graphitic carbon (PGC) stationary phase and an ion trap mass spectrometer. Using this method, separation and detection of several water soluble carbohydrates, ranging from mono-, di-, and oligosaccharides (raffinose, stachyose, and verbascose) to sugar alcohols was achieved in approximately 10 min. This on-line PGC-LC-ESI-MS method shows good linearity with correlation coefficients $R^2 > 0.99$, selectivity, short analysis time, and limits of detection (LOD) ranging from 0.4 to 9 pmol for sugars and 4–20 pmol for sugar alcohols. This PGC-LC-ESI-MS method is sensitive and allowed us to detect even small alterations in carbohydrate levels in *L. albus* stems that resulted from a mild/early water deficit (nmol g^{-1} DW). This paper describes details of our method and its application to the quantitative analysis of water soluble underivatised carbohydrates extracted from *L. albus* stem tissues that have been subjected to early and severe water deficit conditions, followed by a rewatering period.

Keywords: Carbohydrate; Water deficit; Early stress; Severe stress; Porous graphitic carbon; Mass spectrometry; *Lupinus albus*; Stem

1. Introduction

Lupinus albus L. is an important grain legume crop widely cultivated in intensive farming systems. Fully developed lupin grains are of great nutritional value and are widely used in diets of ruminants, primarily due to their unique carbohydrate properties, characterised by negligible levels of starch, and high levels of proteins [1]. Lupins are also cultivated for human consumption (high nutritional protein and oil contents) and as an environmentally friendly fertilizer; they increase the percentage of nitrogen, phosphorus, and organic matter in the soil, and therefore contribute to the improvement of water retention, and other soil characteristics [2].

L. albus is able to withstand water deficit (WD). It has been previously reported that it can survive severe drought conditions during both vegetative and reproductive growth [3,4]. When occurring during vegetative growth, WD affects several organs in different ways. Despite the loss of leaves, *L. albus* plants recover upon rewatering (RW), the stems being the fundamental structures that allow the plant to survive [3]. Furthermore, the metabolism of the two stem components (cortex and stele) was differently affected by WD, suggesting that these two components are important systems for studying the biochemical alterations that allow the plant to survive this stress.

It has been generally proposed that the alterations in the carbohydrate content of a plant under WD act as a metabolic signal to the plant's stress response system; carbohydrates (mainly soluble sugars and sugar alcohols) are also known to

* Corresponding author. Tel.: +44 1904 43 4459; fax: +44 1904 43 2516.
E-mail addresses: cipa500@york.ac.uk (C. Antonio), pinheiro@itqb.unl.pt (C. Pinheiro), mchaves@itqb.unl.pt (M.M. Chaves), ricardo@itqb.unl.pt (C.P. Ricardo), agr004@cebas.csic.es (M.F. Ortuño), jeto1@york.ac.uk (J. Thomas-Oates).

0021-9673/$ – see front matter © 2008 Elsevier B.V. All rights reserved.
doi:10.1016/j.chroma.2008.02.010

act as osmolytes during dehydration [5]. Although they are thus important analytes for understanding the biochemical processes underlying drought resistance, carbohydrates are difficult compounds to analyse due to their high polarity, poor UV absorbance, and the structural variety of isomeric structures. Highly polar compounds are poorly or completely unretained on reversed-phase columns and generally elute close to the void volume without chromatographic separation.

High performance anion-exchange liquid chromatography (HPAEC) with pulsed amperometric detection (PAD) has been used very often for the detection of carbohydrates, and commercial HPAEC-PAD systems are available from Dionex [6–8]. However, the mobile phases used with commercial HPAEC systems contain high concentrations of sodium hydroxide and sodium acetate, and therefore are not compatible with electrospray ionization mass spectrometry (ESI-MS). The high salt content in the samples suppresses ionization and causes capillary blockages and ion source contamination, thus compromising sensitivity [9,10]. To overcome this problem, post-column membrane suppressors were developed by Dionex that were designed to remove the salt from the mobile phase following separation [11]. Although the ion suppressor does desalt, it is not effective enough to make on-line coupling with ESI-MS routinely applicable.

Porous graphitic carbon (PGC) is an LC stationary phase developed by Knox and co-workers as an alternative to the commonly used reversed-phase (RP-) silica packings, and became commercially available in 1988 under the trade name Hypercarb™ [12,13]. The retention mechanism of PGC has been defined as the Polar Retention Effect on Graphite (PREG) [14] determined by a balance of two factors: (i) hydrophobic eluent–analyte repulsions, which occur between a hydrophilic eluent and any nonpolar segments of the analyte, (ii) the interaction of polarizable or polarized functional groups in the analyte with the graphite. PGC stationary phases have advantages over classical RP- and HPAEC columns of stability over the entire pH range, and the use of MS compatible mobile phases without the need for ion-pairing reagents, hence allowing efficient coupling with electrospray ionization. The use of PGC columns has been reported for the separation of mono-, di- and oligosaccharides [15,16], underivatised water soluble oligosaccharides extracted from *Triticum aestivum* stems [17], and more recently for the separation of water soluble sugars and sugar phosphates extracted from *Arabidopsis thaliana* leaves [18]. Here we report the application of a robust on-line LC-ESI-MS method using a PGC stationary phase and an ion trap instrument to follow the alterations in carbohydrate content of *L. albus* stems subjected to a gradual imposition of WD from the early phases to the most severe stress, followed by a rewatering (RW) period.

2. Experimental

2.1. Chemicals

Water and solvents used for chromatography were of HPLC grade and purchased from Fisher (Fisher Scientific, Loughborough, UK). All standards were purchased from Sigma (Poole, UK). Standard stock solutions were prepared in water at a concentration of 1.0 mg mL^{-1} and stored at −20 °C prior to use. Further dilutions were prepared in water.

2.2. Plant material

L. albus L. plants (cv. Rio Maior) were cultivated on a sterilised soil, peat, sand mixture (1:1:1, v/v) in controlled-environment growth chambers: photon flux density 290–320 μmol m^{-2} s^{-1} photosynthetically active radiation (PAR), photoperiod (12 h), temperature (19/25 °C, night/day) and relative humidity (65–70%). Twenty-three days after sowing, WD was induced by withholding watering (this caused a natural and slow induction of WD). Plants were collected 4 and 13 days after withholding water (DAW), and 6 and 26 h after rewatering (RW). Control plants were watered throughout the whole period. Sample collection took place 3–5 h after the beginning of the light period. The stem was cut at both extremities (cotyledon level and the shoot/root junction) to separate the vascular (stele) and cortical (cortex) tissues. A small vertical incision produced at the cotyledon extremity allowed the cortex to be peeled off the stele. As the separation occurred at the cambium level, the stele included both the parenchymatous pith tissue and the xylem while the cortex included parenchymatous tissue and the phloem. Stele and cortex tissues were immediately frozen in liquid nitrogen, lyophilised, and stored at −80 °C prior to extraction and LC-mass spectrometric analysis.

2.3. Characterisation of soil and plant water status

Soil water content (Ψ_{soil}) was measured with a ThetaProbe soil moisture sensor (ML2x ThetaProbe coupled with ThetaMeter type HH2 from Delta-T Devices). Leaf water potential was measured with a Sholander pressure chamber (PMS instrument Co, Corvallis, Oregon, USA) at predawn ($\Psi_{leaf\ pd}$). The relative water content (RWC) for leaflets, stems (cortex and stele) was determined according to Rodrigues et al. [19].

2.4. Extraction of water soluble carbohydrates from L. albus stems

Water soluble carbohydrates were extracted from *L. albus* stem tissues (cortex and stele) in chloroform/methanol [18]. Lyophilised stem material was finely ground in liquid nitrogen using a pre-cooled mortar and pestle. Approximately 10–12 mg plant material were transferred to a polypropylene microfuge tube (2.0 mL) containing 250 μL ice-cold chloroform:methanol (3:7, v/v), vortex-mixed, and the frozen mixture was incubated at −20 °C for 2 h to stop metabolism and extract water soluble metabolites. After incubation, 200 μL ice-cold water were added to the tube, and the tube was kept at 4 °C with continuous shaking. The samples were then centrifuged at 17,900 × *g*, at 4 °C, for 10 min. The upper phase was transferred to a new polypropylene microfuge tube (1.5 mL) and kept at 4 °C. The lower chloroform phase was re-extracted with 200 μL ice-cold water, centrifuged as described above, and the second upper phase was added to the first. The combined extract was evaporated to dryness using

a centrifugal concentrator (Savant SpeedVac system, Thermo Electron Corporation, Runcorn, UK). Samples were reconstituted in 100 μL water and centrifuged at 6800 × *g* at 20 °C for 30 min followed by liquid chromatography ion trap mass spectrometric analysis.

2.5. Liquid chromatography-ion trap mass spectrometry conditions

LC-MS analyses were performed on a Thermo Finnigan Surveyor HPLC system coupled to an ion trap mass spectrometer (LCQ DECA XP Plus, Thermo Electron, San Jose, CA, USA), equipped with a Thermo Finnigan orthogonal electrospray interface. Neutral carbohydrates were detected in the negative ion mode using the following MS parameters: ion source voltage −3.0 kV, capillary voltage −20 V, tube lens offset −60 V, capillary temperature 300 °C, sheath gas 40 (arbitrary units) and auxiliary gas 30 (arbitrary units). Mass spectra were acquired over the scan range *m/z* 50–1000, and data were processed using Xcalibur 1.3 software (Thermo Finnigan, San Jose, CA, USA). Precursor ions were selected with an isolation width of 2 Th and activated for 30 ms. Collision induced dissociation (CID) experiments used helium as the collision gas and normalised collision energy settings were in the range 20–30%, depending on the analyte. Chromatographic separation was carried out using a PGC Hypercarb™ column (5 μm, 100 mm × 4.6 mm; Thermo Electron, Runcorn, Cheshire, UK) at a flow rate of 600 μL min^{-1}. The sample injection volume was 20 μL and the PGC column was used at ambient temperature (25 °C). Two binary mobile phases were used during method development. Mobile phase 1 was composed of (A) water and (B) acetonitrile. Mobile phase 2 was composed of (A) water modified with 0.1% (v/v) of formic acid (FA) and (B) acetonitrile modified with 0.1% (v/v) of FA. The gradient elution profile was as follows: 0–5 min, 96% A + 4% B to 92% A + 8% B; 5–7 min, 92% A + 8% B to 75% A + 25% B, and maintained for 3 min, followed by column re-equilibration: 10–12 min, 75% A + 25% B to 50% A + 50% B, and maintained for 4 min; 16–18 min, 50% A + 50% B to 96% A + 4% B and maintained for 10 min.

3. Results and discussion

3.1. PGC-LC-ESI-MS method development

Separation of mono-, di-, and oligosaccharides on PGC columns have been reported by several different groups to be successful using mobile phases composed mainly of acetonitrile and water [15–18]. We therefore started by optimising our LC separation using mobile phases composed of different ratios of water:acetonitrile (mobile phase 1, details in Section 2) and making use of a solution containing a mixture of authentic standard neutral soluble sugars and sugar alcohols that are known to act as osmolytes in plants during dehydration.

The standard mixture was constituted in order to contain representatives of the main compound types: neutral monosaccharide glucose (Glc), neutral disaccharide sucrose (Suc), neutral trisaccharide (raffinose), neutral tetrasaccharide (stachyose), neutral pentasaccharide (verbascose), and the sugar alcohols mannitol (monosaccharide alcohol), and maltitol (disaccharide alcohol). This mixture was separated on a PGC column without derivatisation and all standard compounds were detected in the negative ion mode as formylated molecules

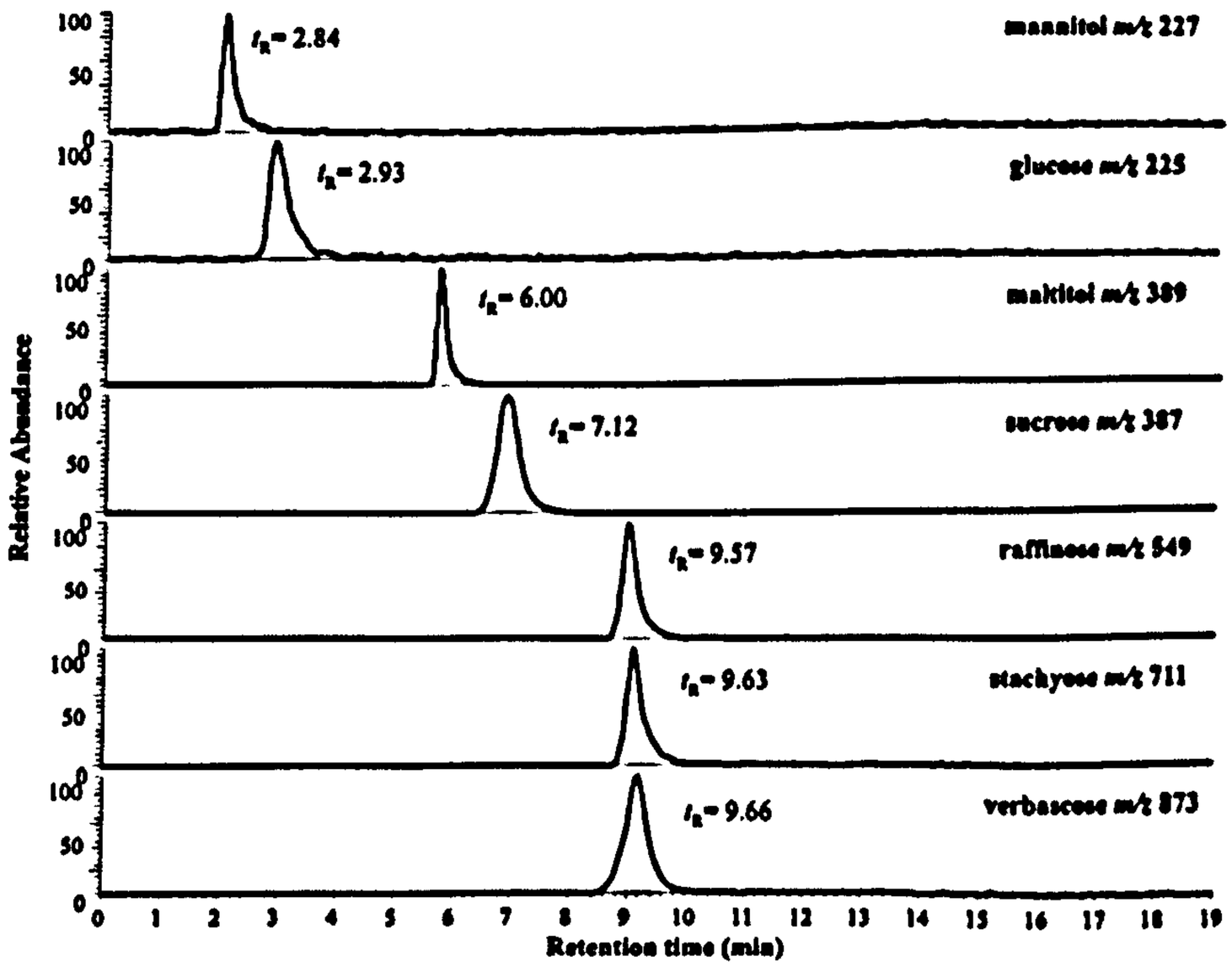

Fig. 1. Extracted ion chromatograms obtained using mobile phase 1 and porous graphitic carbon (PGC) negative ion mode ESI-MS for the separation of a standard mixture of neutral sugars and sugar alcohols (50 μg mL^{-1}). All compounds were detected as formylated molecules $[M + HCOO]^-$.

Table 1
Intra-day and inter-day repeatability of retention times, limits of detection (LOD), limits of quantification (LOQ), and linearity of calibration curves obtained for standard compounds using negative ion PGC-LC-ESI-MS

Standard compounds	Diagnostic ion (*m/z*)	t_R (min)	t_R (intra RSD)[a] (%, $n=3$)	t_R (inter RSD)[b] (%, $n=6$)	LOD[c] (μM)	LOQ[d] (μM)	Amount LOD[e] (pmol)	R^{2f}
Inositol	225 $[M+HCOO]^-$	2.44	0.47	1.48	0.60	2.00	12	0.9981
Mannitol	227 $[M+HCOO]^-$	2.84	0.54	0.96	1.00	3.33	20	0.9985
Fru	225 $[M+HCOO]^-$	2.86	0.68	0.77	2.00	6.70	40	0.9958
Glc	225 $[M+HCOO]^-$	2.93	0.20	1.15	0.45	1.60	9	0.9956
Sorbitol	227 $[M+HCOO]^-$	2.95	0.78	1.47	1.00	3.33	20	0.9989
Galactinol	387 $[M+HCOO]^-$	4.31	0.48	0.50	0.08	0.25	2	0.9958
Maltitol	389 $[M+HCOO]^-$	6.00	0.35	1.11	0.08	0.25	2	0.9991
Suc	387 $[M+HCOO]^-$	7.12	0.41	0.59	0.08	0.25	2	0.9995
Maltose	387 $[M+HCOO]^-$	8.34	0.37	0.71	0.08	0.25	2	0.9931
Raffinose	549 $[M+HCOO]^-$	9.57	0.12	0.50	0.10	0.33	2	0.9966
Stachyose	711 $[M+HCOO]^-$	9.63	0.21	0.41	0.06	0.20	1	0.9970
Verbascose	873 $[M+HCOO]^-$	9.66	0.26	0.42	0.02	0.07	0.4	0.9997

HPLC conditions: Mobile phase 1, Hypercarb PGC column (4.6 mm × 100 mm), 20 μL injection, flow rate 600 μL/min.
[a] Intra-day relative standard deviation (RSD) of retention times ($n=3$ independent measurements).
[b] Inter-day relative standard deviation (RSD) of retention times ($n=6$ independent measurements).
[c] Concentration limit of detection (LOD) calculated at a signal-to-noise ratio (S/N) of 3.
[d] Limit of quantification (LOQ) calculated at a signal-to-noise ratio (S/N) of 10.
[e] LOD of the amount loaded onto column calculated at a signal-to-noise ratio (S/N) of 3.
[f] Correlation coefficients for the standard curves (five points) of relative peak areas against concentration (0–100 μM). Each point on the standard curve is the mean value of 3 independent measurements.

$[M+HCOO]^-$ using electrospray ion trap mass spectrometry (Fig. 1).

Neutral carbohydrates were also observed to ionise as formylated molecules on direct infusion negative ion mode ESI analyses of standard solutions in methanol:water (50:50, v/v) (data not shown), thus showing their affinity for low levels of background formate anions present in the instrument.

In order to ensure that our data would be reproducible in other laboratories using other LC-systems (where formate anions may not be present in the background) we have tested the effect of addition of small amounts (0.1%) of formate to the mobile phase (mobile phase 2, details in Section 2). In this experiment, solvent (A) was water modified with 0.1% of formic acid and (B) acetonitrile modified with 0.1% of formic acid, to ensure that formate anions are present. The same standard mixture as in Fig. 1 was separated on the PGC column using mobile phase 2. We verified that the same elution profile was obtained as before (when no formic acid was present in the mobile phase), as well as that the retention times remained unchanged (all were the same within the standard deviation). We also determined the LODs for all the standard compounds listed in Table 1, and again verified that they were the same (within the standard deviation) as when using mobile phase 1.

Since in our hands good PGC-LC separation and identification of all standard compounds was achieved in approximately 10 min using a binary gradient composed of water and acetonitrile (without the need for addition of formate), we carried out the remainder of the experiments using mobile phase 1. Although raffinose ($t_R=9.57$ min), stachyose ($t_R=9.63$ min), and verbascose ($t_R=9.66$ min) elute very close together, since these compounds have different masses it was decided not to attempt to separate them further, as this would have required extending the gradient and thus the run time. Instead, we chose to make use of the conveniently short run time, by exploiting the ability to differentiate these compounds mass spectrometrically.

Following the optimisation of the LC separation, we have further developed this PGC-method by performing LC-tandem mass spectrometry experiments (MS^n) on the individual authentic standard compounds to record their retention times (t_R), mass-to-charge ratios (*m/z*) (Table 1) and their characteristic ion trap mass spectrometric fragmentation behaviour. Specific ions (formylated molecules $[M+HCOO]^-$, Table 1) were selected as precursors for fragmentation in order to collect MS^2 and MS^3 data. Galactinol ($t_R=4.31$ min), Suc ($t_R=7.12$ min) and maltose ($t_R=8.34$ min) are isomeric compounds detected at *m/z* 387 (formylated molecules $[M+HCOO]^-$, Table 1) and it is clear from their retention times that these are resolved using PGC.

To illustrate typical MS^n data obtainable using this PGC-based method, we describe experimental data for the non-reducing trisaccharide raffinose ($[M+HCOO]^-$ at *m/z* 549) (Fig. 2). Raffinose is a member of the raffinose family oligosaccharides (RFOs), which are non-reducing carbohydrates, consisting of galactose units linked to Suc via α-1,6 glycosidic linkages.

Fig. 2a illustrates the extracted ion chromatogram for raffinose at *m/z* 549 from the full scan negative ion ESI-MS, the extracted ion chromatogram for *m/z* 503 from the full scan product ion spectrum of *m/z* 549, and the extracted ion chromatogram for *m/z* 179 from the full scan product ion spectrum of *m/z* 503 (Fig. 2a). The collision induced dissociation (CID) MS^2 product ion spectrum of raffinose produced an intense ion at *m/z* 503 ($[M-H]^-$) corresponding to the loss of formic acid [HCOOH] (Fig. 2b). Subsequent CID MS^3 analysis, readily achieved using ion trap MS, of the $[M-H]^-$ ion at *m/z* 503 produced intense ions at *m/z* 341 and at *m/z* 179, which are formed by cleavage of the glycoside bond with the loss of one hexose $C_6H_{10}O_5$

(−162 Da), and the loss of two hexoses $C_6H_{10}O_5$ (−324 Da), respectively, and produced cross-ring fragment ions at *m/z* 221, 251, 281, and 311 which are formed by multiple neutral losses of CH_2O (−30 Da) (Fig. 2c).

3.2. Linearity and limits of detection (LOD) of the PGC-LC-ESI-MS method

The potential of the method for quantitative analysis of water soluble carbohydrates from stem tissues of *L. albus* was evaluated by testing intra and interday repeatability of retention times, and the linearity of response of the PGC-LC-ESI-MS method. Intraday repeatability was measured by injecting the same standard solution three times in a single day. Interday repeatability was measured by analysing the same standard solution over 6 different days. Intraday and interday repeatability of retention times using our method gave relative standard deviations (RSD) of less than 2% (Table 1). The linearity of the PGC-LC-ESI-MS response was measured for several analytes ranging from mono- to pentasaccharides and sugar alcohols by recording the responses at different concentrations over the range 0–100 μM. Five-point standard curves were obtained by plotting integrated peak areas versus concentration. Each point on the calibration curve is the mean value of three independent measurements using the PGC-LC-ESI-MS method. The limit of detection (LOD) for each compound was calculated as the min-

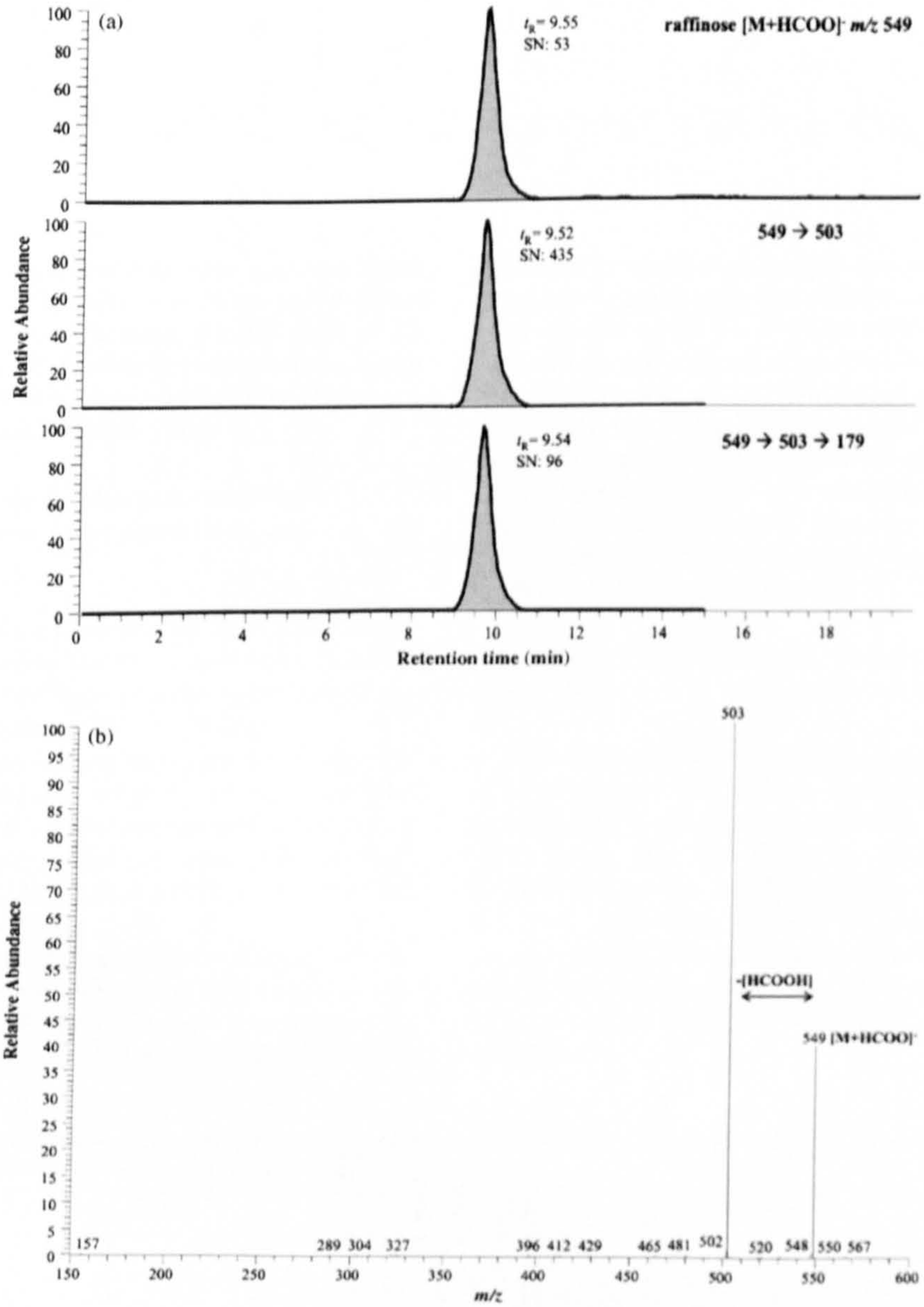

Fig. 2. (a) Extracted ion chromatograms obtained (mobile phase 1) on porous graphitic carbon (PGC) negative ion mode ESI-MS showing the specificity of detection provided by CID MS^n for a standard solution (10 μM) of raffinose, detected at *m/z* 549 ($[M + HCOO]^-$). (b) CID MS^2 spectrum of raffinose (precursor ion $[M + HCOO]^-$ at *m/z* 549). (c) CID MS^3 spectrum of raffinose (precursor ion $[M - H]^-$ at *m/z* 503).

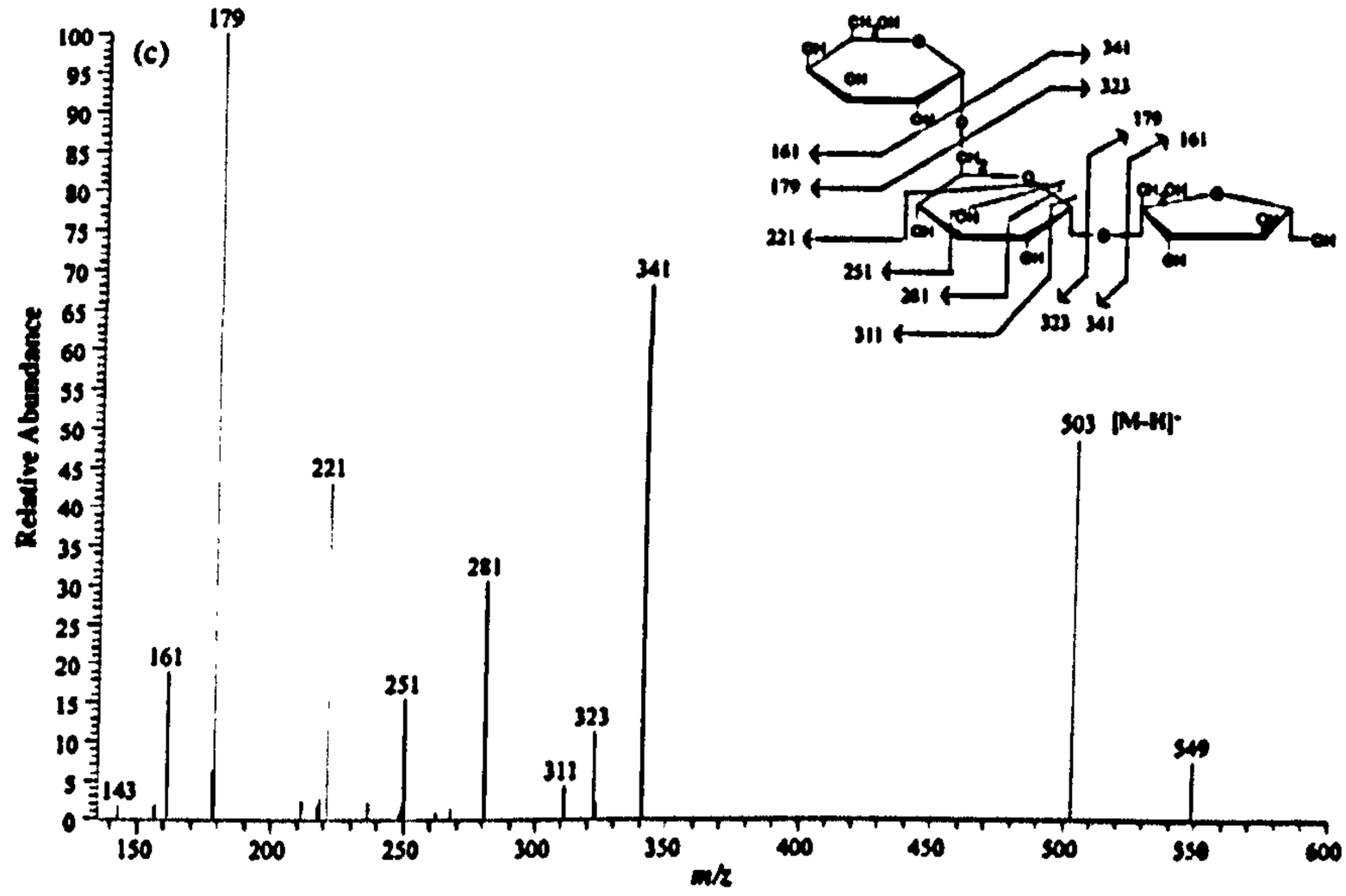

Fig. 2. (*Continued*).

imum amount injected which gave a detector response higher than three times the signal-to-noise ratio (S/N), and the limit of quantification (LOQ) was calculated at a S/N ratio of 10. The on-line PGC-LC-ESI-MS method showed good linearity of response over the concentration range 0–100 μM for all analytes, with correlation coefficients $R^2 > 0.99$ (Table 1).

3.3. Characterisation of the *L. albus* plant water status during early/mild and severe water deficit (WD), and recovery conditions

The characterisation of the *L. albus* plant water status during development and stress imposition was monitored by means of soil water content (Ψ_{soil}), leaf water potential at predawn (Ψ_{pd}), and relative tissue water content (RWC) (Table 2).

At 4 DAW, the soil water content had decreased by approximately 30–40% when compared to that of well watered (WW) control plants, but the plant water status was barely affected, as the leaf and stem RWCs decreased by only around 5%. Although there was a clear soil water shortage at 4 DAW the stress on the plant can be considered as mild.

At 13 DAW, the soil water content was extremely reduced (by approximately 80%) when compared to WW control plants, and this was significantly reflected in the plant water status: leaf Ψ_{pd} decreased by about 5-fold (down to −1.7 MPa), leaf RWC decreased by approximately 50%, and stem RWC decreased by around 15%. It was clear from these results that at 13 DAW the plant is under severe water deficit. However, the stem components (cortex and stele) were much less affected during the WD period than leaves, as they showed a higher capacity to retain water (only 15% reduction). It was also clear that *L. albus* can withstand severe WD, since upon rewatering (RW) the plant water status was rapidly restored (Table 2). In fact, 6 h after water reintroduction the RWC of leaves and stems was already restored and after 26 h of rewatering the plant water status was similar to that of the control plants.

3.4. PGC-LC-ESI-MS analysis of water soluble carbohydrates from *L. albus* stem extracts

The results described above (Section 3.3) indicate that two very distinct water deficit phases can be studied in *L. albus* plants corresponding to early stress (4 DAW), and severe stress (13 DAW), and it was shown [3,4] that the stems are fundamental systems that allow *L. albus* plants to survive such WD. We have, thus, applied our on-line PGC-LC-ESI-MS system as a sensitive method to study the effect of water deficit on the water soluble carbohydrate components of *L. albus* stem tissues (cortex and stele) at 4 DAW and 13 DAW, and 6 and 26 h after rewatering.

Table 2
Soil water potential (Ψ_{soil}), leaf water potential at pre-dawn (Ψ_{pd}) and leaf, stem stele and stem cortex relative water content (RWC) during the period of water deficit (WD) imposition and rewatering (RW). WW, well watered plants (control)

DAW	Ψ_{soil} (MPa)		$\Psi_{leaf\ pd}$ (MPa)		Leaf RWC (%)		Stem stele RWC (%)		Stem cortex RWC (%)	
	WW	WD	WW	WD	WW	WD	WW	WD	WW	WD
4 d	64 ± 1.1	35 ± 1.7	−0.23 ± 0.01	−0.28 ± 0.01	90 ± 1.7	87 ± 0.8	91 ± 1.0	92 ± 0.1	68 ± 4.6	64 ± 0.5
13 d	60 ± 8.0	12 ± 0.2	−0.33 ± 0.02	−1.74 ± 0.05	86 ± 2.7	46 ± 4.7	91 ± 0.5	77 ± 0.7	66 ± 3.7	55 ± 2.9
6 h RW	57 ± 3.1	48 ± 4.3	–	–	–	84 ± 2.1	–	91 ± 1.0	–	67 ± 0.3
26 h RW	49 ± 0.5	42 ± 3.2	−0.31 ± 0.03	−0.35 ± 0.04	88 ± 4.2	86 ± 1.7	94 ± 5.3	90 ± 3.0	67 ± 1.7	71 ± 0.3

The application of our on-line PGC-LC-ESI-MS method allowed the separation and identification in a single run of three water deficit responsive metabolites from *L. albus* stem extracts: the water soluble carbohydrates Glc, Suc, and raffinose. The presence of Glc, Suc, and raffinose in stem extracts was demonstrated based on the retention times, masses, and characteristic fragmentation patterns (MS^2 and MS^3) of peaks obtained on analysis of the stem extracts, and their comparison with those obtained for authentic standard compounds (Table 1). Glc, Suc, and raffinose were quantified by PGC-LC-ESI-MS using the calibration curves (Table 1), and the ions at *m/z* 225 for Glc ($[M+HCOO]^-$), *m/z* 387 for Suc ($[M+HCOO]^-$), and *m/z* 549 for raffinose ($[M+HCOO]^-$).

Fig. 3 shows the quantitative results obtained using PGC-LC-ESI-MS for *L. albus* stems (cortex and stele) at 4 DAW (early/mild stress), 13 DAW (severe stress), and subsequent rewatering (RW) for 6 and 26 h for Glc (Fig. 3A), Suc (Fig. 3B), and raffinose (Fig. 3C). Quantitative values for the control plants (well watered) at 4 and 13 days are also shown.

Using this PGC-LC-ESI-MS method, at 4 DAW (early stress) we determined levels of $2.58 \pm 0.32\ \mu mol\ g^{-1}$ of dry weight (DW) for Glc, $1.35 \pm 0.05\ \mu mol\ g^{-1}$ DW for Suc, and much lower levels of $9.34 \pm 1.00\ nmol\ g^{-1}$ DW for raffinose in stem cortex extracts of *L. albus*. In comparison with the early stress, a decrease in sugar amounts was observed at 13 DAW (severe stress) in stem cortex extracts of *L. albus*, with levels determined to be $1.14 \pm 0.08\ \mu mol\ g^{-1}$ DW for Glc, $1.12 \pm 0.03\ \mu mol\ g^{-1}$ DW for Suc, and $2.18 \pm 0.50\ nmol\ g^{-1}$ DW for raffinose. RW caused a subsequent decrease in the levels of Glc and Suc, but not raffinose.

In the stem stele extracts of *L. albus*, the levels of these water soluble carbohydrates were found to be much lower than those in the stem cortex; 4 DAW stele levels of $0.34 \pm 0.06\ \mu mol\ g^{-1}$ DW for Glc, and $0.16 \pm 0.05\ \mu mol\ g^{-1}$ DW for Suc were obtained (raffinose was not detected). In contrast to what is observed in stem cortex tissues, an increase in sugar amounts was observed at 13 DAW (severe stress) in stem stele extracts when compared to early stress, with levels of $0.49 \pm 0.05\ \mu mol\ g^{-1}$ DW for Glc, and $0.38 \pm 0.01\ \mu mol\ g^{-1}$ DW for Suc determined. RW caused the steady decrease of glucose and sucrose.

It was observed that *L. albus* stems accumulate water soluble sugars (Glc, Suc, and raffinose) during WD, and despite the small variations of the plant water status, or the small variations of the stem RWC (Table 2), WD causes large alterations in the carbohydrate content of *L. albus* stems both 4 DAW and 13 DAW. In addition, by using PGC coupled to ESI-MS, we could separate, identify, and detect very small amounts of raffinose ($nmol\ g^{-1}$ DW) in stem cortex tissues, which was found to be highly responsive to WD, reacting rapidly to small changes in the plant water status. Interestingly, its response is higher in early stress (when the plant water status is still largely unaffected) and on RW (when the plant water status is re-established).

Raffinose is a member of the raffinose family oligosaccharides (RFOs). It has been proposed that the primary roles of RFOs in seeds and vegetative tissues are to store and transport carbohydrates, and to function as osmoprotection molecules against abiotic stresses, such as drought, salinity or cold [20,21]. The accumulation of raffinose during seed maturation has also been associated with the development of desiccation tolerance in mature seeds [20,22].

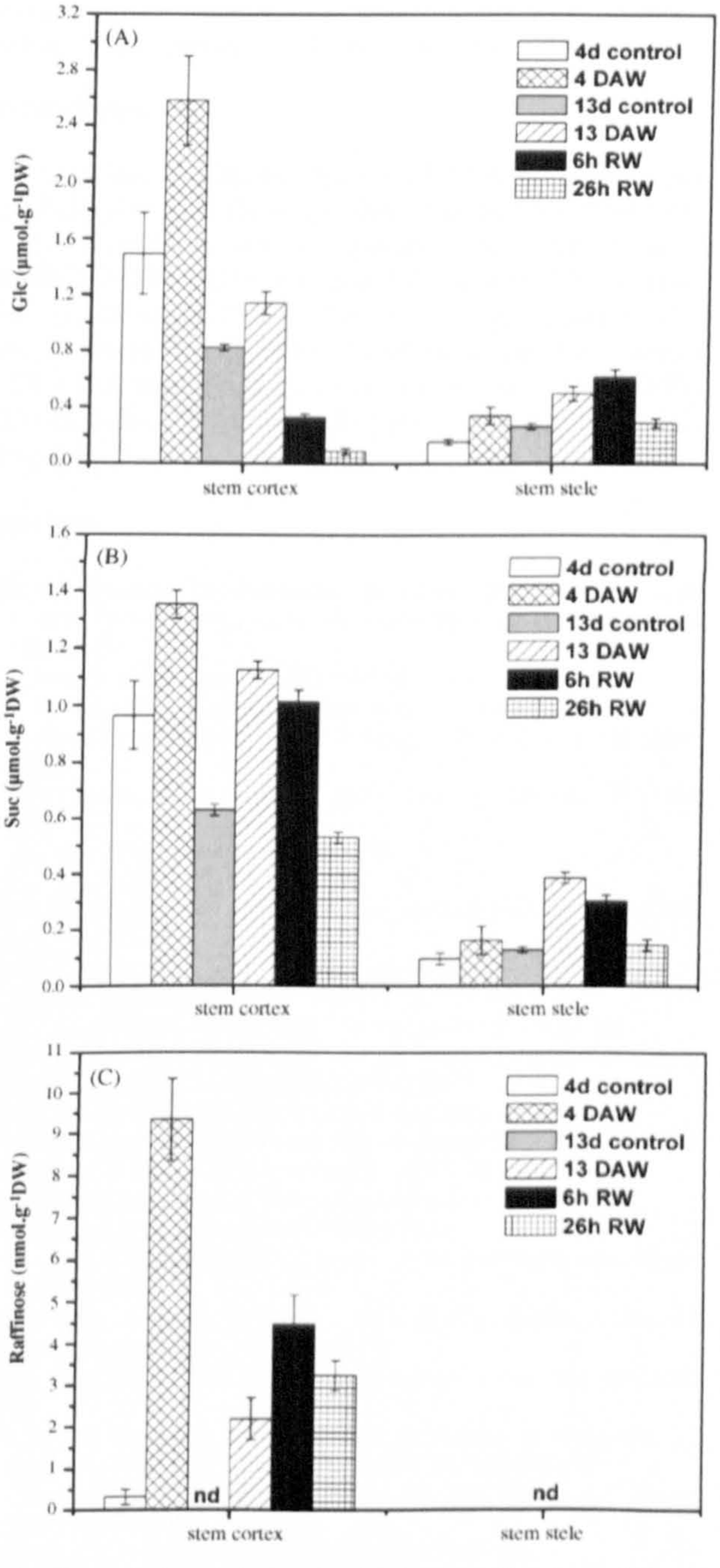

Fig. 3. Water soluble carbohydrate levels in *Lupinus albus* stems obtained by PGC-LC-ESI-MS at 4 days after withholding water (DAW; early water stress), 13 days after withholding water (severe water stress), 6 and 26 h after rewatering (RW). (A) Glucose, (B) sucrose, and (C) raffinose. Data are mean ± S.D. of $n = 2$–3 biological replicates. Each biological replicate is the mean value of $n = 2$–3 independent LC-MS measurements. DW, dry weight. Control, well watered plants.

The presence of raffinose has been previously detected in vegetative tissues of different plant systems exposed to WD (mainly using HPLC with refractive index detection or HPAEC-PAD). In coleus leaves, raffinose levels remained unchanged in response to WD, and were found to vary between 0.1 and 0.2 μmol g^{-1} FW [23]. In perennial ryegrass leaves, raffinose levels decreased in response to WD, leaf bases being less affected (from 0.7 to 0.2 μmol g^{-1} DW) than leaf blades (from 3.1 to 0.7 μmol g^{-1} DW) [24]. On the other hand, in *Arabidopsis thaliana* plants, raffinose was found to be highly responsive to progressive WD, accumulating up to 0.4 μmol g^{-1} FW [20], and a similar response was found recently in the leaves of the angiosperm resurrection plant *Xerophyta viscosa*, where raffinose accumulated up to 35 μmol g^{-1} DW [25].

In *L. albus* stem cortex tissues, not only did we determine much lower levels of raffinose (nmol g^{-1} DW) than those cited above for the leaves of other plants, but we also showed that raffinose does not increase steadily under progressive WD (i.e. a transient accumulation is observed between early and severe stress) which brings into question the role of raffinose in desiccation tolerance in stems. Taking into account that the stem cortex included parenchymatous tissue and the phloem, our results are in agreement with the hypothesis that raffinose is more effectively retained in the phloem leading to higher transport efficiency [26]. However, to our knowledge, transient accumulation of raffinose at such early stages in WD has never been reported. A further study of the effects of progressive WD in other lupin organs (leaves and roots) is underway in order to better understand the physiological role of raffinose in *L. albus* plants.

4. Conclusions

The aim of this study was to develop a robust LC-MS system using a porous graphitic carbon column, suitable for on-line coupling with ESI ion trap tandem MS, for the sensitive analysis of water soluble carbohydrates extracted from the stem tissues of *L. albus* plants subjected to early and severe water deficit conditions, followed by a rewatering period. We have demonstrated that this PGC-LC-based method is capable of separating, detecting and measuring in a single run, water soluble sugars (Glc, Suc and raffinose) in the concentration range 2.18 nmol g^{-1} DW to 2.58 μmol g^{-1} DW from *L. albus* stem tissue extracts.

Such an early stress study (4 d) requires a sensitive technique that can measure small amounts of water deficit responsive metabolites as well as tissue specific responses in *L. albus* stems, induced by a mild drought. This PGC-LC-ESI-MS method provides good linearity, selectivity, short analysis times (approximately 10 min), and LODs in the picomole range (0.4–20 pmol) for a wide variety of sugars and sugar alcohols. It combines the separation power of the LC system with ion trap MS that can perform multistage tandem MS, thus, providing useful structural identification of metabolites from a single sample analysis.

Acknowledgements

C.A. gratefully acknowledges the CHEMCELL Marie Curie Early Stage Research Training Fellowship of the European Community's Sixth Framework Programme under contract number MEST-CT-2004-504345 for financial support. J.T.-O. gratefully acknowledges Thermo Finnigan's support and funding from the Analytical Chemistry Trust Fund, the RSC Analytical Division, and EPSRC. C.P. acknowledges a grant SFRH/BPD/14535/2003 from Fundação para a Ciência e Tecnologia, Portugal.

References

[1] D.S. Petterson, in: J.S. Gladstones, C.A. Atkins, J. Hamblin (Eds.), Lupin as Crop Plants: Biology, Production and Utilization, CAB International, 1998, p. 353.
[2] C. Huyghe, Field Crops Res. 53 (1997) 147.
[3] C. Pinheiro, M.M. Chaves, C.P. Ricardo, J. Exp. Bot. 52 (2001) 1063.
[4] C. Pinheiro, J.A. Passarinho, C.P. Ricardo, J. Plant Physiol. 161 (2004) 1203.
[5] M.M. Chaves, J.P. Maroco, J.S. Pereira, Funct. Plant Biol. 30 (2003) 239.
[6] Y.C. Lee, Anal. Biochem. 189 (1990) 151.
[7] Y.C. Lee, J. Chromatogr. A 720 (1996) 137.
[8] R.R. Townsend, M.R. Hardy, Y.C. Lee, Methods Enzymol. 179 (1989) 65.
[9] J.-P. Antignac, K. de Wasch, F. Monteau, H. De Brabander, F. Andre, B. Le Bizec, Anal. Chim. Acta 529 (2005) 129.
[10] L.L. Jessome, D.A. Volmer, LCGC North America 24 (2006) 498.
[11] W.M.A. Niessen, R.A.M. van der Hoeven, J. van der Greef, H.A. Schols, A.G.J. Voragen, J. Chromatogr. 647 (1993) 319.
[12] M.T. Gilbert, J.H. Knox, B. Kaur, Chromatographia 16 (1982) 138.
[13] J.H. Knox, B. Kaur, G.R. Millward, J. Chromatogr. 352 (1986) 3.
[14] J.H. Knox, P. Ross, Adv. Chromatogr. 37 (1997) 73.
[15] K. Koizumi, Y. Okada, M. Fukuda, Carbohydr. Res. 215 (1991) 67.
[16] K. Koizumi, J. Chromatogr. A 720 (1996) 119.
[17] S. Robinson, E. Bergström, M. Seymour, J. Thomas-Oates, Anal. Chem. 79 (2007) 2437.
[18] C. Antonio, T. Larson, A. Gilday, I. Graham, E. Bergström, J. Thomas-Oates, J. Chromatogr. A 1172 (2007) 170.
[19] M.L. Rodrigues, C.M.A. Pacheco, M.M. Chaves, J. Exp. Bot. 46 (1995) 947.
[20] T. Taji, C. Ohsumi, S. Luchi, M. Seki, M. Kasuga, M. Kobayashi, K. Yamaguchi-Shinozaki, K. Shinozaki, Plant J. 29 (2002) 417.
[21] E. Zuther, K. Büchel, M. Hundertmark, M. Stitt, D.K. Hincha, A.G. Heyer, FEBS Lett. 576 (2004) 169.
[22] K.L. Koster, A.C. Leopold, Plant Physiol. 88 (1988) 829.
[23] W. Pattanagul, M.A. Madore, Plant Physiol. 121 (1999) 987.
[24] V. Amiard, A. Morvan-Bertrand, J.-P. Billard, C. Huault, F. Keller, M.-P. Prud'homme, Plant Physiol. 132 (2003) 2218.
[25] S. Peters, S.G. Mundree, J.A. Thomson, J.M. Farrant, F. Keller, J. Exp. Bot. 58 (2007) 1947.
[26] M.A. Hannah, E. Zuther, K. Buchel, A.G. Heyer, J. Exp. Bot. 57 (2006) 3801.

Appendix III

Hydrophilic interaction chromatography/electrospray mass spectrometry analysis of carbohydrate-related metabolites from *Arabidopsis thaliana* leaf tissue

Carla Antonio[a], Tony Larson[b], Alison Gilday[b], Ian Graham[b], Ed Bergström[a] and Jane Thomas-Oates[a]

[a] Department of Chemistry,
University of York,
UK

[b] Centre for Novel Agricultural Products,
Department of Biology,
University of York,
UK

Rapid Communications in Mass Spectrometry, 22 (2008) 1399-1407

RAPID COMMUNICATIONS IN MASS SPECTROMETRY
Rapid Commun. Mass Spectrom. 2008; 22: 1399–1407
Published online in Wiley InterScience (www.interscience.wiley.com) DOI: 10.1002/rcm.3519

Hydrophilic interaction chromatography/electrospray mass spectrometry analysis of carbohydrate-related metabolites from *Arabidopsis thaliana* leaf tissue

Carla Antonio[1], Tony Larson[2], Alison Gilday[2], Ian Graham[2], Ed Bergström[1] and Jane Thomas-Oates[1]*

[1]Department of Chemistry, University of York, Heslington, York YO10 5DD, UK
[2]Centre for Novel Agricultural Products, Department of Biology, University of York, York YO10 5YW, UK

Received 13 February 2008; Revised 29 February 2008; Accepted 3 March 2008

This work describes the development and application of an on-line liquid chromatography/mass spectrometry (LC/MS) method using hydrophilic interaction chromatography (HILIC) coupled to negative ion mode electrospray ionisation ion trap mass spectrometry (ESI-MS) for the analysis of highly polar carbohydrate-related metabolites commonly found in plants, ranging from reducing and non-reducing sugars and sugar alcohols to sugar phosphates. Using this method, separation and detection of a mixture of eight authentic standard compounds containing glucose (Glc), sucrose (Suc), raffinose, verbascose, mannitol, maltitol, glucose-6-phosphate (Glc6P) and trehalose-6-phosphate (Tre6P) were achieved in less than 15 min. The method is rapid, robust, selective, and sensitive, with limits of detection (LODs) ranging from 0.2 μM obtained for neutral sugars, to 1.0 μM obtained for sugar alcohols, and 2.0 μM obtained for negatively charged sugar phosphates. We have studied the negative ion collision-induced dissociation (CID) fragmentation behaviour of the non-reducing raffinose family oligosaccharides (RFOs) raffinose, stachyose, and verbascose. Mainly B_i and C_i glycosidic and A_i cross-ring structurally informative cleavages are observed. We have applied this HILIC/ESI-MS method for the analysis of *Arabidopsis thaliana* wild-type Columbia-0 (Col-0) and its starchless phosphoglucomutase mutant (*pgm1*) leaf extracts. The method was used to quantify Glc, Suc, raffinose, and Glc6P in *A. thaliana* extracts. Data obtained using this HILIC/ESI-MS method were compared with those obtained using a comparable porous graphitic carbon-based LC/ESI-MS method. Copyright © 2008 John Wiley & Sons, Ltd.

Studies of the plant metabolome include the analysis of a wide range of chemical species with diverse physical properties, from ionic inorganic compounds to biochemically derived hydrophilic carbohydrates, organic and amino acids, and a range of hydrophobic lipid-related compounds. This complexity poses huge challenges to the analytical technologies employed in current plant metabolomic programs, and powerful analytical tools are thus required for both the separation and characterisation of this extremely high compound diversity present in biological sample matrices.[1,2]

Mass spectrometry (MS) with electrospray ionisation (ESI) is a well-established technique used in plant metabolomic analysis.[3] The coupling of MS with on-line separations, typically liquid chromatography (LC) and gas chromatography (GC), allows the separation, detection and identification of a wide range of plant metabolites from a single sample analysis.[4–7] However, most published LC/MS applications use reversed-phase liquid chromatography (RP-LC), and highly polar metabolites, such as carbohydrates, sugar phosphates and intermediary metabolites, are poorly retained or completely unretained on these columns.[8] Such compounds are also difficult to analyse due to their poor volatility, instability, and the wide variety of isomeric structures which contain no UV chromophore.

High-performance anion-exchange chromatography (HPAEC) coupled to pulsed amperometric detection (PAD) has been a powerful technique for the analysis of polar compounds.[9–11] Nevertheless, this technique is not MS-compatible due to the high salt content used in the mobile phase. The high ionic strength suppresses sample ionisation, thus compromising sensitivity.[12,13] The use of post-column membrane suppressors that can remove some salt from the mobile phase[14] offers some improvement, but still does not provide robust direct coupling of HPAEC with on-line ESI-MS for the analysis of more than a few samples at a time.

*Correspondence to: J. Thomas-Oates, Department of Chemistry, University of York, Heslington, York YO10 5DD, UK.
E-mail: jeto1@york.ac.uk
Contract/grant sponsor: CHEMCELL Marie Curie Early Stage Research Training Fellowship of the European Community's Sixth Framework Programme; contract/grant number: MEST-CT-2004-504345.

RCM

Porous graphitic carbon (PGC) stationary phases have been developed as an alternative to RP columns for the analysis of polar compounds.[15–17] PGC columns use MS-friendly mobile phases, with no ion-pairing agents, and therefore enable efficient coupling with ESI-MS. PGC has been reported for the separation of carbohydrates in a wide range of applications,[18–21] and new PGC/ESI-MS methods have been recently reported for the separation of underivatised water-soluble oligosaccharides present in *Triticum aestivum* stems[22] and water-soluble sugars and sugar phosphates extracted from *Arabidopsis thaliana* leaves.[23] These methods offer the advantage of robust and rapid separations of carbohydrate compounds from plant tissues using MS-friendly eluents. However, elution of highly polar compounds often requires extensive method development and the inclusion of significant amounts of carboxylic acids (formic or acetic acid) in the mobile phase to provide anions (formate or acetate) for electronic interaction with the PGC surface, and thus to elute the more retained compounds. This has prompted us to investigate alternative column chemistries for these applications.

One suitable approach for the separation of very polar compounds is hydrophilic interaction chromatography (HILIC). HILIC columns contain a stationary phase that is hydrophilic, and the separation is achieved by partitioning of the analytes into this hydrophilic environment.[24,25] HILIC performance is orthogonal to RP-LC, and similar to that of normal-phase (NP)-LC, but the non-aqueous mobile phase used in NP-LC is replaced by an aqueous/organic mixture (typically acetonitrile in water or a volatile buffer) making this technique also well suited for on-line coupling with ESI-MS. HILIC coupled to ESI-MS has been reported for the analysis of food samples,[26] and the separation and quantitation of water-soluble metabolites extracted from *Escherichia coli*,[27] and it has recently been applied in metabonomic studies of urine.[28] In plant metabolomic studies, the use of HILIC/ESI-MS was introduced by Tolstikov and Fiehn[29] for the analysis of oligosaccharides and sugar nucleotides from *Cucurbita maxima* phloem tissues. In that study, sucrose, raffinose family oligosaccharides (RFOs), such as raffinose, stachyose, and verbascose, UDP-glucose, amino acids, and other larger oligosaccharides were detected using HILIC/ESI-MS. The method was used to quantify stachyose in C. *maxima* phloem tissues, and it was found to be present in the range 1–7 mM. Although these few studies have proven that HILIC/ESI-MS is an important tool for the analysis of polar compounds in complex mixtures, its potential for studying the plant metabolome needs to be further developed.

Here we report the development and application of an on-line HILIC method coupled to negative ion mode ion trap ESI-MS for the analysis of a range of hydrophilic compounds (neutral sugars, sugar alcohols, and sugar phosphates) commonly found in the plant metabolome, which are generally very difficult to retain on traditional RP-LC columns. The results obtained with this HILIC/ESI-MS method were compared with those obtained using a PGC/ESI-MS method recently reported for the separation of water-soluble sugars and sugar phosphates extracted from *A. thaliana* leaves.[23]

EXPERIMENTAL

Materials and chemicals

Authentic standard compounds, formic acid, and ammonium acetate were purchased from Sigma (Poole, UK). Water and all solvents used for extraction and chromatography were of HPLC grade and supplied by Fisher Scientific (Loughborough, UK).

Sample preparation

Standard stock solutions were prepared in water at a concentration of 1.0 mg mL^{-1} and stored at −20°C prior to use. Further dilutions were prepared in acetonitrile/water (50:50, v/v).

Plant material

Arabidopsis thaliana wild-type (WT) Columbia (Col-0) and starchless *pgm1* [30] mutant seeds were cold-treated at 4°C and imbibed in the dark for 4 days on plates with ½-strength Murashige and Skoog medium.[31] Plants were grown in controlled-environment growth chambers: photoperiod 16 h light/8 h dark, temperature 22/17°C, humidity 70/60% (day/night regime) and photosynthetic photon flux density (PPFD) of 150 μmol m^{-2} s^{-1}. *A. thaliana* rosettes were harvested at developmental growth stage 6.0,[32] quenched by immediately freezing in the light at liquid nitrogen temperature, and stored at −80°C prior to extraction and HILIC/MS analysis.

Extraction of polar metabolites from *A. thaliana* tissues

A. thaliana tissue extracts were prepared in chloroform/methanol from approximately 10–12 mg of frozen plant material as described by Antonio *et al.*[23] Tissue extracts were reconstituted in 100 μL acetonitrile/water (50:50, v/v), centrifuged for 30 min at 6800 *g* at 20°C, and filtered through a 0.2 μm PVDF membrane syringe filter (VWR International Ltd., Lutterworth, UK) into sample vials fitted with 100 μL inserts (Thermo Electron Corp., Runcorn, UK) for HILIC/MS analysis.

HILIC/MS conditions

HILIC/MS analyses were carried out on a ThermoFinnigan Surveyor HPLC system coupled to an ion trap mass spectrometer (LCQ DECA XP Plus™, now Thermo Scientific, San Jose, CA, USA), equipped with a ThermoFinnigan orthogonal electrospray interface. Chromatographic separation was performed on a zwitterionic ZIC®-HILIC stationary phase (3.5 μm, 150 mm × 2.1 mm i.d.; SeQuant, Umeå, Sweden). The flow rate was 200 μL/min, the sample injection volume was 0.5 μL, and the HILIC column was used at ambient temperature (25°C). The solution used for washing the autosampler syringe and injection needle was acetonitrile/water (95:5, v/v). Mobile phase A was composed of acetonitrile modified with 0.1% (v/v) formic acid (FA), and mobile phase B was composed of 5 mM ammonium acetate modified with 0.1% (v/v) FA (pH 4), adapted from Cubbon *et al.*[28] The gradient elution profile started with a linear increase from 10% B to 90% B in 19 min. The mobile phase was allowed to return to the starting conditions within 1 min,

DOI: 10.1002/rcm

followed by column re-equilibration for 10 min. The ion trap mass spectrometer was operated in the negative ion mode with the ion source voltage set to −3.0 kV, capillary voltage −20 V, tube lens offset −60 V, capillary temperature 300°C, sheath gas 40 (arbitrary units) and auxiliary gas 30 (arbitrary units). Mass spectra were acquired over the scan range *m/z* 50 to 1000. Precursor ions were selected with an isolation width of 2 *m/z* units and activated for 30 ms. Collision-induced dissociation (CID) experiments used helium as the collision gas and normalised collision energy settings were in the range 20–30%, depending on the compound. Data were processed using Xcalibur 1.3 software (ThermoFinnigan, now Thermo Scientific).

RESULTS AND DISCUSSION

HILIC/ESI-MS method development

Typical gradients used for HILIC consist of organic solvents (60–95%) in water or a volatile buffer, with acetonitrile being the most popular choice as it provides better retention of analytes than methanol.[24–27] Buffers used for HILIC are typically ammonium salts of acetate and formate (5–20 mM) due to their solubility at such high percentages of organic solvent. A suitable pH range for HILIC is 3–8.[33] In order to establish our HILIC separations, different solutions containing mixtures of authentic standards and a mobile phase composed of acetonitrile and 5 mM ammonium acetate, adjusted to pH 4 with the addition of 0.1% (v/v) of FA (adapted from Cubbon *et al.*[28]), were used as the starting point for our plant metabolomic applications.

The standard mixtures were constituted in order to contain representatives of different polar compound types commonly found in plants: soluble neutral sugars, sugar alcohols, and phosphorylated sugars. We started optimising our HILIC separation by using a standard mixture of soluble neutral sugars containing the monosaccharide glucose (Glc), disaccharide sucrose (Suc), trisaccharide (raffinose), tetrasaccharide (stachyose), and pentasaccharide (verbascose) (Fig. 1). Good separation, sharp peaks, and retention of all compounds were achieved using negative ion mode HILIC/ESI-MS. Neutral sugars were detected as formylated molecules $[M+HCOO]^-$ and the analytes were eluted in the order monosaccharide < disaccharide < trisaccharide < tetrasaccharide < pentasaccharide, with the more polar and hydrophilic compound (the pentasaccharide verbascose) being retained longest on the HILIC column.

In order to assess the suitability of this gradient method for the separation of other polar compounds, we tested the separation of a standard solution of sugar alcohols containing: mannitol (monosaccharide alcohol), maltitol and galactinol (disaccharide alcohols) plus *myo*-inositol (Fig. 2). Good separation and retention for all compounds were achieved using HILIC, and these alcohols were also detected as formylated molecules $[M+HCOO]^-$.

The same gradient conditions were then evaluated against a complex standard mixture containing representatives of

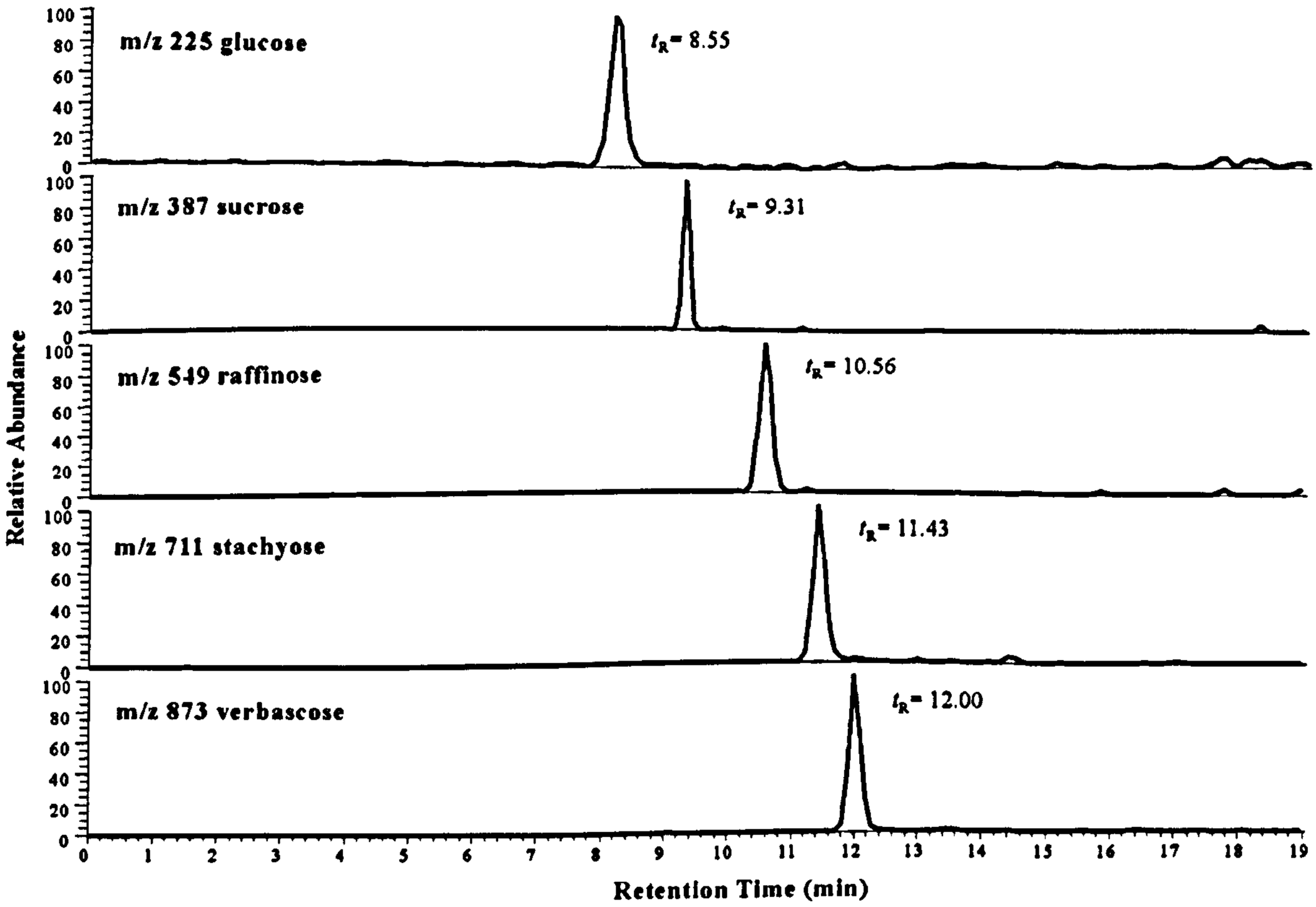

Figure 1. Extracted ion chromatograms obtained on HILIC/ESI-MS separation of a standard solution of neutral sugars (50 μM in each) detected as formylated molecules $[M+HCOO]^-$ by negative ion ESI-MS. HPLC conditions: ZIC®-HILIC column (3.5 μm, 150 mm × 2.1 mm i.d.), 200 μL.min^{-1}, 0.5 μL injection.

DOI: 10.1002/rcm

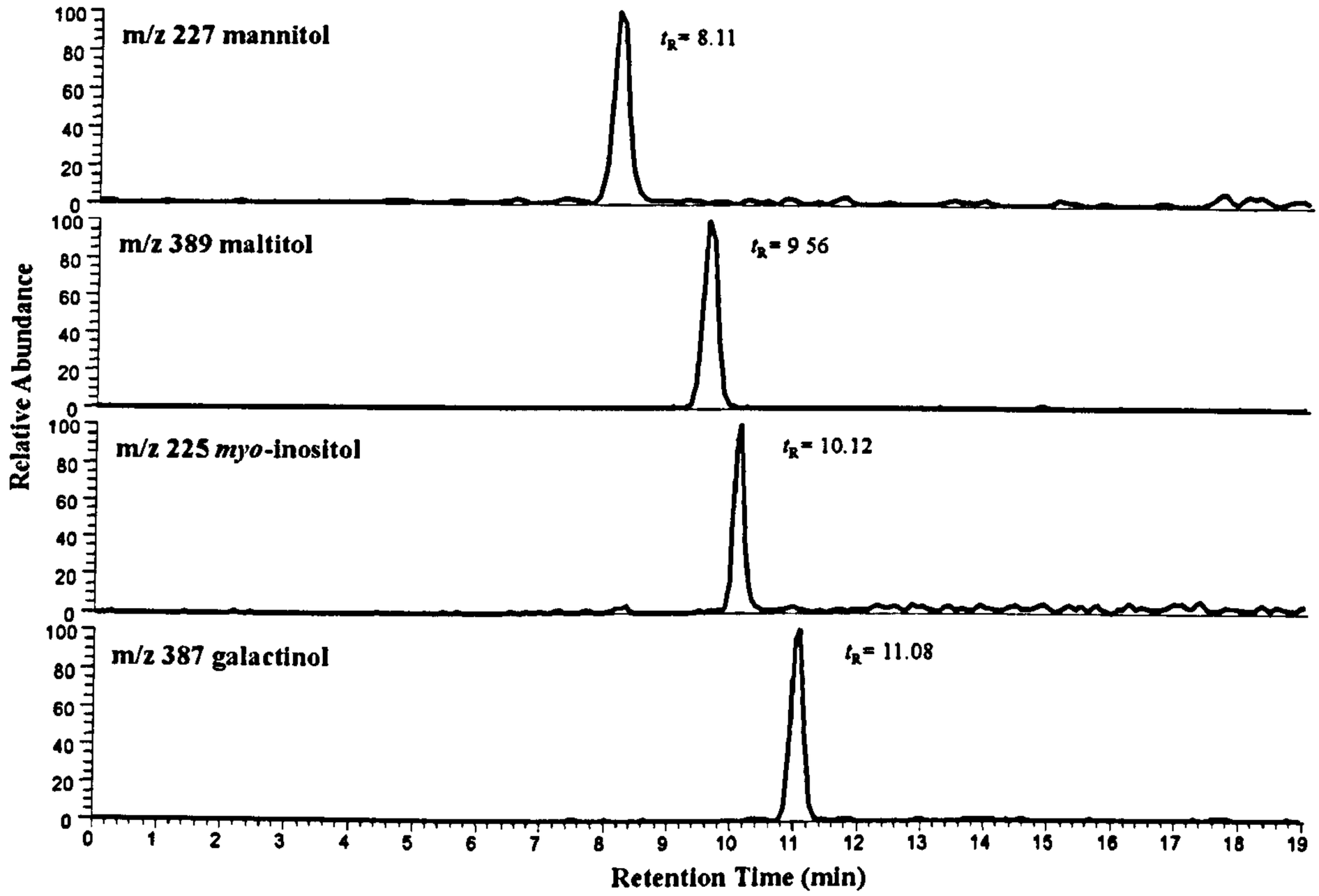

Figure 2. Extracted ion chromatograms obtained on HILIC/ESI-MS separation of a standard solution of sugar alcohols and *myo*-inositol (50 μM in each) detected as formylated molecules $[M+HCOO]^-$ by negative ion ESI-MS. HPLC conditions: ZIC®-HILIC column (3.5 μm, 150 mm × 2.1 mm i.d.), 200 $\mu L.min^{-1}$, 0.5 μL injection.

different polar compound types found in plants, ranging from neutral soluble sugars (Glc, Suc, raffinose and verbascose), to sugar alcohols (mannitol and maltitol), and negatively charged sugar phosphates, such as glucose-6-phosphate (Glc6P) (phosphorylated monosaccharide) and trehalose-6-phosphate (Tre6P) (phosphorylated disaccharide) (Fig. 3).

Figure 3 shows that the same mobile phase has also proven to be successful for the separation of a complex standard mixture containing a wide range of polar compounds; we have therefore used these experimental conditions for further experiments (details in the Experimental section).

HILIC was also tested for the separation of isomeric compounds. Figure 4 depicts the extracted ion chromatograms obtained using negative ion mode HILIC/ESI-MS of different standard solutions (50 μM in each) containing the isomeric disaccharides Suc and trehalose (Tre), detected as formylated molecules $[M+HCOO]^-$ at *m/z* 387 (Fig. 4(a)), the isomeric monosaccharide phosphates glucose-1-phosphate (Glc1P) and Glc6P, detected as deprotonated molecules $[M-H]^-$ at *m/z* 259 (Fig. 4(b)), and the isomeric disaccharide phosphates sucrose-6-phosphate (Suc6P) and Tre6P, detected as deprotonated molecules $[M-H]^-$ at *m/z* 421 (Fig. 4(c)).

Using HILIC/ESI-MS, satisfactory chromatographic separation was achieved for these isomeric compounds, and identification and differentiation are possible based on their retention times. Moreover, under the same HILIC/ESI-MS conditions, the product ion spectra of deprotonated Glc1P and Glc6P are different and show characteristic product ions that can also be used for unambiguous identification.[23,34]

Better chromatographic separation of the isomeric disaccharides Suc and Tre was recently reported using a porous graphitic carbon (PGC)/ESI-MS method;[23] however, the isomeric phosphorylated sugars Glc1P/Glc6P and Suc6P/Tre6P could not be resolved using PGC/ESI-MS. Using this HILIC/ESI-MS method, better chromatographic separation was achieved for these isomeric phosphorylated compounds, without the need for extensive method development or the inclusion of high concentrations of formic acid.

Negative ion CID behaviour of non-reducing RFOs using HILIC/ESI-MS^n

LC/tandem mass spectrometry (MS^n) of authentic standard compounds was performed to record their retention times (t_R) (Table 1) and their characteristic mass spectrometric fragmentation behaviour.

RFOs are non-reducing sugars widely distributed in the plant kingdom, and consist of galactose (Gal) units linked to the glucose moiety of sucrose via α-(1→6) glycosidic linkages. Scheme 1 represents the structure of these carbohydrates showing the nomenclature for carbohydrate fragmentation of Domon and Costello.[35] In the case of these non-reducing glycans, the galactose-containing portion of the molecule is taken as the classical non-reducing terminus, so that its B ion fragments are labelled sequentially from B_1; the 'reducing' terminus is thus attributed to the fructose residue of the sucrose moiety, and its fragments are thus labelled B_n and Y_1, respectively (this extension of the Domon and Costello nomenclature was proposed by B. Domon, personal communication).

DOI: 10.1002/rcm

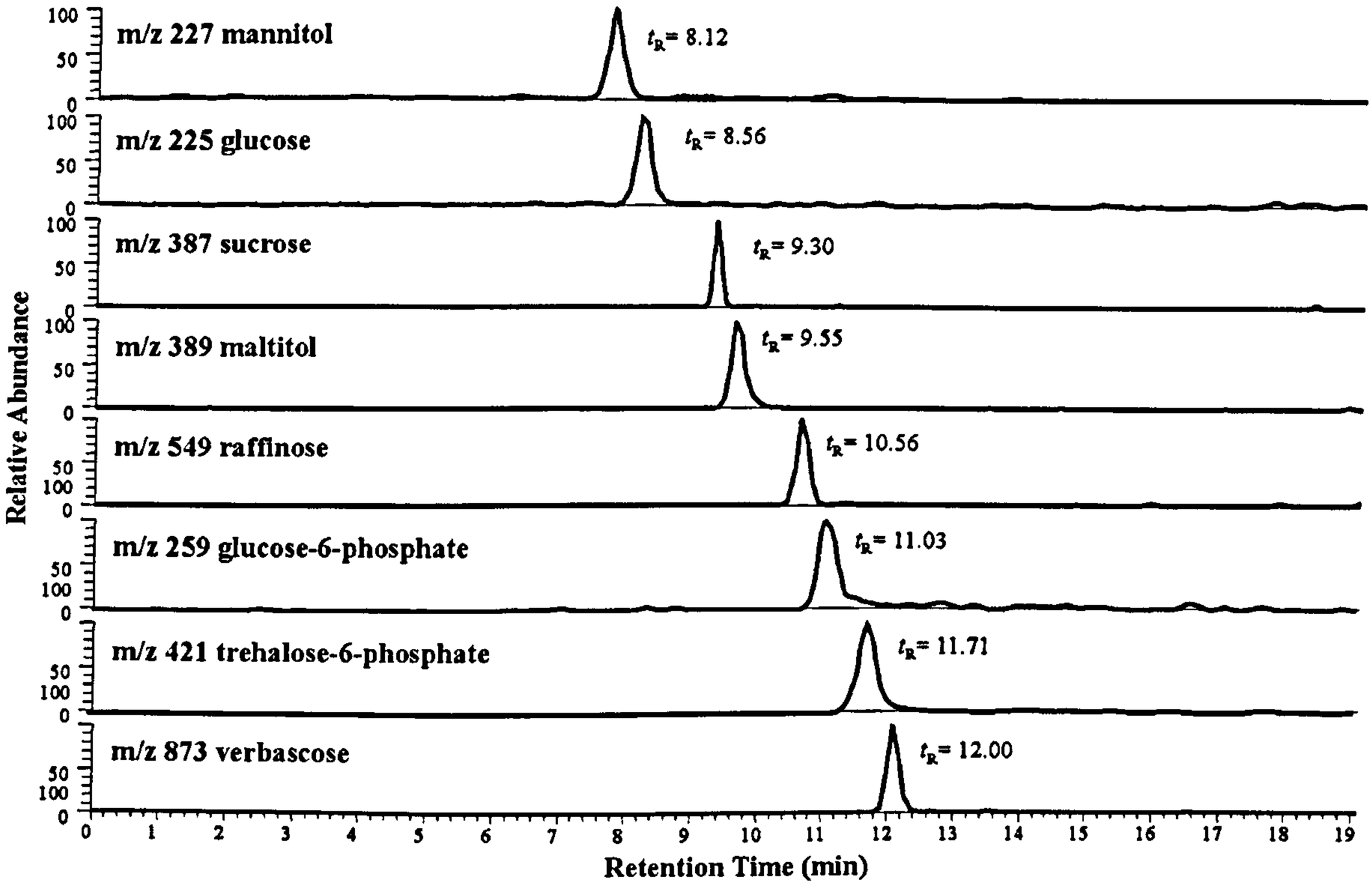

Figure 3. Extracted ion chromatograms obtained on HILIC/ESI-MS separation of a standard solution containing 50 μM neutral sugars (formylated molecules $[M+HCOO]^-$), sugar alcohols (formylated molecules $[M+HCOO]^-$), and sugar phosphates (deprotonated molecules $[M-H]^-$) by negative ion ESI-MS. HPLC conditions: ZIC®-HILIC column (3.5 μm, 150 mm × 2.1 mm i.d.), 200 μL.min^{-1}, 0.5 μL injection.

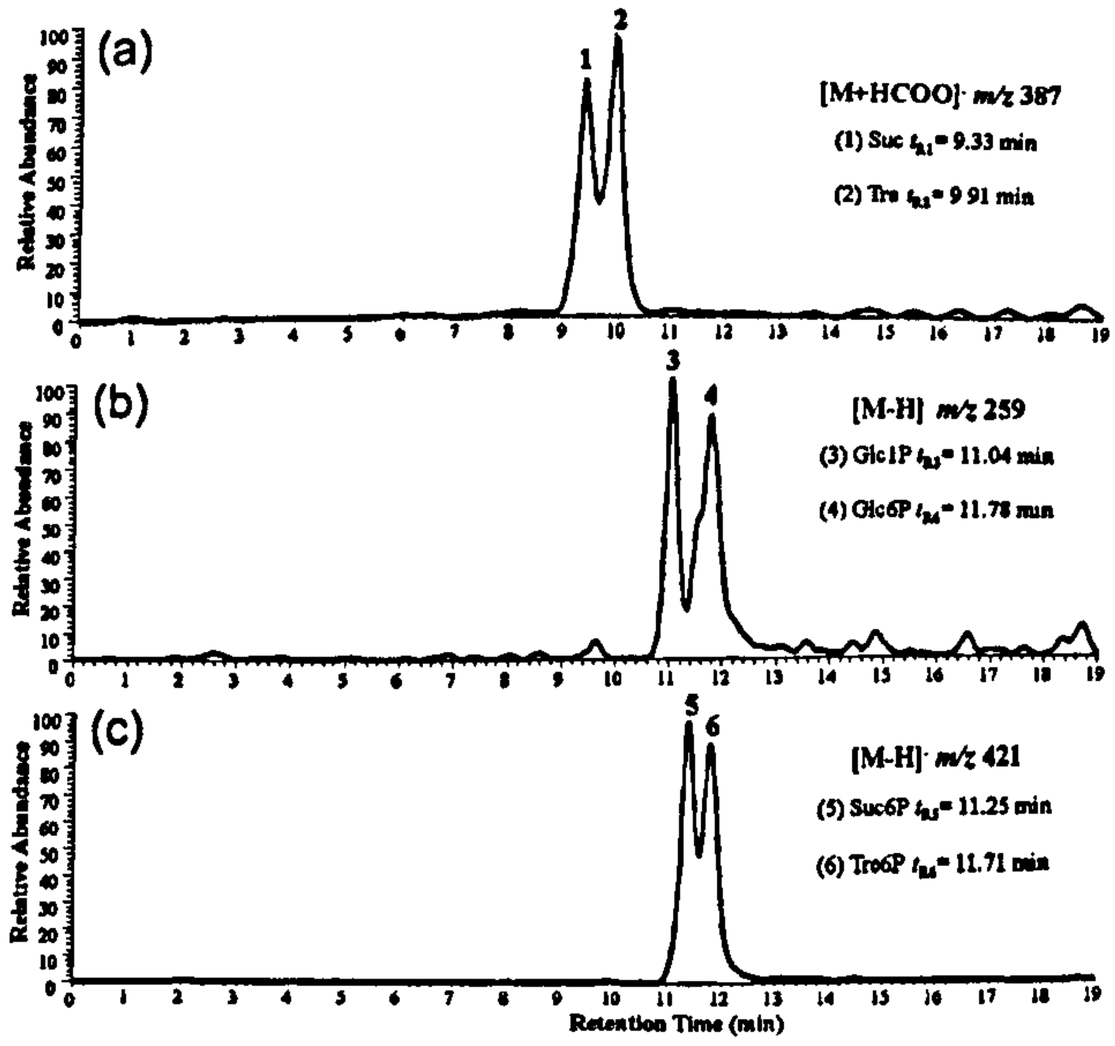

Figure 4. Extracted ion chromatograms obtained on HILIC/ESI-MS separation of different standard solutions (50 μM in each) containing (a) isomeric disaccharides Suc t_{R1} = 9.33 min and Tre t_{R2} = 9.91 min; (b) isomeric monosaccharide phosphates Glc1P t_{R3} = 11.04 min and Glc6P t_{R4} = 11.78 min; (c) isomeric disaccharide phosphates Suc6P t_{R5} = 11.25 min and Tre6P t_{R6} = 11.71 min. HPLC conditions: ZIC®-HILIC column (3.5 μm, 150 mm × 2.1 mm i.d.), 200 μL.min^{-1}, 0.5 μL injection.

The negative ion CID MS^2 product ion spectrum of the formylated trisaccharide raffinose (*m/z* 549 $[M+HCOO]^-$) produced an abundant ion at *m/z* 503 $[M-H]^-$, formed by the loss of formic acid. Subsequent CID MS^3 analysis of the $[M-H]^-$ ion at *m/z* 503 produced characteristic mass spectrometric fragmentation. However, negative ion CID MS^2 analysis of the formylated tetrasaccharide stachyose (*m/z* 711 $[M+HCOO]^-$) and pentasaccharide verbascose (*m/z* 873 $[M+HCOO]^-$) did not produce product ions, even when the normalised collision energy was varied between 30 and 40%, presumably because their formylated molecules $[M+HCOO]^-$ are very stable. For this reason, CID MS^2 analysis of these carbohydrates was obtained using the low-abundance $[M-H]^-$ ions at *m/z* 665 for stachyose and *m/z* 827 for verbascose as precursor ions. Figure 5 illustrates the CID fragmentation obtained using negative ion HILIC/ESI-MS^n for raffinose (Fig. 5(a)), stachyose (Fig. 5(b)), and verbascose (Fig. 5(c)).

Negative ion CID fragmentation of non-reducing sugars gave predominantly two different product ion types, which, according to the nomenclature for carbohydrate fragmentation of Domon and Costello,[35] are formed by: (i) glycosidic bond cleavages to give C_i and B_i ions, and (ii) multiple neutral losses of $(CH_2O)_n$, where $n = 2$, 3, or 4, to give cross-ring cleavage A_i ions.

CID MS^3 analysis of the deprotonated trisaccharide raffinose (*m/z* 503 $[M-H]^-$) produced abundant ions at *m/z* 341 and 179 which correspond to C_2 and C_1 ions formed by the loss of one and two hexose moieties, respectively, and

DOI: 10.1002/rcm

Table 1. Retention times, and nominal *m/z* values, intra-day and inter-day repeatabilities of retention times, LOD, and LOQ obtained for *myo*-inositol, sugars, sugar alcohols, and sugar phosphate standard compounds using negative ion ZIC®-HILIC/ESI-MS

Standard compounds	Diagnostic ion (*m/z*)	t_R (min)	t_R (intra RSD)[a] (%, n = 3)	t_R (inter RSD)[b] (%, n = 5)	LOD[c] (μM)	LOQ[d] (μM)	Amout LOD[e] (pmol)
myo-inositol	225 $[M+HCOO]^-$	10.08	1.00	1.25	1.0	3.0	0.5
Sugars:							
Fru	225 $[M+HCOO]^-$	7.50	1.53	1.93	1.0	3.0	0.5
Glc	225 $[M+HCOO]^-$	8.55	0.95	1.15	1.0	3.0	0.5
Suc	387 $[M+HCOO]^-$	9.33	0.70	1.12	0.2	0.7	0.1
Tre	387 $[M+HCOO]^-$	9.93	1.43	1.78	0.2	0.7	0.1
Raffinose	549 $[M+HCOO]^-$	10.55	0.70	1.67	0.2	0.7	0.1
Stachyose	711 $[M+HCOO]^-$	11.44	1.46	1.89	0.2	0.7	0.1
Verbascose	873 $[M+HCOO]^-$	12.01	1.00	1.12	0.2	0.7	0.1
Sugar alcohols:							
Sorbitol	227 $[M+HCOO]^-$	8.00	1.00	1.72	1.0	3.0	0.5
Mannitol	227 $[M+HCOO]^-$	8.11	0.82	1.58	1.0	3.0	0.5
Maltitol	389 $[M+HCOO]^-$	9.55	1.53	1.94	1.0	3.0	0.5
Galactinol	387 $[M+HCOO]^-$	11.04	0.87	1.65	1.0	3.0	0.5
Sugar phosphates:							
Glc1P	259 $[M-H]^-$	11.03	1.00	1.12	2.0	6.7	1.0
Fru6P	259 $[M-H]^-$	11.09	0.58	1.11	2.0	6.7	1.0
Suc6P	421 $[M-H]^-$	11.28	0.58	1.73	1.0	3.0	0.5
Tre6P	421 $[M-H]^-$	11.69	1.15	1.83	1.0	3.0	0.5
Glc6P	259 $[M-H]^-$	11.81	0.58	0.95	2.0	6.7	1.0
Fru1,6BP	339 $[M-H]^-$	13.73	0.94	1.92	2.0	6.7	1.0

HPLC conditions: ZIC®-HILIC column (3.5 μm, 150 mm × 2.1 mm i.d.), 200 $\mu L.min^{-1}$, 0.5 μL injection.
[a] Intra-day RSD of retention times (n = 3 independent measurements).
[b] Inter-day RSD of retention times (n = 5 independent measurements).
[c] Concentration LOD calculated at an S/N ratio of 3.
[d] LOQ calculated at an S/N ratio of 10.
[e] LOD of the amount loaded onto column calculated at an S/N ratio of 3.

multiple cross-ring cleavages to form A-type ions at *m/z* 311 ($^{0,1}A_2$), 281 ($^{0,2}A_2$), 251 ($^{0,3}A_2$), and 221 ($^{0,4}A_2$) (Fig. 5(a)). CID MS^2 analysis of the deprotonated tetrasaccharide stachyose[29] (*m/z* 665 $[M-H]^-$) produced a C_3 ion at *m/z* 503 due to loss of one hexose residue, an abundant C_2 ion at *m/z* 341 formed by the loss of two hexose moieties, and multiple cross-ring cleavages to form the A_2 and A_3 ions at *m/z* 443 ($^{0,2}A_3$), 413 ($^{0,3}A_3$), and 383 ($^{0,4}A_3$) (Fig. 5(b)). CID MS^2 analysis of the deprotonated pentasaccharide verbascose (*m/z* 827 $[M-H]^-$) produced a low-abundance C_4 ion at *m/z* 665 from loss of one hexose residue, an abundant C_3 ion at *m/z* 503 formed by the loss of two hexose moieties, and multiple cross-ring cleavages to form the A_2 and A_3 ions and A_4 ions at *m/z* 605 ($^{0,2}A_4$) and 545 ($^{0,4}A_4$) (Fig. 5(c)). These A-type product ions must derive from cross-ring cleavage of the α-(1 → 6) linked Glc (in the case of raffinose) and/or Gal residues (for stachyose and verbascose). Their formation involves loss of the fructose moiety, as well as parts or all (raffinose and verbascose) of the Glc, and internal Gal residues.

Such linkage-specific cross-ring fragmentations have been previously reported in negative ion data from this family of non-reducing glycans using fast atom bombardment (FAB) collisional activation (CA) on a magnetic sector instrument[36] and liquid secondary ion mass spectrometry (LSIMS) low-energy CA by Fourier transform mass spectrometry (FT-MS).[37]

The mechanism proposed by the group of Lebrilla[37] for the formation of cross-ring A-type fragments in negative ion mode involves loss of the fructose residue to yield a C_{n-1} ion in which the negative charge is borne by the newly generated reducing terminal anomeric oxygen. This 6-substituted residue was then proposed to undergo subsequent ring opening and cleavage of the C-backbone to allow neutral loss of one or more CH_2O (multiples of 30 Da) moieties from the monosaccharide. Interestingly, this mechanism cannot explain the formation of the A-type ions observed in our experiments, since these were carried out in a quadrupole ion trap. If cleavage of the α-(1 → 2) Glc–Fru bond occurred to yield the C_{n-1} ion, this would not fragment further in an ion trap, since the auxiliary rf voltage applied to activate the precursor ion activates only ions within a narrow *m/z* range. Product ions resonate with different secular frequencies from the precursor ion and thus are not activated; the C_{n-1} product ion would thus not fragment further. A concerted mechanism such as those proposed by Dallinga and Heerma[36] in which fragmentation takes place in a single step must therefore be postulated for the cleavages observed in the ion trap.

Repeatability, limits of detection (LODs) and limits of quantification (LOQs) of the HILIC/ESI-MS method

Intra-day repeatability was measured by injecting the same standard solution three times in a single day. Inter-day repeatability was measured by analysing the same standard solution over five different days. Intra- and inter-day repeatability of retention times using the HILIC/ESI-MS method gave relative standard deviations (RSDs) of less than 2% (Table 1). The LOD for each compound was calculated as

DOI: 10.1002/rcm

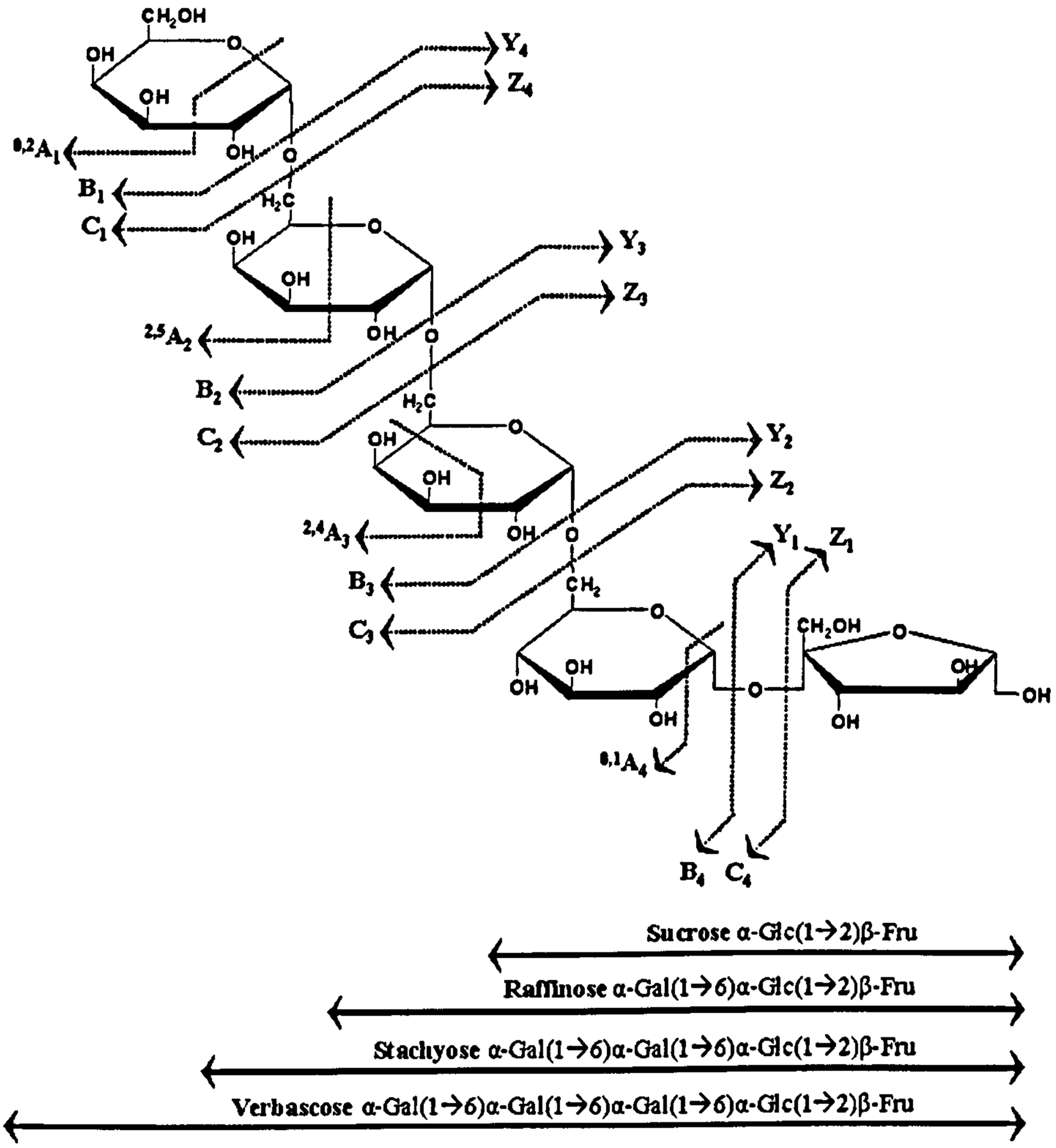

Scheme 1. Structure of non-reducing RFOs showing carbohydrate fragmentation according to the nomenclature of Domon and Costello.[35]

the minimum amount injected which gave a detector response higher than three times the signal-to-noise (S/N) ratio, and the LOQ was calculated at an S/N ratio of 10. The method gave LODs ranging from 0.2 μM obtained for neutral sugars, to 1.0 μM obtained for sugar alcohols and *myo*-inositol, and 2.0 μM obtained for the sugar phosphates, which are comparable with those reported for these compounds using PGC/ESI-MS.[23]

Quantification of carbohydrate-related metabolites in *A. thaliana* wild-type Col-0 and *pgm1* leaf extracts using HILIC/ESI-MS

To evaluate the potential of this on-line HILIC/ESI-MS method as a tool for the separation and characterisation of carbohydrate-related metabolites present in the complex biological matrices typically encountered in plant metabolomics studies, we have applied it for the analysis of *A. thaliana* wild-type (WT) Columbia-0 (Col-0) and *pgm1* mutant chloroform/methanol leaf extracts. *A. thaliana pgm1* mutant plants lack plastidial phosphoglucomutase (PGM) activity, an enzyme that catalyses the interconversion of Glc6P and Glc1P, which is essential for starch synthesis.[30,38] For this reason, *pgm1* plants are unable to synthesise starch and high levels of the soluble sugars Glc and Suc accumulate in the leaves during the day, as they are not converted into starch for storage.

The application of this HILIC/ESI-MS method allowed the separation and identification of four metabolites present in *A. thaliana* plant extracts: Glc, Suc, raffinose, and Glc6P. Metabolite identification was based on the comparison of retention times, masses, and ion trap tandem mass spectra with those obtained for standard compounds (Table 1). In order to quantify Glc, Suc, raffinose, and Glc6P by HILIC/ESI-MS, the linearity of the method was measured for these compounds by recording the response of each at different concentrations over the range 0–100 μM. Five-point standard curves were obtained by plotting integrated peak areas versus concentration. Each point on the calibration curve was the mean value of three independent measurements using the HILIC/ESI-MS method. The on-line HILIC/ESI-MS method showed good linearity of response over the concentration range 0–100 μM for these analytes, with correlation coefficients $R^2 > 0.99$ (Table 2).

Figure 6(A) shows the results obtained for the quantification of Glc, Suc, raffinose and Glc6P in *A. thaliana* WT Col-0 and *pgm1* mutant leaf extracts using HILIC/ESI-MS. The

DOI: 10.1002/rcm

RCM

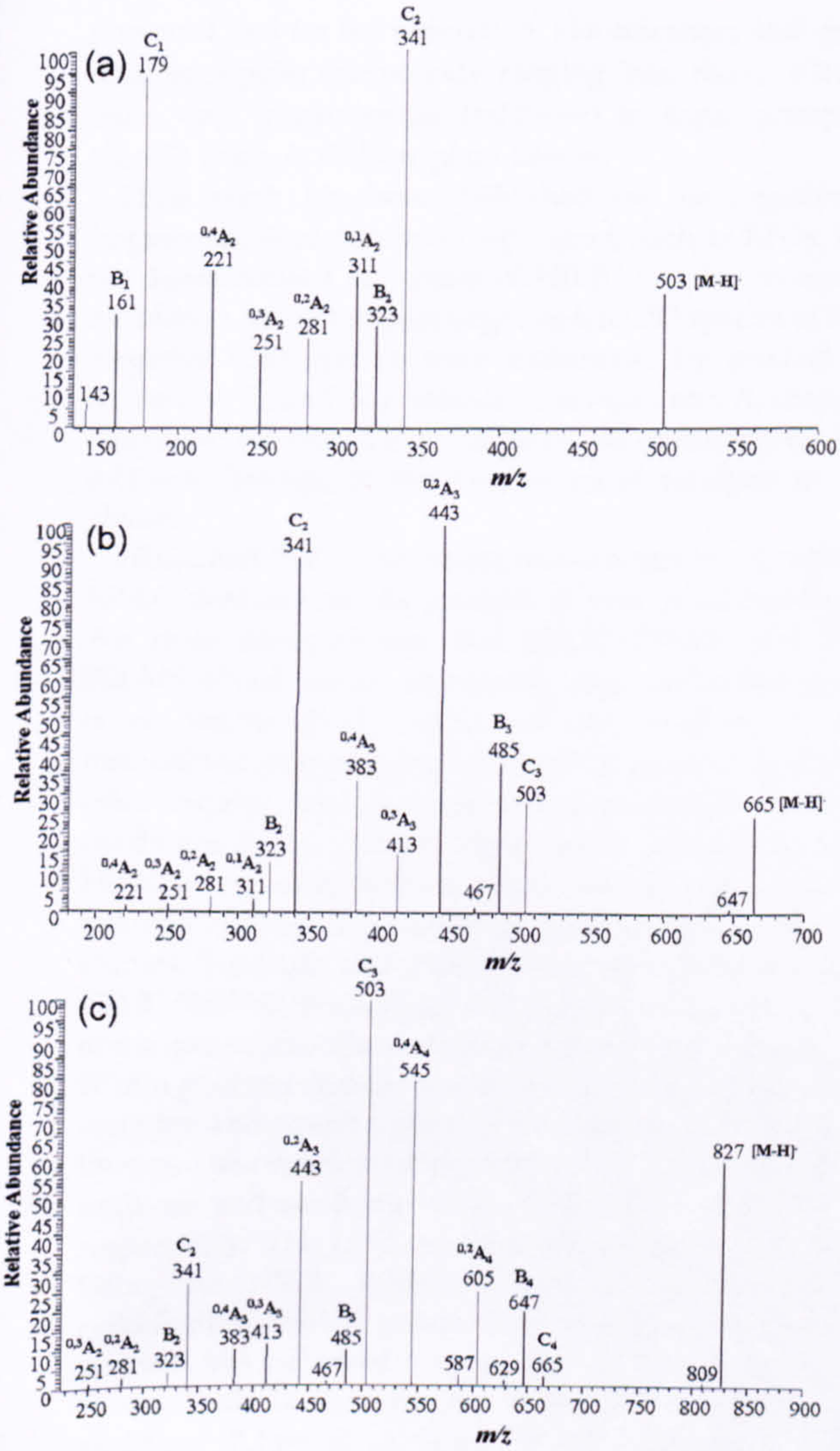

Figure 5. Negative ion CID spectra of non-reducing RFOs obtained by HILIC/ESI-MS^n showing nomenclature of Domon and Costello.[35] (a) CID MS^3 spectrum of raffinose (precursor ion $[M–H]^-$ *m/z* 503); (b) CID MS^2 spectrum of stachyose (precursor ion $[M–H]^-$ *m/z* 665); (c) CID MS^2 spectrum of verbascose (precursor ion $[M–H]^-$ *m/z* 827).

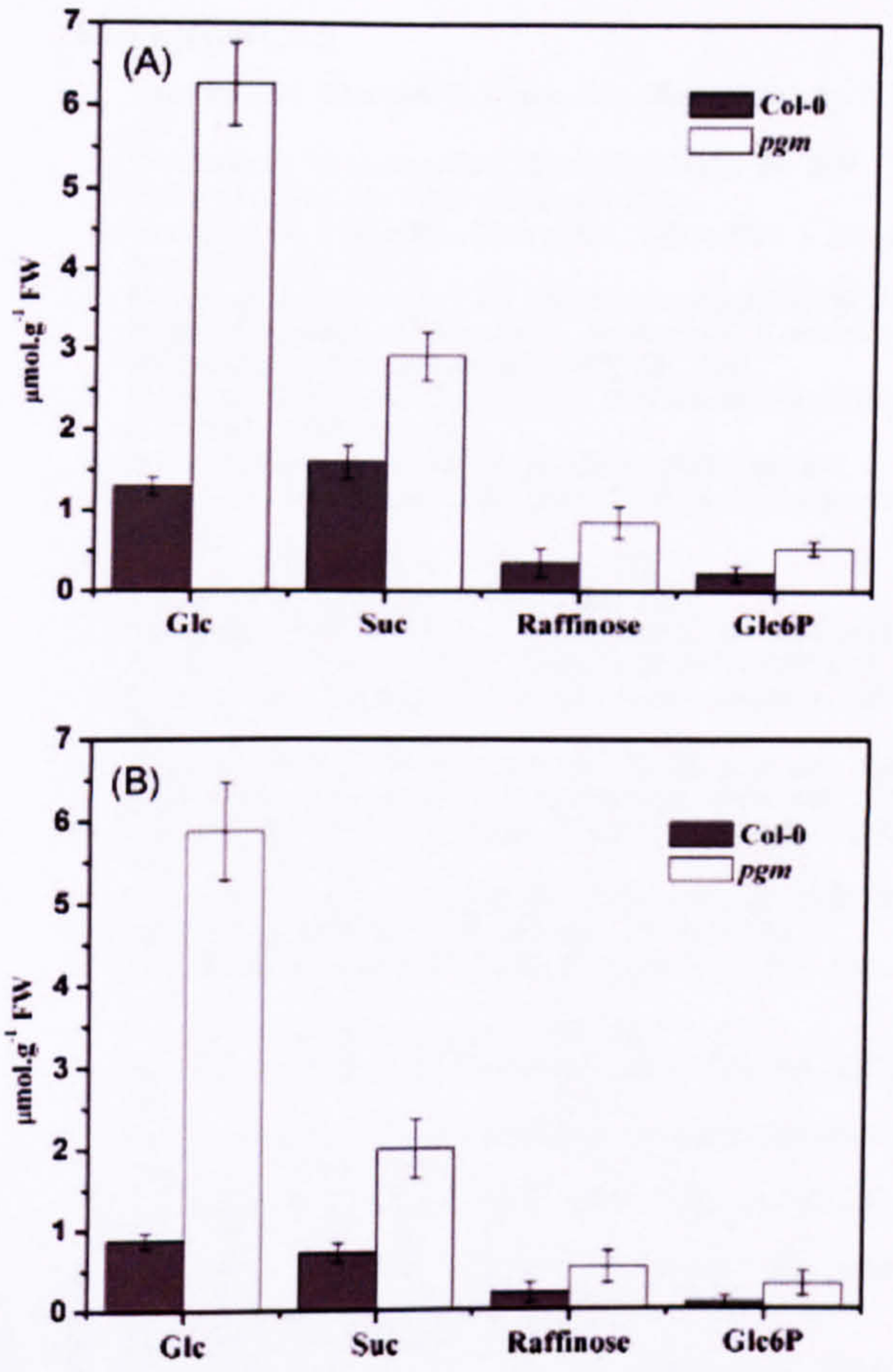

Figure 6. Metabolite levels (Glc, Suc, raffinose, and Glc6P) determined in *Arabidopsis thaliana* Col-0 and *pgm* chloroform/methanol leaf extracts using (A) ZIC®-HILIC/ESI-MS and (B) Hypercarb™ PGC-LC/ESI-MS. Plants were grown under a 16 h light/8 h dark photoperiod and harvested at developmental stage 6.0. Values are mean ± SD (n = 3 biological replicates, each containing leaves from three rosettes). Each biological replicate is the mean value of n = 3 independent LC/MS measurements. FW, fresh weight.

levels of soluble sugars found in *pgm1* leaf extracts were $6.26 \pm 0.50\ \mu mol.g^{-1}$ fresh weight (FW) for Glc, $2.92 \pm 0.30\ \mu mol.g^{-1}$ FW for Suc, $0.85 \pm 0.20\ \mu mol.g^{-1}$ FW for raffinose, and $0.53 \pm 0.09\ \mu mol.g^{-1}$ FW for Glc6P. In contrast, *A. thaliana* Col-0 leaves accumulate much lower levels of soluble sugars, with levels of $1.30 \pm 0.10\ \mu mol.g^{-1}$ FW for Glc, $1.60 \pm 0.20\ \mu mol.g^{-1}$ FW for Suc, $0.35 \pm 0.17\ \mu mol.g^{-1}$ FW for raffinose, and $0.22 \pm 0.09\ \mu mol.g^{-1}$ FW for Glc6P. Figure 6(B) shows the quantification of Glc, Suc, raffinose, and Glc6P using PGC/ESI-MS[23] from an equivalent but separate set of Col-0 and *pgm1* preparations,[23] which gave results very comparable with those obtained using HILIC/ESI-MS.

Table 2. Linearity of standard curves obtained for Glc, Suc, raffinose, and Glc6P standard compounds using negative ion ZIC®-HILIC/ESI-MS

Standard compounds	Diagnostic ion (*m/z*)	R^2
Glc	225 $[M+HCOO]^-$	0.9975
Suc	387 $[M+HCOO]^-$	0.9968
Raffinose	549 $[M+HCOO]^-$	0.9985
Glc6P	259 $[M–H]^-$	0.9981

CONCLUSIONS

This work describes the use of HILIC coupled to negative ion mode ion trap ESI-MS for the analysis of several polar metabolites, ranging from neutral sugars and sugar alcohols to negatively charged sugar phosphates, which generally are not retained on typical RP-LC columns. This method is robust, selective, rapid (less than 15 min), with LODs in the low µM range (0.2–2.0 µM), and uses MS-friendly mobile phases, enabling efficient coupling with on-line ESI-MS. We have demonstrated that our HILIC/ESI-MS method is a

DOI: 10.1002/rcm

powerful tool for the separation, identification, and quantification of polar compounds, ranging from mono- (Glc), di- (Suc), and trisaccharides (raffinose) to sugar phosphates (Glc6P) from *A. thaliana* plant tissues.

Little work has been published on the negative ion fragmentation of non-reducing sugars, such as RFOs. Here, we demonstrated the utility of HILIC coupled to ion trap multistage MS to produce negative ion CID spectra of RFOs. Negative CID spectra were dominated by product ions formed by C_i and B_i glycosidic cleavages and A_i cross-ring cleavages; the cross-ring fragments are characteristic of the α-(1→6) linkage of the hexopyranose residues in these glycans.

HILIC and PGC columns are two alternatives to traditional RP-LC methods for the analysis of very polar metabolites. We have demonstrated that HILIC/ESI-MS and PGC/ESI-MS afford robust, repeatable, and comparable quantitative results (and LODs) for the analysis of plant metabolites. However, the fact that PGC gradient separations often require extensive method development and strong conditions for elution of highly polar compounds makes HILIC a very suitable and more convenient approach for the analysis of these compounds in routine plant metabolomic studies. Tolstikov and Fiehn[29] have previously reported a HILIC/ESI-MS method for the analysis of oligosaccharides and sugar nucleotides from plant tissues. That method uses a 60 min gradient elution, which was necessary to separate the complex and diverse mixture of analytes in those experiments. The retention times obtained for the standards Suc, raffinose and stachyose were 29.57, 35.57, and 40.21 min, respectively. The LOD reported for stachyose was 0.5 ng. Using our HILIC method, aimed at the separation of carbohydrate-related metabolites, separation of these compounds was achieved in significantly less time (around 10 min, Table 1). In addition, a better LOD was obtained for stachyose (0.1 pmol, i.e. 66 pg), which represents a distinct improvement for these analytes over the more broadly targeted method of Tolstikov and Fiehn.

Acknowledgements

The authors gratefully acknowledge the CHEMCELL Marie Curie Early Stage Research Training Fellowship of the European Community's Sixth Framework Programme under contract number MEST-CT-2004-504345 for financial support. J.T.-O. gratefully acknowledges support from ThermoFinnigan and funding from the Analytical Chemistry Trust Fund, the RSC Analytical Division, and EPSRC.

REFERENCES

1. Sumner LW, Mendes P, Dixon RA. *Phytochemistry* 2003; **62**: 817.
2. Weckwerth W. *Annu. Rev. Plant Biol.* 2003; **54**: 669.
3. Fiehn O. *Plant Mol. Biol.* 2002; **48**: 155.
4. Sumner LW, Paiva NL, Dixon RA, Geno PW. *J. Mass Spectrom.* 1996; **31**: 472.
5. Huhman DV, Sumner LW. *Phytochemistry* 2002; **59**: 347.
6. Fiehn O, Kopka J, Dörmann P, Altmann T, Trethewey RN, Willmitzer L. *Nat. Biotechnol.* 2000; **18**: 1157.
7. Roessner U, Wagner C, Kopka J, Trethewey RN, Willmitzer L. *Plant J.* 2000; **23**: 131.
8. Dunn W, Ellis D. *Trends Anal. Chem.* 2005; **24**: 285.
9. Townsend RR, Hardy MR, Lee YC. *Methods Enzymol.* 1989; **179**: 65.
10. Lee YC. *Anal. Biochem.* 1990; **189**: 151.
11. Lee YC. *J. Chromatogr. A* 1996; **720**: 137.
12. Antignac J-P, de Wasch K, Monteau F, De Brabander H, Andre F, Le Bizec B. *Anal. Chim. Acta* 2005; **529**: 129.
13. Jessome LL, Volmer DA. *LCGC North America* 2006; **24**: 498.
14. Niessen WMA, van der Hoeven RAM, van der Greef J, Schols HA, Voragen AGJ. *J. Chromatogr.* 1993; **647**: 319.
15. Gilbert MT, Knox JH, Kaur B. *Chromatographia* 1982; **16**: 138.
16. Knox JH, Kaur B, Millward GR. *J. Chromatogr.* 1986; **352**: 3.
17. Knox JH, Ross P. *Adv. Chromatogr.* 1997; **37**: 73.
18. Koizumi K, Okada Y, Fukuda M. *Carbohydr. Res.* 1991; **215**: 67.
19. Koizumi K. *J. Chromatogr. A* 1996; **720**: 119.
20. Buchholz A, Takors R, Wandrey C. *Anal. Biochem.* 2001; **295**: 129.
21. Xing J, Apedo A, Tymiak A, Zhao N. *Rapid Commun. Mass Spectrom.* 2004; **18**: 1599.
22. Robinson S, Bergström E, Seymour M, Thomas-Oates J. *Anal. Chem.* 2007; **79**: 2437.
23. Antonio C, Larson T, Gilday A, Graham I, Bergström E, Thomas-Oates J. *J. Chromatogr. A* 2007; **1172**: 170.
24. Alpert AJ. *J. Chromatogr.* 1990; **499**: 177.
25. Alpert AJ, Shukla M, Shukla AK, Zieske LR, Yuen SW, Ferguson MAJ, Mehlert A, Pauly M, Orlando R. *J. Chromatogr. A* 1994; **676**: 191.
26. Schlichtherle-Cerny H, Affolter M, Cerny C. *Anal. Chem.* 2003; **75**: 2349.
27. Bajad SU, Lu W, Kimball EH, Yuan J, Peterson C, Rabinowitz JD. *J. Chromatogr. A* 2006; **1125**: 76.
28. Cubbon S, Bradbury T, Wilson J, Thomas-Oates J. *Anal. Chem.* 2007; **79**: 8911.
29. Tolstikov V, Fiehn O. *Anal. Biochem.* 2002; **301**: 298.
30. Caspar T, Huber SC, Somerville C. *Plant Physiol.* 1985; **79**: 11.
31. Murashige T, Skoog F. *Physiol. Plant.* 1962; **15**: 473.
32. Boyes DC, Zayed AM, Ascenzi R, McCaskill AJ, Hoffman NE, Davis KR. *Plant Cell* 2001; **13**: 1499.
33. Guo Y, Gaiki S. *J. Chromatogr. A* 2005; **1074**: 71.
34. Feurle J, Jomaa H, Wilhelm M, Gutsche B, Herderich M. *J. Chromatogr. A* 1998; **803**: 111.
35. Domon B, Costello CE. *Glycoconjugate J.* 1988; **5**: 397.
36. Dallinga JW, Heerma W. *Biol. Mass Spectrom.* 1991; **20**: 215.
37. Carroll JA, Willard D, Lebrilla CB. *Anal. Chim. Acta* 1995; **307**: 431.
38. Caspar T, Lin T-P, Kakefuda G, Benbow L, Preiss J, Somerville C. *Plant Physiol.* 1991; **95**: 1181.